EXPRESSION OF IGF2R, IGF2, TGFβ, AND uPAR IN A RAT MODEL OF OBESITY

A Dissertation

presented to

the Faculty of the Graduate School

at the University of Missouri-Columbia

In Partial Fulfillment

of the Requirements for the Degree

Doctor of Philosophy

By

DAVID BAYLESS

Dr. Harold Laughlin, Dissertation Supervisor

MAY 2017

The undersigned, appointed by the dean of the Graduate School, have examined the dissertation entitled

EXPRESSION OF IGF2R, IGF2, TGFβ, AND uPAR IN A RAT MODEL OF OBESITY

presented by David Bayless, a candidate for the degree of doctor of philosophy,

and hereby certify that, in their opinion, it is worthy of acceptance.

Professor Harold Laughlin

Professor Ronald Korthuis

Professor Frank Booth

Professor Mark Milanick

ACKNOWLEDGEMENTS

I would like to begin by acknowledging Dr. Harold Laughlin, who graciously permitted me to enter his lab following a productive rotation, and who has mentored me for the past four and a half years as I have navigated my way through developing my thesis, participated in the raising of animal cohorts, performed experiments, analyzed data, and wrote. He has displayed patience, support, and understanding at every step of the way and has contributed immensely to my success.

I would also like to acknowledge the members of my committee. Dr. Ronald Korthuis has contributed valuable critiques and advice during the development of my thesis and in response to the data I collected. I also appreciated how, even with the responsibility of heading up the department, he remained accessible and interested in the well-being of the graduate students – including their intellectual well-being derived from attending seminars. Dr. Booth likewise provided valuable commentary during the course of my dissertation, and from all my interactions with him - from working in his lab during my very first rotation, to listening to his lecturing during a skeletal muscle physiology course, to his questions during seminars, I have gained a great appreciation for the raw enthusiasm he has for his work, and a deep respect for his willingness to share how looking back on his own family inspires him to work as hard as he does. Dr. Milanick has provided perspective and alternative interpretations on my data, and has proven an excellent role model as a teacher. I admire his drive to be an effective teacher, from what I observed in the Elements of Physiology laboratory after he took over from Dr. Hurley, and hope that I can emulate his drive when I teach in future.

In my laboratory work, I would first like to thank Pam Thorne, the lab manager for Dr. Laughlin's lab during my time there. Pam displayed grace and patience as I learned the ins and outs of procedures, even as I kept running into what must have been the most absurd roadblocks. I had a very hard time at first getting my Nano-Orange standard curves done consistently, we shall say that much. I wish her the very best in the Emter lab and with whatever remains of her Masters.

For those that have helped me with my dissertation procedures, I would like to begin by thanking the staff of the Veterinary Medical Diagnostic Lab, who patiently worked out how to get my tissues cut and set up on slides for IHC work. I thank Dr. Dae Young Kim of Veterinary Pathobiology for answering my questions about analyzing my IHC slide work. I thank Dr. Darla Tharp for her input on the particulars of dehydrating slides during IHC preparations. I thank Dr. Doug Bowles for his input on assessing staining density in a quantitative fashion.

I appreciate all my fellow students and postdoctoral fellows that I have had a chance to work alongside in the lab during my time here. Drs. Nathan Jenkins, Jaume Padilla, and Michael Roberts provided me with that crucial first step into labwork by bringing me onto their projects. Dr. Jacqui Crissey was also a true pleasure to work with during her time at the University of Missouri as a fellow graduate student. Drs. Ryan Sheldon, Melissa Linden, and Laura Ortinau were wonderful to work with during the raising and harvesting of the rat cohorts used for my own dissertation work. I also want to thank the various faculty whose labs worked hand-in-hand with Dr. Laughlin's lab during my time here, including Dr. Scott Rector, Dr. Victoria Vieira-Potter, and Dr. Craig Emter.

I thank all of my fellow students and the faculty of the Medical Pharmacology and Physiology department, Biomedical Sciences department, and Nutrition and Exercise Physiology departments whom I have had the honor of knowing during my time here.

Finally, saving the best for last, I extend my thanks to my family for their deep and abiding support, even if it was just to be there for me, during my time at the University of Missouri. Thank you Mom and Dad, Peter, and Mare.

TABLE OF CONTENTS

LIST OF FIGURES

LIST OF ABBREVIATIONS

IGF2R: Insulin-like growth factor 2 receptor

IGF2: Insulin-like growth factor 2

TGFβ: Transforming growth factor beta

uPAR: Urokinase plasminogen receptor

LETO: Long-Evans Tokushima Otsuka

OLETF: Otsuka Long-Evans Tokushima Fatty

HFD: High fat, high sucrose diet

CON: Control diet

SED: Sedentary

EX: Exercise training intervention

CR: Calorie restriction intervention

ABSTRACT

We tested the hypothesis that induction of obesity in lean Long Evans Tokushima Otsuka (LETO) and obesity-prone Otsuka Long Evans Tokushima Fatty (OLETF) would cause the insulin growth factor 2 receptor (IGF2R) and factors it regulates, including insulin growth factor 2 (IGF2), transforming growth factor beta (TGFB), and urokinase-plasminogen receptor (uPAR) to be changed in expression away from a pro-angiogenic state. This would arise from an increase in IGF2R and TGFB, and a decrease in IGF2 and uPAR. LETO and OLETF rats were raised from age 4 to 32 weeks, with each strain subdivided into a control diet (CON) and high-fat diet (HFD) group. We also raised a cohort of OLETF HFD rats which either underwent weight control interventions (exercise training (EX) or calorie restriction (CR)) or did not undergo intervention (sedentary (SED)). Interventions began at age 20 weeks and continued until 32 weeks. We found significant increases in both body weight and body fat percentage, and in decrease in capillarity in both biceps brachii (BB) and vastus lateralis (VL) muscle, in comparing non-obese to obese animals ($p < 0.05$). When examining diet and strain induction of obesity, we found significant increases in body weight and body fat percentage from control lean animals, but with no significant change in capillarity. We did not observe any significant effects on body weight or body fat percentage in EX or CR relative to

SED. We observed multiple significant changes in skeletal and adipose feed arteries with obesity induction on IGF2R, IGF2, TGFβ, and uPAR. However, most of these changes did not occur in accordance with our hypothesis. Overall, we find LETO and OLETF rats to be a viable model for examining mechanisms driving changes in tissue capillarity in obesity, and that the IGF2R system we proposed does not appear to agree with the data. We propose that the IGF2R system is moderated in a static-to-proangiogenic state during obesity, and decreases in overall capillarity are driven by other mechanisms.

1. INTRODUCTION

a. Obesity

Obesity has been and is steadily increasing as a health concern in the United States, as well as other countries across the world. Many secondary health concerns arise from obesity, including metabolic syndrome, cardiovascular disease, cancer, diabetes, and others. Obesity has also been shown to affect mental health as well, with low self-esteem, difficulty forming social relationships, depression, and other issues (1). Mental health in obesity has been identified as a major barrier to success in resolving obesity, with patients' distress making it difficult to follow long-term plans(2). The economic impact of obesity is also targeted as a significant issue going forward, both in regards to healthcare costs, as well as secondary economic losses arising from ill health.

With the drastic impact of obesity at both personal and societal levels, much research has been directed towards determining how to successfully treat obesity. The primary avenues used to treat obesity include exercise training and calorie restriction (conventionally known as dieting). Surgical interventions are also used to treat either the aesthetic or functional consequences of obesity, including liposuction and various alterations to the gastrointestinal tract (known as bariatric surgery).

However, physiological changes during obesity may hamper efforts to return to good health by way of physical remodeling. Previous studies in this laboratory have illustrated that obesity can induce dyslipidemia, insulin

insensitivity, hypertension, impaired vasodilation responsiveness, and increased inflammatory agent release from adipose tissue beds in both pig and rat models of obesity(3-6). Additionally, previous studies have also looked at cross-talk between adipose depot and skeletal muscle in obesity(7). One topic pertinent to vascular dysfunction but not studied in great detail previously by this laboratory is the decrease in capillarity observed during obesity(8). This decrease is hypothesized to be caused by mechanisms acting to block new vessel growth resulting in vascular senescence, mechanisms acting to promote the degradation of existing vessels, or both.

In the course of literature review, a proposed mechanism for control of vascular senescence came to the forefront as shown in Figure 1, suggesting that the insulin growth factor 2 receptor (IGF2R) was responsible for mediating senescence by way of degradation of insulin growth factor 2 (IGF2), activation of transforming growth factor beta (TGFβ), and degradation of the urokinase-plasminogen receptor (uPAR)(9). Given previous work in the lab which established physiological dysfunction in animals such as the LETO and OLETF rats and Ossabaw pigs, the prospect of investigating this mechanism as a potential cause of decreased vessel density and subsequent physiological dysfunction was compelling.

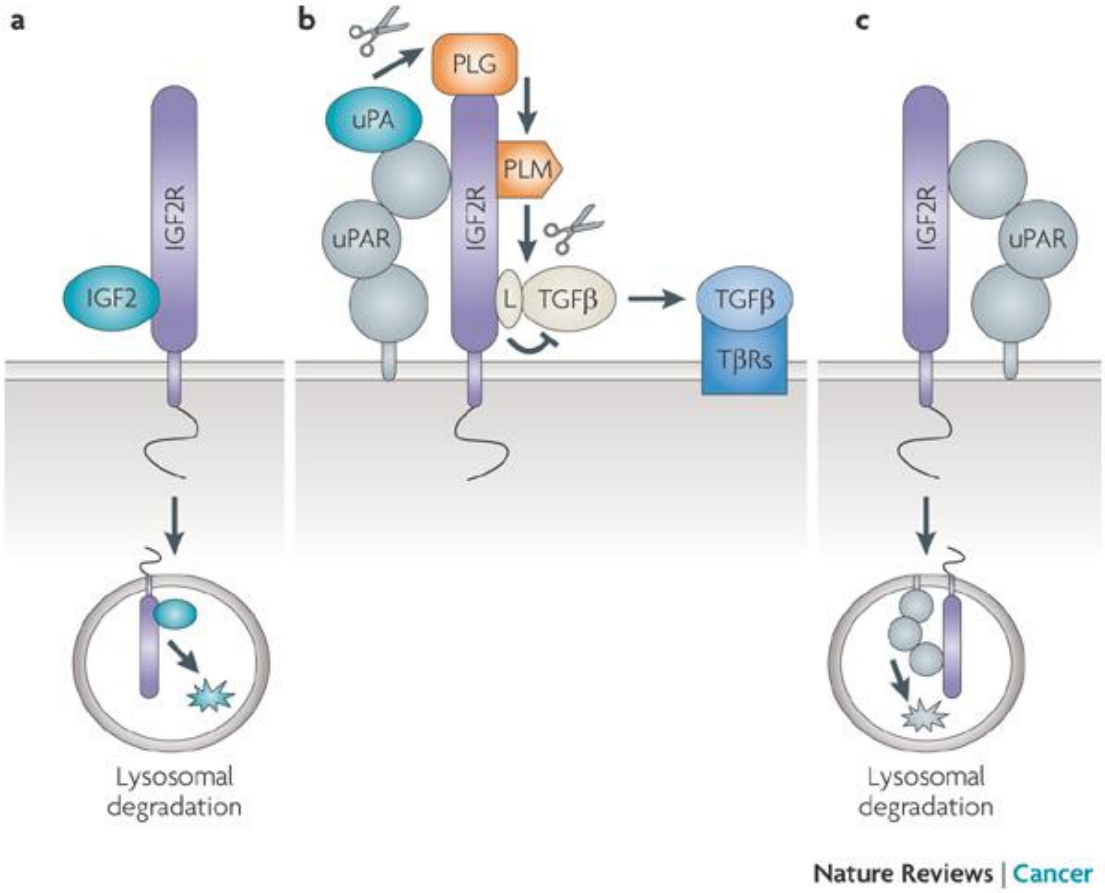

Figure 1. Senescence mechanism coordinated around IGF2R. Adapted from Kuilman, Thomas and Daniel S. Peeper. "Senescence-messaging secretome: SMS-ing cellular stress." Nature Reviews Cancer. 2009. 9(2): 81-94. IGF2R: Insulin-like growth factor 2 receptor. IGF2: Insulin-like growth factor 2. uPA: urokinase-plasminogen activator. uPAR: urokinase plasminogen activator receptor. PLG: plasminogen. PLM: plasmin. L: Latent (TGFβ). TβR: TGFβ receptor.

b. Obesity and changes in the vasculature

There are a host of physiological changes in obesity, including decrease in capillarity, which invites investigation into underlying mechanisms to understand what is changing and how it can be effectively treated. During obesity, the adipose tissue beds expand in mass, with a distinction drawn between hypertrophy of individual adipocytes and proliferation of adipocytes, with the latter being considered more conducive to a healthy phenotype and being less likely to be vulnerable to metabolic syndrome(10). Total expansion of adipose tissue during obesity development may be constrained by various factors, resulting in abnormal deposition of lipids in other body tissues such as the liver, skeletal muscle, and near β-cells, resulting in lipotoxicity(11). This lipotoxicity may be a local and systemic driver for insulin resistance seen in the development of type 2 diabetes.

Vascular dysfunction is also observed to occur in adipose tissue before insulin resistance develops. Decreases in capillarity are upstream of hypoxia and inflammation, and while hypoxia initially stimulates vascular remodeling and subsequent increases in energy expenditure as a reaction to obesity, hypoxic response soon becomes insufficient to overcome the factors affecting capillarity in obesity(12, 13).

Inflammation is observed in adipose tissue during obesity, with M1 macrophage recruitment increasing and forming clusters around adipocytes, resulting in a “crown-like” structure. Immune response and inflammation results

in changes to the adipose tissue environmental secretome, resulting in the release of pro-inflammatory agents including, but not limited to, leptin, TNF-α, IL-6, resistin, CCL2, and CXCL5(14). Expansion of particular depots can be relevant in this regard, as while both subcutaneous and visceral adipose tissue expansion are correlated with health outcomes, visceral adipose tissue expansion correlates with more severe health outcomes than subcutaneous adipose tissue(15).

In skeletal muscle, HFD has been shown to decrease the capillary/fiber ratio(8). Capillarity has also been shown to decrease with advancing glucose intolerance and decreasing insulin sensitivity, suggesting issues with skeletal muscle uptake of glucose may be due in part to decreased delivery avenues(16). This change is not believed to be due to decreases in VEGF expression, as a decrease in capillarity did not display a concomitant change in VEGF expression in humans(17). In fact, VEGF is noted to increase as BMI increases, and inducing VEGF overexpression can assist with metabolism, though it is not known why VEGF action is ineffective at normal physiological levels(18).

These changes in capillarity in skeletal muscle may have downstream effects in terms of functional capacity during obesity and T2D. Obese human subjects have been observed to have lower fatigue resistance during strength exercises, and in terms of power output, studies have characterized either a decrease in strength overall, or higher absolute but lower relative strength compared to lean counterparts(19, 20).

In addition to changes in density, other pathophysiological changes in the vasculature are observed in obesity and type 2 diabetes. Arterial stiffness is present and is believed to be due to both diminished NO response as well as deposition of noncompliant factors in the vessel wall(21, 22).

From these studies, we know that capillarity decreases in obesity, and that a proposed mechanism, IGF2R coordination of IGF2, TGFβ, and uPAR, may act as a driving force behind this decrease. In addition to measuring these factors, we must ask if we can treat these changes in obesity by way of common interventions. Exercise training is one prospect, as it has been shown in numerous studies to increase human capillarity in direct proportion to training, although this phenomenon is less consistent in animal models(23-26). Capillarization appears to be greatest in fast oxidative glycemic muscle, followed by slow oxidative and fast glycemic, respectively, and training seems to promote capillarization increase in all fiber types in humans – though for animals, the effect is observed mostly in fast oxidative glycemic muscle(25, 27). Exercise training also increases arteriolar density, which in conjunction with capillarity and changes in vascular resistance are thought to promote increased blood flow capacity(28-30).

Exercise training is also shown to induce beneficial physiological remodeling of the ventricles of the heart as well as improving systolic and diastolic function, and reduces arterial stiffness through its influence on the NO system(31, 32). Exercise training also promotes muscle and adipose tissue health, as well as improving insulin and glucose responsiveness in muscle tissue

which can help blunt the insulin insensitivity and diminished glucose uptake observed in type 2 diabetes(33). Calorie restriction also promotes weight loss which can be beneficial in terms of reducing mechanical stress and inflammation, but does not yield the same cardiovascular benefits as exercise training. In addition, calorie restriction can result in lean and bone mass loss in addition to adipose mass loss(34).

Of note as a common intervention but not pursued in this study, bariatric surgery has been shown to resolve issues with obesity and the metabolic syndrome, with improvements in lipid blood profiles, remission of diabetes, and significant weight loss, but has its own risks in potential nutritional deficiencies leading to secondary complications(35, 36).

c. Type 2 Diabetes

In addition to obesity, the animal model we work with, the OLETF rat, develops type 2 diabetes at around twenty weeks of age, contingent on ad libitum access to food as well as diet quality. Type 2 diabetes is a chronic disease caused by a combination of genetic and lifestyle factors. It is estimated to affect approximately 8.5% of adults worldwide, and is predicted to be the seventh leading cause of death worldwide by 2030. Lifestyle factors include obesity as well as diet, with diet contributing both directly as well as indirectly via causing obesity(37-39). Type 2 diabetes arises from insulin insensitivity manifested in tissues, which results in decreased glucose uptake. Even with β-cell activity producing more insulin to overcome insulin insensitivity, glucose

levels are difficult to manage by the body's own physiology, and β-cells are observed to diminish over time due to unknown factors, decreasing available insulin production and resulting in glucose intolerance(40). This insulin insensitivity results in a variety of secondary health complications, with cardiovascular disease being the most well-known complication, but also others such as blindness and cognitive decline(41, 42).

Exercise training has been shown to be effective in reducing incidence of type 2 diabetes, increasing insulin sensitivity of muscle while concurrently lowering resting insulin levels(43). Glucose disposal is also observed to increase with exercise training, while glucose production is lowered(44). Overall, exercise training helps mitigate the extreme insulin and glucose serum levels and response seen in untreated diabetes(45-47).

Various pharmacological treatments for type 2 diabetes exist, with the most commonly used being metformin, which has been shown to have therapeutic effects in weight control and reducing cardiovascular mortality(48, 49). Metformin also promotes beneficial changes in glycaemic control, insulemia, and lipids(48). One primary point to note in metformin usage, however, is that it is contradicted in patients with liver and kidney problems. Bariatric surgery has also shown potential in treating type 2 diabetes with its overall effects on adiposity and metabolic syndrome, although treatments vary in efficacy(50).

In our study, we use the OLETF rat, an animal model that develops hyperphagia as a result of CCK-1 receptor deficiency, and which develops type 2 diabetes at around twenty weeks of age in association with the hyperphagic

phenotype, contingent on ab libitum access to food as well as diet composition(51). The purpose of this study was to show that IGF2R and TGFB are elevated in obesity, and IGF2 and uPAR decreased in obesity, and that these changes are associated with a decrease in capillarity in obesity.

d. Vascular remodeling

To understand the role IGF2R, IGF2, TGFB, and uPAR play in assisting vascular remodeling, we must briefly review the process of angiogenesis. During initiation, the basement membrane of the affected vessel, composed of lamins, collagen T4, and perlecan, is disrupted by the presence of VEGF, which in turn is generated by cells responding to external stimuli, commonly wounding or hypoxia(52, 53). Vascular sprouting initiates, forming a fibrillary network composed of fibronectin and T5 collagen, later to be followed by laminin and T4 collagen(54).

As the basement membrane continues to degrade, various factors begin to extravasate from the bloodstream, including fibrinogen, vitronectin, and fibronectin(55). These components form a new temporary ECM with fibrinogen converting to fibrin(56). At this stage, the ECM begins to acquire a lumen and pericytes. Pericytes stimulate matrix bridging proteins, percalan, laminins, and integrins(57). At this stage, morphogenesis ends and the new vessel is stabilized, linking to its parent vessel and permitting blood flow.

e. The role of IGF2R

IGF2R is a multifunction type 1 transmembrane receptor that has been identified as binding various molecules and internalizing the bound complex into the cell for degradation, after which IGF2R is returned to the Golgi apparatus.

IGF2R has been shown to be associated with disease progression in the cardiovascular system, with abnormally elevated expression in myocardial infarction scars as well as pathological hypertrophy(58). This may be linked to CREO binding to IGF2R inducing SMC switching from a contractile to a proliferative phenotype(59). Current literature on IGF2R in obesity indicates that obese dams have increased placental IGF2R(60). With the placenta being the avenue by which nutrients are delivered to the developing fetus, elevated levels of a cardiovascular-disease associated factor could signal dysfunction in nutrient delivery.

IGF2R is also known to be involved in cancer progression. IGF2R loss or mutation is known to increase cancer risk through its modulatory effects on tumorigenicity or invasiveness(61, 62). IGF2R is also linked to cancer progression through its regulatory effects on IGF2, specifically downregulation of IGF2R allowing higher levels of IGF2 to remain present and bind IGF1R.

f. The role of IGF2

IGF2 helps regulate cell proliferation, growth and migration, and while it is especially important in fetal growth and development, it also has been linked to

disease in adults, including cancer and cardiovascular disease. It binds to a variety of receptors, including IGF2R as well as IGF1R.

IGF2 can be handled in a variety of different ways as shown in Figure 2. Binding to IGF2R leads to IGF2 degradation. After binding to IGF1R, however, IGF2 activates the PI3K/Akt pathway, resulting in activation of mTOR and CCND1, promoting cell growth, survival, and apoptosis. Various polymorphisms have been shown to alter cell proliferation and survival, having been linked increased health risk in obese phenotypes, and reoccurrence of tumors and increase in angiogenesis in cancer in a giant cell tumor model(63) (64).

Maternal obesity and diet has been shown to alter IGF2 in the placenta and consequently has an impact on the developing fetus(65). Low protein diet increases IGF2 expression and protein levels in the placenta, which is believed to be a response intended to induce greater angiogenesis in a low-nutrition state to better deliver nutrients(66). Overexpression of IGF2 has also been shown to result in fetal overgrowth and obesity in young children(67). In obesity at large, IGF2 methylation is associated with an increased risk of lipid profile changes and metabolic changes(68).

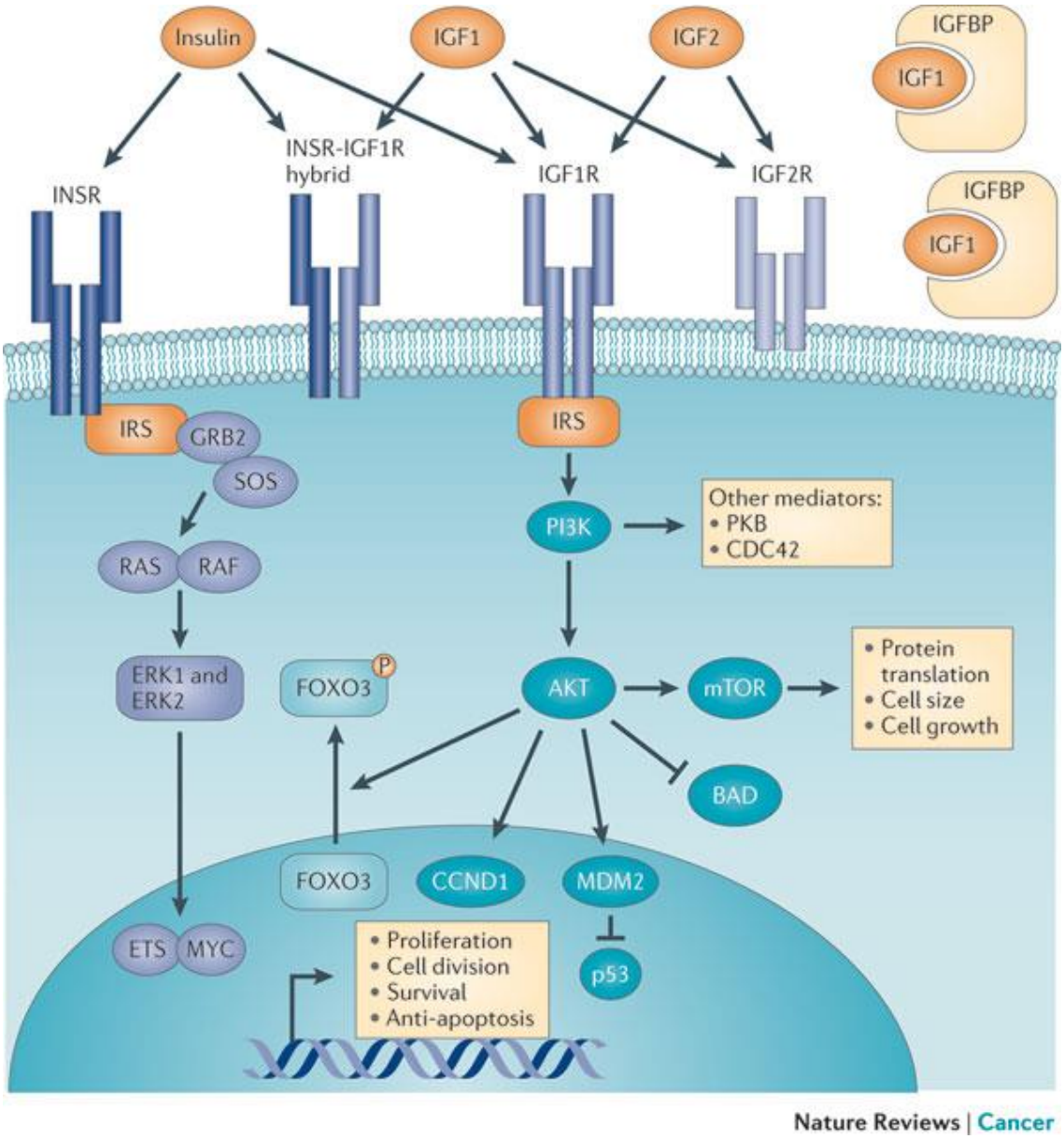

Figure 2. IGF2R and IGF2 pathway. Adapted from Khandehar et al. "Molecular mechanisms of cancer development in obesity." Nature Reviews Cancer. 2011. 11(12): 886-501. IGF1: Insulin-like growth factor 1. IGF2: Insulin-like growth factor 2. IGFBP: Insulin-like growth factor binding protein. INSR: Insulin receptor. IGF1R: Insulin-like growth factor 1 receptor. IGF2R: Insulin-like growth factor 2 receptor. IRS: Insulin receptor substrate. GRB2: Growth factor receptor-bound protein 2. SOS: Son of sevenless. ERK: Extracellluar-related kinase. ETS: E-26 transformation specific. AKT: Protein kinase B. mTOR: Mechanistic target of rapamycin. BAD: BCL-2 antagonist of cell death. FOXO3: Forkhead box O. CCND1: Cyclin D-1. MDM2: E3 ubiquitin-protein ligase Mdm2.

g. The role of uPAR

uPAR is a glycoprotein anchored to the membrane of cells, and binds uPA. It is a part of the plasminogen activation system, and in concert with MMPs, works to reorganize the extracellular matrix (69, 70). uPAR binds uPA resulting in the formation of the urokinase-plasminogen activator, facilitating the conversion of plasminogen to plasmin as shown in Figure 3. This leads to both direct and indirect – via MMP action – degradation of the extracellular matrix and increase in endothelial cell mobility.

In angiogenesis, uPAR has been shown to be involved in ECM proteoloysis and remodeling(71). uPAR responds to VEGF-induced angiogenesis by breakdown of the ECM, increasing vascular permeability to permit blood-bourne components involved in the synthesis of new vessels to the extracellular compartment, and promotes endothelial cell migration to help form the developing vessel(72-74). Angiogenic action is believed to be promoted through the Ser88-Arg-Ser-Arg-Tyr92 sequence, and is moderated through PI3K/Akt, which also plays a role in adipogenesis(72, 75).

uPAR has also been shown to be involved in other disease states, including cancer. Utilizing a competitive antagonist of uPA/uPAR decreases tumor spread, and another study shows that decreasing uPAR induces senescence in carcinoma cells, decreasing migration, invasion, and proliferation of cancerous cells(76, 77). Silencing of uPAR has been shown to decrease movement of mesenchymal and amoeboid cancer cells(74).

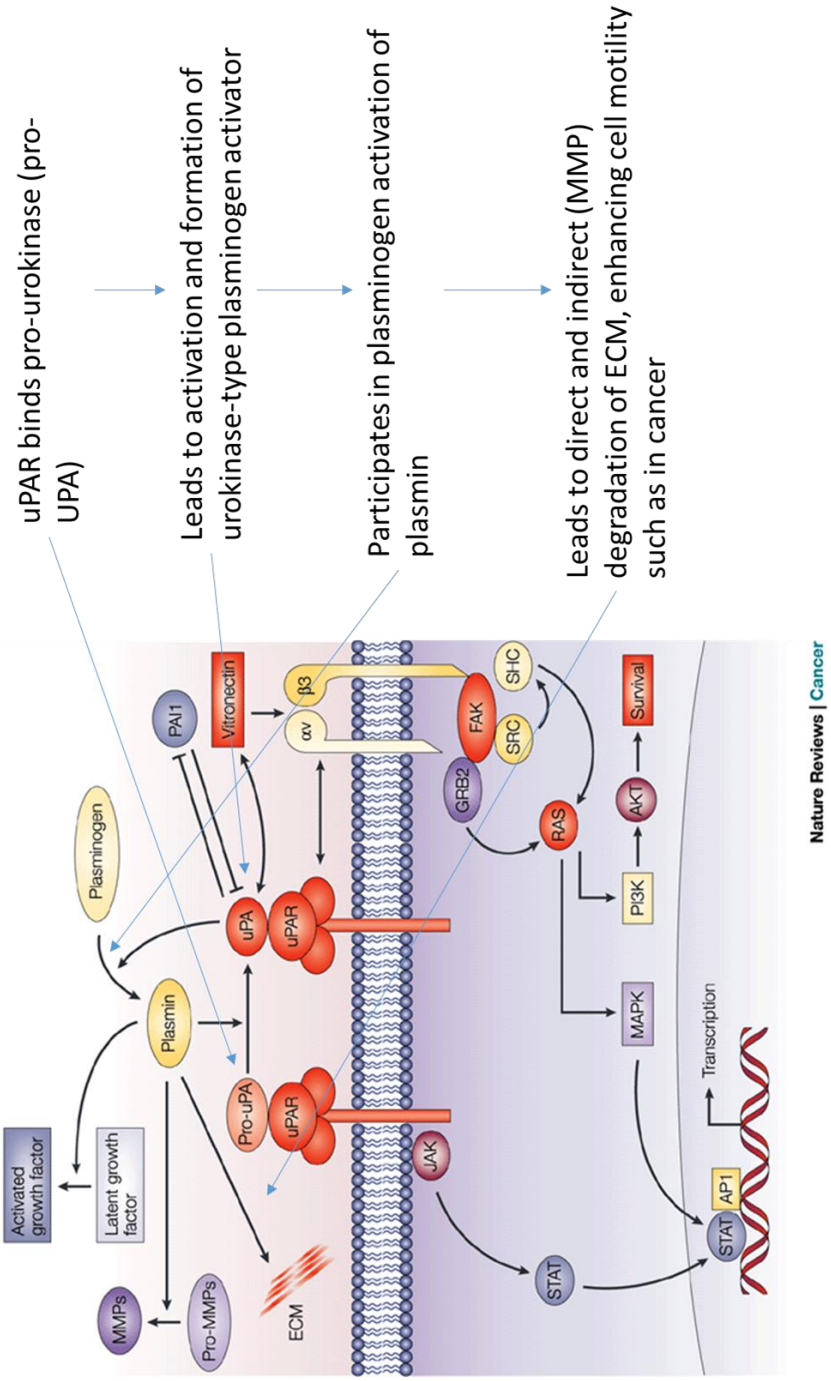

Figure 3. uPAR pathway. Adapted from Jasti S. Rao. "Molecular mechanisms of glioma invasiveness: the role of proteases." Nature Reviews Cancer. 2003. 3(7): 489-501. MMP: Matrix metalloproteinase enzyme. PAI1: Plasminogen activator inhibitor 1. ECM: Extracellular matrix. JAK: Janus kinase 1. STAT: Signal tranducer and activator of transcription protein. AP1: Activator protein-1. MAPK: Mitogen-activated protein kinase. For other abbreviations, please refer to Figure 1 and 2.

h. The role of TGFB

TGFβ is a 112 amino-acid long peptide that is a powerful modulator of cell growth and under typical circumstances acts as a cell growth inhibitor, modulated by the concomitant binding of T1 and T2 receptors, leading to activation of SMAD 2/3, and subsequent activation of SMAD 4 and the MAPK PI3K/AKT pathways as shown in Figure 4(78). Biological output is believed to be dependent on the T1 receptor, with the T2 receptor serving an auxiliary role in this regard(79, 80). Adipose tissue studies have demonstrated TGFβ involvement within the tissue bed. mir21 modulates TGFβ during adipogenic differentiation, and activated TGFβ can inhibit adipogenesis(81-83). On the other hand, TGFβ can switch roles and become a strong cell growth promoter, typically associated with development and progression of cancer(84). Genetic and epigenetic TGFβ events can result in an endothelial to mesenchymal phenotype switch(85, 86).

In obesity, TGFβ is also shown to be altered in other components of the cardiovascular system outside of vessels. TGFβ has been shown to be elevated in the left ventricle as a fibrotic marker in obese animals relative to both control diet animals and animals on an obesity reduction plan involving HFD followed by control diet feeding(87). mRNA expression was also observed to be increased in the airways by diet-induced obesity concomitant with lung inflammation(88). Systemic blockade of TGFβ can improve prognosis in obesity and type 2 diabetes(89).

.

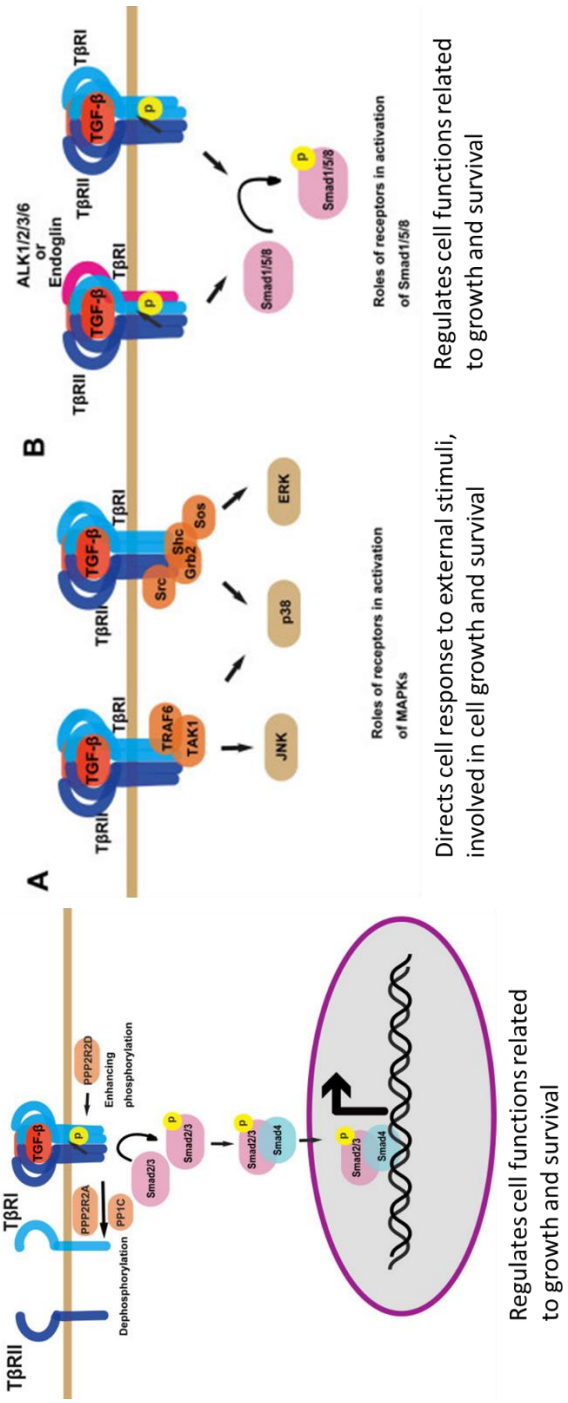

Figure 4. TGFβ pathway. Adapted from Huang et al. "Regulation of TGF-β receptor activity." Cell and Bioscience. 2012. 2:9. JNK: c-Jun N-terminal kinase. TRAF: TNF receptor associated factor. PPP2R: Serine-threonine-protein phosphatase 2A. For other abbreviations, please refer to Figures 1-3.

i. Interactions of the factors IGF2R, IGF2, TGFβ, and uPAR

The four factors described above have been shown to interact under normal physiological conditions. IGF2R is heavily associated with regulation of uPAR. IGF2R silencing is shown to increase both uPAR and plasminogen activation, and IGF2R is known to bind plasminogen and inhibit uPAR activity by way of TACE(90, 91).

In interacting with other factors, it has been shown that IGF2R expression increases uPAR cleavage, although uPAR/IGF2R binding is a low probability event overall(90, 92). IGF2R controls cell invasion by regulating αV integrin expression and increasing uPAR cleavage. uPAR cleavage then results in a loss of urokinase, vitronectin, and integrin sites, hampering vessel formation. uPAR also demonstrates a relationship with TGFβ in that experimental decrease in upAR decreases TGFβ -related proliferation and invasion of cells.

As discussed above, IGF2R, IGF2, uPAR, and TGFβ are altered in obesity and are involved in either promoting or decreasing angiogenesis. The literature indicates that downregulation of IGF2R in cancer can promote tumorigenesis and survival by increasing uPAR and TGF2 presence and activity, while also decreasing TGFB activity(93). Also in cancer, uPAR and IGF2 activity are shown to be increased.

Bringing it all together, we have a proposed mechanism which explains decreased capillarization observed in adipose tissue and skeletal muscle, in obesity, by promotion of vascular senescence, and we have evidence that the

individual components of the mechanism are altered in obesity, although having not been examined in concert in the same study and not examined in adult OLETF rats.

j. Aim of the investigation

As described above, IGF2R and IGF2 have been shown to be altered in obesity, but in pregnancy models and focused on dam, placenta and fetus expression, as opposed to the adult male rats we plan to study(60, 65, 66). TGFβ has also been studied in obesity as well, although not directly in feed arteries for adipose tissue or skeletal muscle beds(94). Additionally, IGF2R and IGF2 have been shown to alter vessel growth in cancer, albeit in opposite fashion from the mechanism we are about to propose, but strengthening our case for investigating their role in obesity. Previous research has not examined these four factors within a single study, and many of these studies have only characterized placental, fetal, and young infant expression and effects of these factors. With evidence indicating that an IGF2R-mediated system controlling uPAR, IGF2, and TGFβ presence and action exists in cancer, the question arises as to whether this system may be present in obesity, but working to downregulate angiogenesis.

It is therefore hypothesized that in obesity concomitant with type 2 diabetes, that IGF2R expression is increased, TGF2 expression is decreased, TGFβ expression is increased, and uPAR expression is decreased. It is also hypothesized that as interventions to treat obesity,

exercise training and calorie restriction will result in a decrease of IGF2R expression, an increase in TGF2 expression, a decrease in TGFβ expression, and an increase in uPAR expression.

This investigation will serve to expand the field by clarifying expression of these factors within a single investigation in adult animals. If the hypothesis is supported, these factors might serve as a target for therapeutics to resolve the pathophysiological capillarity phenotype observed in skeletal muscle and adipose tissue in obesity.

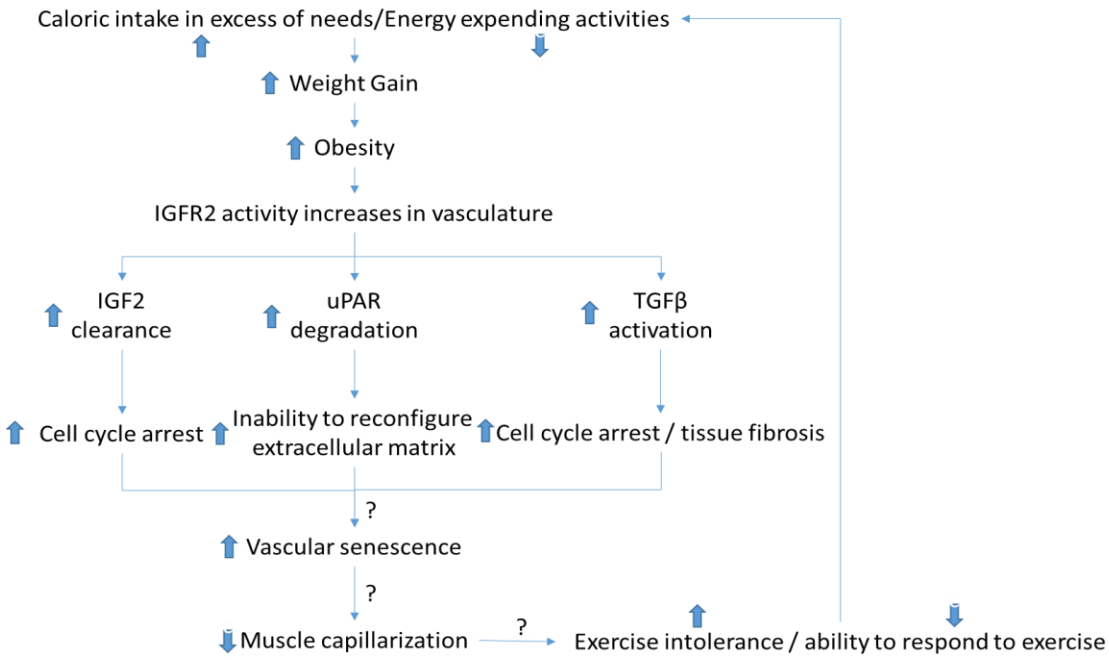

Figure 5. Hypothesized schema by which IGF2R coordinates decrease in muscle capillarization during obesity. For abbreviations, please refer to Figure 1.

k. References

1. Small L, Aplasca A. Child Obesity and Mental Health: A Complex Interaction. Child and adolescent psychiatric clinics of North America. 2016;25(2):269-82. Epub 2016/03/17. doi: 10.1016/j.chc.2015.11.008. PubMed PMID: 26980129.

2. Vallis M. Quality of life and psychological well-being in obesity management: improving the odds of success by managing distress. International journal of clinical practice. 2016;70(3):196-205. Epub 2016/02/05. doi: 10.1111/ijcp.12765. PubMed PMID: 26842304; PubMed Central PMCID: PMCPMC5067635.

3. Crissey JM, Jenkins NT, Lansford KA, Thorne PK, Bayless DS, Vieira-Potter VJ, et al. Adipose tissue and vascular phenotypic modulation by voluntary physical activity and dietary restriction in obese insulin-resistant OLETF rats. American journal of physiology Regulatory, integrative and comparative physiology. 2014;306(8):R596-606. Epub 2014/02/14. doi: 10.1152/ajpregu.00493.2013. PubMed PMID: 24523340; PubMed Central PMCID: PMCPMC4043131.

4. Padilla J, Jenkins NT, Thorne PK, Lansford KA, Fleming NJ, Bayless DS, et al. Differential regulation of adipose tissue and vascular inflammatory gene expression by chronic systemic inhibition of NOS in lean and obese rats. Physiological reports. 2014;2(2):e00225. Epub 2014/04/20. doi: 10.1002/phy2.225. PubMed PMID: 24744894; PubMed Central PMCID: PMCPMC3966247.

5. Vieira-Potter VJ, Lee S, Bayless DS, Scroggins RJ, Welly RJ, Fleming NJ, et al. Disconnect between adipose tissue inflammation and cardiometabolic dysfunction in Ossabaw pigs. Obesity (Silver Spring, Md). 2015;23(12):2421-9. Epub 2015/11/03. doi: 10.1002/oby.21252. PubMed PMID: 26524201; PubMed Central PMCID: PMCPMC4701582.

6. Jenkins NT, Padilla J, Arce-Esquivel AA, Bayless DS, Martin JS, Leidy HJ, et al. Effects of endurance exercise training, metformin, and their combination on adipose tissue leptin and IL-10 secretion in OLETF rats. Journal of applied physiology (Bethesda, Md : 1985). 2012;113(12):1873-83. Epub 2012/09/29. doi: 10.1152/japplphysiol.00936.2012. PubMed PMID: 23019312; PubMed Central PMCID: PMCPMC3544496.

7. Roberts MD, Bayless DS, Company JM, Jenkins NT, Padilla J, Childs TE, et al. Elevated skeletal muscle irisin precursor FNDC5 mRNA in obese OLETF rats. Metabolism: clinical and experimental. 2013;62(8):1052-6. Epub 2013/03/19. doi: 10.1016/j.metabol.2013.02.002. PubMed PMID: 23498898; PubMed Central PMCID: PMCPMC3688677.

8. Nascimento AR, Machado M, de Jesus N, Gomes F, Lessa MA, Bonomo IT, et al. Structural and functional microvascular alterations in a rat model of metabolic syndrome induced by a high-fat diet. Obesity (Silver Spring, Md). 2013;21(10):2046-54. Epub 2013/03/21. doi: 10.1002/oby.20358. PubMed PMID: 23512529.

9. Kuilman T, Peeper DS. Senescence-messaging secretome: SMS-ing cellular stress. Nature reviews Cancer. 2009;9(2):81-94. Epub 2009/01/10. doi: 10.1038/nrc2560. PubMed PMID: 19132009.

10. Arner E, Westermark PO, Spalding KL, Britton T, Ryden M, Frisen J, et al. Adipocyte turnover: relevance to human adipose tissue morphology. Diabetes. 2010;59(1):105-9. Epub 2009/10/23. doi: 10.2337/db09-0942. PubMed PMID: 19846802; PubMed Central PMCID: PMCPMC2797910.

11. Virtue S, Vidal-Puig A. It's Not How Fat You Are, It's What You Do with It That Counts. PLoS Biology. 2008;6(9). doi: 10.1371/journal.pbio.0060237. PubMed PMID: 18816166; PubMed Central PMCID: PMCPMC2553843.

12. Ye J. Adipose tissue vascularization: its role in chronic inflammation. Current diabetes reports. 2011;11(3):203-10. Epub 2011/02/18. doi: 10.1007/s11892-011-0183-1. PubMed PMID: 21327583; PubMed Central PMCID: PMCPMC3119578.

13. Pasarica M, Sereda OR, Redman LM, Albarado DC, Hymel DT, Roan LE, et al. Reduced adipose tissue oxygenation in human obesity: evidence for rarefaction, macrophage chemotaxis, and inflammation without an angiogenic response. Diabetes. 2009;58(3):718-25. Epub 2008/12/17. doi: 10.2337/db08-1098. PubMed PMID: 19074987; PubMed Central PMCID: PMCPMC2646071.

14. Ouchi N, Parker JL, Lugus JJ, Walsh K. Adipokines in inflammation and metabolic disease. Nature reviews Immunology. 2011;11(2):85-97. doi: 10.1038/nri2921. PubMed PMID: 21252989; PubMed Central PMCID: PMCPMC3518031.

15. Preis SR, Massaro JM, Robins SJ, Hoffmann U, Vasan RS, Irlbeck T, et al. Abdominal subcutaneous and visceral adipose tissue and insulin resistance in the Framingham heart study. Obesity (Silver Spring, Md). 2010;18(11):2191-8. Epub 2010/03/27. doi: 10.1038/oby.2010.59. PubMed PMID: 20339361; PubMed Central PMCID: PMCPMC3033570.

16. Solomon TP, Haus JM, Li Y, Kirwan JP. Progressive hyperglycemia across the glucose tolerance continuum in older obese adults is related to skeletal muscle capillarization and nitric oxide bioavailability. The Journal of clinical endocrinology and metabolism. 2011;96(5):1377-84. Epub 2011/02/04. doi: 10.1210/jc.2010-2069. PubMed PMID: 21289242; PubMed Central PMCID: PMCPMC3085198.

17. Gavin TP, Stallings HW, 3rd, Zwetsloot KA, Westerkamp LM, Ryan NA, Moore RA, et al. Lower capillary density but no difference in VEGF expression in obese vs. lean young skeletal muscle in humans. Journal of applied physiology (Bethesda, Md : 1985). 2005;98(1):315-21. Epub 2004/08/10. doi: 10.1152/japplphysiol.00353.2004. PubMed PMID: 15298982.

18. Loebig M, Klement J, Schmoller A, Betz S, Heuck N, Schweiger U, et al. Evidence for a relationship between VEGF and BMI independent of insulin sensitivity by glucose clamp procedure in a homogenous group healthy young men. PloS one. 2010;5(9):e12610. Epub 2010/09/11. doi: 10.1371/journal.pone.0012610. PubMed PMID: 20830305; PubMed Central PMCID: PMCPMC2935379.

19. Maffiuletti NA, Jubeau M, Munzinger U, Bizzini M, Agosti F, De Col A, et al. Differences in quadriceps muscle strength and fatigue between lean and obese subjects. European journal of applied physiology. 2007;101(1):51-9. Epub 2007/05/04. doi: 10.1007/s00421-007-0471-2. PubMed PMID: 17476522.

20. Morley JE, Malmstrom TK, Rodriguez-Manas L, Sinclair AJ. Frailty, sarcopenia and diabetes. Journal of the American Medical Directors Association. 2014;15(12):853-9. Epub 2014/12/03. doi: 10.1016/j.jamda.2014.10.001. PubMed PMID: 25455530.

21. Wu CF, Liu PY, Wu TJ, Hung Y, Yang SP, Lin GM. Therapeutic modification of arterial stiffness: An update and comprehensive review. World journal of cardiology. 2015;7(11):742-53. Epub 2015/12/05. doi: 10.4330/wjc.v7.i11.742. PubMed PMID: 26635922; PubMed Central PMCID: PMCPMC4660469.

22. Kozakova M, Palombo C. Diabetes Mellitus, Arterial Wall, and Cardiovascular Risk Assessment. International journal of environmental research and public health. 2016;13(2):201. Epub 2016/02/11. doi: 10.3390/ijerph13020201. PubMed PMID: 26861377; PubMed Central PMCID: PMCPMC4772221.

23. Brodal P, Ingjer F, Hermansen L. Capillary supply of skeletal muscle fibers in untrained and endurance-trained men. The American journal of physiology. 1977;232(6):H705-12. Epub 1977/06/01. PubMed PMID: 879309.

24. Ingjer F, Brodal P. Capillary supply of skeletal muscle fibers in untrained and endurance-trained women. European journal of applied physiology and occupational physiology. 1978;38(4):291-9. Epub 1978/05/30. PubMed PMID: 668683.

25. Carrow RE, Brown RE, Van Huss WD. Fiber sizes and capillary to fiber ratios in skeletal muscle of exercised rats. The Anatomical record. 1967;159(1):33-9. Epub 1967/09/01. doi: 10.1002/ar.1091590106. PubMed PMID: 6062782.

26. Adolfsson J, Ljungqvist A, Tornling G, Unge G. Capillary increase in the skeletal muscle of trained young and adult rats. The Journal of physiology. 1981;310:529-32. Epub 1981/01/01. PubMed PMID: 7230047; PubMed Central PMCID: PMCPMC1274756.

27. Mai JV, Edgerton VR, Barnard RJ. Capillarity of red, white and intermediate muscle fibers in trained and untrained guinea pigs. Experientia. 1970;26(11):1222-3. Epub 1970/11/15. PubMed PMID: 5485285.

28. Laughlin MH, Korthuis RJ, Sexton WL, Armstrong RB. Regional muscle blood flow capacity and exercise hyperemia in high-intensity trained rats. Journal of applied physiology (Bethesda, Md : 1985). 1988;64(6):2420-7. Epub 1988/06/01. PubMed PMID: 3403424.

29. Laughlin MH, Ripperger J. Vascular transport capacity of hindlimb muscles of exercise-trained rats. Journal of applied physiology (Bethesda, Md : 1985). 1987;62(2):438-43. Epub 1987/02/01. PubMed PMID: 3558204.

30. Laughlin MH, Cook JD, Tremble R, Ingram D, Colleran PN, Turk JR. Exercise training produces nonuniform increases in arteriolar density of rat soleus and gastrocnemius muscle. Microcirculation (New York, NY : 1994). 2006;13(3):175-86. Epub 2006/04/22. doi: 10.1080/10739680600556829. PubMed PMID: 16627360; PubMed Central PMCID: PMCPMC2646594.

31. Andersen LJ, Hansen PR, Sogaard P, Madsen JK, Bech J, Krustrup P. Improvement of systolic and diastolic heart function after physical training in sedentary women. Scandinavian journal of medicine & science in sports. 2010;20 Suppl 1:50-7. Epub 2010/02/09. doi: 10.1111/j.1600-0838.2009.01088.x. PubMed PMID: 20136765.

32. Vaitkevicius PV, Fleg JL, Engel JH, O'Connor FC, Wright JG, Lakatta LE, et al. Effects of age and aerobic capacity on arterial stiffness in healthy adults. Circulation. 1993;88(4 Pt 1):1456-62. Epub 1993/10/01. PubMed PMID: 8403292.

33. Marson EC, Delevatti RS, Prado AK, Netto N, Kruel LF. Effects of aerobic, resistance, and combined exercise training on insulin resistance markers in overweight or obese children and adolescents: A systematic review and meta-analysis. Preventive medicine. 2016;93:211-8. Epub 2016/11/05. doi: 10.1016/j.ypmed.2016.10.020. PubMed PMID: 27773709.

34. Locher JL, Goldsby TU, Goss AM, Kilgore ML, Gower B, Ard JD. Calorie restriction in overweight older adults: Do benefits exceed potential risks? Experimental gerontology. 2016. Epub 2016/03/21. doi: 10.1016/j.exger.2016.03.009. PubMed PMID: 26994938; PubMed Central PMCID: PMCPMC5026870.

35. Azim S, Kashyap SR. Bariatric Surgery: Pathophysiology and Outcomes. Endocrinology and metabolism clinics of North America. 2016;45(4):905-21. Epub 2016/11/09. doi: 10.1016/j.ecl.2016.06.011. PubMed PMID: 27823611.

36. Nostedt JJ, Switzer NJ, Gill RS, Dang J, Birch DW, de Gara C, et al. The Effect of Bariatric Surgery on the Spectrum of Fatty Liver Disease. Canadian journal of gastroenterology & hepatology. 2016;2016:2059245. Epub 2016/10/26. doi: 10.1155/2016/2059245. PubMed PMID: 27777925; PubMed Central PMCID: PMCPMC5061986.

37. McMorrow AM, Connaughton RM, Lithander FE, Roche HM. Adipose tissue dysregulation and metabolic consequences in childhood and adolescent obesity: potential impact of dietary fat quality. The Proceedings of the Nutrition Society. 2015;74(1):67-82. Epub 2014/12/17. doi: 10.1017/s002966511400158x. PubMed PMID: 25497038.

38. Riserus U, Willett WC, Hu FB. Dietary fats and prevention of type 2 diabetes. Progress in lipid research. 2009;48(1):44-51. Epub 2008/11/27. doi: 10.1016/j.plipres.2008.10.002. PubMed PMID: 19032965; PubMed Central PMCID: PMCPMC2654180.

39. Malik VS, Popkin BM, Bray GA, Despres JP, Hu FB. Sugar-sweetened beverages, obesity, type 2 diabetes mellitus, and cardiovascular disease risk. Circulation. 2010;121(11):1356-64. Epub 2010/03/24. doi: 10.1161/circulationaha.109.876185. PubMed PMID: 20308626; PubMed Central PMCID: PMCPMC2862465.

40. Kahn SE, Cooper ME, Del Prato S. PATHOPHYSIOLOGY AND TREATMENT OF TYPE 2 DIABETES: PERSPECTIVES ON THE PAST, PRESENT AND FUTURE. Lancet. 2014;383(9922):1068-83. doi: 10.1016/s0140-6736(13)62154-6. PubMed PMID: 24315620; PubMed Central PMCID: PMCPMC4226760.

41. Ripsin CM, Kang H, Urban RJ. Management of blood glucose in type 2 diabetes mellitus. American family physician. 2009;79(1):29-36. Epub 2009/01/17. PubMed PMID: 19145963.

42. Pasquier F. Diabetes and cognitive impairment: how to evaluate the cognitive status? Diabetes & metabolism. 2010;36 Suppl 3:S100-5. Epub 2011/01/08. doi: 10.1016/s1262-3636(10)70475-4. PubMed PMID: 21211730.

43. Kirwan JP, del Aguila LF, Hernandez JM, Williamson DL, O'Gorman DJ, Lewis R, et al. Regular exercise enhances insulin activation of IRS-1-associated PI3-kinase in human skeletal muscle. Journal of applied physiology (Bethesda, Md : 1985). 2000;88(2):797-803. Epub 2000/02/05. PubMed PMID: 10658053.

44. Dela F, Mikines KJ, von Linstow M, Secher NH, Galbo H. Effect of training on insulin-mediated glucose uptake in human muscle. The American journal of physiology. 1992;263(6 Pt 1):E1134-43. Epub 1992/12/01. PubMed PMID: 1476187.

45. O'Gorman DJ, Krook A. Exercise and the treatment of diabetes and obesity. The Medical clinics of North America. 2011;95(5):953-69. Epub 2011/08/23. doi: 10.1016/j.mcna.2011.06.007. PubMed PMID: 21855702.

46. Orozco LJ, Buchleitner AM, Gimenez-Perez G, Roque IFM, Richter B, Mauricio D. Exercise or exercise and diet for preventing type 2 diabetes mellitus. The Cochrane database of systematic reviews. 2008(3):Cd003054. Epub 2008/07/23. doi: 10.1002/14651858.CD003054.pub3. PubMed PMID: 18646086.

47. Bunker AK, Arce-Esquivel AA, Rector RS, Booth FW, Ibdah JA, Laughlin MH. Physical activity maintains aortic endothelium-dependent relaxation in the obese type 2 diabetic OLETF rat. American journal of physiology Heart and circulatory physiology. 2010;298(6):H1889-901. Epub 2010/03/23. doi: 10.1152/ajpheart.01252.2009. PubMed PMID: 20304812; PubMed Central PMCID: PMCPMC2886626.

48. Saenz A, Fernandez-Esteban I, Mataix A, Ausejo M, Roque M, Moher D. Metformin monotherapy for type 2 diabetes mellitus. The Cochrane database of systematic reviews. 2005(3):Cd002966. Epub 2005/07/22. doi: 10.1002/14651858.CD002966.pub3. PubMed PMID: 16034881.

49. Maruthur NM, Tseng E, Hutfless S, Wilson LM, Suarez-Cuervo C, Berger Z, et al. Diabetes Medications as Monotherapy or Metformin-Based Combination Therapy for Type 2 Diabetes: A Systematic Review and Meta-analysis. Annals of internal medicine. 2016;164(11):740-51. Epub 2016/04/19. doi: 10.7326/m15-2650. PubMed PMID: 27088241.

50. Ganguly S, Tan HC, Lee PC, Tham KW. Metabolic bariatric surgery and type 2 diabetes mellitus: an endocrinologist's perspective. Journal of biomedical research. 2015;29(2):105-11. Epub 2015/04/11. doi: 10.7555/jbr.29.20140127. PubMed PMID: 25859264; PubMed Central PMCID: PMCPMC4389109.

51. Moran TH, Bi S. Hyperphagia and obesity in OLETF rats lacking CCK-1 receptors. Philosophical Transactions of the Royal Society B: Biological Sciences. 2006;361(1471):1211-8. doi: 10.1098/rstb.2006.1857. PubMed PMID: 16815799; PubMed Central PMCID: PMCPMC1642702.

52. Hallmann R, Horn N, Selg M, Wendler O, Pausch F, Sorokin LM. Expression and function of laminins in the embryonic and mature vasculature. Physiological reviews. 2005;85(3):979-1000. Epub 2005/07/01. doi: 10.1152/physrev.00014.2004. PubMed PMID: 15987800.

53. Chang SH, Kanasaki K, Gocheva V, Blum G, Harper J, Moses MA, et al. VEGF-A induces angiogenesis by perturbing the cathepsin-cysteine protease inhibitor balance in venules, causing basement membrane degradation and mother vessel formation. Cancer research. 2009;69(10):4537-44. Epub 2009/05/14. doi: 10.1158/0008-5472.can-08-4539. PubMed PMID: 19435903; PubMed Central PMCID: PMCPMC2683911.

54. Nicosia RF, Madri JA. The microvascular extracellular matrix. Developmental changes during angiogenesis in the aortic ring-plasma clot model. The American journal of pathology. 1987;128(1):78-90. Epub 1987/07/01. PubMed PMID: 2440308; PubMed Central PMCID: PMCPMC1899791.

55. Senger DR. Molecular framework for angiogenesis: a complex web of interactions between extravasated plasma proteins and endothelial cell proteins induced by angiogenic cytokines. The American journal of pathology. 1996;149(1):1-7. Epub 1996/07/01. PubMed PMID: 8686733; PubMed Central PMCID: PMCPMC1865245.

56. Grant DS, Kleinman HK. Regulation of capillary formation by laminin and other components of the extracellular matrix. Exs. 1997;79:317-33. Epub 1997/01/01. PubMed PMID: 9002225.

57. Stratman AN, Malotte KM, Mahan RD, Davis MJ, Davis GE. Pericyte recruitment during vasculogenic tube assembly stimulates endothelial basement membrane matrix formation. Blood. 2009;114(24):5091-101. Epub 2009/10/14. doi: 10.1182/blood-2009-05-222364. PubMed PMID: 19822899; PubMed Central PMCID: PMCPMC2788982.

58. Chang MH, Kuo WW, Chen RJ, Lu MC, Tsai FJ, Kuo WH, et al. IGF-II/mannose 6-phosphate receptor activation induces metalloproteinase-9 matrix activity and increases plasminogen activator expression in H9c2 cardiomyoblast cells. Journal of molecular endocrinology. 2008;41(2):65-74. Epub 2008/05/23. doi: 10.1677/jme-08-0051. PubMed PMID: 18495691.

59. Han Y, Luan B, Sun M, Guo L, Guo P, Tao J, et al. Glycosylation-independent binding to extracellular domains 11-13 of mannose-6-phosphate/insulin-like growth factor-2 receptor mediates the effects of soluble CREG on the phenotypic modulation of vascular smooth muscle cells. Journal of molecular and cellular cardiology. 2011;50(4):723-30. Epub 2011/01/05. doi: 10.1016/j.yjmcc.2010.12.013. PubMed PMID: 21195083.

60. Jungheim ES, Schoeller EL, Marquard KL, Louden ED, Schaffer JE, Moley KH. Diet-induced obesity model: abnormal oocytes and persistent growth abnormalities in the offspring. Endocrinology. 2010;151(8):4039-46. Epub 2010/06/25. doi: 10.1210/en.2010-0098. PubMed PMID: 20573727; PubMed Central PMCID: PMCPMC2940512.

61. Probst OC, Puxbaum V, Svoboda B, Leksa V, Stockinger H, Mikula M, et al. The mannose 6-phosphate/insulin-like growth factor II receptor restricts the tumourigenicity and invasiveness of squamous cell carcinoma cells. International journal of cancer. 2009;124(11):2559-67. Epub 2009/02/06. doi: 10.1002/ijc.24236. PubMed PMID: 19195023.

62. Hoyo C, Schildkraut JM, Murphy SK, Chow WH, Vaughan TL, Risch H, et al. IGF2R polymorphisms and risk of esophageal and gastric adenocarcinomas. International journal of cancer. 2009;125(11):2673-8. Epub 2009/07/25. doi: 10.1002/ijc.24623. PubMed PMID: 19626700; PubMed Central PMCID: PMCPMC3008656.

63. Zhang K, Zhou M, Chen H, Wu G, Chen K, Yang H. Expression of IMP3 and IGF2 in giant cell tumor of spine is associated with tumor recurrence and angiogenesis. Clinical & translational oncology : official publication of the Federation of Spanish Oncology Societies and of the National Cancer Institute of Mexico. 2015;17(7):570-5. Epub 2015/03/06. doi: 10.1007/s12094-015-1280-4. PubMed PMID: 25740666.

64. Queiroz EM, Candido AP, Castro IM, Bastos AQ, Machado-Coelho GL, Freitas RN. IGF2, LEPR, POMC, PPARG, and PPARGC1 gene variants are associated with obesity-related risk phenotypes in Brazilian children and adolescents. Brazilian journal of medical and biological research = Revista brasileira de pesquisas medicas e biologicas. 2015;48(7):595-602. Epub 2015/04/30. doi: 10.1590/1414-431x20154155. PubMed PMID: 25923461; PubMed Central PMCID: PMCPMC4512097.

65. Belobrajdic DP, Frystyk J, Jeyaratnaganthan N, Espelund U, Flyvbjerg A, Clifton PM, et al. Moderate energy restriction-induced weight loss affects circulating IGF levels independent of dietary composition. European journal of endocrinology. 2010;162(6):1075-82. Epub 2010/03/10. doi: 10.1530/eje-10-0062. PubMed PMID: 20212016.

66. Vomhof-DeKrey E, Darland D, Ghribi O, Bundy A, Roemmich J, Claycombe K. Maternal low protein diet leads to placental angiogenic compensation via dysregulated M1/M2 macrophages and TNFalpha expression in Sprague-Dawley rats. Journal of reproductive immunology. 2016;118:9-17. Epub 2016/09/07. doi: 10.1016/j.jri.2016.08.009. PubMed PMID: 27596280.

67. Kadakia R, Josefson J. The Relationship of Insulin-Like Growth Factor 2 to Fetal Growth and Adiposity. Hormone research in paediatrics. 2016;85(2):75-82. Epub 2016/01/27. doi: 10.1159/000443500. PubMed PMID: 26812688.

68. Deodati A, Inzaghi E, Liguori A, Puglianiello A, Germani D, Brufani C, et al. IGF2 methylation is associated with lipid profile in obese children. Hormone research in paediatrics. 2013;79(6):361-7. Epub 2013/06/19. doi: 10.1159/000351707. PubMed PMID: 23774180.

69. Alfano D, Franco P, Vocca I, Gambi N, Pisa V, Mancini A, et al. The urokinase plasminogen activator and its receptor: role in cell growth and apoptosis. Thrombosis and haemostasis. 2005;93(2):205-11. Epub 2005/02/16. doi: 10.1160/th04-09-0592. PubMed PMID: 15711734.

70. Ploug M. Structure-function relationships in the interaction between the urokinase-type plasminogen activator and its receptor. Current pharmaceutical design. 2003;9(19):1499-528. Epub 2003/07/23. PubMed PMID: 12871065.

71. Fleetwood AJ, Achuthan A, Schultz H, Nansen A, Almholt K, Usher P, et al. Urokinase plasminogen activator is a central regulator of macrophage three-dimensional invasion, matrix degradation, and adhesion. Journal of immunology (Baltimore, Md : 1950). 2014;192(8):3540-7. Epub 2014/03/13. doi: 10.4049/jimmunol.1302864. PubMed PMID: 24616477.

72. Bifulco K, Longanesi-Cattani I, Gala M, G DIC, Masucci MT, Pavone V, et al. The soluble form of urokinase receptor promotes angiogenesis through its Ser(8)(8)-Arg-Ser-Arg-Tyr(9)(2) chemotactic sequence. Journal of thrombosis and haemostasis : JTH. 2010;8(12):2789-99. Epub 2010/10/01. doi: 10.1111/j.1538-7836.2010.04075.x. PubMed PMID: 20880257.

73. Breuss JM, Uhrin P. VEGF-initiated angiogenesis and the uPA/uPAR system. Cell adhesion & migration. 2012;6(6):535-615. Epub 2012/10/19. doi: 10.4161/cam.22243. PubMed PMID: 23076133; PubMed Central PMCID: PMCPMC3547900.

74. Margheri F, Luciani C, Taddei ML, Giannoni E, Laurenzana A, Biagioni A, et al. The receptor for urokinase-plasminogen activator (uPAR) controls plasticity of cancer cell movement in mesenchymal and amoeboid migration style. Oncotarget. 2014;5(6):1538-53. Epub 2014/04/01. doi: 10.18632/oncotarget.1754. PubMed PMID: 24681666; PubMed Central PMCID: PMCPMC4039230.

75. Kanno Y, Matsuno H, Kawashita E, Okada K, Suga H, Ueshima S, et al. Urokinase-type plasminogen activator receptor is associated with the development of adipose tissue. Thrombosis and haemostasis. 2010;104(6):1124-32. Epub 2010/10/05. doi: 10.1160/th10-02-0101. PubMed PMID: 20886176.

76. Nowicki TS, Zhao H, Darzynkiewicz Z, Moscatello A, Shin E, Schantz S, et al. Downregulation of uPAR inhibits migration, invasion, proliferation, FAK/PI3K/Akt signaling and induces senescence in papillary thyroid carcinoma cells. Cell cycle (Georgetown, Tex). 2011;10(1):100-7. Epub 2010/12/31. doi: 10.4161/cc.10.1.14362. PubMed PMID: 21191179; PubMed Central PMCID: PMCPMC3048079.

77. Sato S, Kopitz C, Schmalix WA, Muehlenweg B, Kessler H, Schmitt M, et al. High-affinity urokinase-derived cyclic peptides inhibiting urokinase/urokinase receptor-interaction: effects on tumor growth and spread. FEBS letters. 2002;528(1-3):212-6. Epub 2002/09/26. PubMed PMID: 12297307.

78. Shi Y, Massague J. Mechanisms of TGF-beta signaling from cell membrane to the nucleus. Cell. 2003;113(6):685-700. Epub 2003/06/18. PubMed PMID: 12809600.

79. Attisano L, Wrana JL. Signal transduction by the TGF-beta superfamily. Science (New York, NY). 2002;296(5573):1646-7. Epub 2002/06/01. doi: 10.1126/science.1071809. PubMed PMID: 12040180.

80. Derynck R, Jarrett JA, Chen EY, Eaton DH, Bell JR, Assoian RK, et al. Human transforming growth factor-beta complementary DNA sequence and expression in normal and transformed cells. Nature. 1985;316(6030):701-5. Epub 1985/08/22. PubMed PMID: 3861940.

81. Du B, Cawthorn WP, Su A, Doucette CR, Yao Y, Hemati N, et al. The transcription factor paired-related homeobox 1 (Prrx1) inhibits adipogenesis by activating transforming growth factor-beta (TGFbeta) signaling. The Journal of biological chemistry. 2013;288(5):3036-47. Epub 2012/12/20. doi: 10.1074/jbc.M112.440370. PubMed PMID: 23250756; PubMed Central PMCID: PMCPMC3561528.

82. Kim YJ, Hwang SJ, Bae YC, Jung JS. MiR-21 regulates adipogenic differentiation through the modulation of TGF-beta signaling in mesenchymal stem cells derived from human adipose tissue. Stem cells (Dayton, Ohio). 2009;27(12):3093-102. Epub 2009/10/10. doi: 10.1002/stem.235. PubMed PMID: 19816956.

83. Tsurutani Y, Fujimoto M, Takemoto M, Irisuna H, Koshizaka M, Onishi S, et al. The roles of transforming growth factor-beta and Smad3 signaling in adipocyte differentiation and obesity. Biochemical and biophysical research communications. 2011;407(1):68-73. Epub 2011/03/02. doi: 10.1016/j.bbrc.2011.02.106. PubMed PMID: 21356196.

84. Perrot CY, Javelaud D, Mauviel A. Insights into the Transforming Growth Factor-beta Signaling Pathway in Cutaneous Melanoma. Annals of dermatology. 2013;25(2):135-44. Epub 2013/05/30. doi: 10.5021/ad.2013.25.2.135. PubMed PMID: 23717002; PubMed Central PMCID: PMCPMC3662904.

85. Miyazono K. Transforming growth factor-beta signaling in epithelial-mesenchymal transition and progression of cancer. Proceedings of the Japan Academy Series B, Physical and biological sciences. 2009;85(8):314-23. Epub 2009/10/20. PubMed PMID: 19838011; PubMed Central PMCID: PMCPMC3621568.

86. Wendt MK, Tian M, Schiemann WP. Deconstructing the mechanisms and consequences of TGF-beta-induced EMT during cancer progression. Cell and tissue research. 2012;347(1):85-101. Epub 2011/06/22. doi: 10.1007/s00441-011-1199-1. PubMed PMID: 21691718; PubMed Central PMCID: PMCPMC3723118.

87. Wang HT, Liu CF, Tsai TH, Chen YL, Chang HW, Tsai CY, et al. Effect of obesity reduction on preservation of heart function and attenuation of left ventricular remodeling, oxidative stress and inflammation in obese mice. Journal of translational medicine. 2012;10:145. Epub 2012/07/13. doi: 10.1186/1479-5876-10-145. PubMed PMID: 22784636; PubMed Central PMCID: PMCPMC3551744.

88. Jung SH, Kwon JM, Shim JW, Kim DS, Jung HL, Park MS, et al. Effects of diet-induced mild obesity on airway hyperreactivity and lung inflammation in mice. Yonsei medical journal. 2013;54(6):1430-7. Epub 2013/10/22. doi: 10.3349/ymj.2013.54.6.1430. PubMed PMID: 24142648; PubMed Central PMCID: PMCPMC3809850.

89. Yadav H, Quijano C, Kamaraju AK, Gavrilova O, Malek R, Chen W, et al. Protection from obesity and diabetes by blockade of TGF-beta/Smad3 signaling. Cell metabolism. 2011;14(1):67-79. Epub 2011/07/05. doi: 10.1016/j.cmet.2011.04.013. PubMed PMID: 21723505; PubMed Central PMCID: PMCPMC3169298.

90. Schiller HB, Szekeres A, Binder BR, Stockinger H, Leksa V. Mannose 6-phosphate/insulin-like growth factor 2 receptor limits cell invasion by controlling alphaVbeta3 integrin expression and proteolytic processing of urokinase-type plasminogen activator receptor. Molecular biology of the cell. 2009;20(3):745-56. Epub 2008/11/28. doi: 10.1091/mbc.E08-06-0569. PubMed PMID: 19037107; PubMed Central PMCID: PMCPMC2633380.

91. Leksa V, Loewe R, Binder B, Schiller HB, Eckerstorfer P, Forster F, et al. Soluble M6P/IGF2R released by TACE controls angiogenesis via blocking plasminogen activation. Circulation research. 2011;108(6):676-85. Epub 2011/01/29. doi: 10.1161/circresaha.110.234732. PubMed PMID: 21273553.

92. Kreiling JL, Byrd JC, Deisz RJ, Mizukami IF, Todd RF, 3rd, MacDonald RG. Binding of urokinase-type plasminogen activator receptor (uPAR) to the mannose 6-phosphate/insulin-like growth factor II receptor: contrasting interactions of full-length and soluble forms of uPAR. The Journal of biological chemistry. 2003;278(23):20628-37. Epub 2003/04/01. doi: 10.1074/jbc.M302249200. PubMed PMID: 12665524.

93. Khandekar MJ, Cohen P, Spiegelman BM. Molecular mechanisms of cancer development in obesity. Nature reviews Cancer. 2011;11(12):886-95. Epub 2011/11/25. doi: 10.1038/nrc3174. PubMed PMID: 22113164.

94. Wang X, Abraham S, McKenzie JA, Jeffs N, Swire M, Tripathi VB, et al. LRG1 promotes angiogenesis by modulating endothelial TGF-beta signalling. Nature. 2013;499(7458):306-11. Epub 2013/07/23. doi: 10.1038/nature12345. PubMed PMID: 23868260; PubMed Central PMCID: PMCPMC3836402.

2. IGF2R, IGF2, TGFB, AND UPAR IN A RAT MODEL OF OBESITY

a. Methods

Animal Cohorts

All animal protocols were approved by the University of Missouri Institutional Animal Care and Use Committee.

Cohort 1: Male age 4 weeks LETO (n = 20) and OLETF (n = 20) rats were procured from Tokushima Research Institute, Otsuka Pharmaceutical, Japan. Rats were individually housed on a 12 hour light, 12 hour cycle and provided water and standard chow (70% kcal carbohydrate, 20% kcal protein, 10% kcal fat, 3.5% sucrose) (D09071604, Research Diets Inc., New Brunswick, N.J., USA) *ab libitum* until age 8 weeks. At age 8 weeks, LETO and OLETF were subdivided into two groups and each group was assigned to either maintenance of control diet or to a high fat, high sucrose diet (45% kcal fat, 35% kcal carbohydrate, 17% sucrose, 1% cholesterol)(D12110704, Research Diets Inc.) from age 8 to 32 weeks (L-CON, L-HFD, O-CON, O-HFD, n = 10 for all four). Rats were anesthetized and sacrificed at age 32 weeks.

Cohort 2: Male age 4 weeks OLETF (n = 30) rats were procured from Tokushima Research Institute, Otsuka Pharmaceutical, Japan. Rats were individually housed on a 12 hour light, 12 hour cycle and provided water and standard chow (10% kcal fat, 3.5% sucrose) *ab libitum* until age 8 weeks. At age

8 weeks, rats were placed on high fat, high sucrose diet from age 8 to 32 weeks. At age 20 weeks, rats were either sacrificed (n = 4) or assigned to a sedentary group (O-SED, n - 6), an exercise training group (O-EX, n = 10, treadmill running 20 m / min, 15% incline, 60 min /day, 5 day / week), or a calorie restriction group (O-CR, n = 9, 25% kcal reduction in intake relative to O-SED)(1). All remaining rats were sacrificed at age 32 weeks.

Tissue Sampling and Composition Analysis.

Prior to sacrifice, body composition was analyzed using a Hologic QDR-1000/w dual-energy X-ray absorptiometry machine calibrated for rats, and rats were weighed to the nearest 0.01g.

Feed arteries for the biceps brachii, vastus lateralis, and gastrocnemius muscles were removed and stored at -80C. Biceps brachii and vastus lateralis muscles were removed, flash frozen in liquid nitrogen, wrapped in foil, and stored at -80C. Feed artery for retroperitoneal and epididymal fad pats were removed and stored at -80C. Retroperitoneal and epididymal fat samples were removed, flash frozen in liquid nitrogen, and stored at -80C.

Protein Quantification

Nano-Orange protein solution was prepared from Nano-Orange Protein Kit (N-6666, Thermo-Fisher, Waltham, MA). 3 uL was used for each sample and samples were run in duplicate (6 uL total used). Samples were briefly vortexed and spun down, then boiled for five minutes, then sonicated for ten seconds,

repeated three times. Preparations were placed in a Fisher 96-well plate and read with a Tecan Safire plate reader.

Western Blot

Samples were loaded at 10ug protein/lane. Tris-acetate 3-8% gels were used (EA03752BOX, Invitrogen, Waltham, MA) and HiMark Prestained Protein Standard was used (LC5699, ThermoFisher, Waltham, MA.) Gels were run at 150V for 1 hr 15 min. Membranes were prepared by washing for five minutes with methanol, rinsed twice with ddH_2O, shook in ddH_2O for fifteen minutes, then incubated in transfer buffer. Blot was loaded according to Invitrogen directions and run at 34V for one hour. PVDF membrane was incubated in 5% milk (TBST) for one hour at room temperature (RT). 10 mL primary antibody solution was added and membrane was placed on a shaker overnight at RT. Antibodies are listed in Table 1.

Next-day processing of membranes entailed removal of primary antibody, quick rinse with TSBT, four 10 minute rinses of membrane with TSBT, incubation with secondary antibody for one hour at RT on shaker, followed by four more 10 minute TSBT rinses.

Imaging proceeded with pouring off TSBT and incubating for one minute with HRP substrate (WBLUF0500, Millapore, Billerica, MA). Membranes were exposed between one and three minutes on a Kodak Image Station 4000R with Kodak MI Network as the image capture program.

Membranes were stripped with a blot restore kit (2520, Millipore, Bellerica, MA), incubated in 5% milk (TBST) for one hour at RT, then incubated overnight at RT with 10 mL primary antibody. Next-day procedure proceeded as above.

Immunohistochemistry

Slides were prepared by the Veterinary Medical Diagnostic Lab at the Veterninary Medical Building of the University of Missouri. Hydrophobic barriers were drawn with a barrier pen around samples on slides. Slides were washed twice with TBS in five minute intervals, then incubated for two hours in 10% goat serum. Antibody was applied and slides were stored at 4C in a fridge overnight.

The following day, slides were washed with TBS twice in five minute intervals, then secondary antibody was applied for one hour. Slides were then incubated for seven minutes with chromagen (RAEC810L, Biocare Medical, Concord, CA), then quickly rinsed with hematoxylin. Slides were then incubated in ddH_2O, 70% ethanol, 90% ethanol, and two each of 100% ethanol and xylene baths at three minutes apiece, followed by application of xylene mounting medium (245-691, Fisher Scientific, Waltham, MA) and slide cover. Slides were left to dry for at least one hour.

Imaging of Slides

Slides were examined with an Olympus BX60 photomicroscope (Olympus, Melville, NY) and photographed at x20 magnification using a Spot Insight digital camera (Diagnostic Instruments, Sterling Heights, MI).

Image Analysis of TGFβ and uPAR

TGFβ and uPAR were quantified by using threshold tools in Photoshop and adjusting sensitivity settings on a per-image basis to incorporate all stained sections.

Antibody target	Manufacturer	Antibody code
IGF2R	Abcam	Ab124767
IGF2	Sigma-Aldrich	HPA002037
TGFβ	Abcam	Ab66043
uPAR	Santa Cruz Biotechnology	SC-10815
Goat anti-rabbit (secondary)	Abcam	Ab6721
Alkaline phosphatase	Abcam	Ab95462

Table 1: List of antibodies used. Please refer to figure 1 for abbreviations.

1. Linden MA, Sheldon RD, Meers GM, Ortinau LC, Morris EM, Booth FW, et al. Aerobic exercise training in the treatment of non-alcoholic fatty liver disease related fibrosis. The Journal of physiology. 2016;594(18):5271-84. Epub 2016/04/23. doi: 10.1113/jp272235. PubMed PMID: 27104887; PubMed Central PMCID: PMCPMC5023692.

b. Results

Whole-body and tissue-level parameters

We found that when comparing non-obese (L-CON only) rats to obese (O-CON, O-HFD, O-SED, O-EX, and O-CR), non-obese rats had significantly lower final body weight and body fat percentage at age 32 weeks (Fig. 6)($p < 0.05$ for both). Examining our two cohorts individually, Cohort 1 (L-CON, L-HFD, O-CON, O-HFD) demonstrated general increases in both body weight and body fat percentage with induction of obesity by way of either LETO to OLETF, or CON to HFD, or by double induction of obesity as with L-CON versus O-HFD (Fig. 7) ($p < 0.05$ or $p < 0.01$). There are four exceptions to this trend in that L-CON versus L-HFD displays no significant difference in either final body weight or body fat percentage, that L-HFD versus O-CON does not display a significant difference in terms of final body weight, and that O-CON versus O-HFD does not display a significant difference in terms of final body fat percentage. In Cohort 2, we found no significant difference between O-SED, O-EX, and O-CR in terms of final body weight or final body composition (Fig. 8).

Examining capillarity in biceps brachii and vastus lateralis muscle (Fig. 9), we find that non-obese animals have a significantly high capillarity in both biceps brachii and vastus lateralis than their non-obese counterparts(Fig. 10)($p< 0.05$ for both muscles). In Cohort 1, we found only one instance of a significant change in capillarity with L-HFD having a higher capillarity than O-CON (Fig. 11) ($p < 0.05$).

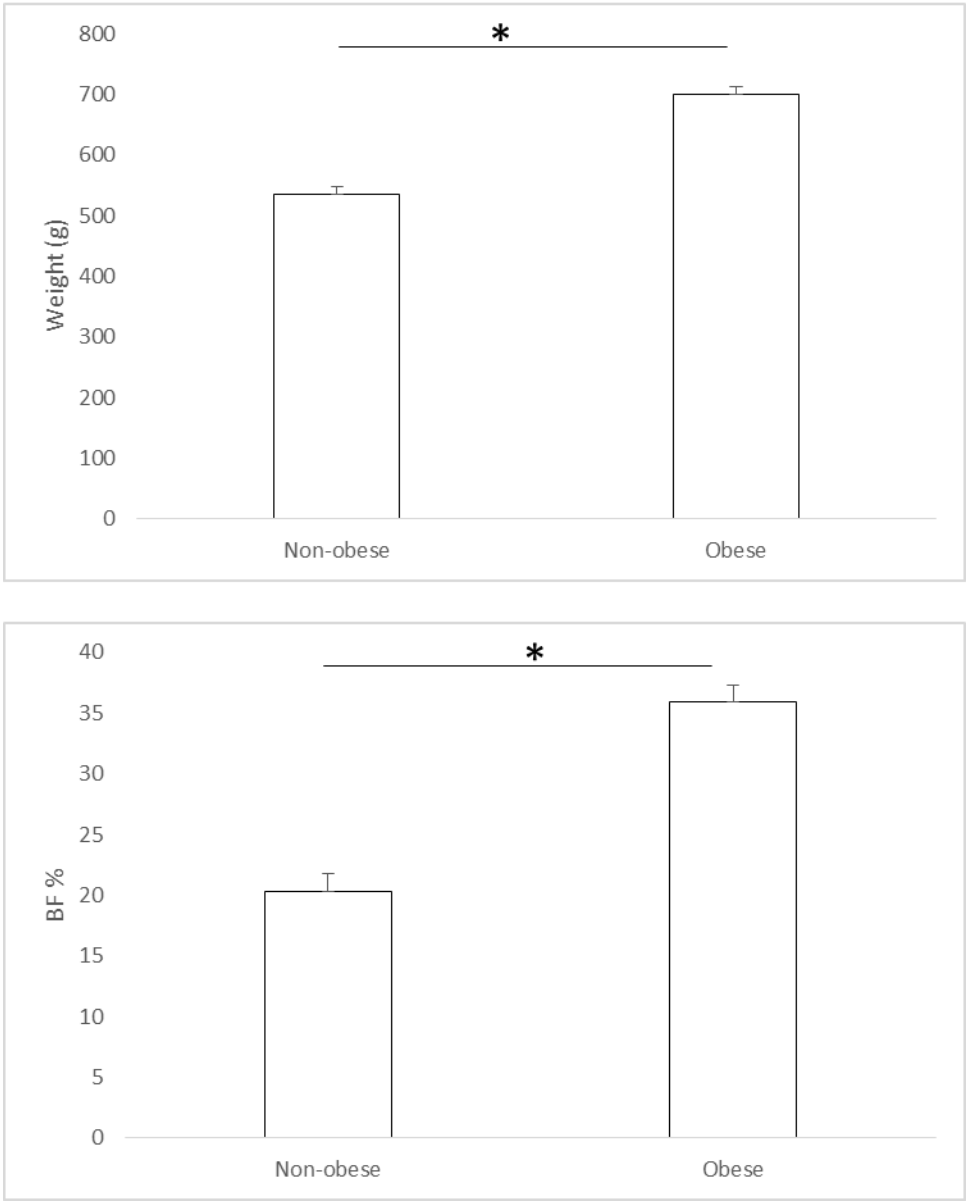

Figure 6: Average final weight and body fat percentage in non-obese and obese animals. (*: $p < 0.05$)

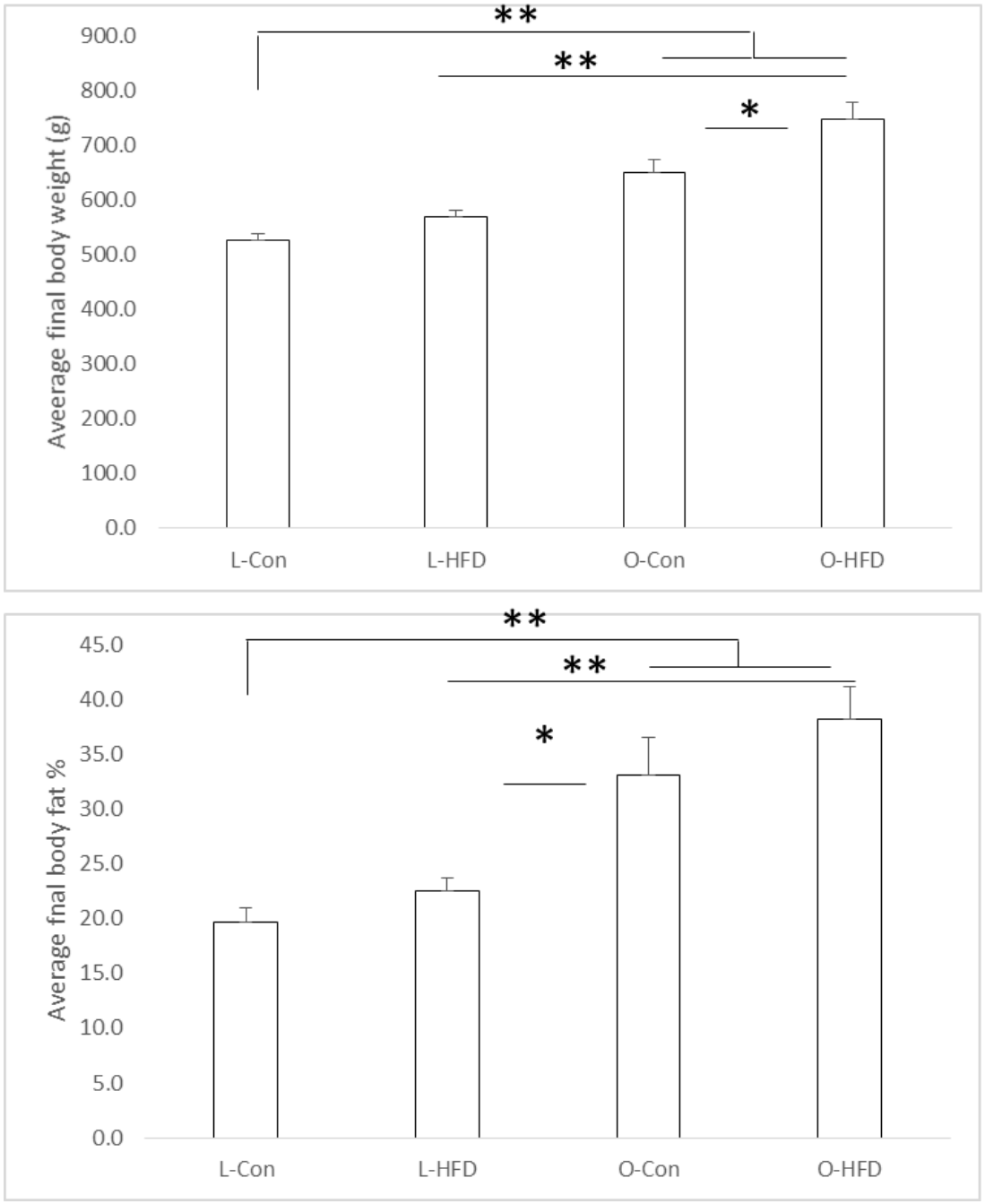

Figure 7: Average final body weight and body fat percentage in Cohort 1, representing diet and strain induction of obesity. (*: $p < 0.05$, **: $p < 0.01$) L-CON: LETO control diet. L-HFD: LETO high-fat diet. O-CON: OLETF control diet. O-HFD: OLETF high-fat diet.

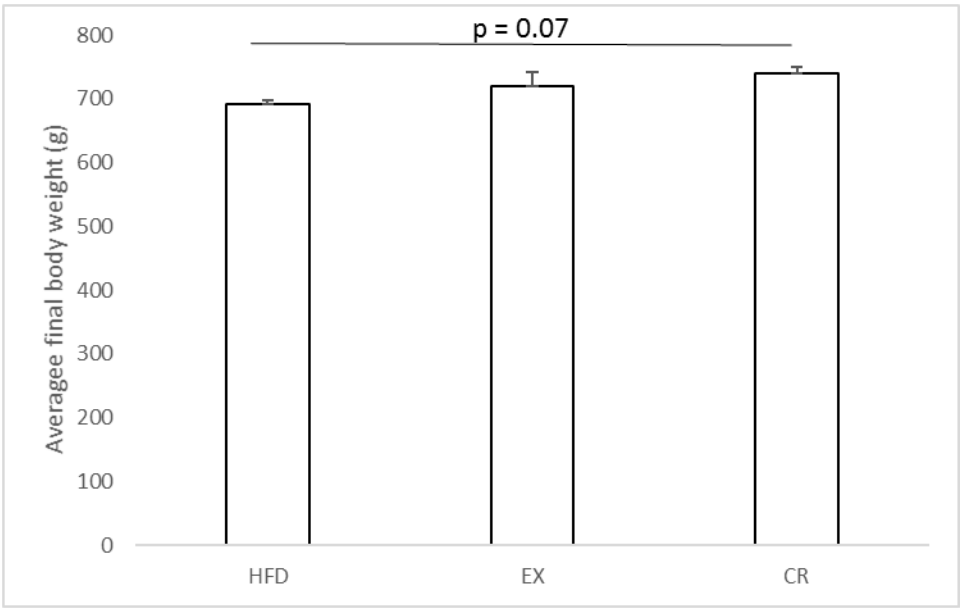

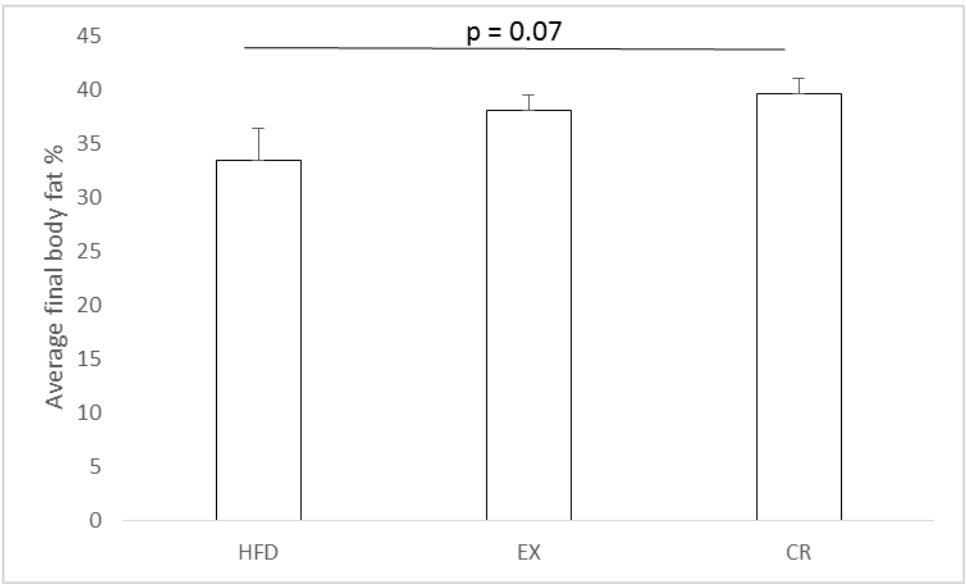

Figure 8: Average final body weight and body fat percentage of Cohort 2, representing exercise and calorie restriction intervention in obesity. HFD: High fat, high sucrose diet only animals, without intervention. EX: Exercise intervention high fat, high sucrose diet animals. CR: Calorie restriction high fat, high sucrose diet animals.

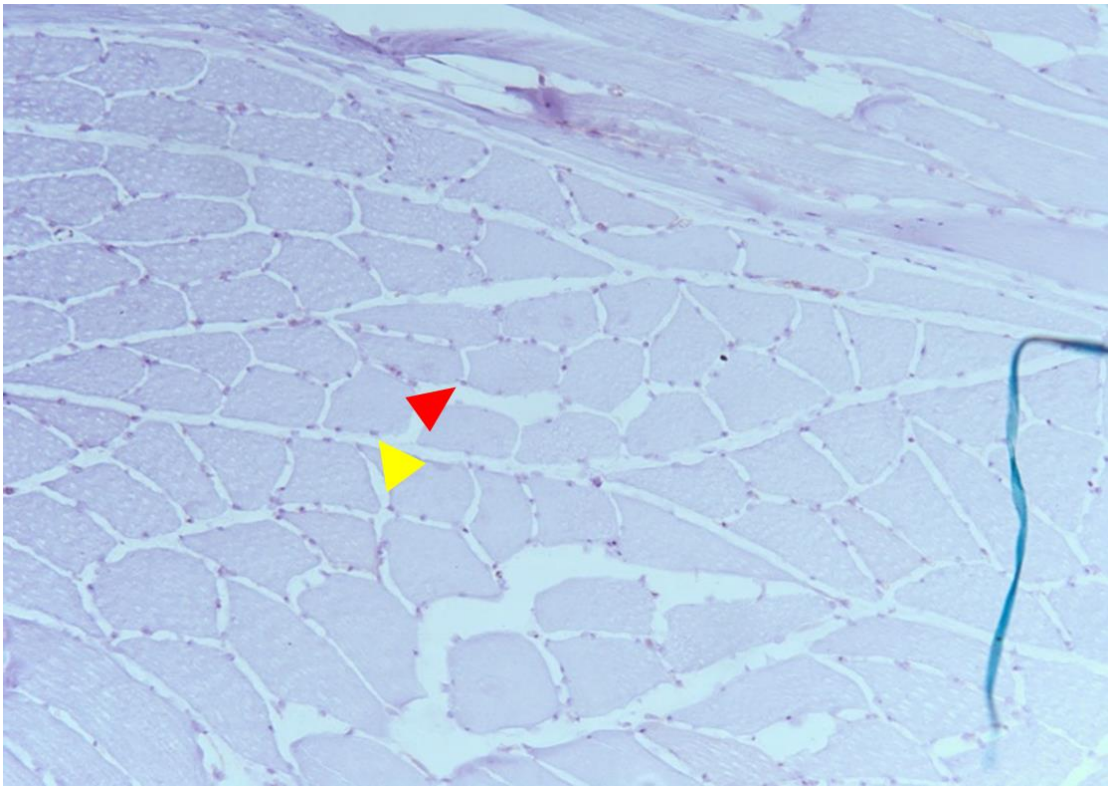

Figure 9: A representative image showing field of view during capillarity measurements. Yellow arrow indicates a nucleus, red arrow indicates a capillary.

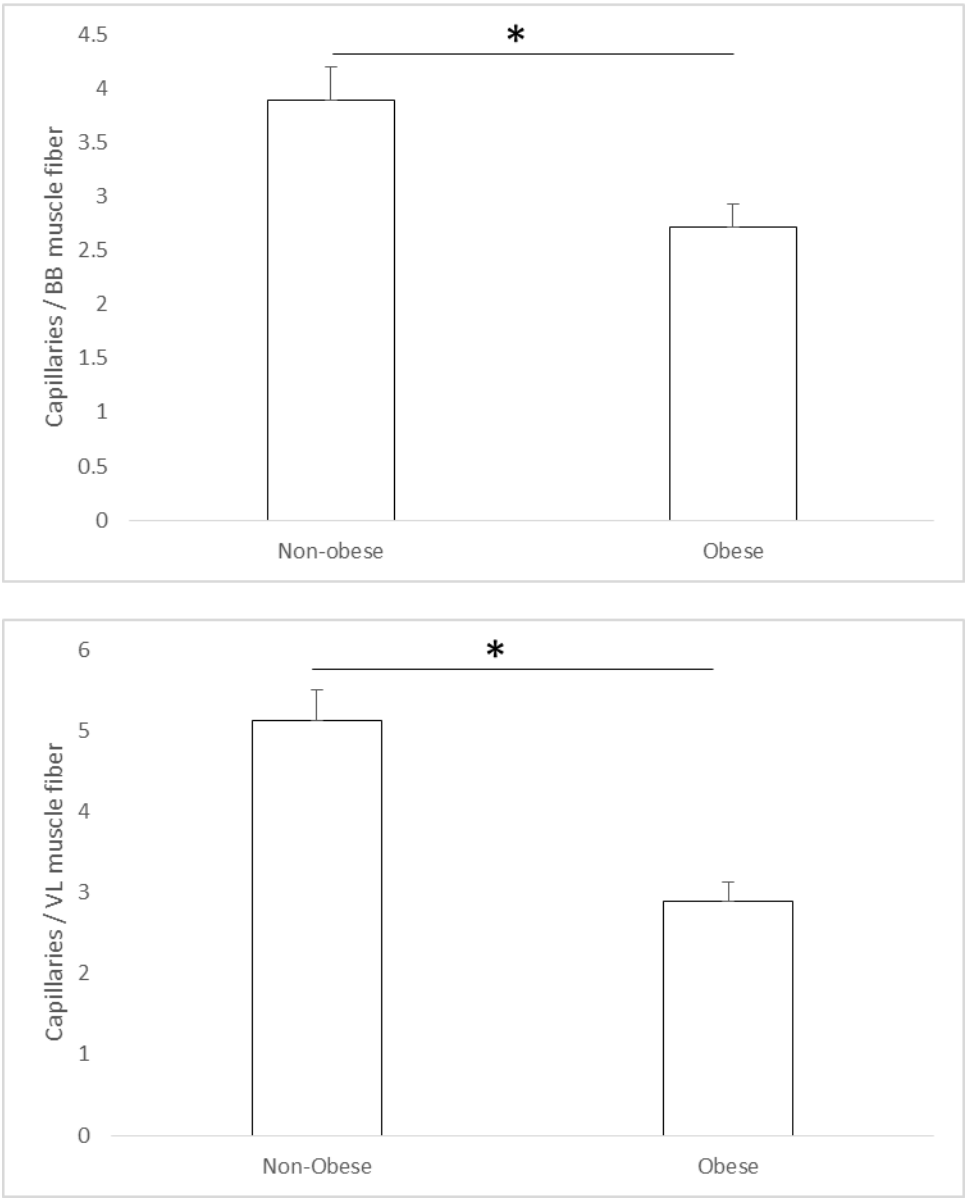

Figure 10: Measurement of capillarity in non-obese versus obese animals, expressed as (# capillaries / # muscle fibers). (*: $p < 0.05$). BB: Biceps brachii. VL: Vastus lateralis.

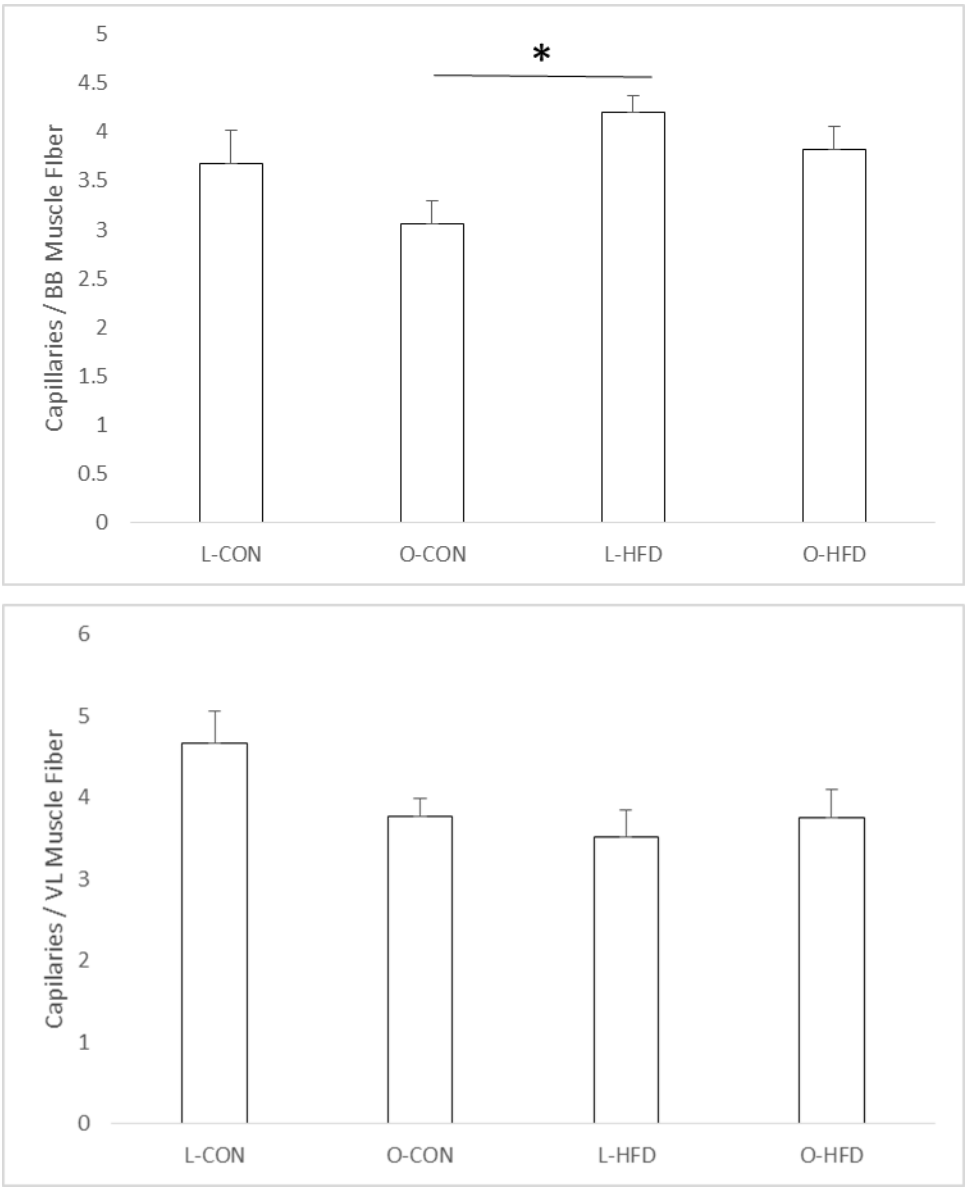

Figure 11: Measurement of capillarity in Cohort 1, expressed as (# capillaries / # muscle fibers). (*: $p < 0.05$)

Western blotting and immunohistochemistry

We assessed levels of IGF2R, IGF2, TGFβ, and uPAR in terms of non-obese versus obese rats, as well as in terms of strain and diet induction of obesity (Cohort 1) and intervention in obesity (Cohort 2), in both adipose tissue feed arteries and skeletal muscle feed arteries. In terms of raw data values from Western blotting adipose tissue feed arteries (Fig. 12), we found no significant difference between non-obese and obese animals in terms of IGF2R, IGF2, TGFβ, or uPAR. When normalizing the data, we find a significant decrease in TGFβ in obese animals, but no change in any of the other three factors (Fig. 13) ($p < 0.05$).

Breaking the raw data for adipose tissue feed arteries down by cohort, we find that Cohort 1 displays no significant differences between groups (Fig. 14), but when data is normalized (Fig. 15), we find that IGF2 displays significant decreases from L-CON to L-HFD ($p < 0.01$) as well from O-CON to O-HFD ($p < 0.05$), and a significant increase in IGF2 from L-HFD to O-HFD ($p < 0.05$). TGFB also shows a significant decrease from L-CON in both O-CON and O-HFD ($p < 0.05$ for both), while O-CON shows a significant increase in uPAR relative to L-HFD. Cohort 2 is not shown here, but no significant difference was found between groups in terms of raw data, while normalized data suggested IGF2 was significantly decreased in CR relative to SED, and significantly increased in EX relative to CR. Also in Cohort 2 normalized data, both TGFB and uPAR was significantly decreased in both EX and CR relative to SED.

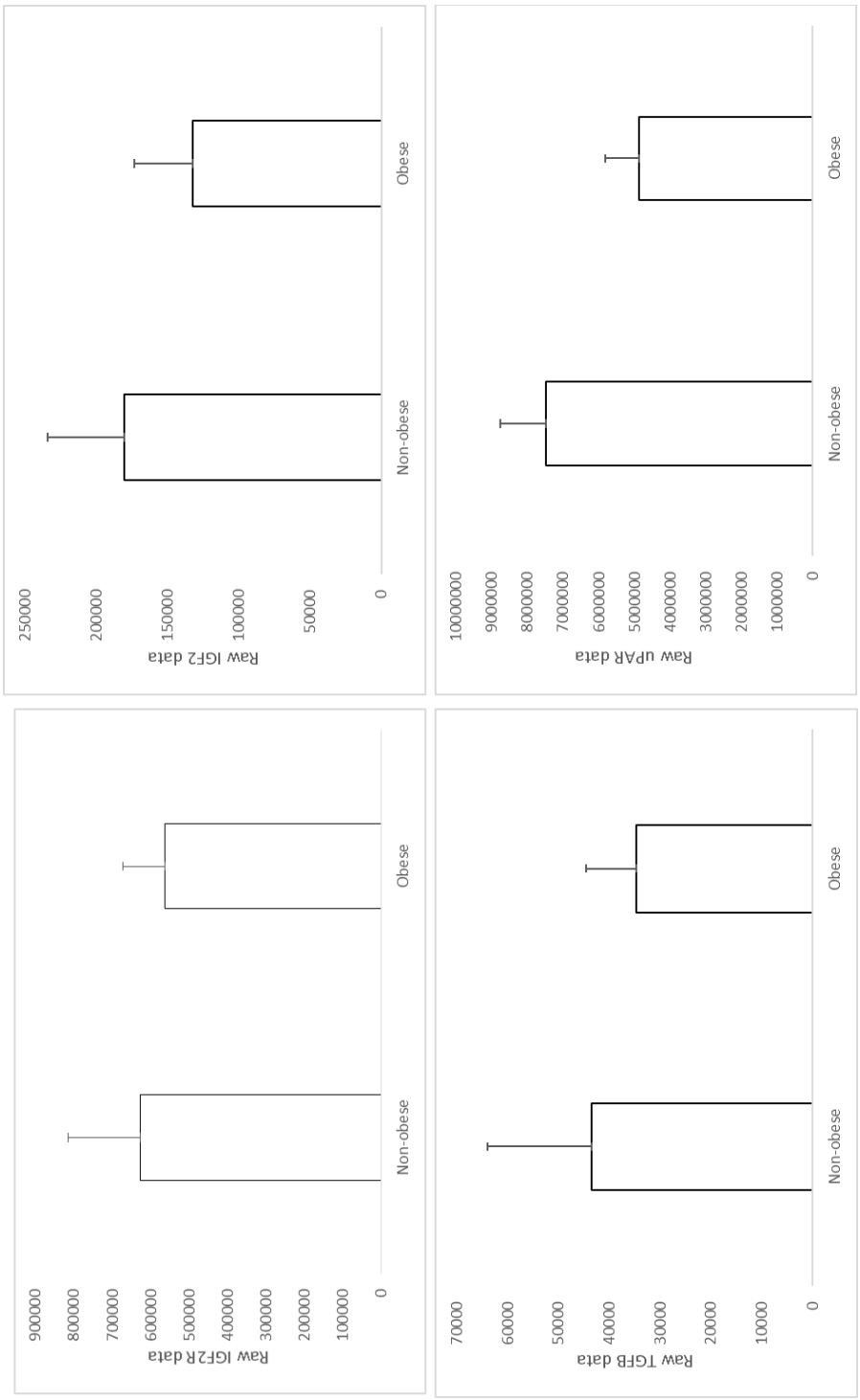

Figure 12: Adipose tissue feed artery raw data values for non-obese versus obese animals.

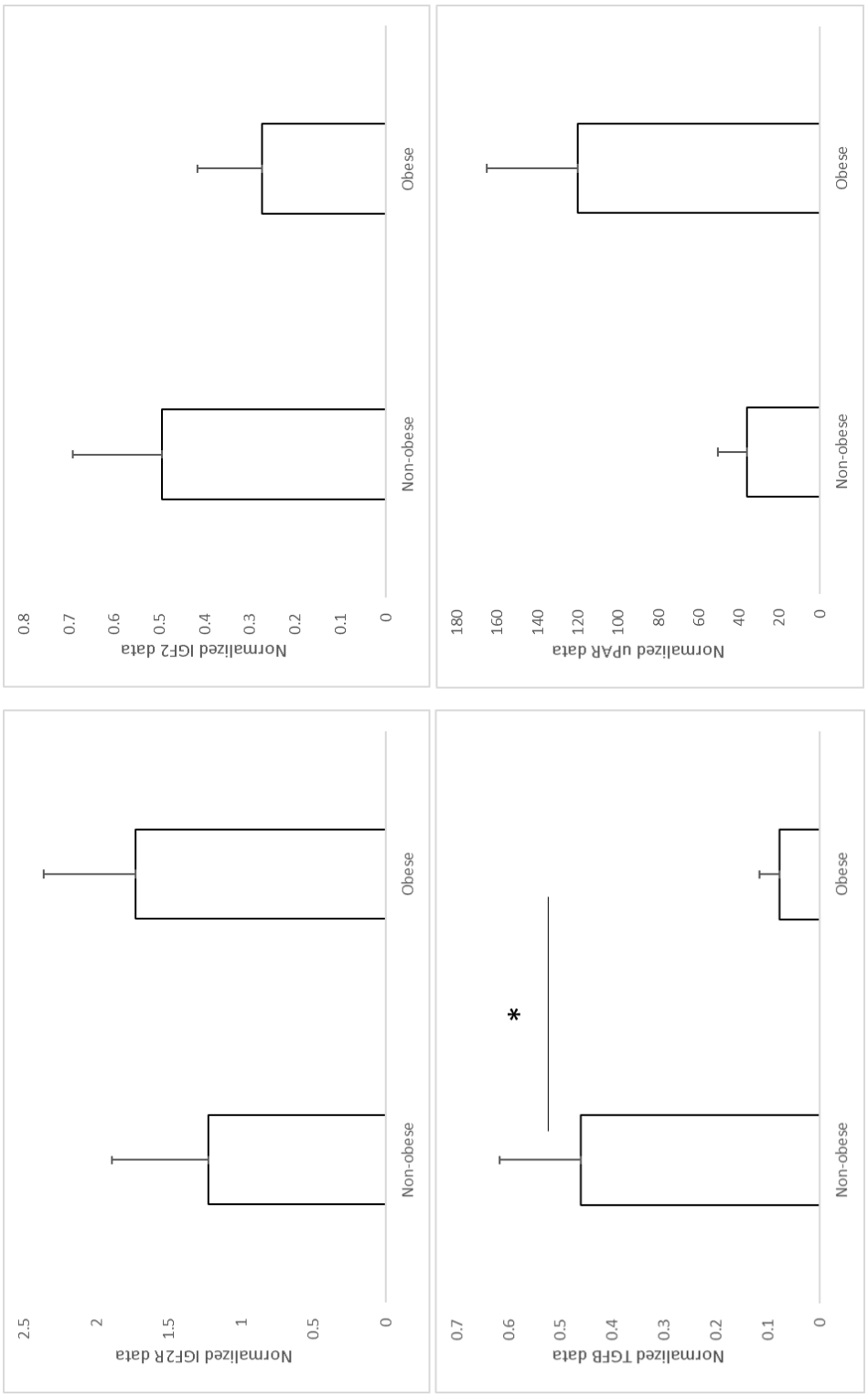

Figure 13: Adipose tissue feed artery normalized data values for non-obese versus obese animals. (*: $p < 0.05$)

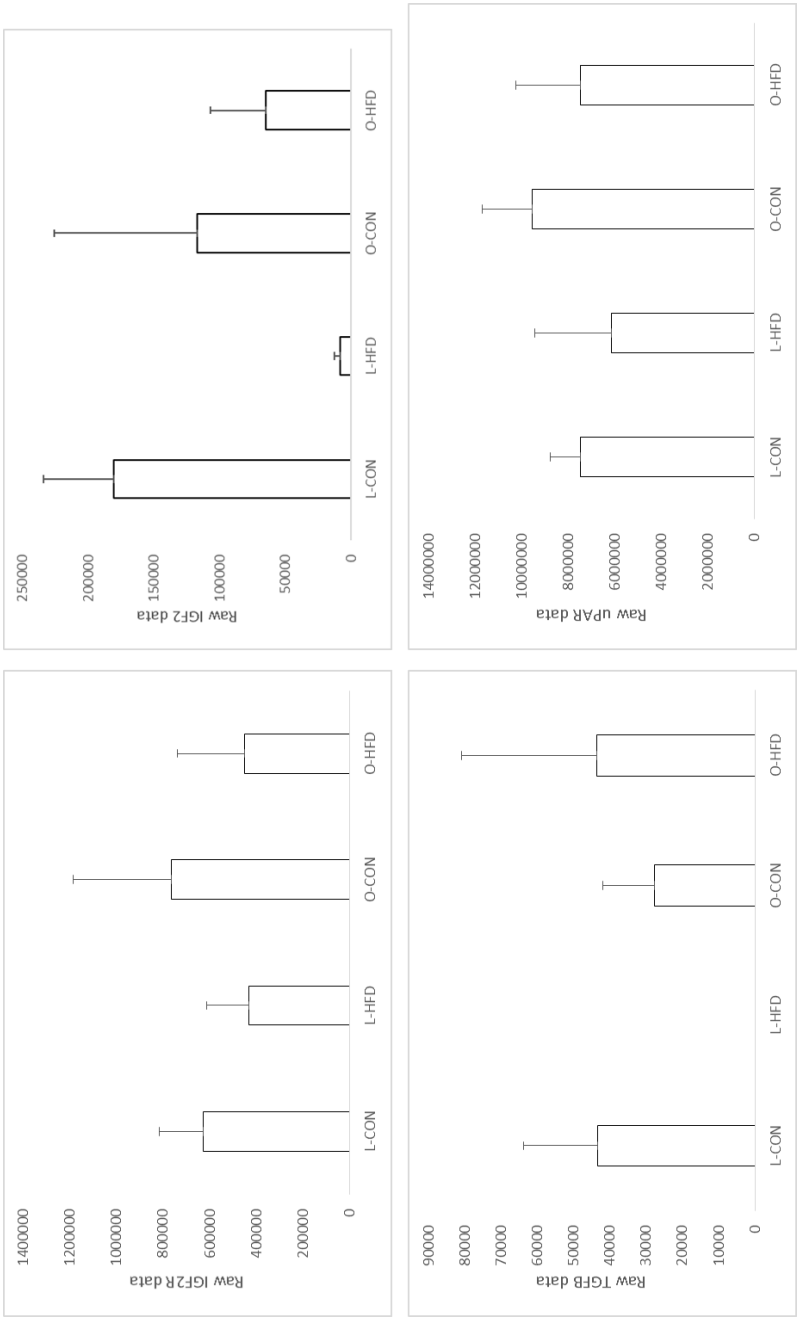

Figure 14: Adipose tissue feed artery raw data values for Cohort 1

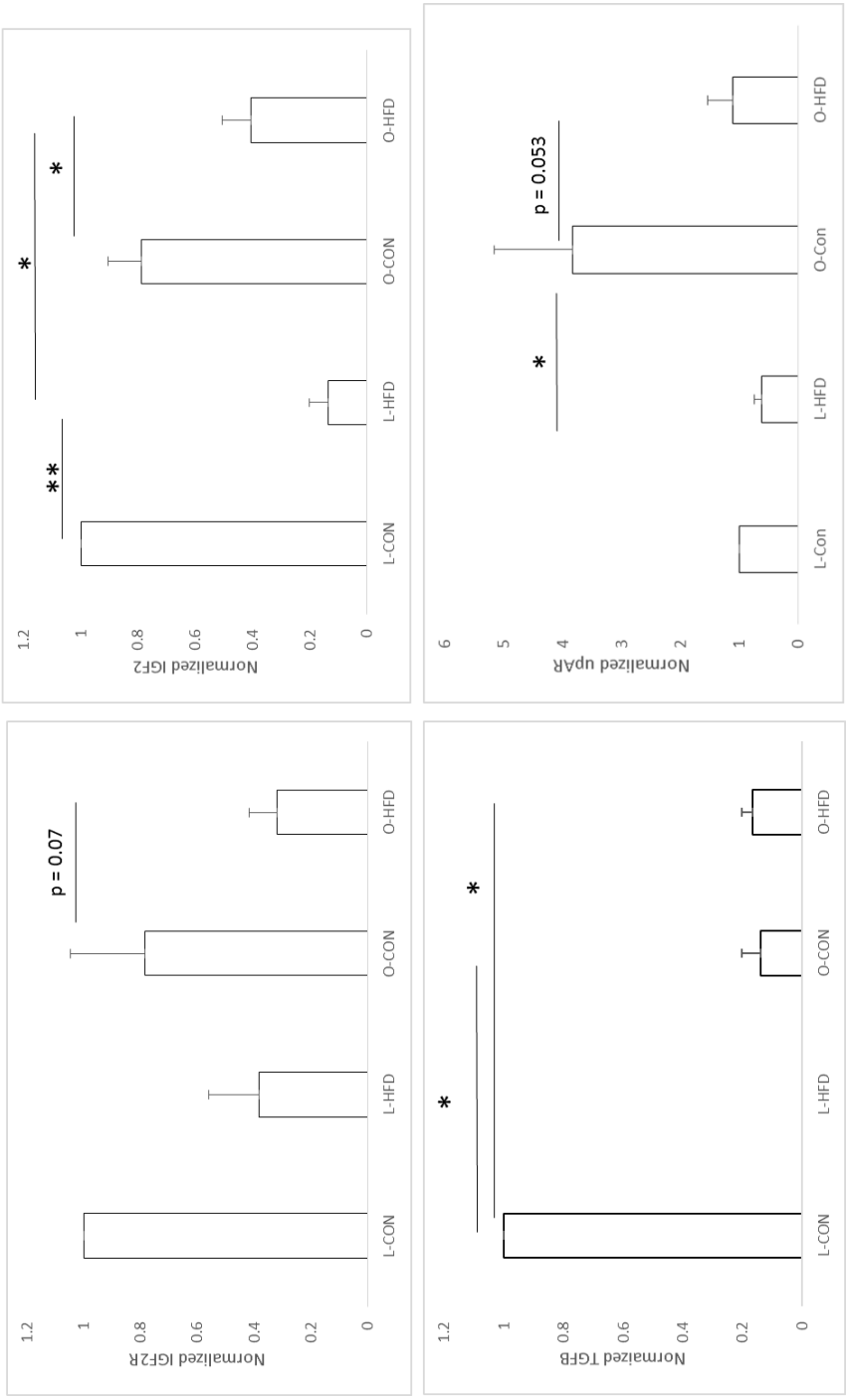

Figure 15: Adipose tissue feed artery normalized data values for Cohort 1. (*: $p < 0.05$, **: $p < 0.01$)

Examining factor expression in skeletal muscle feed arteries, we find no significant difference between obese and non-obese rats in terms of raw data (Fig. 16) or normalized data (Fig. 17) for any of the four factors. Cohort 1 shows a significant increase in TGFB in O-HFD from both L-HFD and O-CON in terms of raw data values (Fig. 18) ($p < 0.05$), while normalized data (Fig. 19) shows a significant increase in IGF2R in O-HFD relative to L-HFD ($p < 0.05$), significant increase in IGF2 in O-HFD relative to both L-HFD and O-CON ($p< 0.05$ for both), and significant increase in O-HFD uPAR relative to L-HFD ($p < 0.05$). Cohort 2 is not shown, but no significant difference is found among groups for either raw or normalized data, excepting a significant increase in IGF2 in EX relative to SED, in terms of raw data. We also performed immunohistochemistry on skeletal muscle from animals in Cohort 2 to detect TGFB and uPAR. However, we found no significant difference between groups for either TGFB or uPAR as measured with IHC.

Correlational analyses

To test the hypothesis that obesity and/or body fat percentage are major determinants of the major parameters measured in this study, we performed multiple correlational analyses, which are described in Table 2. These analyses yielded no strong correlations ($r^2 \geq 0.80$) when examining raw or normalized factor data, or capillarity, versus body weight, body fat percentage, or capillarity in either biceps brachii or vastus lateralis skeletal muscle. We observed correlations of 0.41 in normalized TGFB (adipose feed artery) versus body

weight, 0.58 in normalized uPAR (adipose feed artery) versus body weight, and 0.45 in normalized uPAR (adipose feed artery) versus body fat percentage.

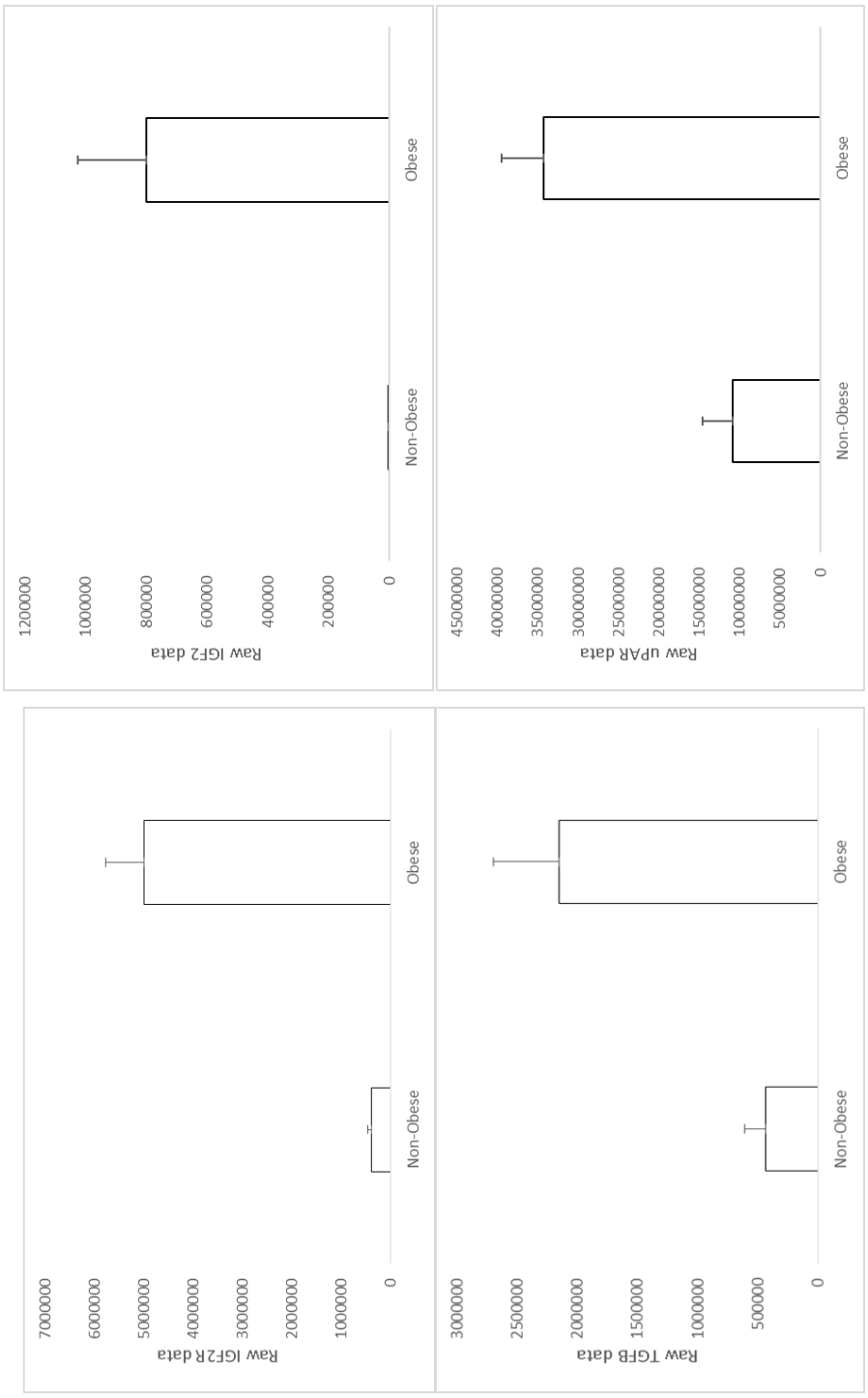

Figure 16: Skeletal muscle feed artery raw data values for non-obese versus obese animals.

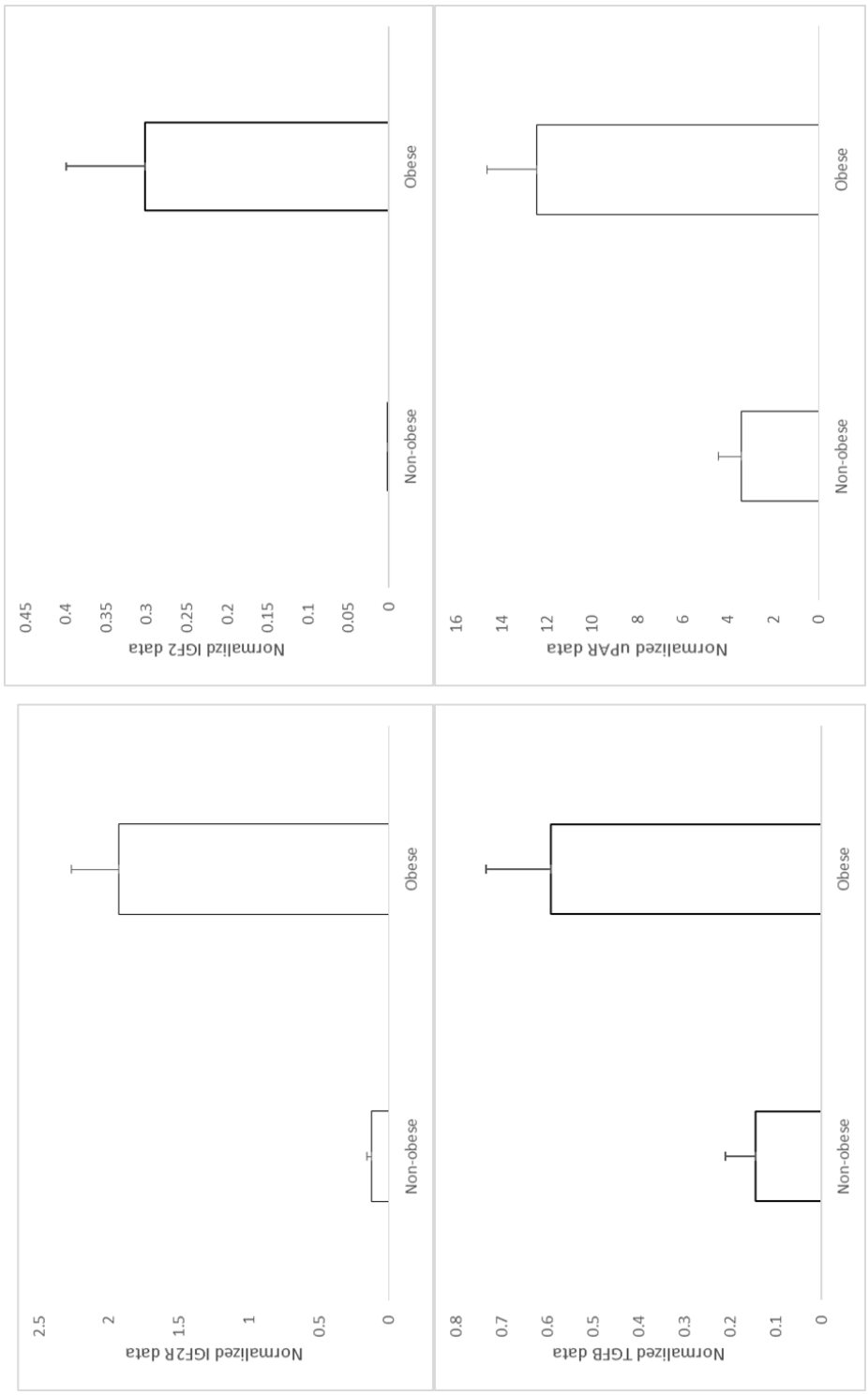

Figure 17: Skeletal muscle feed artery normalized data values for non-obese versus obese animals.

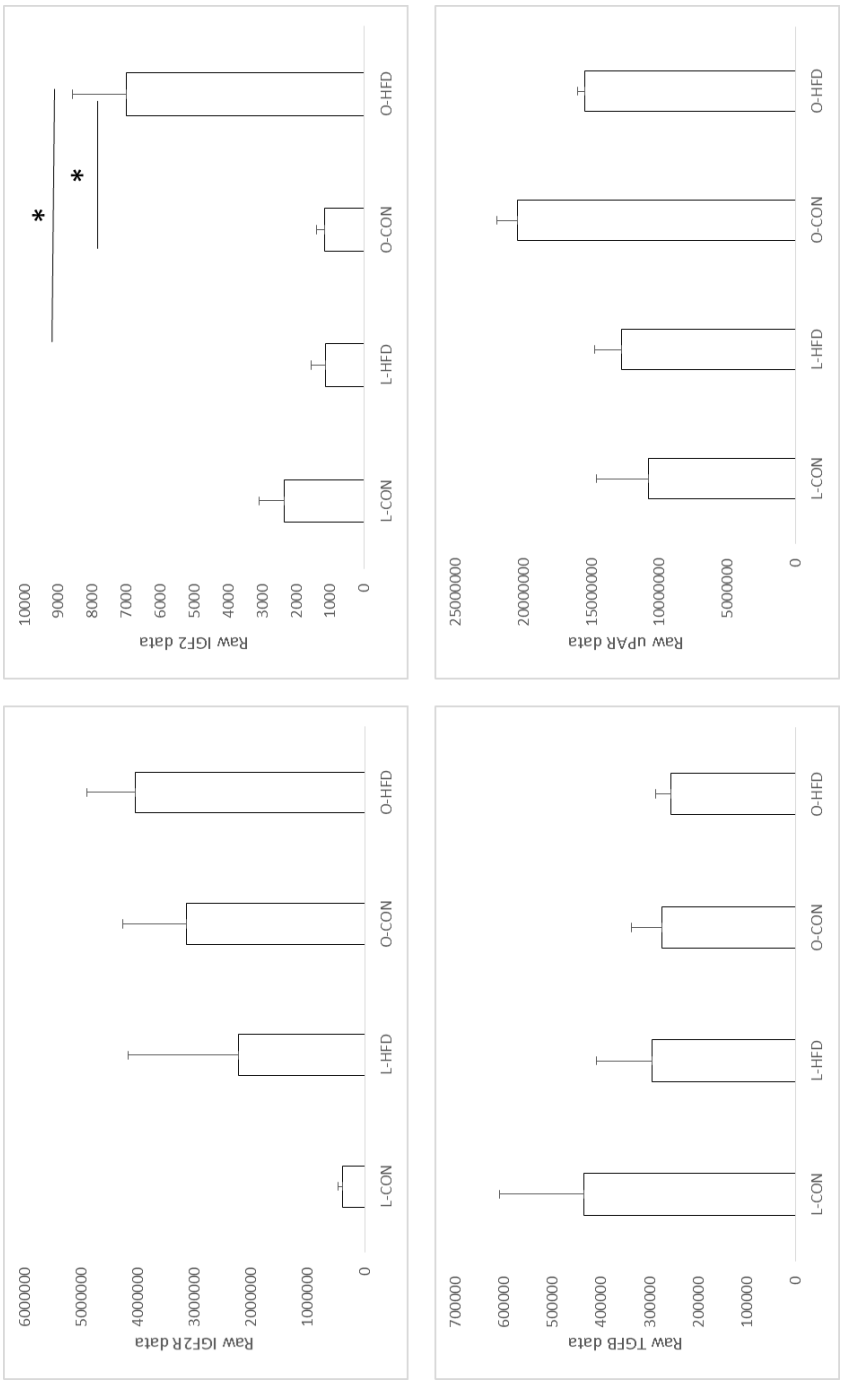

Figure 18: Skeletal muscle feed artery raw data values for Cohort 1. (*: $p < 0.05$).

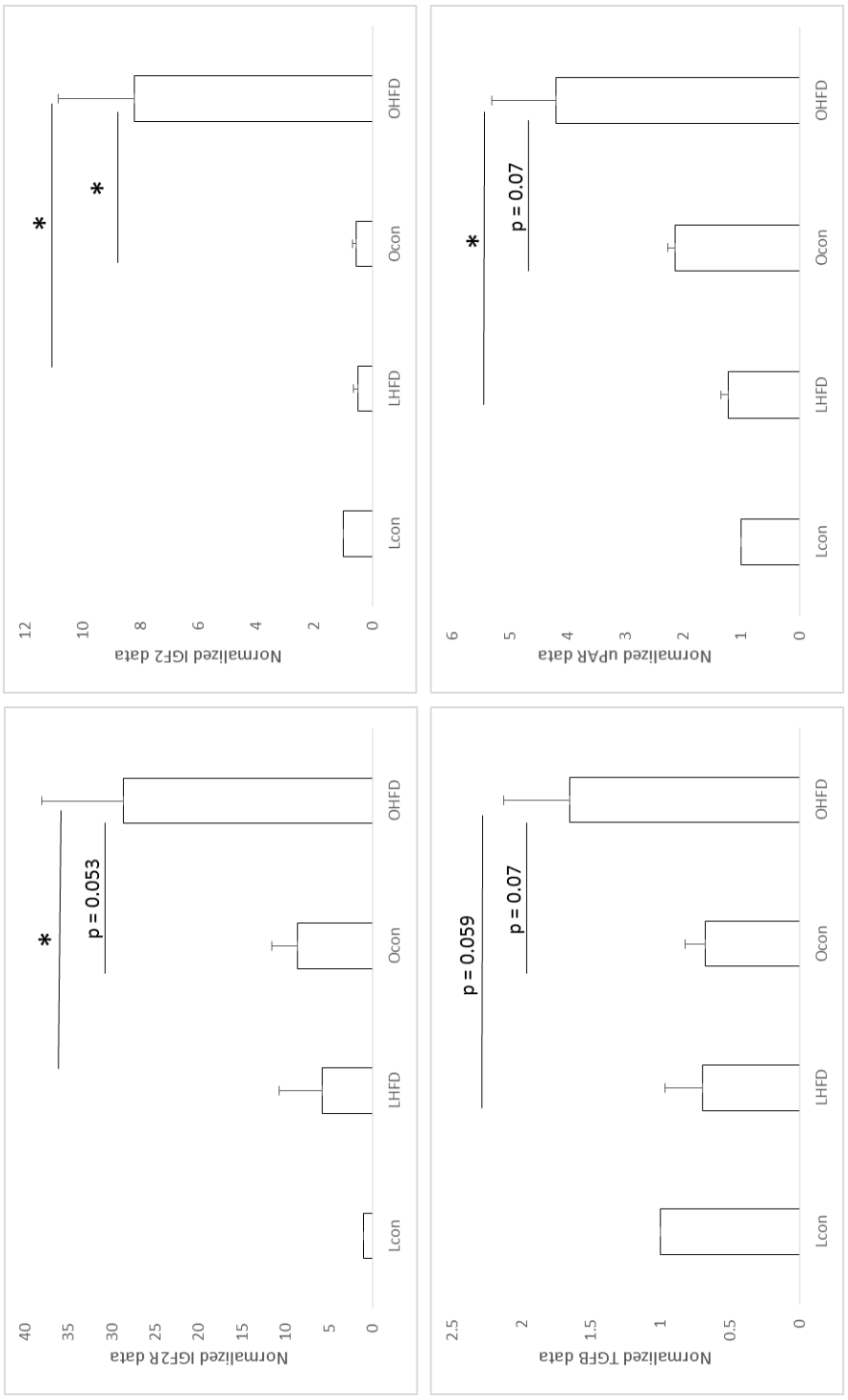

Figure 19: Skeletal muscle feed artery normalized data values. (*: $p < 0.05$)

	Body weight	Body fat %	Cap. Density (BB)	Cap. Density (VL)
Raw IGF2R	N.C.	N.C	N.C.	N.C.
Raw IGF2R	N.C.	N.C	N.C.	N.C.
Raw TGFB	N.C.	N.C	N.C.	N.C.
Raw uPAR	N.C.	N.C	N.C.	N.C.
Norm. IGF2R	N.C.	N.C	N.C.	N.C.
Norm. IGF2R	N.C.	N.C	N.C.	N.C.
Norm. TGFB	N.C.	N.C	N.C.	0.49
Norm. uPAR	0.54	N.C	N.C.	0.51
Cap. Density (BB)	N.C.	N.C	-	-
Cap. Density (VL)	N.C.	N.C	-	-

Table 2: List of correlational comparisons made during data analysis. N.C.: No correlation. *: Exception to no correlation status, see text.

c. Discussion

LETO and OLETF rat in modeling weight gain, body composition change, and capillarity change in obesity

In our study, we have shown that obesity can be successfully induced in in a cohort of LETO and OLETF rats by way of both strain and diet, reflected in increases in both total body weight as well as in body fat percentage. This corresponds with previous literature indicating that OLETF rat gains weight rapidly owing to hyperphagia, and that diet can cause obesity(1-4). Owing to previous literature indicating that obesity is associated with decreases in capillarity, we hypothesized that obesity induction would result in a decrease in capillarity in skeletal muscle, which was supported by the data in comparing non-obese versus obese animals(5).

The biceps brachii is predominantly type IIa and IIb fibers, while the vastus lateralis is primarily type IIb fibers with type IIa fibers present in a lesser proportion than in the biceps brachii(6, 7). Capillarity is highest in fast oxidative glycolytic muscle, followed by slow oxidative and fast glycolytic muscle(8). In addition, exercise training in animal models has been shown to have a greater effect in increasing capillarity in fast oxidative glycolytic muscle than in the other two subtypes(9). However, in our study, in comparing non-obese versus obese animals, the vastus lateralis had a higher average capillary to fiber ratio in non-obese animals than the biceps brachii, and both muscles displayed significant decreases in capillarity following obesity induction. This indicates either that the

difference between the biceps brachii and vastus lateralis type IIb to other fiber types' ratio is either insufficient to drive differences in lean capillarity, or that our rat strains differ from the strains characterized in the literature in terms of fiber density in muscle with different fiber types. However, both muscles still displayed decreases in capillarization in response to obesity.

We then examined Cohort 1, which contained several subgroups of obesity induction contributing to our generic obesity induction group, including induction on the basis of diet and strain. We find no significant differences among groups in either the biceps brachii or the vastus lateralis, except for LETO animals on HFD having a greater bicep brachii capillarity than OLETF animals on HFD. However, density averages display consistent, though non-significant differences in the biceps brachii, with LETO rats having a higher average density than their OLETF diet counterpart, and HFD animals having a higher density than their CON counterparts. In the vastus lateralis as well, induction of obesity by diet, strain, or both shows a lower average density than the L-CON group.

Overall, the data indicates that obesity in our animals used resulted in decreases in capillarity across both muscle beds, as summarized in Figure 20. Given the decreases in capillarity in our obese rats, it is reasonable to use tissues from these rats for investigation of mechanisms controlling vascular growth and retraction, including that of IGF2R mediating IGF2 degradation, TGFB activation, and uPAR degradation.

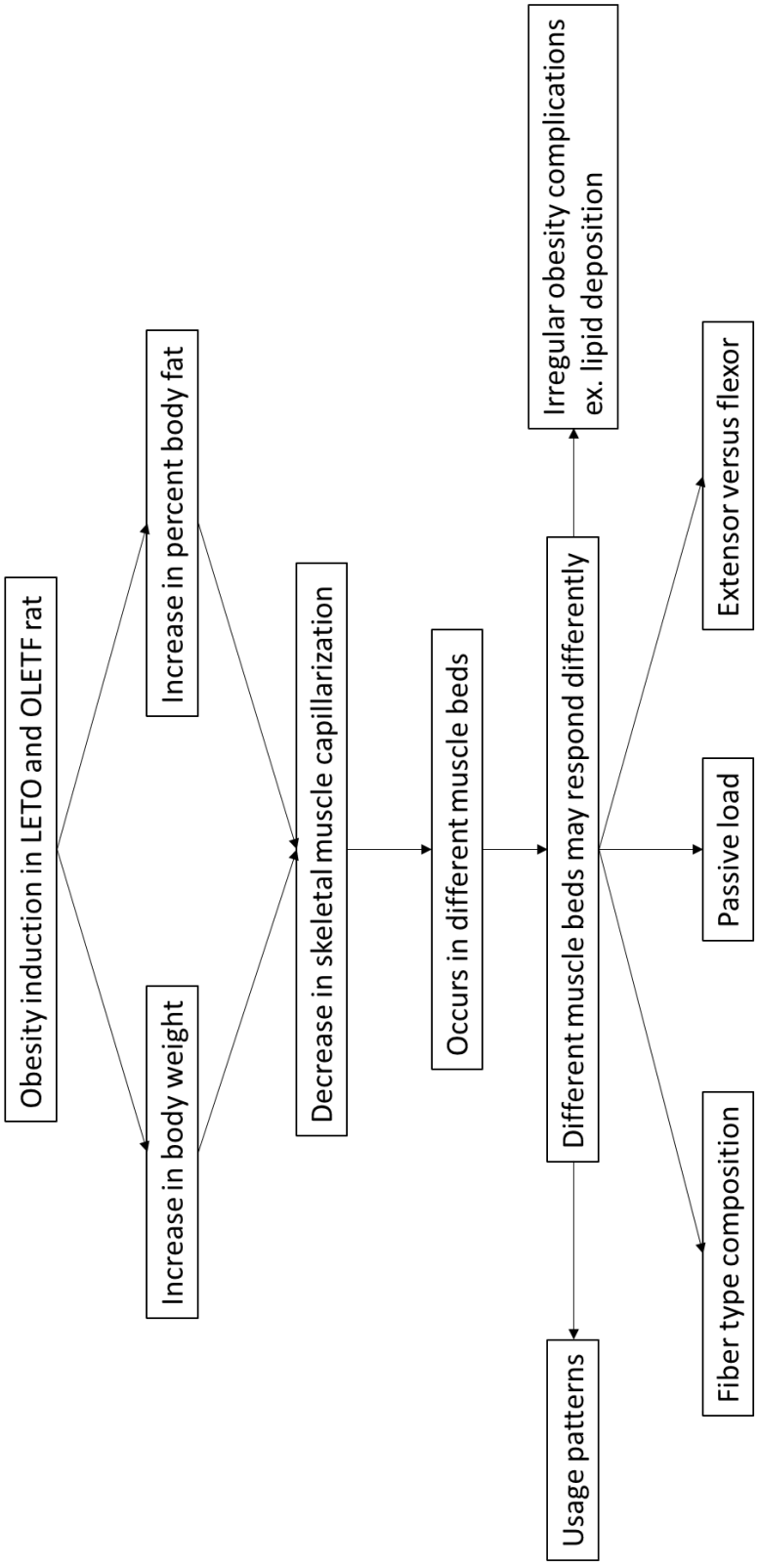

Figure 20: Schema of changes in capillarization during obesity.

Changes in factors during induction of obesity in the OLETF rat

Previous literature has indicated that IGF2R is increased in obese dams, with IGF2 increased in dam placenta and the developing fetus(10, 11). TGFB has also been shown to be elevated in obesity, with blockade improving prognosis(12, 13). With decreases in capillarity in obesity and the known regulation of IGF2, TGFB, and uPAR by IGF2R, we hypothesized that IGF2R would be increased in obesity in adult rats, with IGF2 expression decreased, TGFB expression increased, and uPAR decreased.

In the non-obese versus obese animal cohort, as illustrated in Figure 21, only TGFB changed in adipose tissue feed arteries, decreasing significantly in obese animals as compared to non-obese animals which was directly opposite to what we hypothesized. In all other evaluations of raw and normalized data, none of the four factors changed at all.

More differences were observed when evaluating the raw and normalized data on the basis of strain or diet-induced obesity, but many of these results did not support our hypothesis, as summarized in Figure 22. On the basis of raw data values, IGF2 expression increased in skeletal muscle feed artery in O-HFD as compared to L-HFD, and in O-HFD as compared to O-CON. In the first set, addition of strain-induced obesity increased IGF2 expression, and in the second set, addition of diet-induced obesity increased IGF2 expression. We also did not find any changes in IGF2R, IGF2, TGFB, or uPAR on the basis of raw data for adipose tissue feed arteries.

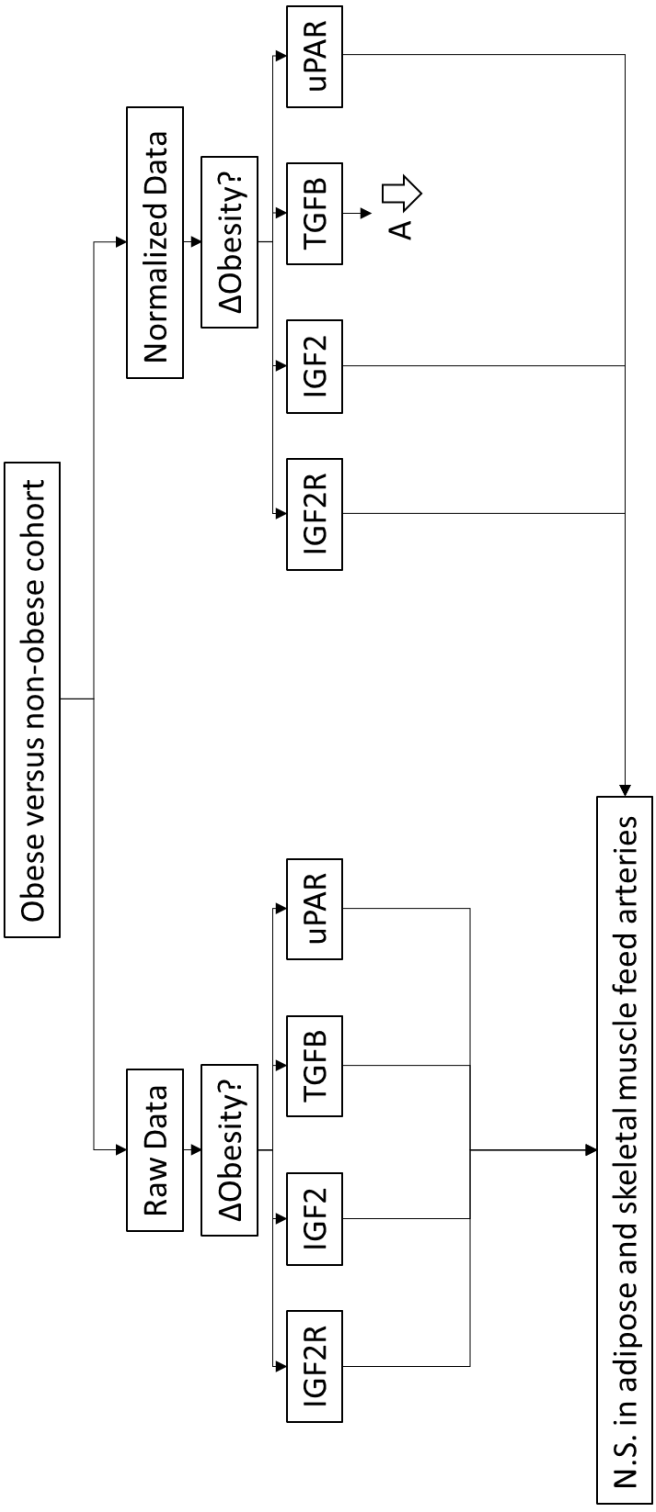

Figure 21: Schema showing changes in factors in terms of raw data and normalized data when comparing non-obese to obese animals. White arrows indicate changes contrary to hypothesis as well as direction of change.
A: Adipose feed artery. N.S.: Not significant.

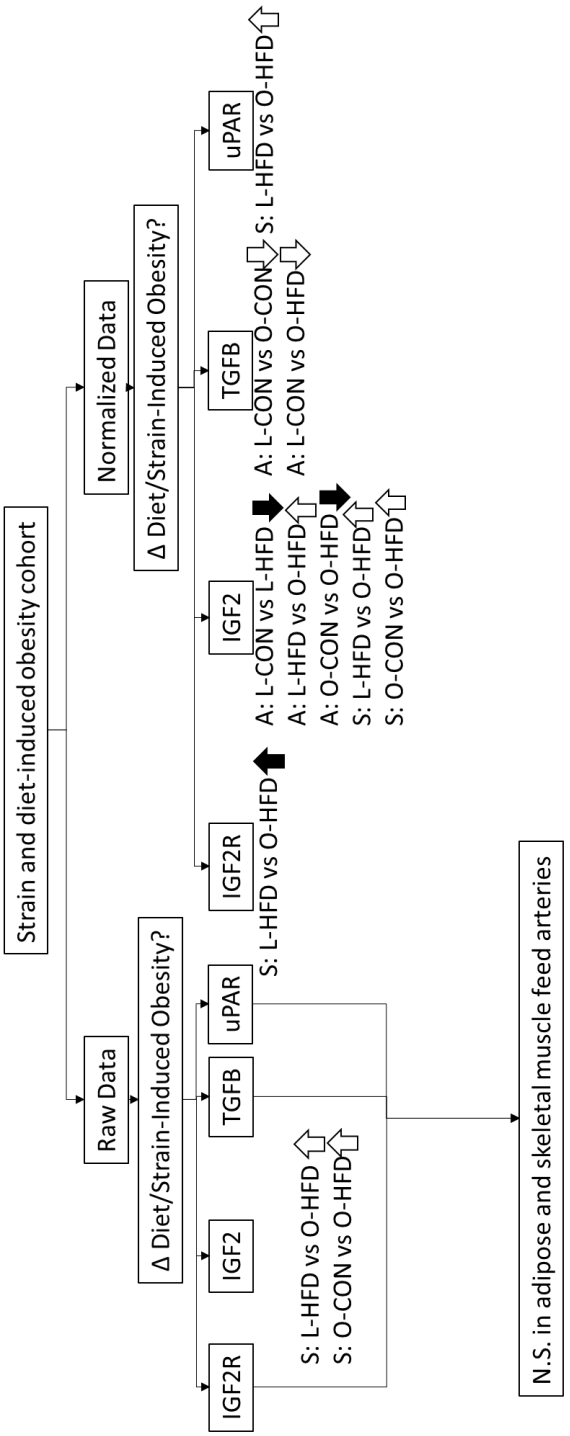

Figure 22: Schema showing changes in factors in terms of raw and normalized data when comparing induction of obesity on the basis of diet or strain. White arrows indicate changes contrary to hypothesis as well as direction of change. Black arrows indicate changes in concurrence with hypothesis as well as direction of change. A: Adipose feed artery. S: Skeletal muscle feed artery. N.S.: Not significant.

Examining normalized data in the strain and diet-induced obesity cohort, IGF2R increased in skeletal muscle feed arteries in accordance with our hypothesis but only on the basis of one of two strain-induced obesity comparisons (in O-HFD as compared to L-HFD). Adipose feed artery normalized data, by comparison, did not show a significant change in IGF2R between any of the groups. IGF2 displayed several changes in expression between groups, with adipose tissue feed artery data showing a decrease on the basis of diet-induced obesity, as hypothesized, but in strain-induced obesity (O-HFD as compared to L-HFD) showing an increase in IGF2 which was not in accordance with the hypothesis. In skeletal muscle feed artery data, IGF2 increased with diet (O-HFD as compared to O-CON) and strain (O-HFD as compared to L-HFD, which was contrary to our hypothesis. TGFB displayed changes in terms of adipose tissue feed artery data, decreasing in expression on the basis of strain (O-CON and O-HFD as compared to L-CON), while uPAR demonstrated an increase on the basis of strain-induced obesity (O-HFD as compared to L-HFD. These changes in TGFB and uPAR were contrary to our hypothesis as well.

Our data indicates that our hypothesis that IGF2R is elevated in obesity, leading to IGF2 degradation, TGFB activation, and uPAR degradation, is not supported. In adipose tissue feed arteries, we observed mixed results with respect to IGF2, decreases in TGFB, and no significant changes in IGF2R or uPAR. In skeletal muscle feed arteries, we observed one instance of IGF2R increase, increases in IGF2 contrary to the hypothesis, no change in TGFB, and one instance of uPAR increase contrary to the hypothesis. When staining muscle

for TGFB and uPAR, we observed no significant difference in these markers across groups undergoing intervention versus without intervention.

Given these data, we suggest an alternative schema, as seen in Figure 23, where in tissue feed arteries IGF2 remains increased in an response to sustain angiogenesis in adult rats, similar to observations in dam and fetal studies, while IGF2R, uPAR, and TGFB remain similar in expression to lean individuals, or decreased in the case of TGFB. Overall, the net effect is pro-angiogenic, with growth factors increased or steady in obesity and with growth-freezing factors either steady or decreased. Tissue rarefaction, then, is due to either another anti-angiogenic mechanism such as the originally hypothesized schema in which IGF2R degrades IGF2 and uPAR while activating TGFB, or a mechanism promoting increased retraction of capillaries, either of which have greater effect and result in net capillarity decrease.

In summary, we show that the LETO and OLETF rats both exhibit decreased capillarity in obesity, similar to other animal and human models. Further, results indicate that these capillarity decreases occur in two different muscle beds. We also demonstrate that IGF2R, IGF2, TGFB, and uPAR are not consistently altered in an anti-angiogenic fashion in obesity induction in LETO or OLETF rats. These results suggest that other mechanisms are at work in producing the capillarity decrease observed with obesity in LETO and OLETF rats.

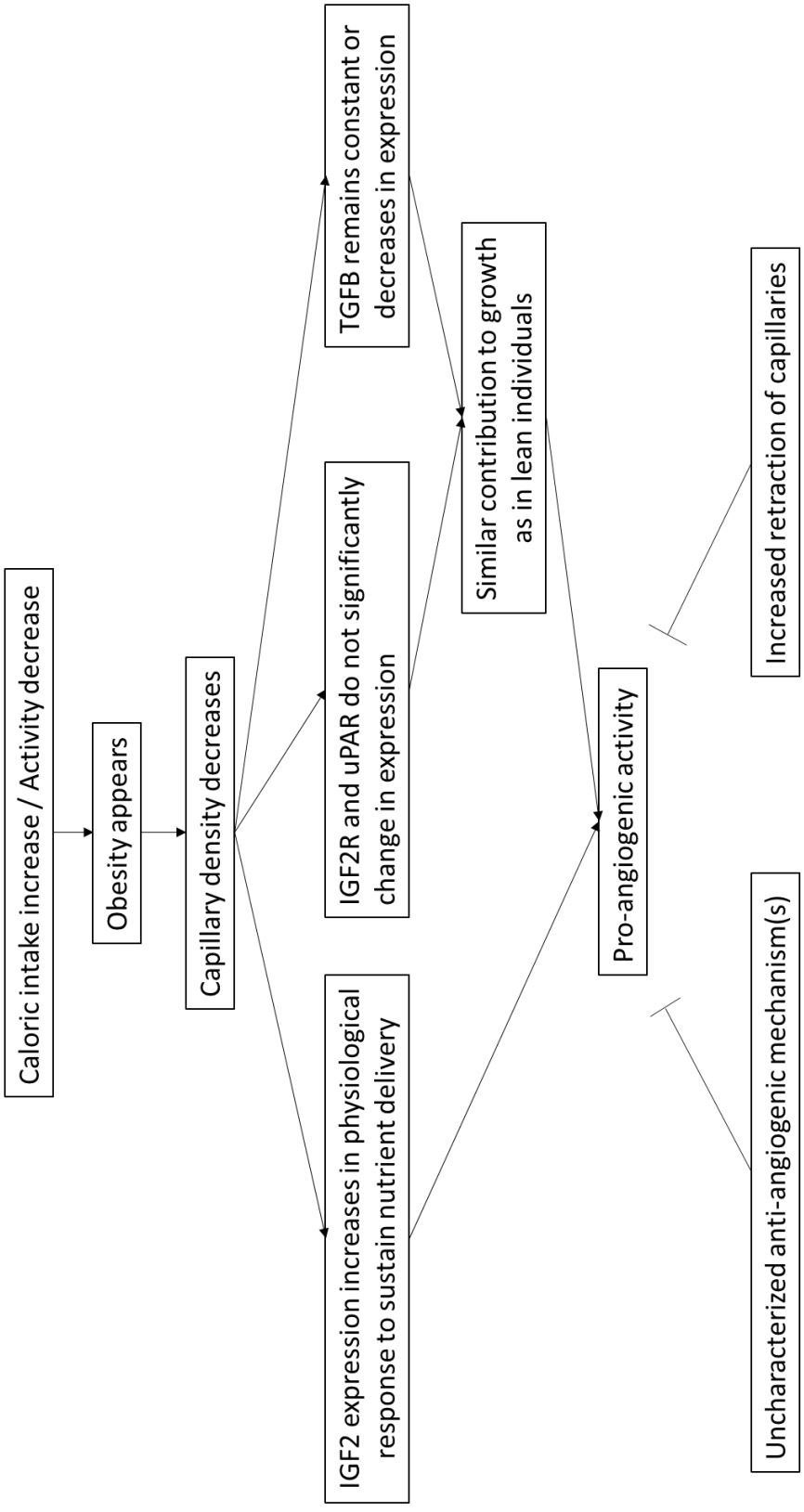

Figure 23: New proposed schema for IGF2R and coordinated factors in obesity

d. References

1. Rector RS, Thyfault JP, Uptergrove GM, Morris EM, Naples SP, Borengasser SJ, et al. Mitochondrial dysfunction precedes insulin resistance and hepatic steatosis and contributes to the natural history of non-alcoholic fatty liver disease in an obese rodent model. Journal of hepatology. 2010;52(5):727-36. Epub 2010/03/30. doi: 10.1016/j.jhep.2009.11.030. PubMed PMID: 20347174; PubMed Central PMCID: PMCPMC3070177.

2. McMorrow AM, Connaughton RM, Lithander FE, Roche HM. Adipose tissue dysregulation and metabolic consequences in childhood and adolescent obesity: potential impact of dietary fat quality. The Proceedings of the Nutrition Society. 2015;74(1):67-82. Epub 2014/12/17. doi: 10.1017/s002966511400158x. PubMed PMID: 25497038.

3. Riserus U, Willett WC, Hu FB. Dietary fats and prevention of type 2 diabetes. Progress in lipid research. 2009;48(1):44-51. Epub 2008/11/27. doi: 10.1016/j.plipres.2008.10.002. PubMed PMID: 19032965; PubMed Central PMCID: PMCPMC2654180.

4. Malik VS, Popkin BM, Bray GA, Despres JP, Hu FB. Sugar-sweetened beverages, obesity, type 2 diabetes mellitus, and cardiovascular disease risk. Circulation. 2010;121(11):1356-64. Epub 2010/03/24. doi: 10.1161/circulationaha.109.876185. PubMed PMID: 20308626; PubMed Central PMCID: PMCPMC2862465.

5. Nascimento AR, Machado M, de Jesus N, Gomes F, Lessa MA, Bonomo IT, et al. Structural and functional microvascular alterations in a rat model of metabolic syndrome induced by a high-fat diet. Obesity (Silver Spring, Md). 2013;21(10):2046-54. Epub 2013/03/21. doi: 10.1002/oby.20358. PubMed PMID: 23512529.

6. Eng CM, Smallwood LH, Rainiero MP, Lahey M, Ward SR, Lieber RL. Scaling of muscle architecture and fiber types in the rat hindlimb. The Journal of experimental biology. 2008;211(Pt 14):2336-45. Epub 2008/07/01. doi: 10.1242/jeb.017640. PubMed PMID: 18587128.

7. Fuentes I, Cobos AR. Muscle fibre types and their distribution in the biceps and triceps brachii of the rat and rabbit. 1998;192(Pt 2):203-10. doi: 10.1046/j.1469-7580.1998.19220203.x. PubMed PMID: 9643421; PubMed Central PMCID: PMCPMC1467754.

8. Mai JV, Edgerton VR, Barnard RJ. Capillarity of red, white and intermediate muscle fibers in trained and untrained guinea pigs. Experientia. 1970;26(11):1222-3. Epub 1970/11/15. PubMed PMID: 5485285.

9. Carrow RE, Brown RE, Van Huss WD. Fiber sizes and capillary to fiber ratios in skeletal muscle of exercised rats. The Anatomical record. 1967;159(1):33-9. Epub 1967/09/01. doi: 10.1002/ar.1091590106. PubMed PMID: 6062782.

10. Jungheim ES, Schoeller EL, Marquard KL, Louden ED, Schaffer JE, Moley KH. Diet-induced obesity model: abnormal oocytes and persistent growth abnormalities in the offspring. Endocrinology. 2010;151(8):4039-46. Epub 2010/06/25. doi: 10.1210/en.2010-0098. PubMed PMID: 20573727; PubMed Central PMCID: PMCPMC2940512.

11. Belobrajdic DP, Frystyk J, Jeyaratnaganthan N, Espelund U, Flyvbjerg A, Clifton PM, et al. Moderate energy restriction-induced weight loss affects circulating IGF levels independent of dietary composition. European journal of endocrinology. 2010;162(6):1075-82. Epub 2010/03/10. doi: 10.1530/eje-10-0062. PubMed PMID: 20212016.

12. Wang X, Abraham S, McKenzie JA, Jeffs N, Swire M, Tripathi VB, et al. LRG1 promotes angiogenesis by modulating endothelial TGF-beta signalling. Nature. 2013;499(7458):306-11. Epub 2013/07/23. doi: 10.1038/nature12345. PubMed PMID: 23868260; PubMed Central PMCID: PMCPMC3836402.

13. Yadav H, Quijano C, Kamaraju AK, Gavrilova O, Malek R, Chen W, et al. Protection from obesity and diabetes by blockade of TGF-beta/Smad3 signaling. Cell metabolism. 2011;14(1):67-79. Epub 2011/07/05. doi: 10.1016/j.cmet.2011.04.013. PubMed PMID: 21723505; PubMed Central PMCID: PMCPMC3169298.

3. EFFECTS OF ENDURANCE EXERCISE TRAINING, METFORMIN, AND THEIR COMBINATION ON ADIPOSE TISSUE LEPTIN AND IL-10 SECRETION IN RATS

a. Note to the reader on authorship

This paper was originally authored by Dr. Nathan T. Jenkins, who has granted permission for both the text and figures of this paper to be reproduced in this dissertation. Figure and table numbering has been changed when necessary to follow the numbering scheme of the dissertation. The citation for this paper is as follows:

Jenkins, N.T., et al., *Effects of endurance exercise training, metformin, and their combination on adipose tissue leptin and IL-10 secretion in OLETF rats.* J Appl Physiol (1985), 2012. **113**(12): p. 1873-83.

b. Abstract

Adipose tissue inflammation plays a role in cardiovascular (CV) and metabolic diseases associated with obesity, insulin resistance and type 2 diabetes mellitus (T2DM). The interactive effects of exercise training and metformin, two first-line T2DM treatments, on adipose tissue inflammation are not known. Using the hyperphagic, obese, insulin resistant Otsuka Long Evans Tokushima Fatty (OLETF) rat model, we tested the hypothesis that treadmill training, metformin, and/or their combination reduces the secretion of pro-inflammatory cytokines from adipose tissue. Compared to Long Evans Tokushima Otsuka (LETO) control rats

(L-Sed), sedentary OLETF (O-Sed) animals secreted significantly greater amounts of leptin from retroperitoneal (RP) adipose tissue. Conversely, secretion of interleukin (IL)-10 by O-Sed adipose tissue was lower than that of L-Sed. Examination of leptin and IL-10 secretion from adipose tissue in OLETF groups treated with endurance exercise training (O-EndEx), metformin treatment (O-Met), and combined endurance training and metformin (O-E+M) from 20-32 wks of age indicated that (i) leptin secretion from adipose tissue was reduced in O-Met and O-E+M, but not O-EndEx; (ii) adipose tissue IL-10 secretion was increased in O-EndEx and O-E+M but not in O-Met; and (iii) only the combined treatment (O-E+M) displayed both a reduction in leptin secretion and an increase in IL-10 secretion. Leptin and IL-10 concentrations in adipose tissue-conditioned buffers were correlated with their plasma concentrations as well as with adipocyte diameters and total adiposity. Overall, this study indicates that exercise training and metformin have additive influences on adipose tissue secretion and plasma concentrations of leptin and IL-10.

c. Introduction

Chronic low-grade systemic inflammation is appreciated as a critical biological link between obesity and its association with cardiovascular (CV) and metabolic diseases (1). The etiology of this inflammation seems to be initiated by excessive lipid accumulation and expansion of adipocytes, resulting in the activation of cellular stress pathways, which in turn signal the recruitment and activation of immune cells into adipose tissue (2). These cells are primarily responsible for the

increased circulating concentrations of a number of pro-inflammatory cytokines and the systemic pro-inflammatory state that is recognized as a hallmark of obesity and the metabolic syndrome (3). Indeed, inflamed adipose tissue is implicated in the pathogenesis of insulin resistance, type 2 diabetes mellitus (T2DM), endothelial dysfunction, and atherosclerosis (4).

The current standard of care for patients upon diagnosis of T2DM is pharmacologic treatment with metformin, a prescription for weight loss, and advice to become physically active (5). These therapies are well-established as effective glucose-lowering and insulin-sensitizing approaches when prescribed in isolation to insulin-resistant patient populations (6, 7), and there is some evidence to indicate that the inflammatory component of these pathologies can be ameliorated by exercise or metformin treatment when prescribed individually (8-12). The combined treatments, however, have received less attention. Exercise and metformin produced additive effects on GLUT4 protein expression in skeletal muscle of high fat, high sucrose diet-fed Zucker diabetic fatty rats, suggesting a possible metabolic benefit of the combined therapies (13). On the other hand, recent data from pre-diabetic humans indicate that exercise combined with metformin therapy may not necessarily produce favorable influences on certain metabolic syndrome parameters (7, 14). In fact, the typically-observed insulin sensitization effect of exercise training may be blunted with metformin co-therapy (7). It is unclear why the combined therapies did not produce beneficial effects, but, interestingly, the inflammatory marker C-reactive protein was reduced by both treatments individually but not by the combined therapies (14), raising the

hypothesis that inflammation may have played a role. However, the combined effects of exercise training and metformin on systemic inflammatory markers or on the inflammatory phenotype of particular sources of systemic inflammation (e.g. adipose tissue) have, to our knowledge, never been examined.

The aim of the present investigation was to test the hypothesis that exercise training, metformin, and their combination decrease secretion of inflammatory markers by adipose tissue and as a result normalize plasma concentrations of a panel of cytokines with known roles in insulin resistance and CV disease. The seven cytokines chosen for investigation have established roles in (i) immunity and inflammatory responses [i.e., leptin, interleukin(IL)-6), IL-1β, and tumor necrosis factor (TNF)-α], (ii) recruiting immune cells into inflamed tissue [i.e., IL-12p70, monocyte chemoattractant protein (MCP-1), and Regulated upon Activation, Normal T-cell Expressed, and Secreted (RANTES)], and (iii) anti-inflammatory effects via repression of pro-inflammatory cytokine activity and signaling (i.e., IL-10). Using the hyperphagic, obese, insulin resistant, type 2 diabetic Otsuka Long Evans Tokushima Fatty (OLETF) rat model, we tested the hypothesis that endurance exercise treadmill training, metformin, and/or their combination would favorably influence the secretion of these cytokines from adipose tissue. We also hypothesized that treatment effects on adipose tissue cytokine secretion would be related to effects on circulating cytokine levels, adipocyte diameter, and body composition.

d. Methods

Animals and experimental design

Male Long Evans Tokushima Otsuka (LETO; n = 10) and OLETF rats (n = 48) were obtained at four weeks of age (Tokushima Research Institute, Otsuka Pharmaceutical; Tokushima, Japan). The OLETF rat, characterized by a mutated cholestykinin-1 receptor which results in a hyperphagic phenotype, is an established model of obesity, insulin resistance, and T2DM (15). Animals were individually housed in a temperature-controlled (21°C) environment with 0600-1800 light and 1800-0600 dark cycles. At age 19 weeks, all OLETFs were exposed to 15 m/min treadmill running for 5 min/d to allow for acclimation to the running stimulus. The OLETF rats were then randomly assigned to one of four groups (n = 12/group): 1) sedentary (O-Sed), 2) endurance exercise (O-EndEx), 3) metformin treatment (O-Met), or 4) endurance exercise and metformin combined (O-E+M). Sedentary LETO (L-Sed) animals were used as healthy, non-hyperphagic controls. Treatments began at 20 weeks of age, as our group has documented that the OLETF rat becomes hyperglycemic and hyperinsulinemic at this age and elevated HbA1c (16-19). EndEx treatment initially consisted of treadmill running at a speed of 15 m/min on a 15% incline for 5 min/d. Duration and speed were gradually increased by 2-3 min/day and 1-2 m/min per wk such that by wk 4 the animals were running at a speed of 20 m/min on a 15% incline for 60 min/d, 5 d/wk. This training volume was maintained for the remainder of the experiment until animals were sacrificed. Metformin (Bosche Scientific) was administered in drinking water (150 mg/kg/d during first week, 300 mg/kg/d thereafter) (20). All groups were given

ad libitum access to standard chow with a macronutrient composition of 56% carbohydrate, 17% fat, and 27% protein (Formulab 5008, Purina Mills, St Louis, MO). Rats were anesthetized at 30-32 weeks of age with an intraperitoneal injection of sodium pentobarpital (100 mg/kg). Tissues were then harvested and the animals were killed by exsanguination. The last exercise bout for O-EndEx and O-E+M animals was performed ~18 hours prior to sacrifice. Food was removed from the cages 12 hours prior to sacrifice, and water (including metformin-treated water for O-Met and O-E+M groups) was removed on the morning of the experiment (~1 hour prior to sacrifice). All protocols were approved by the University of Missouri Animal Care and Use Committee.

Body weight, body composition, and food intake

Body weights and food intakes were monitored and recorded on a weekly basis. Weekly food intakes were averaged across the period of the intervention (age 20-30 wks). Body composition was assessed by dual energy x-ray absorptiometry (DXA; Hologic QDR-1000, calibrated for rodents) on the day of sacrifice. Omental and retroperitoneal (RP) adipose tissue depots were then removed and weighed to the nearest 0.01 g.

Blood parameters

Whole blood was collected on the day of euthanasia for analysis of glycosylated hemoglobin (HbA1c) by the boronate-affinity HPLC method (Primus Diagnostics, Kansas City, MO) in the Diabetes Diagnostics Lab at the University of Missouri. Serum samples were prepared by centrifugation and stored at -80°C until analysis. Glucose, triglyceride (TG), and non-esterified fatty acids (NEFA) assays were

performed by a commercial laboratory (Comparative Clinical Pathology Services, Columbia, MO) on an Olympus AU680 automated chemistry analyzer (Beckman-Coulter, Brea, CA) using commercially available assays according to manufacturer's guidelines. Plasma insulin concentrations were determined using a commercially available, rat-specific ELISA (Alpco Diagnostics, Salem, NH). Samples were run in duplicate and manufacturer's controls and calibrators were used according to assay instructions.

Immunohistochemistry

Formalin-fixed RP adipose tissue samples were processed through paraffin embedment, sectioned at five microns, stained with hematoxylin and eosin for morphometric determinations. Sections were examined using an Olympus BX60 photomicroscope (Olympus, Melville, NY) and photographed at 10x magnification using with a Spot Insight digital camera (Diagnostic Instruments, Inc., Sterling Heights, MI). For each sample, no less than five fields of view were selected for the analysis. The diameters of at least 100 adipocytes were measured using Image Pro imaging software (MediaCybernetics Inc., Bethesda, MD, USA). The average value of these 100 individually-measured adipocyte diameters was calculated for each rat. In addition, the distribution of cells of discrete size categories was examined as described previously (16, 21). A single blinded operator performed all imaging and adipocyte diameter measurements.

Preparation of Adipose Tissue-Conditioned Buffers

At sacrifice, RP adipose tissue depots were harvested for preparation of adipose-conditioned buffer as described previously (22), with minor modifications.

Briefly, one of the two RP fat pads were incubated in filter-sterilized physiological saline solution (pH 7.4; 6 g tissue/mL PSS) for 60 min at 37°C in a shaking water bath. In pilot experiments of 30, 60, and 120 min adipose tissue incubations, the 60 min incubation protocol produced optimal results for the purposes of the present study. PSS contained (in mM): 25 MOPS, 1.2 NaH_2PO_4, 5.0 glucose, 2.0 pyruvate, 0.02 EDTA, 145 NaCl, 4.7 KCl, 2.0 $CaCl_2$, and 1.17 $MgSO_4$. Following incubation, the tissue was discarded and the conditioned buffers were aliquoted and stored at -80°C for future analysis. Our modified approach of using 6 g tissue/mL PSS instead of 3 g tissue/mL PSS as described by Payne et al. (22) was chosen in light of the fact that their adipose tissue conditioned medium contained concentrations of cytokines that were at or near the lower limit of detection of the assay. Thus, with a more concentrated conditioned media preparation we expected to observe concentrations of cytokines that were well within the normal limits of the multiplex assay that we employed [and importantly, also used by Payne et al. (22)]. Additionally, an alternative approach would have been to use a fixed amount of adipose tissue for the conditioned buffers, rather than the whole RP fat pad and adjusting the volume of sterile PSS added to achieve the desired concentration of 6 g/mL. However, this approach would have required cutting and handling the tissue, which might have been problematic given observations from our group indicating that mincing/cutting of adipose tissue induces substantial (~200 fold) expression of inflammatory genes such as TNF-α (J.M. Company and F.W. Booth, unpublished data). Thus, all samples were handled with minimal cutting of the tissue beyond that required for the dissection and were rapidly weighed and placed

in sterile PSS. It was ensured that buffer volumes were sufficient to cover the entire sample. Finally, the use of a strong buffering agent (i.e., high concentration of MOPS) was employed to prevent unwanted confounding effects of hypoxia and any consequent metabolic acidosis.

Cytokine Concentrations in Conditioned Buffers and Plasma

Adipose tissue-conditioned buffers and plasma samples were assayed in duplicate for concentrations of leptin, IL-1β, IL-6, IL-10, IL-12p70, MCP-1, TNF-α, and RANTES using a multiplex cytokine assay (Millipore Milliplex, cat no. RCYTOMAG-80K; Billerica, MA, USA) on a MAGPIX instrument (Luminex Technologies; Luminex Corp., Austin, TX, USA) according to the manufacturer's instructions.

Statistics

One-way analysis of variance (ANOVA) was used to test for differences among groups in body weights, food intakes, % body fat, fat pad weights, adipocyte diameters, and cytokine concentrations in adipose tissue-conditioned buffers and plasma. Fisher's Least Significant Difference (LSD) post hoc comparisons were performed in the event of a significant omnibus ANOVA. All analyses were performed using SPSS version 19 (IBM, Chicago, IL, USA). Data are presented as means ± SEM, and $P \leq 0.05$ was used as the criterion for statistical significance.

e. Results

Body weight, body composition, and food intake

Mean body weights, percent body fat, fat pad masses, and food intake were all significantly greater in the O-Sed group compared to L-Sed (Fig 1A-G, $P < 0.05$).

O-EndEx, O-Met, and O-E+M groups had 15%, 6%, and 21% lower body weights than the O-Sed group, respectively (all $P < 0.05$ vs. O-Sed and $P < 0.05$ vs. each other; Fig 1A). The food intake data (Fig 1B) displayed similar patterns to the body weights, as EndEx, O-Met, and O-E+M had 12%, 7%, and 22% lower mean food intakes during wk 20-32 than the O-Sed animals, respectively (all $P < 0.05$ vs. O-Sed and $P < 0.05$ vs. each other; Fig 1B). When these food intake values were normalized to grams of body weight, OLETF groups remained significantly elevated compared to L-Sed, consistent with their hyperphagic phenotype ($P < 0.05$, Fig 1C). However, there were no differences among OLETF groups in normalized food intake ($P > 0.05$). O-EndEx and O-E+M, but not O-Met, had significantly lower % body fat than O-Sed ($P < 0.05$; Fig 1D). Similarly, O-Met RP mass was not significantly different from that of O-Sed ($P > 0.05$), whereas O-EndEx and O-E+M had 41% and 50% lower RP mass than O-Sed, respectively ($P < 0.05$; Fig 1E). O-EndEx, O-Met, and O-E+M had 55%, 25%, and 67% lower omental fat pad mass than O-Sed (all $P < 0.05$; Fig 1F). O-EndEx and O-E+M omental fat masses were not different from each other, but were significantly lower than O-Met ($P < 0.05$). Importantly, omental fat mass was not significantly different between O-E+M and L-Sed ($P > 0.05$). Epididymal fat mass also lower in O-EndEx and O-E+M groups compared to O-Sed ($P < 0.05$), but again the difference between O-Met and O-Sed was not significant ($P > 0.05$; Fig 1G). Epididymal fat mass of O-E+M was lower than that of O-EndEx and O-Met, but greater than that of L-Sed (all $P < 0.05$).

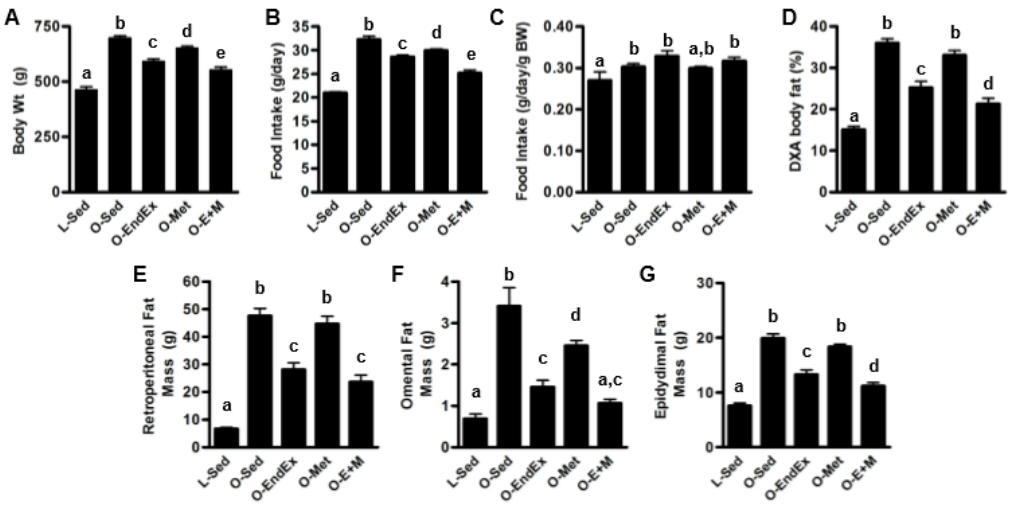

Figure 24: Effects of endurance exercise training, metformin, and their combination on (A) body weight, (B) food intake, (C) food intake normalized to body weight, (D) % body fat, and retroperitoneal (E), omental (F), and epididymal (G) fat pad masses. L-Sed, sedentary LETO; O-Sed, sedentary OLETF; O-EndEx, endurance-trained OLETF; O-Met, metformin-treated OLETF; O-E+M, combined endurance-trained and metformin-treated OLETF. Data with unlike letters are significantly different from each other ($P < 0.05$).

Blood parameters

Blood parameters are presented in Table 1. HbA1c levels were lower ($P = 1.1 \times 10^{-14}$) in L-Sed than O-Sed. Analysis of intervention effects indicated that O-EndEx, O-Met, and O-E+M had lower HbA1c levels than O-Sed (all $P < 0.05$), although only O-E+M levels were restored to levels of L-Sed such that the pairwise comparison between the two groups was not statistically significant (see exact P-values in footnote of Table 1). Serum glucose, insulin, TG, and NEFA levels were all significantly greater in O-Sed than in L-Sed (all $P < 0.05$). In O-Met these parameters were not different from levels in O-Sed, whereas O-EndEx and O-E+M levels were significantly lower than O-Sed ($P < 0.05$). Further, insulin levels were completely normalized in O-EndEx rats to L-Sed levels, while lucose, insulin and TG were all completely normalized in O-E+M (although the P-values for TG approached statistical significance; see footnote of Table 1).

Table 3. Blood Parameters

	L-Sed	O-Sed	O-EndEx	O-Met	O-E+M
Glucose (mg/dl)	152 ± 4[a]	300 ± 12[b]	236 ± 22[c]	283 ± 21[b]	189 ± 9[a]
Insulin (ng/ml)	3.1 ± 0.4[a]	8.2 ± 2.1[b]	4.4 ± 0.5[a]	7.1 ± 1.0[b]	4.3 ±0.3[a]
HbA1c (%)	4.9 ± 0.04[a]	7.0 ± 0.13[b]	5.4 ± 0.03[c]	5.3 ± 0.06[c]	5.0 ± 0.04[a,c]
TG (mg/dl)	44 ± 3[a]	360 ± 40[b]	121 ± 15[a*]	337 ± 46[b]	125 ± 26[a*]
NEFA (mmol/l)	0.28 ± 0.02[a]	0.92 ± 0.06[b]	0.57 ± 0.05[c]	0.89 ± 0.06[b]	0.53 ± 0.07[c]

Data are means ± SEM. Values with like letters are significantly different from each other. P-values for HbA1c vs L-Sed were as follows: O-EndEx: P = 0.01; O-Met: P = 0.05; O-E+M: P = 0.52

**P = 0.08 and 0.07 for O-EndEx vs. L-Sed and O-E+M vs. L-Sed comparisons, respectively.*

Adipocyte Diameters

The O-Sed group had significantly more adipocytes of larger sizes, i.e. the RP adipocyte diameter distribution curve of the O-Sed group was shifted to the right, relative to the L-Sed group (Fig 2A). Among the OLETF intervention groups, only the O-E+M rats displayed an adipocyte diameter distribution that resembled that of the L-Sed (Fig 2A). Analysis of adipocyte diameter summary data (Fig 2B) indicated that O-Sed had significantly larger average adipocyte diameters compared to L-Sed ($P < 0.05$), and O-E+M average adipocyte diameters were significantly smaller than those of O-Sed and not significantly different from L-Sed ($P > 0.05$; Fig 2B). O-EndEx adipocyte diameters did not differ from other intervention groups.

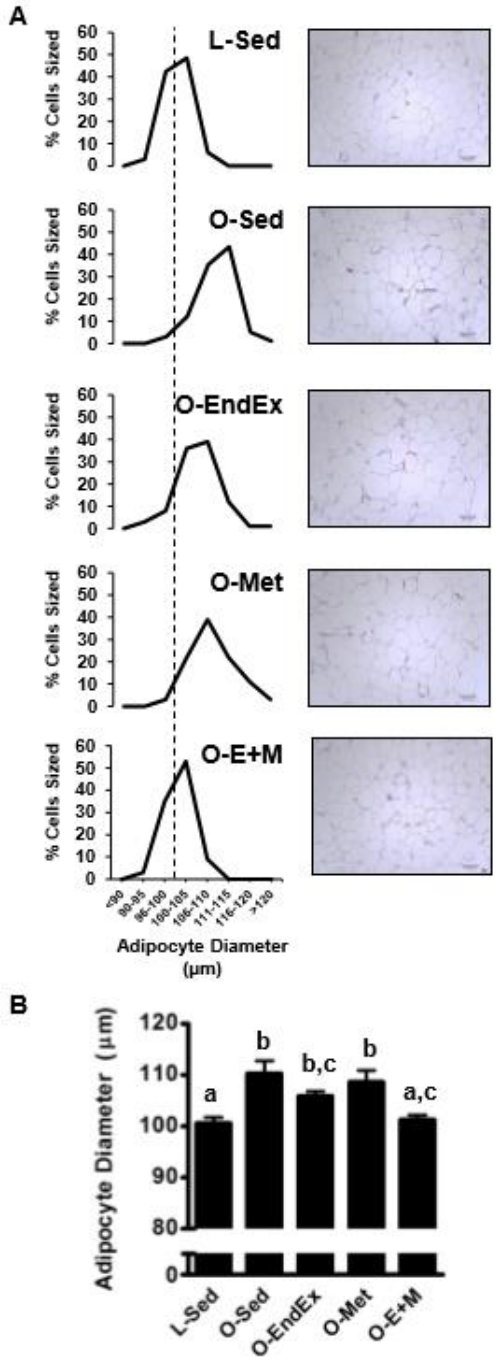

Figure 25. Distribution of retroperitoneal adipocyte diameters (A) and summary data (B) among groups (L-Sed, sedentary LETO; O-Sed, sedentary OLETF; O-EndEx, endurance-trained OLETF; O-Met, metformin-treated OLETF; O-E+M, combined endurance-trained and metformin-treated OLETF). Data with unlike letters are significantly different from each other ($P < 0.05$).

Retroperitoneal Adipose Tissue Cytokine Secretion and Plasma Cytokine Concentrations.

RP Adipose tissue-secreted leptin (Fig 3A) was greater in O-Sed than L-Sed (2.6-fold, $P < 0.05$), while that in O-EndEx, O-Met, and O-E+M were lower than O-Sed by 18% (trend: $P = 0.07$), 33% ($P < 0.05$), and 50% ($P < 0.05$), respectively. IL-10 secretion was 43% lower in O-Sed than L-Sed ($P < 0.05$; Fig 3B). O-EndEx and O-E+M had IL-10 secretion levels that were ~130-140% greater than O-Sed levels ($P = 0.02$ and $P = 0.03$, respectively) and not different from L-Sed levels ($P = 0.75$ and $P = 0.94$, respectively), while O-Met IL-10 secretion was not different from O-Sed, O-EndEx, or O-E+M groups (Fig 3B). As there were substantial differences among groups in RP mass, it is possible that the contribution of this depot to systemic (plasma) levels of leptin and IL-10 were linked to differences in RP mass. Thus, to account for differences in fat pad weights, we calculated secretion levels from the whole fat pad as the product of leptin and IL-10 concentrations in the conditioned buffer (pg/mL) × RP mass (g). O-Sed levels of leptin secretion from the whole RP pad were ~17-fold higher than those of the L-Sed group ($P < 0.05$), while O-EndEx, O-Met, and O-E+M had 57%, 45%, and 77% lower levels than O-Sed (all $P < 0.05$; Fig 3C). O-Sed levels of IL-10 secretion from the whole RP pad were ~3-fold greater than those of the L-Sed group ($P < 0.05$), whereas there were no significant differences among O-Sed and the intervention groups ($P > 0.05$; Fig 3D).

Plasma leptin levels were 9-fold higher in O-Sed compared to L-Sed ($P < 0.05$), whereas O-EndEx and O-E+M had 65% and 75% lower plasma leptin levels compared to O-Sed, respectively ($P < 0.05$; Fig 3E). Plasma IL-10 levels were

greater in all OLETF groups than L-Sed ($P < 0.05$), and although the mean IL-10 levels were highest in O-EndEx, the differences among OLETF groups were not statistically significant (Fig 3F).

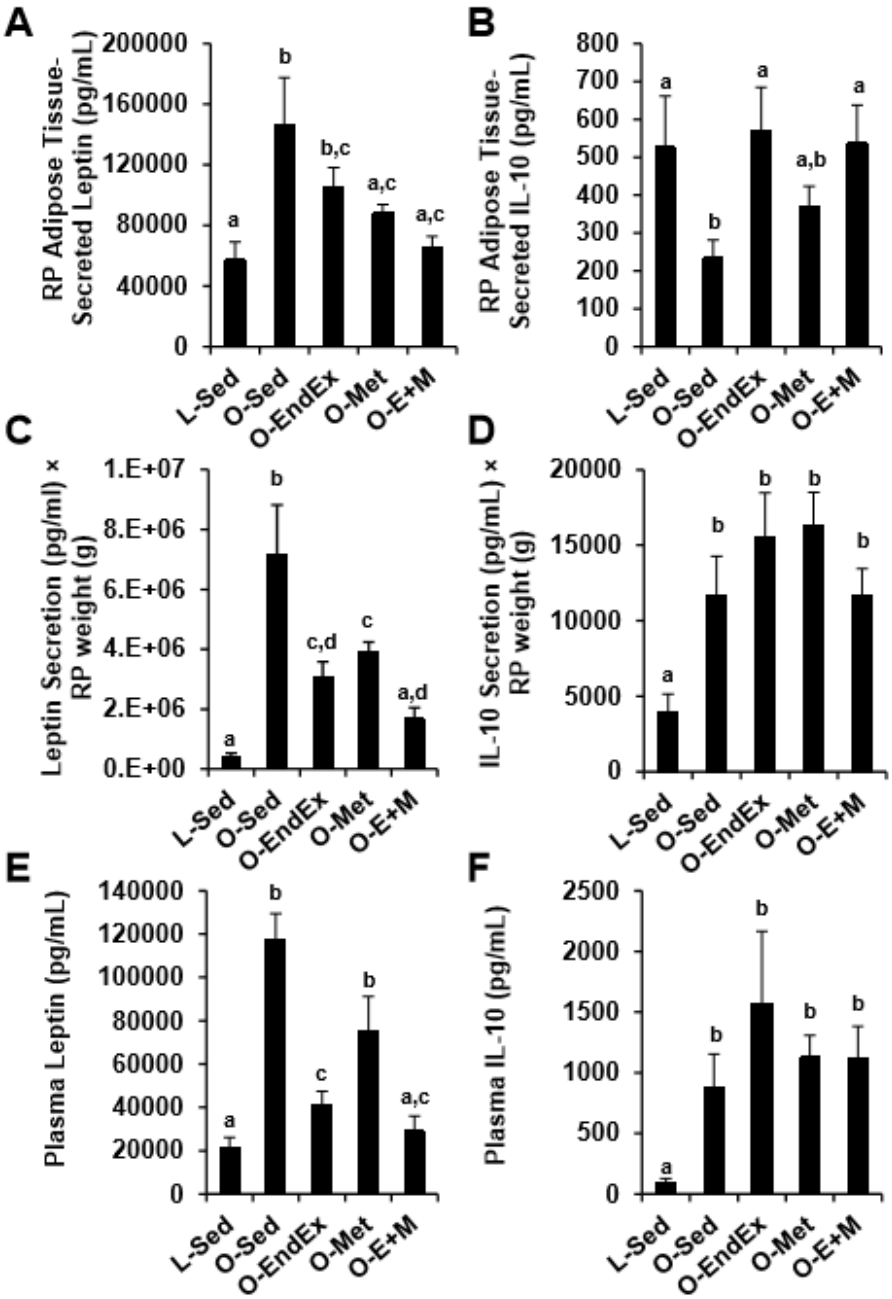

Figure 26. Effects of endurance exercise training, metformin, and their combination on leptin secretion from retroperitoneal (RP) adipose tissue (A), IL-10 secretion from RP adipose tissue (B), leptin secretion × RP mass (C), IL-10 secretion × RP mass (D), plasma leptin concentrations (E), and plasma IL-10 concentrations (F). L-Sed, sedentary LETO; O-Sed, sedentary OLETF; O-EndEx, endurance-trained OLETF; O-Met, metformin-treated OLETF; O-E+M, combined endurance-trained and metformin-treated OLETF. Data with unlike letters are significantly different from each other ($P < 0.05$).

To investigate the functional implications of the effects of the endurance exercise training, metformin, and combined interventions on adipose tissue cytokine secretion, we examined the relationships among mean concentrations of leptin (Fig 4A) and IL-10 (Fig 4B) present in adipose tissue-conditioned buffers vs. their mean plasma concentrations. There was a positive linear relationship between concentrations of leptin in adipose tissue-conditioned buffers and plasma across group means ($r = 0.85$, Fig 4A). Similarly, there was a strong relationship between secreted and circulating IL-10 concentrations ($r = 0.81$, Fig 4B), although this relationship was only observed within the OLETF rats (i.e., when L-Sed means were excluded from the analysis; there was no apparent relationship with all groups included). The relationships among group means in plasma leptin and IL-10 concentrations with their respective secretion levels from the whole fat pad (pg/mL × g tissue) were quite strong ($r = 0.97$ for leptin, $r = 0.92$ for IL-10; Fig 4C and D).

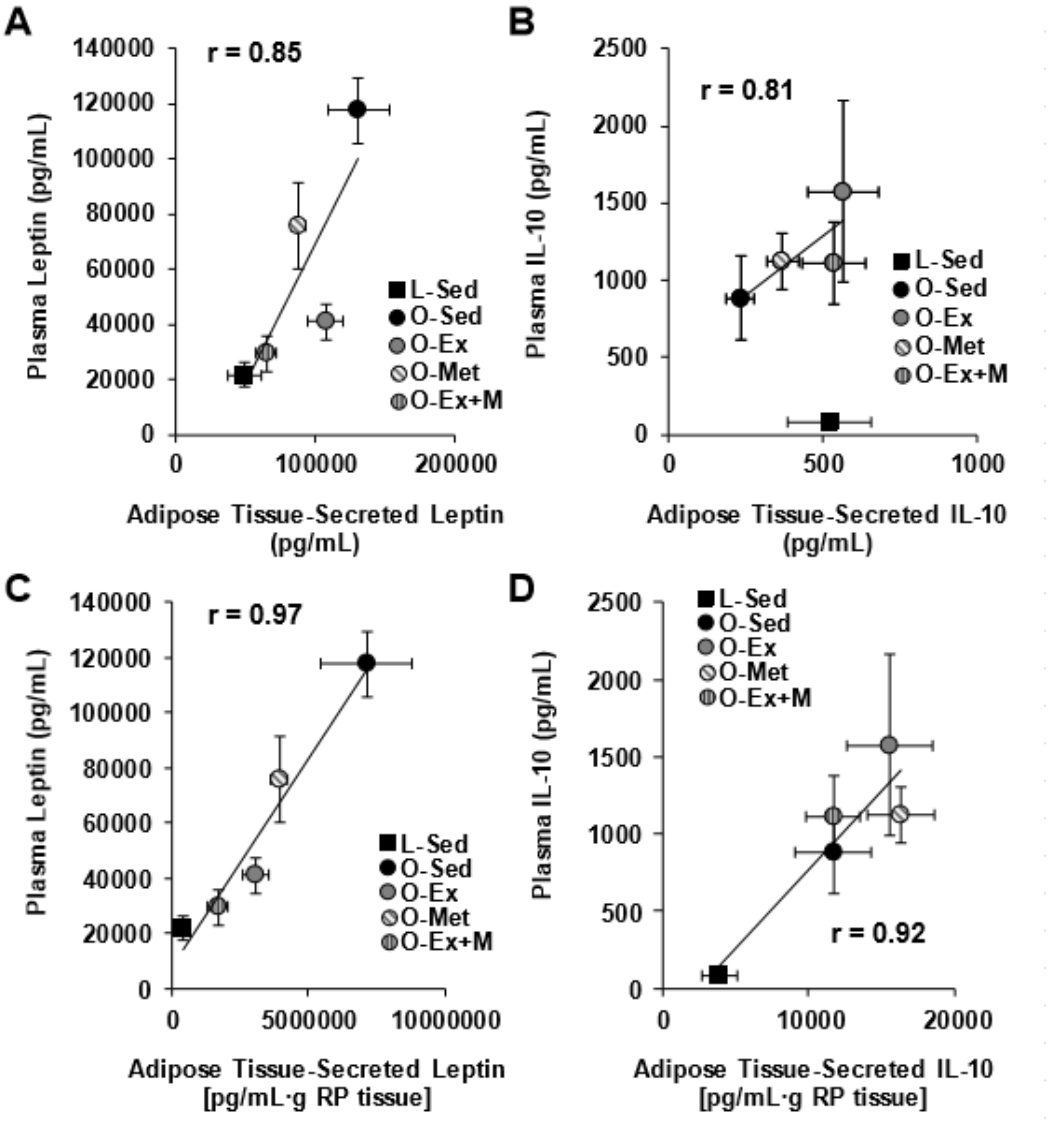

Figure 27. Correlations between (A) leptin concentrations in RP adipose tissue-conditioned buffers and plasma leptin concentrations; (B) IL-10 concentrations in RP adipose tissue-conditioned buffers and plasma IL-10 concentrations; (C) the product of leptin secretion × RP mass and plasma leptin concentrations; and (D) the product of IL-10 secretion × RP mass and plasma IL-10 concentrations. L-Sed, sedentary LETO; O-Sed, sedentary OLETF; O-EndEx, endurance-trained OLETF; O-Met, metformin-treated OLETF; O-E+M, combined endurance-trained and metformin-treated OLETF. Note that relationship shown for IL-10 (B) is among OLETF groups only.

Adipocyte diameter group means were strongly and positively related to means for adipose tissue-secreted leptin (r = 0.87; Fig 5A) and negatively related to means for adipose tissue-secreted IL-10 (r = -0.81; Fig 5B). Similarly, % body fat means were positively related to adipose tissue-secreted leptin (r = 0.83; Fig 5C) and negatively related to adipose tissue-secreted IL-10 (r = -0.83; Fig 5D).

To gain insight into whether these treatment effects on leptin and IL-10 RP adipose tissue secretion and their plasma concentrations were related to our observations of improved HbA1c levels, we also examined correlations among mean concentrations of plasma leptin and IL-10 concentrations vs. HbA1c levels. Although there was only a weak relationship between plasma IL-10 and HbA1c among the groups (r = 0.20), the relationship between plasma leptin and HbA1c was robust (r = 0.91, Fig 6).

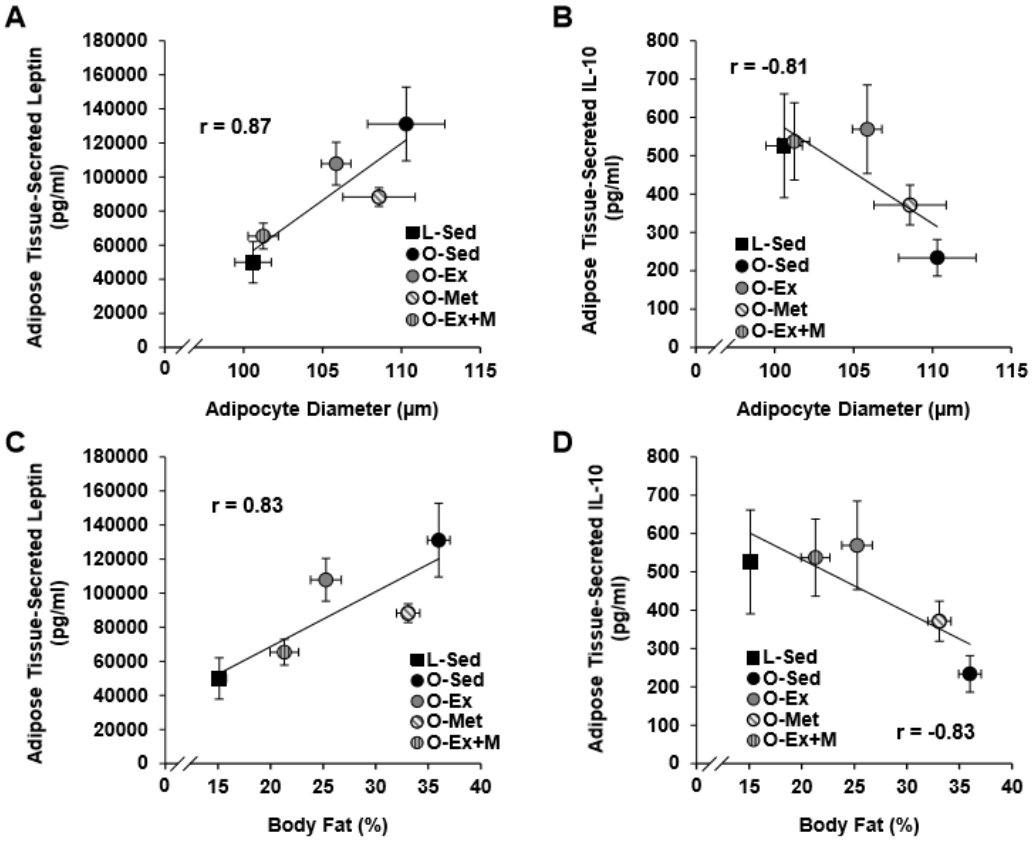

Figure 28. Correlations between adipocyte diameters and retroperitoneal (RP) adipose tissue-secreted leptin (A) and IL-10 (B), as well as % body fat and secreted leptin (C) and IL-10 (D). L-Sed, sedentary LETO; O-Sed, sedentary OLETF; O-EndEx, endurance-trained OLETF; O-Met, metformin-treated OLETF; O-E+M, combined endurance-trained and metformin-treated OLETF.

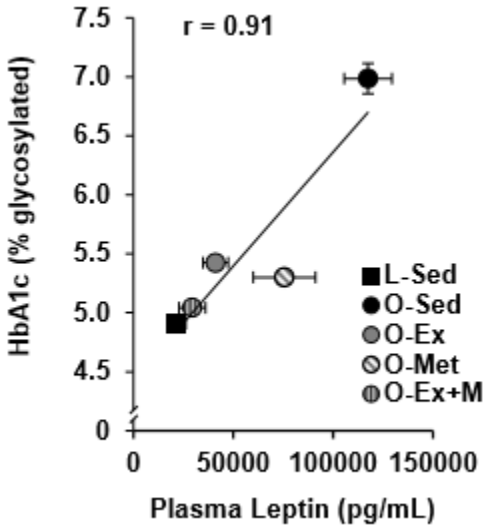

Figure 29. Correlation between plasma leptin and HbA1c levels. L-Sed, sedentary LETO; O-Sed, sedentary OLETF; O-EndEx, endurance-trained OLETF; O-Met, metformin-treated OLETF; O-E+M, combined endurance-trained and metformin-treated OLETF.

The remaining cytokines examined are presented in Table 2 (adipose tissue) and Table 3 (plasma). There were few statistically significant differences among groups in these cytokines in adipose tissue-conditioned buffers, with the exceptions of higher MCP-1 and IL-6 secretion in L-Sed compared to the other groups, and TNF-α and IL12-p70 being lowest in O-E+M (all $P < 0.05$; Table 2A). Secretion levels of IL-1β, IL-12p70, MCP-1, and RANTES from the whole RP fat pad (pg/mL × g RP mass) were significantly greater in O-Sed than L-Sed (all $P < 0.05$; Table 2B). The elevations in O-Sed animals in IL-1β were partially corrected in O-EndEx and O-E+M ($P < 0.05$ vs. O-Sed) but not restored to level of L-Sed, while O-Met levels were higher than those of L-Sed and not different from O-Sed. IL-12p70, MCP-1, and TNF-α were completely normalized (i.e., not different from L-Sed) in the O-EndEx and O-E+M groups, but not in O-Met. RANTES secretion levels from the RP pad were partially reversed in the O-EndEx group, not different between O-Met and O-Sed, and completely reversed in the O-E+M group.

In plasma (Table 3), O-Sed had significantly higher IL-6 and IL12p70 concentrations than L-Sed, but there were no differences among O-Sed and the OLETF intervention groups ($P > 0.05$). Plasma MCP-1 concentrations were lower in O-EndEx and O-E+M than all other groups ($P < 0.05$). There were no significant relationships between adipose tissue-conditioned buffer and plasma concentrations among cytokines other than leptin and IL-10.

Table 4. Adipose tissue-conditioned buffer cytokine concentrations.

A. Conditioned-Buffer (pg/mL)	L-Sed	O-Sed	O-EndEx
IL-1β	458 ± 180	260 ± 34	318 ± 55
IL-6	445 ± 128[a]	140 ± 50[b]	129 ± 41[b]
IL-12p70	18 ± 4 [a,b]	15 ± 3 [a,b]	12 ± 1 [a,b]
MCP-1	98 ± 22[a]	62 ± 8[b]	57 ± 7[b]
TNF-α	11 ± 2[a]	8 ± 2[a,b]	7 ± 1[a,b]
RANTES	674 ± 191	537 ± 49	574 ± 106
B. Conditioned-Buffer (pg/mL) × RP mass (g)	L-Sed	O-Sed	O-EndEx
IL-1β	3316 ± 1329[a]	12728 ± 1815[b]	8781 ± 1315[c]
IL-6	3280 ± 1146	7203 ± 2704	3173 ± 794
IL-12p70	130 ± 39[a]	717 ± 111[b,c]	351 ± 53[a,b]
MCP-1	725 ± 193[a]	3042 ± 457[b]	1577 ± 226[a,c]
TNF-α	74 ± 19[a]	367 ± 90[b]	179 ± 46[a,c]
RANTES	4861 ± 1449[a]	26276 ± 3370[b]	15955 ± 3243[c]

Data are means ± SEM. Values with unlike letters are significantly different from each other (P < 0.05).

Table 5. Plasma cytokine concentrations.

	L-Sed
IL-1β	ND
IL-6	14 ± 10[a]
IL-12p70	10 ± 3[a]
MCP-1	36 ± 16[a]
TNF-α	3 ± 1
RANTES	1213 ± 189

Data are means ± SEM. Units are pg/mL. Values with unlike letters are significantly different from each other (P < 0.05).

f. Discussion

The major findings of the current study are (i) leptin secretion from adipose tissue is reduced by metformin with or without endurance exercise treadmill training; (ii) IL-10 secretion from adipose tissue is increased by treadmill exercise training with or without metformin; and (iii) only the combination of endurance training and metformin is effective in both reducing leptin secretion and increasing IL-10 secretion in the OLETF rat model of obesity and insulin resistance. These treatment effects on adipose tissue leptin and IL-10 secretion were closely linked to effects on adipocyte diameter and body composition as well as to effects on plasma concentrations. Importantly, our finding that IL-10 secretion was enhanced by exercise training is the first indication to our knowledge that exercise training can increase secretion of an anti-inflammatory factor from adipose tissue. These data highlight the notion put forth by our group (23) and others that exercise has a beneficial impact on other tissues besides skeletal muscle. Overall, this study provides evidence from an obese rodent model that treatment of insulin resistance/T2DM with exercise training, metformin, and particularly the two treatments combined can favorably alter adipose tissue secretion and plasma concentrations of leptin and IL-10 and shift the adipose tissue towards an anti-inflammatory phenotype.

Leptin is secreted primarily from white adipose tissue and while originally thought to just function as a satiety hormone, it is now known that in excess, it may have potent deleterious effects on numerous tissues (24-26). The most consistent circulating leptin-lowering effects of exercise have been observed when weight

loss is achieved (27-32). Indeed the available data suggest that regular exercise without weight loss has little effect on circulating leptin concentrations (27, 30) or leptin gene expression in adipose tissue (33, 34). Our data are in line with these previous observations, as leptin secretion and circulating levels were restored in O-E+M to the lower levels seen in the L-Sed rats. As this reversal was not observed in either O-EndEx or O-Met alone, our data stimulate the hypothesis for future studies that combined metformin therapy and lifestyle modification with exercise training may be optimal for the reduction of circulating leptin concentrations in obese, insulin resistant humans. Furthermore, data from rodents (16, 35, 36) and humans (28, 29) also support the idea that alterations in adipocyte size are closely associated with circulating leptin concentrations. This is in agreement with our observed relationship between adipocyte diameters and adipose tissue leptin secretion, which was, in turn, related to plasma leptin concentrations (whether expressed as concentrations in the conditioned buffers or as secretion from the whole fat pad). There is some evidence that metformin also is effective in reducing plasma leptin concentrations (9) and *in vitro* secretion from cultured adipose tissue (37); however, the combined treatments have not been previously investigated. Therefore, our study provides the first evidence that the combination of exercise and metformin treatment initiated at the onset of T2DM and moderate insulin resistance not only reduces the secretion of leptin from adipose tissue, but restores leptin secretion to the level seen in lean healthy rats (L-Sed).

The anti-inflammatory actions of IL-10 include suppression of NFκB induction by pro-inflammatory cytokines (e.g. TNF-α and IL-1β) and stimulation of an anti-inflammatory gene expression program (38). It seems possible that the effect on adipose tissue IL-10 could have systemic consequences for circulating levels of IL-10, as secreted and plasma IL-10 levels were correlated within the OLETF groups. Thus, given the well-established anti-inflammatory role of IL-10, our data suggest that adipose tissue-derived IL-10 may be a signal participating in the beneficial effects of exercise on numerous tissues. Our data are generally consistent with previous findings regarding the effects of endurance training on IL-10 secretion/expression by different cell types. Basal IL-10 production by circulating monocytes has been documented to increase by ~10 fold following 6 months of moderate endurance exercise training in patients at risk for ischemic heart disease (39). Exercise training also increased IL-10 expression in RP fat in a cachectic rodent model (40) as well as in healthy rats (41). To the best of our knowledge, the effects of metformin on adipose tissue-secreted or circulating levels of IL-10 have not been previously studied. The present study suggests that metformin therapy alone does not alter IL-10 secretion from adipose tissue.

Although we have focused the present report on our leptin and IL-10 data, there were some notable findings regarding the other cytokines included in our panel. First, our findings of greater adipose tissue IL-6 secretion in L-Sed compared to all OLETF groups (Table 2A) with greater IL-6 plasma concentrations in O-Sed compared to L-Sed (Table 3) were unexpected. However, based on prior evidence that IL-6 can stimulate lipolysis in adipocytes (42), and the smallest adipocyte

diameters being associated with the highest IL-6 secretion in L-Sed and O-E+M groups in our study, we can speculate that the greater IL-6 release from adipose tissue in these groups may reflect the known lipolytic effects of IL-6. Regarding our plasma IL-6 data, chronic circulating IL-6 concentrations are elevated in patients with inflammatory conditions such as CV disease and T2DM, consistent with our findings. However, IL-6 unequivocally has anti-inflammatory effects on several organs and tissues (12, 43), and it is now that a high circulating level of IL-6 in chronic low-grade inflammatory states does not necessarily mean that IL-6 is pro-inflammatory in every condition (11). In addition, plasma MCP-1 and IL-12p70 were elevated in O-Sed and reduced to near L-Sed levels in O-EndEx, further supporting the efficacy of regular exercise for the reduction of systemic inflammation. However, these effects were not totally consistent with concentrations observed in adipose tissue-conditioned buffers. Indeed secretion of MCP-1 and several other cytokines (although only MCP-1 reached statistical significance) was, surprisingly, higher in L-Sed than all OLETF groups. A possible explanation for these dissociations between cytokine concentrations in the RP adipose tissue-conditioned buffers (Table 2A) and plasma concentrations (Table 3) might be the fact that hyperphagia/obesity (O-Sed) and the different interventions produced markedly different total RP weights among the groups (Fig 1E). Thus, the total contribution of adipose tissue-derived cytokines to the plasma concentrations might be driven by not only the amount of secretion per unit of tissue but also by the tissue mass. To gain insight into this issue, we calculated the product of cytokine concentrations in the conditioned buffers × RP mass (Fig

4C and D and Table 2B). This metric seems to provide an index of RP adipose tissue contribution to the systemic circulation, as (i) total RP secretions of leptin and IL-10 were closely linked to their plasma concentrations, (ii) the differences between L-Sed and O-Sed groups in MCP-1 secretion from the whole RP pad were more in line with plasma concentrations, and (iii) O-EndEx and O-E+M animals experienced partial or complete restoration to L-Sed levels of several cytokines (IL-1β, IL-12p70, MCP-1, TNF-α, and RANTES) when taking into account the differences among groups in RP fat mass in this manner. Thus, taken together, these data indicate that exercise training, metformin, and particularly their combination might favorably influence the mass and the inflammatory phenotype of the adipose tissue in the OLETF rat, with potential functional relevance for systemic (plasma) levels of the adipose-derived cytokines we examined.

Metformin increases fat oxidation during exercise (44), which could explain why our O-E+M rats had smaller adipocyte diameters, lower % fat, and lower omental fat mass than the O-EndEx group. As the current literature supports the idea that the key initiating step in adipose tissue inflammation is adipocyte hypertrophy and subsequent infiltration of inflammatory immune cells (1, 45), we speculate that the normalization (i.e., complete restoration to L-Sed levels) of adipocyte diameter in the O-E+M group is an important mechanism underlying our observation of normalized HbA1c levels in this group. In support of this speculation, our data indicate that only O-E+M animals exhibited complete normalization in adipocyte diameter, which was also associated with complete normalization of leptin secretion, and plasma leptin levels, which were, in turn, associated with the

normalized HbA1c levels (Fig 6). These data are consistent with the notion that adipocyte hypertrophy (more so than increases in % fat or adipose tissue mass, which were *not* restored to L-Sed levels in any OLETF intervention group) is a key therapeutic target for the treatment of obesity-related CV and metabolic complications (45).

Recent studies in humans indicate that adding metformin to exercise training might actually *blunt* favorable training-induced adaptations in CV/metabolic variables in the OLETF rat such as insulin sensitivity (7) and metabolic syndrome score (14). In contrast, we observed additive beneficial effects of the combined therapies on glucose, insulin and HbA1c, such that O-E+M levels were restored to L-Sed levels. Thus, there is clearly a need for further work to reconcile the discrepancy between the previous findings from humans and the present data from the OLETF rat model. Nevertheless, our findings of improved HbA1c, glucose, and insulin levels were closely linked to adipose tissue-secreted leptin and plasma leptin concentrations. As leptin can inhibit insulin-stimulated glucose uptake in skeletal muscle and adipose tissue (46-48), it seems possible that attenuated adipose tissue-derived leptin secretion might play a mechanistic role in the favorable effects of combined endurance training and metformin treatment on glycemic control in the OLETF rat model.

In summary, combined metformin and exercise training treatment had more potent effects than either treatment alone on adipose tissue secretion and plasma concentrations of IL-10 and leptin in OLETF rats. These effects of combined exercise training and metformin were associated with complete reversal of

elevations in serum glucose and insulin levels, HbA1c, omental fat mass, and adipocyte diameters. Overall, we conclude that the combination of exercise training and metformin therapy may be an effective approach to attenuate the adipose tissue inflammation associated with obesity and metabolic disease.

g. References

1. Bays HE. Adiposopathy is "sick fat" a cardiovascular disease? J Am Coll Cardiol. 2011;57(25):2461-73. Epub 2011/06/18. doi: S0735-1097(11)01312-X [pii] 10.1016/j.jacc.2011.02.038. PubMed PMID: 21679848.

2. Shoelson SE, Lee J, Goldfine AB. Inflammation and insulin resistance. J Clin Invest. 2006;116(7):1793-801. Epub 2006/07/11. doi: 10.1172/JCI29069. PubMed PMID: 16823477; PubMed Central PMCID: PMC1483173.

3. Fain JN. Release of inflammatory mediators by human adipose tissue is enhanced in obesity and primarily by the nonfat cells: a review. Mediators Inflamm. 2010;2010:513948. Epub 2010/05/29. doi: 10.1155/2010/513948. PubMed PMID: 20508843; PubMed Central PMCID: PMC2874930.

4. Donath MY, Shoelson SE. Type 2 diabetes as an inflammatory disease. Nature reviews Immunology. 2011;11(2):98-107. Epub 2011/01/15. doi: nri2925 [pii]10.1038/nri2925. PubMed PMID: 21233852.

5. Standards of medical care in diabetes--2012. Diabetes care. 2012;35 Suppl 1:S11-63. Epub 2012/01/04. doi: 35/Supplement_1/S11 [pii] 10.2337/dc12-s011. PubMed PMID: 22187469.

6. Diabetes. Reduction in the Incidence of Type 2 Diabetes with Lifestyle Intervention or Metformin. New England Journal of Medicine. 2002;346(6):393-403. doi:10.1056/NEJMoa012512.

7. Malin SK, Gerber R, Chipkin SR, Braun B. Independent and combined effects of exercise training and metformin on insulin sensitivity in individuals with prediabetes. Diabetes care. 2012;35(1):131-6. Epub 2011/11/02. doi: dc11-0925 [pii] 10.2337/dc11-0925. PubMed PMID: 22040838; PubMed Central PMCID: PMC3241331.

8. Tan BK, Heutling D, Chen J, Farhatullah S, Adya R, Keay SD, et al. Metformin decreases the adipokine vaspin in overweight women with polycystic ovary syndrome concomitant with improvement in insulin sensitivity and a decrease in insulin resistance. Diabetes. 2008;57(6):1501-7. Epub 2008/04/01. doi: db08-0127 [pii]

10.2337/db08-0127. PubMed PMID: 18375437.
9. Gomez-Diaz RA, Talavera JO, Pool EC, Ortiz-Navarrete FV, Solorzano-Santos F, Mondragon-Gonzalez R, et al. Metformin decreases plasma resistin concentrations in pediatric patients with impaired glucose tolerance: a placebo-controlled randomized clinical trial. Metabolism: clinical and experimental. 2012. Epub 2012/03/20. doi: S0026-0495(12)00072-8 [pii]10.1016/j.metabol.2012.02.003. PubMed PMID: 22424822.

10. Pedersen BK. The diseasome of physical inactivity--and the role of myokines in muscle--fat cross talk. The Journal of physiology. 2009;587(Pt 23):5559-68. Epub 2009/09/16. doi: jphysiol.2009.179515 [pii]10.1113/jphysiol.2009.179515. PubMed PMID: 19752112; PubMed Central PMCID: PMC2805368.

11. Pedersen BK, Febbraio MA. Muscles, exercise and obesity: skeletal muscle as a secretory organ. Nat Rev Endocrinol. 2012. Epub 2012/04/05. doi: 10.1038/nrendo.2012.49 [pii]. PubMed PMID: 22473333.

12. Petersen AM, Pedersen BK. The anti-inflammatory effect of exercise. Journal of Applied Physiology. 2005;98(4):1154-62.

13. Smith AC, Mullen KL, Junkin KA, Nickerson J, Chabowski A, Bonen A, et al. Metformin and exercise reduce muscle FAT/CD36 and lipid accumulation and blunt the progression of high-fat diet-induced hyperglycemia. Am J Physiol Endocrinol Metab. 2007;293(1):E172-81. Epub 2007/03/22. doi: 00677.2006 [pii] 10.1152/ajpendo.00677.2006. PubMed PMID: 17374701.

14. Malin SK, Nightingale J, Choi SE, Chipkin SR, Braun B. Metformin modifies the exercise training effects on risk factors for cardiovascular disease in impaired glucose tolerant adults. Obesity (Silver Spring, Md). 2012. Epub 2012/05/26. doi: 10.1038/oby.2012.133 oby2012133 [pii]. PubMed PMID: 22628020.

15. Kawano K, Hirashima T, Mori S, Saitoh Y, Kurosumi M, Natori T. Spontaneous long-term hyperglycemic rat with diabetic complications. Otsuka Long-Evans Tokushima Fatty (OLETF) strain. Diabetes. 1992;41(11):1422-8. Epub 1992/11/01. PubMed PMID: 1397718.

16. Laye MJ, Rector RS, Warner SO, Naples SP, Perretta AL, Uptergrove GM, et al. Changes in visceral adipose tissue mitochondrial content with type 2 diabetes and daily voluntary wheel running in OLETF rats. The Journal of physiology. 2009;587(Pt 14):3729-39. Epub 2009/06/06. doi: jphysiol.2009.172601 [pii] 10.1113/jphysiol.2009.172601. PubMed PMID: 19491243; PubMed Central PMCID: PMC2742294.

17. Bunker AK, Arce-Esquivel AA, Rector RS, Booth FW, Ibdah JA, Laughlin MH. Physical activity maintains aortic endothelium-dependent relaxation in the obese type 2 diabetic OLETF rat. American journal of physiology Heart and circulatory physiology. 2010;298(6):H1889-901. Epub 2010/03/23. doi: 10.1152/ajpheart.01252.2009. PubMed PMID: 20304812; PubMed Central PMCID: PMCPMC2886626.

18. Rector RS, Uptergrove GM, Borengasser SJ, Mikus CR, Morris EM, Naples SP, et al. Changes in skeletal muscle mitochondria in response to the development of type 2 diabetes or prevention by daily wheel running in hyperphagic OLETF rats. Am J Physiol Endocrinol Metab. 2010;298(6):E1179-87. Epub 2010/03/18. doi: ajpendo.00703.2009 [pii] 10.1152/ajpendo.00703.2009. PubMed PMID: 20233940; PubMed Central PMCID: PMC2886529.

19. Rector RS, Thyfault JP, Uptergrove GM, Morris EM, Naples SP, Borengasser SJ, et al. Mitochondrial dysfunction precedes insulin resistance and hepatic steatosis and contributes to the natural history of non-alcoholic fatty liver disease in an obese rodent model. Journal of hepatology. 2010;52(5):727-36. Epub 2010/03/30. doi: 10.1016/j.jhep.2009.11.030. PubMed PMID: 20347174; PubMed Central PMCID: PMCPMC3070177.

20. Matsumoto T, Noguchi E, Ishida K, Kobayashi T, Yamada N, Kamata K. Metformin normalizes endothelial function by suppressing vasoconstrictor prostanoids in mesenteric arteries from OLETF rats, a model of type 2 diabetes. American journal of physiology Heart and circulatory physiology. 2008;295(3):H1165-H76. Epub 2008/07/22. doi: 00486.2008 [pii] 10.1152/ajpheart.00486.2008. PubMed PMID: 18641273.

21. Laye MJ, Thyfault JP, Stump CS, Booth FW. Inactivity induces increases in abdominal fat. J Appl Physiol. 2007;102(4):1341-7. Epub 2006/11/24. doi: 01018.2006 [pii]10.1152/japplphysiol.01018.2006. PubMed PMID: 17122374.

22. Payne GA, Borbouse L, Bratz IN, Roell WC, Bohlen HG, Dick GM, et al. Endogenous adipose-derived factors diminish coronary endothelial function via inhibition of nitric oxide synthase. Microcirculation (New York, NY : 1994). 2008;15(5):417-26. Epub 2008/06/25. doi: 792840150 [pii] 10.1080/10739680701858447. PubMed PMID: 18574744; PubMed Central PMCID: PMC3042130.

23. Thyfault JP, Rector RS. Exercise: not just a medicine for muscle? The Journal of physiology. 2010;588(Pt 15):2687-8. Epub 2010/08/03. doi: 588/15/2687 [pii]

10.1113/jphysiol.2010.193797. PubMed PMID: 20675815; PubMed Central PMCID: PMC2956892.

24. Knudson JD, Payne GA, Borbouse L, Tune JD. Leptin and mechanisms of endothelial dysfunction and cardiovascular disease. Curr Hypertens Rep. 2008;10(6):434-9. Epub 2008/10/31. PubMed PMID: 18959828.

25. Parola M, Marra F. Adipokines and redox signaling: impact on fatty liver disease. Antioxid Redox Signal. 2011;15(2):461-83. Epub 2011/01/05. doi: 10.1089/ars.2010.3848. PubMed PMID: 21194387.

26. Hall JE, da Silva AA, do Carmo JM, Dubinion J, Hamza S, Munusamy S, et al. Obesity-induced hypertension: role of sympathetic nervous system, leptin, and melanocortins. The Journal of biological chemistry. 2010;285(23):17271-6. Epub 2010/03/30. doi: R110.113175 [pii]

10.1074/jbc.R110.113175. PubMed PMID: 20348094; PubMed Central PMCID: PMC2878489.

27. Lowndes J, Zoeller RF, Caplan JD, Kyriazis GA, Moyna NM, Seip RL, et al. Leptin responses to long-term cardiorespiratory exercise training without concomitant weight loss: a prospective study. J Sports Med Phys Fitness. 2008;48(3):391-7. Epub 2008/11/01. PubMed PMID: 18974728.

28. Kraemer RR, Kraemer GR, Acevedo EO, Hebert EP, Temple E, Bates M, et al. Effects of aerobic exercise on serum leptin levels in obese women. European journal of applied physiology and occupational physiology. 1999;80(2):154-8. Epub 1999/07/17. PubMed PMID: 10408327.

29. Polak J, Klimcakova E, Moro C, Viguerie N, Berlan M, Hejnova J, et al. Effect of aerobic training on plasma levels and subcutaneous abdominal adipose tissue gene expression of adiponectin, leptin, interleukin 6, and tumor necrosis factor alpha in obese women. Metabolism: clinical and experimental. 2006;55(10):1375-81. Epub 2006/09/19. doi: S0026-0495(06)00213-7 [pii]10.1016/j.metabol.2006.06.008. PubMed PMID: 16979409.

30. Thong FS, Hudson R, Ross R, Janssen I, Graham TE. Plasma leptin in moderately obese men: independent effects of weight loss and aerobic exercise. Am J Physiol Endocrinol Metab. 2000;279(2):E307-13. Epub 2000/07/27. PubMed PMID: 10913030.

31. Perusse L, Collier G, Gagnon J, Leon AS, Rao DC, Skinner JS, et al. Acute and chronic effects of exercise on leptin levels in humans. J Appl Physiol. 1997;83(1):5-10. Epub 1997/07/01. PubMed PMID: 9216937.

32. Kohrt WM, Landt M, Birge SJ, Jr. Serum leptin levels are reduced in response to exercise training, but not hormone replacement therapy, in older women. The Journal of clinical endocrinology and metabolism. 1996;81(11):3980-5. Epub 1996/11/01. PubMed PMID: 8923847.

33. Vieira VJ, Valentine RJ, Wilund KR, Antao N, Baynard T, Woods JA. Effects of exercise and low-fat diet on adipose tissue inflammation and metabolic complications in obese mice. Am J Physiol Endocrinol Metab. 2009;296(5):E1164-71. Epub 2009/03/12. doi: 00054.2009 [pii]

10.1152/ajpendo.00054.2009. PubMed PMID: 19276393; PubMed Central PMCID: PMC2681303.

34. Vieira VJ, Valentine RJ, Wilund KR, Woods JA. Effects of diet and exercise on metabolic disturbances in high-fat diet-fed mice. Cytokine. 2009;46(3):339-45. Epub 2009/04/14. doi: S1043-4666(09)00094-5 [pii]

10.1016/j.cyto.2009.03.006. PubMed PMID: 19362852; PubMed Central PMCID: PMC2743469.

35. Miyazaki S, Izawa T, Ogasawara JE, Sakurai T, Nomura S, Kizaki T, et al. Effect of exercise training on adipocyte-size-dependent expression of leptin and adiponectin. Life Sci. 2010;86(17-18):691-8. Epub 2010/03/17. doi: S0024-3205(10)00100-1 [pii]10.1016/j.lfs.2010.03.004. PubMed PMID: 20226796.

36. Zachwieja JJ, Hendry SL, Smith SR, Harris RB. Voluntary wheel running decreases adipose tissue mass and expression of leptin mRNA in Osborne-Mendel rats. Diabetes. 1997;46(7):1159-66. Epub 1997/07/01. PubMed PMID: 9200651.

37. Mick GJ, Wang X, Ling Fu C, McCormick KL. Inhibition of leptin secretion by insulin and metformin in cultured rat adipose tissue. Biochimica et biophysica acta. 2000;1502(3):426-32. Epub 2000/11/09. doi: S0925-4439(00)00074-0 [pii]. PubMed PMID: 11068185.

38. Tedgui A, Mallat Z. Cytokines in atherosclerosis: pathogenic and regulatory pathways. Physiological reviews. 2006;86(2):515-81. Epub 2006/04/08. doi: 86/2/515 [pii]

10.1152/physrev.00024.2005. PubMed PMID: 16601268.

39. Smith JK, Dykes R, Douglas JE, Krishnaswamy G, Berk S. Long-term exercise and atherogenic activity of blood mononuclear cells in persons at risk of developing ischemic heart disease. JAMA. 1999;281(18):1722-7. Epub 1999/05/18. doi: jci90017 [pii]. PubMed PMID: 10328073.

40. Lira FS, Yamashita AS, Rosa JC, Koyama CH, Caperuto EC, Batista ML, Jr., et al. Exercise training decreases adipose tissue inflammation in cachectic rats. Horm Metab Res. 2012;44(2):91-8. Epub 2012/01/24. doi: 10.1055/s-0031-1299694. PubMed PMID: 22266827.

41. Lira FS, Rosa JC, Yamashita AS, Koyama CH, Batista ML, Jr., Seelaender M. Endurance training induces depot-specific changes in IL-10/TNF-alpha ratio in rat adipose tissue. Cytokine. 2009;45(2):80-5. Epub 2008/12/23. doi: S1043-4666(08)00775-8 [pii] 10.1016/j.cyto.2008.10.018. PubMed PMID: 19097804.

42. van Hall G, Steensberg A, Sacchetti M, Fischer C, Keller C, Schjerling P, et al. Interleukin-6 stimulates lipolysis and fat oxidation in humans. The Journal of clinical endocrinology and metabolism. 2003;88(7):3005-10. Epub 2003/07/05. PubMed PMID: 12843134.

43. Ellingsgaard H, Hauselmann I, Schuler B, Habib AM, Baggio LL, Meier DT, et al. Interleukin-6 enhances insulin secretion by increasing glucagon-like peptide-1 secretion from L cells and alpha cells. Nat Med. 2011;17(11):1481-9. Epub 2011/11/01. doi: 10.1038/nm.2513

nm.2513 [pii]. PubMed PMID: 22037645.

44. Malin SK, Stephens BR, Sharoff CG, Hagobian TA, Chipkin SR, Braun B. Metformin's effect on exercise and postexercise substrate oxidation. Int J Sport Nutr Exerc Metab. 2010;20(1):63-71. Epub 2010/03/02. PubMed PMID: 20190353.

45. Hajer GR, van Haeften TW, Visseren FL. Adipose tissue dysfunction in obesity, diabetes, and vascular diseases. Eur Heart J. 2008;29(24):2959-71. Epub 2008/09/09. doi: ehn387 [pii]

10.1093/eurheartj/ehn387. PubMed PMID: 18775919.

46. Sweeney G, Keen J, Somwar R, Konrad D, Garg R, Klip A. High leptin levels acutely inhibit insulin-stimulated glucose uptake without affecting glucose transporter 4 translocation in l6 rat skeletal muscle cells. Endocrinology. 2001;142(11):4806-12. Epub 2001/10/19. PubMed PMID: 11606447.

47. Ishizuka T, Ernsberger P, Liu S, Bedol D, Lehman TM, Koletsky RJ, et al. Phenotypic consequences of a nonsense mutation in the leptin receptor gene (fak) in obese spontaneously hypertensive Koletsky rats (SHROB). The Journal of nutrition. 1998;128(12):2299-306. Epub 1998/12/30. PubMed PMID: 9868173.

48. Wang JL, Chinookoswong N, Scully S, Qi M, Shi ZQ. Differential effects of leptin in regulation of tissue glucose utilization in vivo. Endocrinology. 1999;140(5):2117-24. Epub 1999/04/28. PubMed PMID: 10218962.

4. ELEVATED SKELETAL MUSCLE IRISIN PRECURSOR FNDC5 MRNA IN OBESE OLETF RATS

a. Note to the reader on authorship

This paper was originally authored by Dr. Michael Roberts, who has granted permission for both the text and figures of this paper to be reproduced in this dissertation. Figure and table numbering has been changed when necessary to follow the numbering scheme of the dissertation. The citation for this paper is as follows:

Roberts, M.D., et al., *Elevated skeletal muscle irisin precursor FNDC5 mRNA in obese OLETF rats.* Metabolism, 2013. **62**(8): p. 1052-6.

b. Abstract

OBJECTIVE: To examine fibronectin type III domain containing 5 (FNDC5, precursor to irisin) mRNA within skeletal muscle of obese/diabetic-prone Otsuka Long-Evans Tokushima Fatty (OLETF) rats versus lean/healthy Long Evans Tokushima Otsuka (LETO). We hypothesized that FNDC5 expression would differ between obese (OLETF) versus lean (LETO) animals.
MATERIALS/METHODS: Triceps muscle of 30-32 week old OLETF and LETO rats were assayed for FNDC5 and PGC1α mRNA levels. Body composition and circulating biomarkers of the OLETF and LETO rats were also correlated with skeletal muscle FNDC5 mRNA expression patterns in order to examine potential relationships that may exist. RESULTS: OLETF rats exhibited twice the amount

of triceps FNDC5 mRNA compared to LETO rats ($p < 0.01$). Significant positive correlations existed between triceps muscle FNDC5 mRNA expression patterns versus fat mass ($r = 0.70$, $p = 0.008$), as well as plasma leptin ($r = 0.82$, $p < 0.001$). PGC1α mRNA levels were also highly correlated with FNDC5 mRNA ($r = 0.85$, $p < 0.001$). In subsequent culture experiments, low and high physiological doses of leptin had no effect on PGC1α mRNA or FNDC5 mRNA levels in C_2C_{12} myotubes. Paradoxically, circulating irisin concentrations tended to be higher in a second cohort of LETO versus OLETF rats ($p = 0.085$). CONCLUSION: Our data suggest an association between adiposity and skeletal muscle FNDC5 gene expression, although circulating irisin levels tended to be lower in OLETF rats. Further research is needed to examine whether other adipose tissue-derived factors might up-regulate FNDC5 transcription and/or inhibit irisin biosynthesis from FNDC5.

c. Introduction

Fibronectin type III domain containing 5 (FNDC5) has garnered recent attention. The proteolytic FNDC5 cleavage product, irisin, was reported by Boström et al. (1) to a) be up-regulated in a proliferator-activated receptor gamma coactivator 1-α (PGC1α)- and exercise-dependent fashion in rodent and human skeletal muscle (1), and b) increase thermogenesis and decrease bodyweights in mice (1); leading them to propose that FNDC5 and irisin may be novel therapeutic targets in the treatment of obesity. Based upon data by Boström et al. (1), we initially hypothesized that obese/diabetic Otsuka Long-Evans Tokushima Fatty (OLETF) rats would exhibit reduced skeletal muscle

FNDC5 mRNA compared to lean/healthy Long Evans Tokushima Otsuka (LETO) rats. Later during testing of our initial hypothesis, contrasting papers were published. Timmons et al. (2) reported that skeletal muscle FNDC5 mRNA was shown to increase only within a subset of highly active human elderly subjects following 6 weeks of exercise (2). Moreover, FNDC5 mRNA for all subjects correlated with body mass index (BMI), but not with changes in aerobic capacity. Next, Huh et al. (3) similarly reported that circulating irisin increases acutely following a sprint-interval exercise bout in healthy humans. In addition, these same authors reported that surgically-induced weight loss in patients with a BMI > 50 decreased skeletal muscle FNDC5 mRNA as well as circulating irisin leading the authors to conclude that irisin could not be directly involved with health improvements given its positive association with body fat [3]. Thus, we hypothesized that triceps muscle FNDC5 mRNA would be elevated in OLETF rats, and would correlate with fat mass, lean body mass, and plasma leptin.

d. Methods

Animals and experimental design

Experimental protocols were approved by the University of Missouri Animal Care and Use Committee. Four week-old, male LETO (n = 7) and OLETF rats (n = 7) (Tokushima Research Institute, Otsuka Pharmaceutical) were received and individually housed in with 0600-1800 light and 1800-0600 dark cycles at 21°C. Animals were given *ad libitum* access to standard chow (Formulab 5008, Purina Mills). On the day of sacrifice, at 30-32 weeks of age, rats were fasted for 12 h and anesthetized with an intraperitoneal injection of

sodium pentobarbital (100 mg/kg). While animals were under isoflurane anesthesia, body composition was assessed by dual energy x-ray absorptiometry (DXA; Hologic QDR-1000, calibrated for rodents), whole triceps muscles harvested, and animals killed by exsanguination.

Real-time PCR for mRNA expression

For triceps muscle RNA extraction, methods were done as previously described (4). mRNAs for FNDC5, PGC1α, and18S were assayed using with SYBR green-based chemistry (Applied Biosystems) real-time PCR and gene-specific primers. Primer efficiency curves for all genes ranged between 90-110%.

Plasma cytokine and irisin concentrations

EDTA-treated plasma samples were assayed for plasma cytokine concentrations as described (5) in OLETF (n = 7) and LETO (n = 7) rats. EDTA-treated plasma samples were also assayed for plasma irisin concentrations in a separate set of OLETFs (n = 10) and LETOs (n = 10) using an ELISA kit (Phoenix Pharmaceuticals) due to limited plasma samples from the first cohort of rats.

Myotube cell culture adipokine treatment and FNDC5 mRNA expression

C_2C_{12} myoblasts (American Type Culture Collection CRL-1722) were maintained under standard conditions and differentiation was induced 24 h after

growth reached 80-90% confluency with differentiation media [DM; DMEM, 2% (vol/vol) horse serum]. DM was replaced every 24 h for 124 h. Myotubes were then treated with lower (8 ng/ml) and higher (150 ng/ml) dosages of leptin (Sigma) for 24 h and 48 h. After treatments, myotubes were lysed with Trizol, cDNA was made from isolated RNA per the methods described above. 25 ng of cDNA was assayed for FNDC5, PGC1α and GAPDH mRNAs using the aforementioned SYBR green chemistry methods. Murine FNDC5 primers were used as previously used by Bostrom et al. (1).

Statistics

Between-group comparisons for all variables were made using independent samples t-tests. Univariate correlations were performed using Pearson correlation tests. In vitro myotube FNDC5 and PGC1α mRNA expression patterns were made between leptin-treated and control conditions using one-way ANOVAs. Significance was set at $p < 0.05$ and data are presented as mean ± SE.

e. Results

Most general health markers presented in Table 1 were more favorable in LETO versus OLETF rats indicating that LETO rats exhibited a generally healthier phenotype.

Triceps FNDC5 and PGC1α mRNA expression patterns

FNDC5 and PGC1α mRNAs were ~50% and ~45% less in the triceps muscle of LETO versus OLETF rats, respectively (Fig 1A).

Table 6. Between-treatment differences in body composition and serum markers

Variable	OLETF SED (n=7)	LETO SED (n=6)
Body composition variables		
Bodyweight (g)	693 ± 14	474 ± 19***
DXA bfat (%)	37.0 ± 1.6	14.9 ± 0.6***
Lean mass (g)	435 ± 8	407 ± 17
fat mass (g)	257 ± 15	72 ± 5***
Serum markers		
Glucose (mg/dl)	290 ± 14	151 ± 5***
Insulin (mg/dl)	6.2 ± 0.6	2.8 ± 0.6**
HDL-c (mg/dl)	33 ± 2	26 ± 1*
LDL-c (mg/dl)	50 ± 7	61 ± 4
Triglycerides (mg/dl)	319 ± 47	40 ± 5***
Plasma adipokines		
Leptin (ng/ml)	102 ± 11	13 ± 2***
IL-1β (pg/ml)	17 ± 13	ND
IL-6 (pg/ml)	825 ± 222	ND
IL-10 (pg/ml)	927 ± 332	34 ± 10*
IL-12p70 (pg/ml)	125 ± 66	12 ± 5
TNF-α (pg/ml)	8.9 ± 4.2	3.9 ± 1.9
MCP-1 (pg/ml)	49 ± 10	56 ± 28
RANTES (pg/ml)	938 ± 69	1218 ± 334

All data are presented as mean ± SE.
Abbreviations: DXA bfat = dual x-ray absorptiometry body fat percentage, ND = not detectable; *indicate a significant difference between groups ($p < 0.05$), **indicate a significant difference between groups ($p < 0.01$), ***indicate a significant difference between groups ($p < 0.001$).

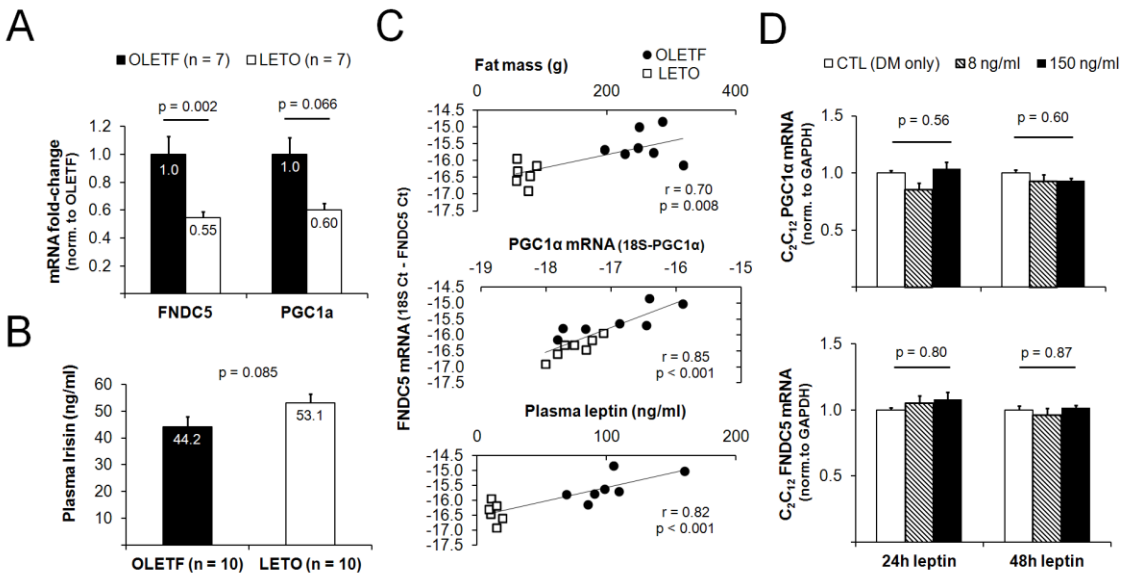

Figure 30. Relationship between muscle FNDC5 mRNA and adiposity. Obese OLETF rats possessed a greater triceps muscle FNDC5 mRNA expression compared to LETO rats (A). In a second cohort of rats, LETO rats tended to present more circulating irisin compared to OLETF rats OLETF (B). In all rats from panel A, positive correlations existed between triceps muscle FNDC5 mRNA expression versus fat mass, triceps muscle PGC1α and plasma leptin (C). Despite the positive association between circulating leptin and triceps muscle FNDC5 mRNA expression, 24-h and 48- treatments with low (8 ng/ml) and high (150 ng/ml) physiological doses of leptin did not alter the mRNA expression of FNDC5 (mRNA precursor to irisin) in C_2C_{12} myoblasts (D). In panel D, all data are normalized to DM-only-treated cells and are presented as mean ± SE (n = 4 wells per treatment).

Correlations between biomarkers and triceps FNDC5 mRNA expression patterns

Triceps FNDC5 mRNA expression was positively associated with total body fat mass ($r = 0.70$, $p = 0.008$; Fig 1B), although there was no association between triceps FNDC5 mRNA expression total lean body mass ($r = -0.06$, $p = 0.76$). There was no association with circulating insulin and triceps FNDC5 mRNA expression ($r = 0.40$, $p = 0.20$). We have previously examined differences in multiple plasma adipokines between the same OLETF and LETO animals as the current study (5). Circulating leptin exhibited the strongest correlation with triceps muscle FNDC5 mRNA expression patterns relative to the other adipokines ($r = 0.82$, $p < 0.001$; Fig 1C), although other adipokines were also associated with triceps muscle FNDC5 mRNA expression patterns [(IL-1β: $r = 0.54$, $p = 0.054$); IL-6: ($r = 0.61$, $p = 0.03$); and IL-10: ($r = 0.64$, $p = 0.02$)]. Plasma leptin was also correlated triceps PGC1α mRNA expression levels ($r = 0.42$, $p = 0.04$). Finally, triceps muscle FNDC5 mRNA expression was also positively associated with triceps muscle PGC1α mRNA ($r = 0.85$, $p < 0.001$; Fig 1D).

Effects of leptin treatment on myotube FNDC5 and PGC1α mRNA levels

Given the strong correlation between triceps FNDC5 mRNA expression and circulating leptin, we next assessed whether leptin-treated C2C12 myotubes exhibited a dose-response increase in FNDC5 gene expression. Contrary to our

hypothesis, FNDC5 *and PGC1α* mRNA expression was not altered in leptin-treated C_2C_{12} myotubes (Fig 1E).

Plasma irisin in a second set of OLETF and LETO rats

Due to limited plasma from the original animals, a second set of OLETF (n = 10) and LETO (n = 10) rats were used to assay plasma irisin. While circulating irisin was not statistically different between these cohorts, LETO rats tended to present greater concentrations of circulating irisin ($p = 0.085$, Fig. 1). Within this second cohort of animals (n = 20 total), there were no correlations between plasma irisin and body weight ($r = -0.19$, $p = 0.42$), or DXA body fat percentage ($r = -0.24$, $p = 0.32$).

f. Discussion

Novel findings of this study are that total body fat and plasma leptin levels are positively associated with higher skeletal muscle FNDC5 mRNA expression in the obese OLETF rat. These data agree with previous studies by Timmons et al. (2), as well as Huh et al. (3), who reported positive associations between BMI and FNDC5 mRNA expression in human skeletal muscle. Likewise, Huh et al. (3) demonstrated that weight loss after bariatric surgery decreased human vastus lateralis muscle FNDC5 mRNA expression as well as circulating leptin concentrations. We also report that OLETF rats tended to express more triceps PGC-1α mRNA, which is a known regulator of FNDC5 gene expression. Importantly, our findings combined with the literature collectively suggest that obesity can increase skeletal muscle PGC1α mRNA in OLETF rats, which may,

in turn, may increase FNDC5 mRNA expression patterns in an exercise-independent manner.

Plasma leptin was positively correlated with triceps FNDC5 mRNA expression levels, as well as PGC1α mRNA expression. Leptin administration to leptin-deficient ob/ob mice is known to increase the expression of PGC1α protein in skeletal muscle through AMPK-mediated signaling (6). Hence, we further speculated that leptin-mediated "crosstalk" between adipose tissue and skeletal muscle might constitute a novel compensatory mechanism to increase thermogenesis and stimulate fat loss via irisin-mediated signaling in the obese OLETF rats. However, longer-term (24 h and 48 h) leptin treatments at low and high physiological doses did not alter PGC1α mRNA or FNDC5 mRNA levels in C_2C_{12} myotubes in culture. Therefore, an increase in triceps muscle FNDC5 gene expression with elevated circulating leptin concentrations may be coincidental with an increase in adiposity. Nevertheless, our findings suggest that an unknown obesity-induced adipose tissue-derived factor could regulate skeletal muscle FNDC5 mRNA expression in an attempt to increase thermogenesis and stimulate fat loss via irisin-mediated signaling in the obese OLETF rats. Future research is needed to test this hypothesis.

Interestingly, in a second set of animals circulating irisin tended to be greater in leaner/healthier LETO versus fatter/unhealthier OLETF rats, although no correlations existed between plasma irisin and body weight or DXA body fat percentage. This finding is in agreement with Huh et al. (3) who demonstrated that BMI was not correlated with circulating irisin in humans. Therefore, while

muscle FNDC5 gene expression may be upregulated in obese skeletal muscle, it remains possible that post-translational proteolytic cleavage mechanisms responsible for the conversion of FNDC5 to irisin are impaired in the obese/diseased OLETFs. Future studies addressing how obesity affects the post-translational modification of FNDC5 would be informative. In addition, despite initial excitement over irisin as a novel myokine [1], our data combined with recent human data [2, 3] suggest that its role in obesity-associated metabolic pathologies is somewhat ambiguous at the present time.

g. References

1. Bostrom P, Wu J, Jedrychowski MP, Korde A, Ye L, Lo JC, et al. A PGC1-alpha-dependent myokine that drives brown-fat-like development of white fat and thermogenesis. Nature. 2012;481(7382):463-8. Epub 2012/01/13. doi: nature10777 [pii]10.1038/nature10777. PubMed PMID: 22237023.

2. Timmons JA, Baar K, Davidsen PK, Atherton PJ. Is irisin a human exercise gene? Nature. 2012;488(7413):E9-10; discussion E-1. Epub 2012/08/31. doi: nature11364 [pii] 10.1038/nature11364. PubMed PMID: 22932392.

3. Huh JY, Panagiotou G, Mougios V, Brinkoetter M, Vamvini MT, Schneider BE, et al. FNDC5 and irisin in humans: I. Predictors of circulating concentrations in serum and plasma and II. mRNA expression and circulating concentrations in response to weight loss and exercise. Metabolism. 2012. Epub 2012/09/29. doi: S0026-0495(12)00332-0 [pii]

10.1016/j.metabol.2012.09.002. PubMed PMID: 23018146.

4. Roberts MD, Childs TE, Brown JD, Davis JW, Booth FW. Early depression of Ankrd2 and Csrp3 mRNAs in the polyribosomal and whole-tissue fractions in skeletal muscle with decreased voluntary running. J Appl Physiol. 2012. Epub 2012/01/28. doi: japplphysiol.01419.2011 [pii]

10.1152/japplphysiol.01419.2011. PubMed PMID: 22282489.

5. Jenkins NT, Padilla J, Arce-Esquivel AA, Bayless DS, Martin JS, Leidy HJ, et al. Effects of Endurance Exercise Training, Metformin, and their Combination on Adipose Tissue Leptin and IL-10 Secretion in OLETF Rats. J Appl Physiol. 2012. Epub 2012/09/29. doi: japplphysiol.00936.2012 [pii] 10.1152/japplphysiol.00936.2012. PubMed PMID: 23019312.

6. Sainz N, Rodriguez A, Catalan V, Becerril S, Ramirez B, Gomez-Ambrosi J, et al. Leptin administration favors muscle mass accretion by decreasing FoxO3a and increasing PGC-1alpha in ob/ob mice. PLoS One. 2009;4(9):e6808. Epub 2009/09/05. doi: 10.1371/journal.pone.0006808. PubMed PMID: 19730740; PubMed Central PMCID: PMC2733298.

5. DIFFERENTIAL REGULATION OF ADIPOSE TISSUE AND VASCULAR INFLAMMATORY GENE EXPRESSION BY CHRONIC SYSTEMIC INHIBITION OF NOS IN LEAN AND OBESE RATS

a. Note to the reader on authorship

This paper was originally authored by Dr. Jaume Padilla, who has granted permission for both the text and figures of this paper to be reproduced in this dissertation. Figure and table numbering has been changed when necessary to follow the numbering scheme of the dissertation. The citation for this paper is as follows:

Padilla, J., et al., *Differential regulation of adipose tissue and vascular inflammatory gene expression by chronic systemic inhibition of NOS in lean and obese rats.* Physiol Rep, 2014. **2**(2): p. e00225.

b. Abstract

We tested the hypothesis that a decrease in bioavailability of nitric oxide (NO) would result in increased adipose tissue (AT) inflammation. In particular, we utilized the obese OLETF rat model (n=20) and lean LETO counterparts (n=20) to determine the extent to which chronic inhibition of NO synthase (NOS) with L-NAME treatment (for 4 weeks) upregulates expression of inflammatory genes and markers of immune cell infiltration in retroperitoneal white AT, subscapular brown

AT, periaortic AT as well as in its contiguous aorta free of perivascular AT. As expected, relative to lean rats (% body fat=13.5±0.7), obese rats (% body fat=27.2±0.8) were hyperlipidemic (total cholesterol 77.0±2.1 vs. 101.0±3.3 mg/dL), hyperleptinemic (5.3±0.9 vs. 191.9±59.9 pg/mL), and insulin resistant (higher HOMA IR index (3.9±0.8 vs. 25.2±4.1)). Obese rats also exhibited increased expression of pro-inflammatory genes in perivascular, visceral, and brown ATs. L-NAME treatment produced a small but statistically significant decrease in percent body fat (24.6±0.9 vs 27.2±0.8%) and HOMA IR index (16.9±2.3 vs 25.2±4.1) in obese rats. Further, contrary to our hypothesis, we found that expression of inflammatory genes in all AT depots examined were generally unaltered with L-NAME treatment in both lean and obese rats. This was in contrast with the observation that L-NAME produced a significant upregulation of inflammatory and pro-atherogenic genes in the aorta. Collectively, these findings suggest that chronic NOS inhibition alters transcriptional regulation of pro-inflammatory genes to a greater extent in the aortic wall compared to its adjacent perivascular AT, or visceral white and subscapular brown AT depots.

c. Introduction

Originally characterized as a mediator of vascular smooth muscle relaxation (1, 2), nitric oxide (NO) has since been implicated in a wide range of physiological processes in different tissues including adipose tissue (AT). For example, a recent study in mice demonstrated that overexpression of endothelial NO synthase (eNOS) prevents diet-induced obesity and that the mechanism of this antiobesogenic effect of eNOS was related to an increase in mitochondrial

abundance and activity in visceral AT (3). Furthermore, while the anti-inflammatory effects of NO on the vasculature are established (4-8), recent evidence indicates that NO also exerts an anti-inflammatory effect in AT. In this regard, eNOS knockout mice exhibit increased inflammation in epidydimal AT, compared to wild-type counterparts, indicating that NO derived from eNOS is crucial for maintenance of a low-inflammatory state within the visceral AT (9). Whether the anti-inflammatory influence of NO signaling is also present in other AT depots beyond the viscera including perivascular and brown AT is uncertain.

Accordingly, we utilized the obese hyperphagic Otsuka Long Evans Tokushima Fatty (OLETF) rat model and lean counterparts [Long Evans Tokushima Otsuka (LETO)] to test the hypothesis that a decrease in NO bioavailability with chronic systemic inhibition of NOS activity would result in AT inflammation as well as to determine whether this effect would be modulated with obesity. Examination of the effects of NOS inhibition in both lean and obese rats is important because obesity is associated with adipose tissue inflammation (10-12) as well as reduced NO bioavailability (13, 14). A question that remains largely unanswered is whether obesity-associated low NO bioavailability mediates adipose tissue inflammation. To begin addressing this question, in our study we created a lean condition with induced low NO bioavailability to compare it to an obese condition with inherent low NO bioavailability. We hypothesized that systemic NOS inhibition would make the adipose tissue of lean animals phenotypically resemble the adipose tissue of obese animals. In particular, expression of inflammatory genes and markers of immune cell infiltration were

assessed in retroperitoneal white AT, subscapular brown AT, periaortic AT and its contiguous aorta free of perivascular AT in lean and obese rats systemically treated or not with NOS inhibitor N^{ω}-nitro-L-arginine methyl ester (L-NAME). The aorta was also included to determine whether the extent of the effects of systemic NOS inhibition on adipose tissue samples were comparable to the effects observed in vascular tissue.

d. Methods

Animals

All animal protocols were approved by the University of Missouri Institutional Animal Care and Use Committee. Male LETO (n=20) and OLETF (n=20) rats (age 4 wk; Tokushima Research Institute, Otsuka Pharmaceutical, Tokushima, Japan) were individually housed on a 12-h:12-h light-dark cycle and provided water and standard rodent chow (Formulab 5008, Purina Mills, St. Louis, MO) *ad libitum* with approximately 26% protein, 18% fat, and 56% carbohydrate. Body weights and food intakes were recorded on a weekly basis. At 16 weeks of age rats were randomly divided into L-NAME-treated (LETO L-NAME, n=10; OLETF L-NAME, n=10) or untreated (LETO CONT, n=10; OLETF CONT, n=10) groups. L-NAME animals received L-NAME daily in drinking water for 4 weeks as described (15). Briefly, L-NAME was dissolved in tap water and the water was supplied fresh every other day to the animals. The concentration of L-NAME in water was individually adjusted for bodyweight and water consumption such that each rat consumed 65-70 mg/kg/day. Similar dose of L-NAME in drinking water has been used in previous studies (5, 15). L-NAME administration was continued until the day of sacrifice (20

weeks of age). On that morning, rats were anesthetized by intraperitoneal injection of pentobarbital sodium (50 mg/kg) following a 12-hr overnight fast. Tissues were harvested and the animals were euthanized by exsanguination in full compliance with the American Veterinary Medical Association Guidelines on Euthanasia.

Body composition, blood parameters, and citrate synthase activity

On the day of the experiments, body mass was measured to the nearest 0.01 g and, following anesthetization, body composition was determined using a dual energy x-ray absorptiometry instrument (Hologic QDR-1000) calibrated for rodents. In addition, retroperitoneal, epididymal, and omental fat pad weights were measured to the nearest 0.01 g. Plasma samples were prepared by centrifugation and stored at -80ºC until analysis. Glucose, triglycerides, and non-esterified fatty acids (NEFA) assays were performed by a commercial laboratory (Comparative Clinical Pathology Services, Columbia, MO) on an Olympus AU680 automated chemistry analyzer (Beckman-Coulter, Brea, CA) using commercially available assays according to manufacturer's guidelines. Plasma insulin concentrations were determined using a commercially available, rat-specific ELISA (Alpco Diagnostics, Salem, NH). In addition, plasma samples were assayed for concentrations of leptin, MCP-1, TNF-α, and IL-6 using a multiplex cytokine assay (Millipore Milliplex, cat no. RCYTOMAG-80K; Billerica, MA, USA) on a MAGPIX instrument (Luminex Technologies; Luminex Corp., Austin, TX, USA) according to the manufacturer's instructions (16, 17). Serum nitrate + nitrite (NOx) levels were measured using the Nitrate/Nitrite Fluorometric Assay Kit (Cayman Chemical, item no. 780051, Ann Arbor, MI) according to manufacturer's instructions. Citrate

synthase activity was determined in retroperitoneal AT homogenates using the methods of Srere (18). AT was homogenized in buffer (25 mM Tris HCl, 1 mM EDTA, pH 7.4), centrifuged, and the infranatant was collected. The citrate synthase activity assay was only performed in the retroperitoneal fat depot because this is where we had AT availability.

Tissue sampling

A segment of the thoracic aorta cleaned of perivascular AT and excess adventitia, as well as the perivascular AT surrounding the thoracic aorta, retroperitoneal white AT, and subscapular brown AT were quickly excised from the anesthetized rat. Isolated aortic segments were kept in RNAlater (Ambion, Austin, TX) for 24 h at 4ºC, then removed from the RNAlater solution and stored at -80ºC until analysis. For each fat depot, a portion was flash frozen and kept at -80ºC for examination of gene expression and a portion was fixed in neutral-buffered 10% formalin for histology analysis. Retroperitoneal AT was studied because it is the largest visceral AT depot in obese rats. Subscapular brown AT was studied because it is a source of healthy AT (19) and a classic depot for the study of brown AT biology (20-23). Periaortic AT was selected because increasing amounts of evidence implicates AT surrounding the arteries as a local source of pro-inflammatory cytokines influencing the athero-susceptibility of the vascular wall (24-31). On the other hand, like others we have found that AT surrounding the descending thoracic aorta is a brown-like AT depot in rodents (32, 33). Last, we studied gene expression in the aorta to determine the extent to which changes in

perivascular AT gene expression induced by NOS inhibition and obesity were comparable to changes in gene expression in the adjacent arterial wall.

RNA extraction and real-time PCR

Adipose tissue and aortic samples were homogenized in TRIzol solution using a tissue homogenizer (TissueLyser LT, Qiagen, Valencia, CA). Total RNA was isolated using the Qiagen's RNeasy Lipid Tissue Kit and assayed using a Nanodrop spectrophotometer (Thermo Scientific, Wilmington, DE) to assess purity and concentration. First-strand cDNA was synthesized from total RNA using the High Capacity cDNA Reverse Transcription kit (Applied Biosystems, Carlsbad, CA). Quantitative real-time PCR was performed as previously described (17, 32) using the CFX Connect™ Real-Time PCR Detection System (BioRad, Hercules, CA). Primer sequences (Table 1) were designed using the NCBI Primer Design tool. All primers were purchased from IDT (Coralville, IA). A 20-µl reaction mixture containing 10 µl iTaq UniverSYBR Green SMX (BioRad, Hercules, CA) and the appropriate concentrations of gene-specific primers plus 4 µl of cDNA template were loaded in each well of a 96-well plate. All PCR reactions were performed in duplicate. PCR was performed with thermal conditions as follows: 95ºC for 10 min, followed by 40 cycles of 95ºC for 15 s and 60ºC for 45 s. A dissociation melt curve analysis was performed to verify the specificity of the PCR products. 18S primers were used to amplify the endogenous control product. Our group has established that 18S is a suitable house-keeping gene for real-time PCR when examining AT gene expression (32, 34). In the present study, 18S CTs were not different among fat depots or groups of animals. Similarly, 18S CTs in the aorta were not different

among groups of animals. mRNA expression values are presented as $2^{\Delta CT}$ whereby ΔCT = 18S CT - gene of interest CT (17, 32). AT mRNA levels were normalized to perivascular AT in the LETO control group of rats, which was always set at 1. Similarly, aorta mRNA levels were normalized to the LETO control group of rats, which was set at 1.

Table 7. Forward and reverse primer sequences for quantitative real-time PCR

	Primer sequence (5'→3')	
Gene	**Forward**	**Reverse**
18S	GCCGCTAGAGGTGAAATTCTTG	CATTCTTGGCAAATGCTTTCG
Leptin	GACACCCTTAGAGGGGGCTA	AACCCAAGCCCCTTTGTTCA
MCP-1	CTGTCTCAGCCAGATGCAGTTAA	AGCCGACTCATTGGGATCAT
TNF-α	AACACACGAGACGCTGAAGT	TCCAGTGAGTTCCGAAAGCC
IL-6	AGAGACTTCCAGCCAGTTGC	AGCCTCCGACTTGTGAAGTG
IL-10	CTGGCTCAGCACTGCTATGT	GCAGTTATTGTCACCCCGGA
IL-18	ACAGCCAACGAATCCCAGAC	ATAGGGTCACAGCCAGTCCT
E-Selectin	GCCATGTGGTTGAATGTAAAGC	GGATTTGAGGAACATTTCCTGACT
VCAM-1	GAAGGAAACTGGAGAAGACAATCC	TGTACAAGTGGTCCACTTATTTCAATT
ICAM-1	CACAAGGGCTGTCACTGTTCA	CCCTAGTCGGAAGATCGAAAGTC
PAI-1	AGCTGGGCATGACTGACATCT	GCTGCTCTTGGTCGGAAAGA
Adiponectin	CAAGGCCGTTCTCTTCACCT	CCCCATACACTTGGAGCCAG
CD4	ACCCTAAGGTCTCTGACCCC	TAGGCTGTGCGTGGAGAAAG
CD8	CACTAGGCTCCAGGTTTCCG	CGCAGCACTTCGCATGTTAG
CD11c	CTGTCATCAGCAGCCACGA	ACTGTCCACACCGTTTCTCC
F4/80	GCCATAGCCACCTTCCTGTT	ATAGCGCAAGCTGTCTGGTT
FoxP3	CTCCAGTACAGCCGGACAC	GGTTGGGCATCAGGTTCTTG
eNOS	AGGCATCACCAGGAAGAAGA	GGCCAGTCTCAGAGCCATAC
iNOS	GGTGAGGGGACTGGACTTTT	CCAACTCTGCTGTTCTCCGT
nNOS	GGACCAGCCAAAGCAGAGAT	GAGCTTTGTGCGATTTGCCA
Endothelin-1	TTGCTCCTGCTCCTCCTTGAT	TAGACCTAGAAGGGCTTCCTAGT
p22phox	ACCTGACCGCTGTGGTGAA	GTGGAGGACAGCCCGGA
p47phox	ACGCTCACCGAGTACTTCAACA	TCATCGGGCCGCACTTT
UCP-1	CCGGTGGATGTGGTAAAAAC	CTCCAAGTCGCCTATGTGGT
PPARGC-1-α	GGGGCACATCTGTTCTTCCA	GAGCTGTTTTCTGGTGCTGC

Histology assessments

Formalin-fixed AT samples were processed through paraffin embedment, sectioned at five microns, stained with hematoxylin and eosin for morphometric determinations. Sections were examined using an Olympus BX60 photomicroscope (Olympus, Melville, NY) and photographed at 40x magnification using with a Spot Insight digital camera (Diagnostic Instruments, Inc., Sterling Heights, MI) (16, 32).

Functional assessment of isolated aortic rings

A segment of the thoracic aorta, trimmed of AT and connective tissue, was sectioned into 2 mm rings in cold Krebs. Rings were then mounted on wire feet connected to isometric force transducers and submerged in 20mL baths containing physiological Krebs solution maintained at 37ºC for 1 hour to allow for equilibration. Aortic rings were stretched to optimal length which ranged from 130 to 140% of passive diameter. Aortic vasomotor function was investigated with cumulative concentration-response curves of acetylcholine (ACh, 10^{-10} to 10^{-4} M), an endothelium-dependent dilator and sodium-nitro-prusside (SNP, 10^{-10} to 10^{-4} M), an endothelium-independent dilator. A submaximal concentration of phenylephrine ($3e^{-7}$ M) was used to preconstrict all vessels prior to ACh and SNP relaxation curves. Relaxation at each concentration was measured and expressed as percent maximum relaxation, where 100% is equivalent to loss of all tension developed in response to phenylephrine (32, 35).

Statistical analysis

The effects of obesity and L-NAME on body composition and plasma markers were evaluated using 2 X 2 (group X condition) ANOVAs. Concentration-response curves from vasomotor function experiments were analyzed using a 2 X 2 X 7 (group X condition X concentration) ANOVAs. In addition, a 2 X 2 X 3 (group X condition X fat depot) ANOVAs were used to evaluate the effects of obesity, L-NAME, and fat depot on gene expression of AT samples. A 2 X 2 (group X condition) ANOVAs were used to evaluate the effects of obesity and L-NAME on gene expression of aortic samples. Simple effects of group, condition, and fat depot were evaluated, and, when appropriate, the Fishers protected LSD post hoc was used. All data are presented as mean ± standard error (SE). For all statistical tests, the alpha level was set at 0.05. All statistical analyses were performed with SPSS V21.0.

e. Results

Daily L-NAME intake averaged 71.2±1.3 mg/kg/day in the LETO + L-NAME group and 67.7±1.6 mg/kg/day in the OLETF + L-NAME group (between group comparison p=0.109). All animals tolerated the L-NAME treatment well throughout the 4-week intervention. As expected (36), treatment of L-NAME resulted in a decrease in serum NOx levels in both groups of rats (Figure 1).

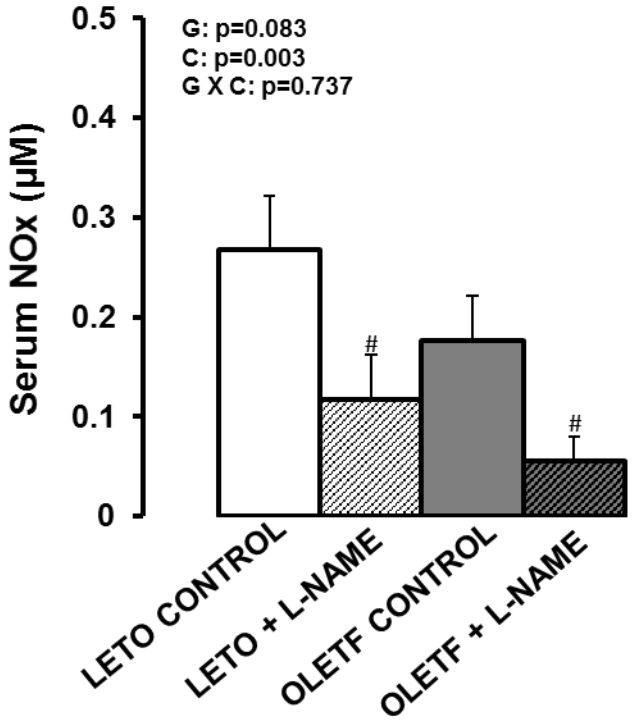

Figure 31. Serum nitrite + nitrate (NOx) levels in LETO and OLETF rats chronically treated without and with L-NAME. Serum was obtained at 20 weeks (time of sacrifice). Values are expressed as means ± SE. #Denotes difference ($p<0.05$) from control rats. G, group; C, condition; G X C, group by condition interaction.

As shown in Figure 2, OLETF rats were heavier and had a greater percent body fat than LETO rats. L-NAME treatment produced a small but statistically significant decrease in percent body fat in OLETF, but not LETO, rats. This effect of L-NAME on the body composition of OLETF rats may be related to decreased food intake induced by L-NAME (Figure 2). Retroperitoneal, epididymal, and omental fat pad weights were greater in the OLETF rats than LETO rats and unaffected by L-NAME treatment. Given that lean mass was unaffected by L-NAME, from these observations, we deduce that the L-NAME-induced reduction in percent body fat of OLETF rats was likely explained by changes in subcutaneous AT; however, total subcutaneous fat mass was not assessed in the present study.

In addition, fasting plasma levels of total cholesterol, high-density lipoprotein (HDL), nonesterified fatty acids, triglycerides, insulin, glucose, HOMA-IR, and leptin were significantly higher in OLETF rats compared to LETO rats (Table 2). Plasma MCP-1 levels were significantly lower in OLETF + L-NAME rats compared to LETO + L-NAME rats. L-NAME significantly increased HDL as well as decreased insulin and HOMA-IR in OLETF rats. These effects were not noted in the LETO rats.

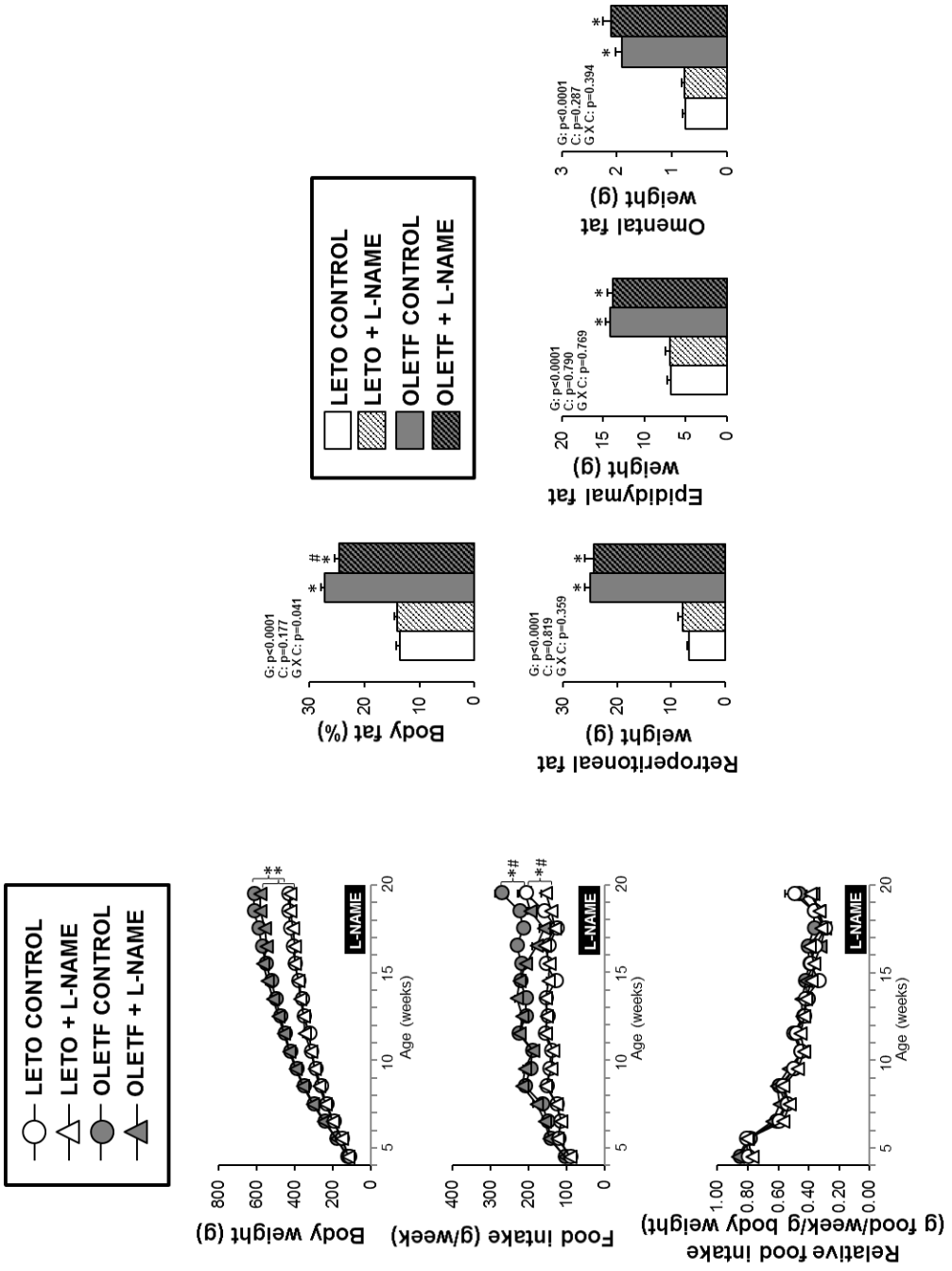

Figure 32. Body composition and food intake in LETO and OLETF rats chronically treated without and with L-NAME. Values are expressed as means ± SE. Body fat and fat pad weights were obtained at 20 weeks (time of sacrifice). *****Denotes difference ($p<0.05$) from LETO rats; $^{\#}$Denotes difference ($p<0.05$) from control rats. For body weight and food intake, statistical analysis was performed at 20 weeks. G, group; C, condition; G X C, group by condition interaction.

Table 8. Fasting plasma characteristics in LETO and OLETF rats chronically treated without and with L-NAME

Variable	LETO CONTROL	LETO + L-NAME	OLETF CONTROL	OLETF + L-NAME
Total cholesterol, mg/dl	77.0±2.1	80.1±2.0	101.0±3.3*	107.3±3.4*
LDL, mg/dl	41.9±1.4	41.3±2.0	40.0±1.9	40.4±2.5
HDL, mg/dl	27.1±0.6	28.2±0.5	32.4±0.7*	34.4±0.7*#
Triglycerides, mg/dl	40.1±2.4	52.9±2.6	142.8±10.0*	162.5±9.0*
NEFA, mmol/l	0.31±0.03	0.32±0.04	0.61±0.04*	0.61±0.03*
Insulin, ng/ml	8.1±1.2	10.1±1.6	32.0±3.8*	22.4±3.1*#
Glucose, mg/dl	186.0±13.7	178.1±5.7	309.8±23.5*	312.1±19.7*
HOMA-IR index	3.9±0.8	4.6±0.8	25.2±4.1*	16.9±2.3*#
Leptin, ng/ml	5.3±0.9	4.9±0.8	191.9±59.9*	205.1±54.7*
MCP-1, pg/ml	282.8±57.6	322.6±45.8	209.1±26.8	167.3±8.9*
TNF-α, pg/ml	5.5±0.5	6.0±0.3	6.8±0.8	5.6±0.2
IL-6, pg/ml	147.0±39.4	196.1±33.5	190.9±58.4	174.3±37.0

Values are expressed as means ± SE. Abbreviations: LDL, low density lipoprotein; HDL, high density lipoprotein; NEFA; non-esterified fatty acids; HOMA-IR, homeostasis model assessment of insulin resistance; MCP-1, monocyte chemotactic protein-1; TNF-α, tumor necrosis factor alpha; IL-6, interleukin 6.

*****Denotes difference ($p<0.05$) from LETO rats; #Denotes difference ($p<0.05$) from control rats.

As illustrated in Figure 3, ACh-mediated relaxation of the aorta was blunted in OLETF rats compared to LETO rats at the highest doses of acetylcholine. Aortas from LETO and OLETF rats treated with L-NAME did not respond to acetylcholine. Dose response curves to SNP were shifted to the right in OLETF rats (Log EC_{50}=-8.55±0.13) compared to LETO rats (Log EC_{50}=-8.96±0.16, $p<0.05$). L-NAME treatment further shifted the SNP dose-response curve to the right in both LETO (Log EC_{50} L-NAME=-8.31±0.17) and OLETF (Log EC_{50} L-NAME=-7.92±0.14) rats (both $p<0.05$).

Figure 4 illustrates representative histological photographs of perivascular AT, retroperitoneal AT, and brow AT. As shown, obesity was associated with increased lipid deposition in perivascular and brown AT as well as increased adipocyte size in retroperitoneal AT. No effects of L-NAME treatment on these parameters were observed in any of the AT depots. Consistent with our previous report (32), a clear structural similarity between thoracic perivascular AT and subscapular brown AT can also be appreciated.

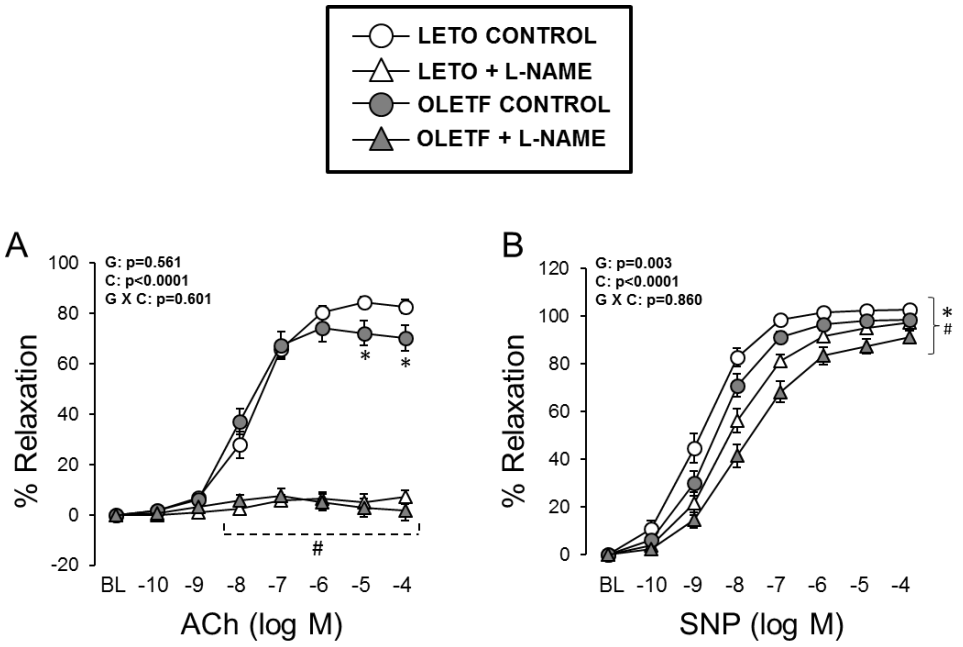

Figure 33. Vasomotor function of thoracic aortic rings in LETO and OLETF rats chronically treated without and with L-NAME. Values are expressed as means ± SE. Panel A: *****Denotes difference ($p<0.05$) from LETO rats; #Denotes difference ($p<0.05$) from control rats. Panel B: *Denotes difference ($p<0.05$) from LETO rats under control conditions at dose -9 log M and from LETO rats under L-NAME conditions at doses -8 to -4 log M. #Denotes difference ($p<0.05$) from control LETO rats at doses -10 to -4 log M and from control OLETF rats at doses -9 to -4 log M. G, group; C, condition; G X C, group by condition interaction.

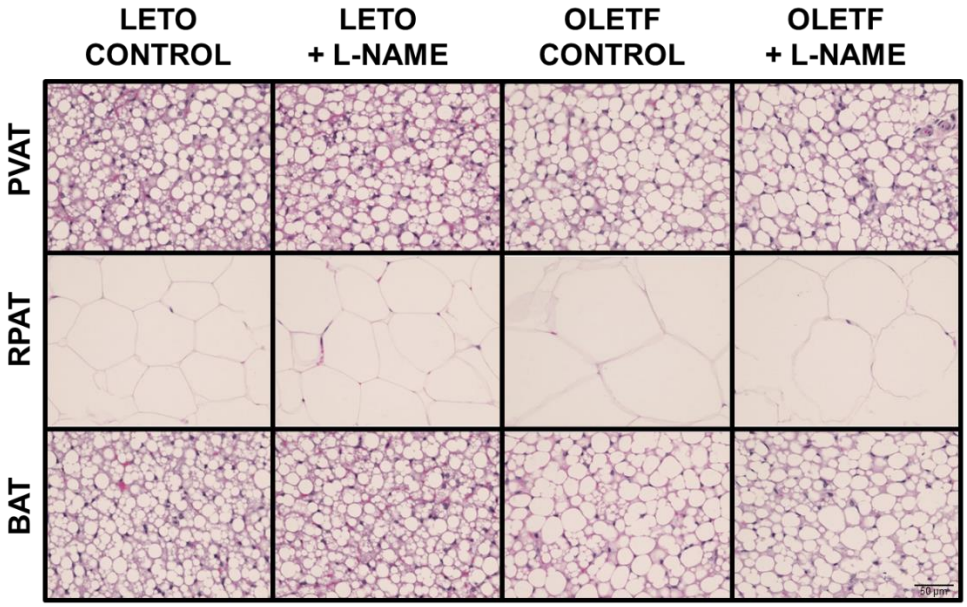

Figure 34. Representative histology photographs (40X magnification) of perivascular (PVAT), retroperitoneal (RPAT) and brown (BAT) ATs in LETO and OLETF rats chronically treated without and with L-NAME.

Figures 5 to 10 summarize the results on AT and vascular gene expression. Specifically, adipokines and inflammation-related genes are presented in Figure 5, adhesion molecule-related genes are presented in Figure 6, immune cell-related genes are presented in Figure 7, nitric oxide isoforms and endothelin-1 are presented in Figure 8, NADPH oxidase-related genes are presented in Figure 9, and mitochondria-related genes are presented in Figure 10. For AT, there was a significant main effect of group for leptin, VCAM-1, ICAM-1, PAI-1, adiponectin, CD4, CD8, CD11c, F4/80, FoxP3, CHOP, p22phox, p47phox, and PPARGC-1-α mRNA (all increased in OLETF relative to LETO rats). A significant main effect of L-NAME treatment was only observed for FoxP3, nNOS, and p22phox mRNA (all three decreased in L-NAME treated rats relative to control rats). A significant main effect of AT depot was observed for all mRNAs examined except for TNF-α ($p=0.097$), FoxP3 ($p=0.590$), and iNOS mRNA ($p=0.208$). A significant group by condition interaction was only observed for FoxP3 mRNA. For clarity and as an example, a statistical interaction occurs when differences between levels (e.g., control vs. L-NAME) within one group (e.g., LETO) are not the same as the differences between levels in other group (e.g., OLETF). A significant group by AT depot interaction was observed for leptin, MCP-1, VCAM-1, PAI-1, CD4, CD8, CD11c, F4/80, FoxP3, nNOS, CHOP, p22phox, and p47hpox mRNA. A significant group by condition by AT depot interaction was only observed for IL-6 mRNA. Figure 11 illustrates the effects of obesity and L-NAME treatment on citrate synthase activity in the retroperitoneal AT. Although not statistically significant, relative to LETO rats, retroperitoneal AT from OLETF rats appeared to have

reduced levels of citrate synthase activity by 35% (p=0.104), an effect that was normalized with L-NAME treatment (p=0.073).

For aortic samples, there was a significant main effect of group for five mRNAs. IL-6 and E-selectin mRNA levels were higher in OLETF relative to LETO rats, and endothlein-1, GRP78, and p47phox mRNA levels were lower in OLETF relative to LETO rats. A significant main effect of L-NAME treatment was observed for MCP-1, IL-6, IL-18, E-selectin, VCAM-1, ICAM-1, CD8, CD11c, F4/80, endothelin-1, and p47phox mRNA (all increased in L-NAME treated rats relative to control rats), as well as for nNOS mRNA, which decreased in L-NAME treated rats relative to control rats. A significant group by condition interaction was only observed for IL-6 and endothelin-1 mRNA. Significant main effects of group, condition, and fat depot on gene expression are depicted in the figures (Figures 5 to 10).

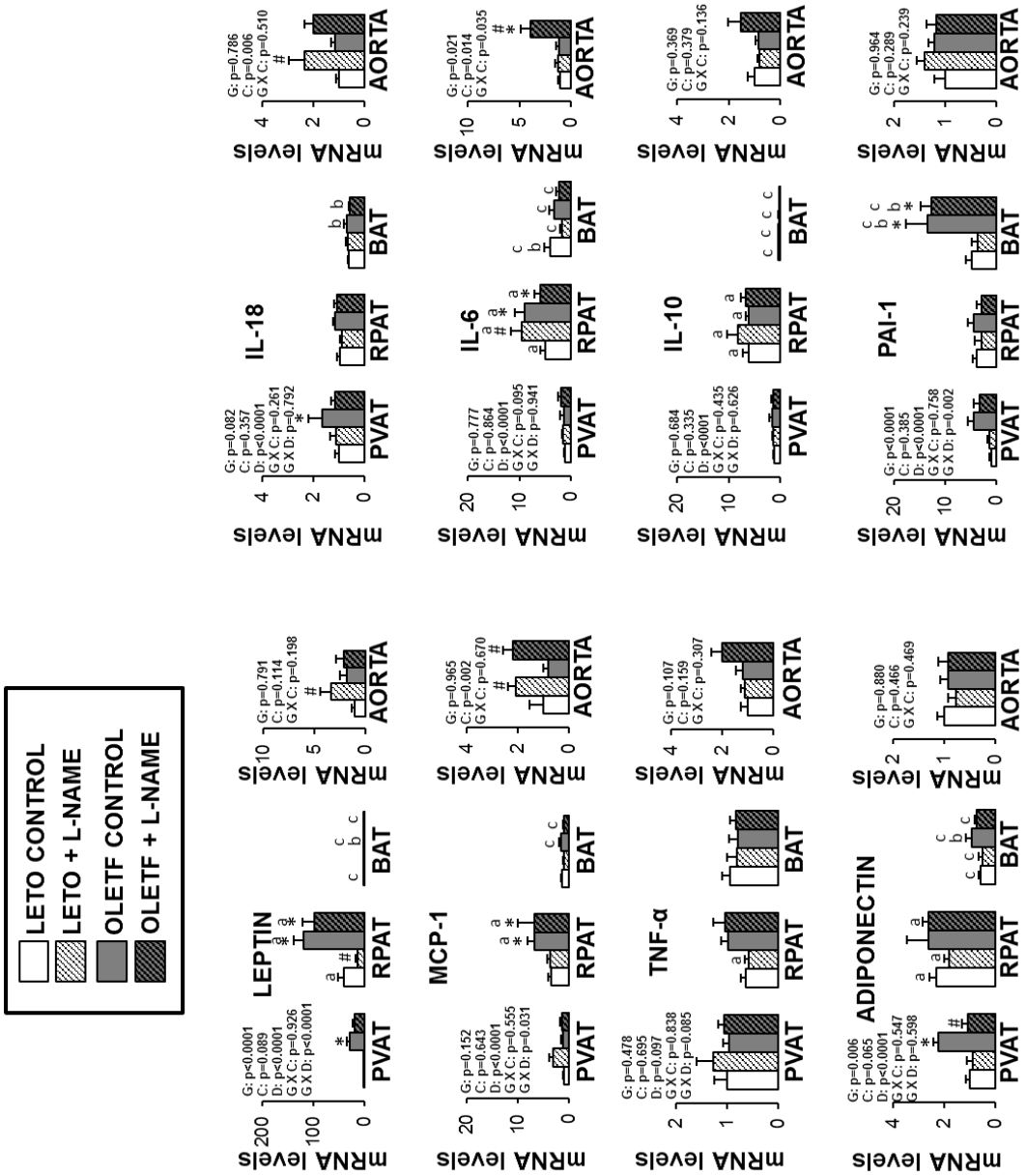

Figure 35. Expression of adipokines and inflammation-related genes in AT and aorta of LETO and OLETF rats chronically treated without and with L-NAME. Values are fold difference in mRNA and expressed as means ± SE. PVAT in the LETO control group of rats is used as the reference tissue and set at 1 for all AT comparisons. For aorta comparisons, the LETO control is used as the reference group and set at 1. *****Denotes difference ($p<0.05$) from LETO rats; [#]Denotes difference ($p<0.05$) from control rats; [a]Denotes difference ($p<0.05$) between PVAT and RPAT; [b]Denotes difference ($p<0.05$) between PVAT and BAT; [c]Denotes difference ($p<0.05$) between RPAT and BAT. G, group; C, condition; D, fat depot.

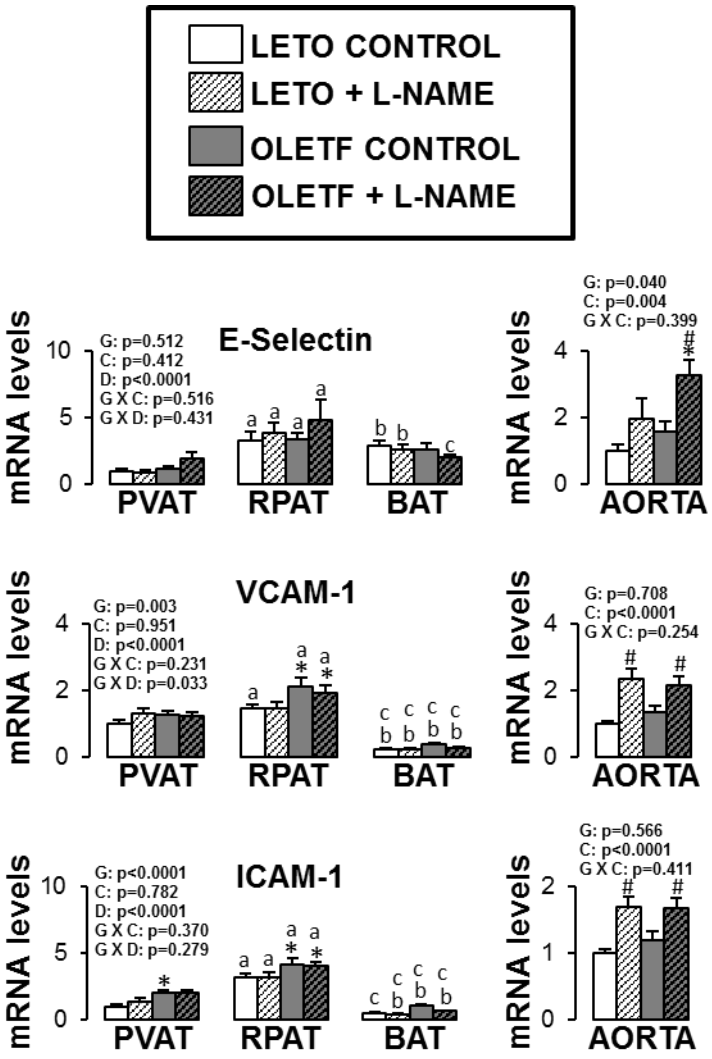

Figure 36. Expression of adhesion molecule-related genes in AT and aorta of LETO and OLETF rats chronically treated without and with L-NAME. Values are fold difference in mRNA and expressed as means ± SE. PVAT in the LETO control group of rats is used as the reference tissue and set at 1 for all AT comparisons. For aorta comparisons, the LETO control is used as the reference group and set at 1. *****Denotes difference ($p<0.05$) from LETO rats; [#]Denotes difference ($p<0.05$) from control rats; [a]Denotes difference ($p<0.05$) between PVAT and RPAT; [b]Denotes difference ($p<0.05$) between PVAT and BAT; [c]Denotes difference ($p<0.05$) between RPAT and BAT. G, group; C, condition; D, fat depot.

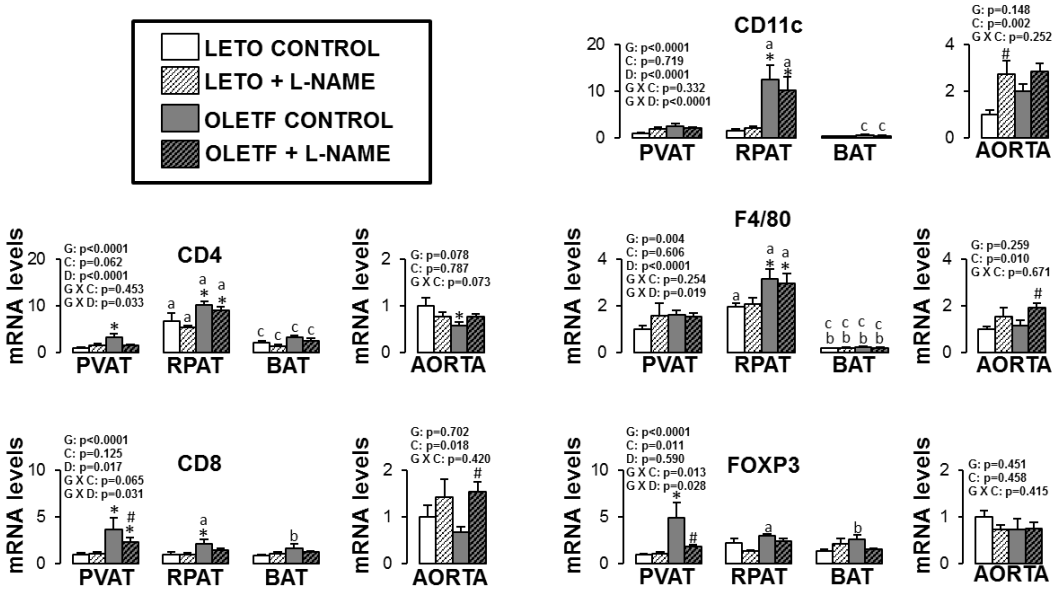

Figure 37. Expression of immune cell-related genes in AT and aorta of LETO and OLETF rats chronically treated without and with L-NAME. Values are fold difference in mRNA and expressed as means ± SE. PVAT in the LETO control group of rats is used as the reference tissue and set at 1 for all AT comparisons. For aorta comparisons, the LETO control is used as the reference group and set at 1. *****Denotes difference ($p<0.05$) from LETO rats; [#]Denotes difference ($p<0.05$) from control rats; [a]Denotes difference ($p<0.05$) between PVAT and RPAT; [b]Denotes difference ($p<0.05$) between PVAT and BAT; [c]Denotes difference ($p<0.05$) between RPAT and BAT. G, group; C, condition; D, fat depot.

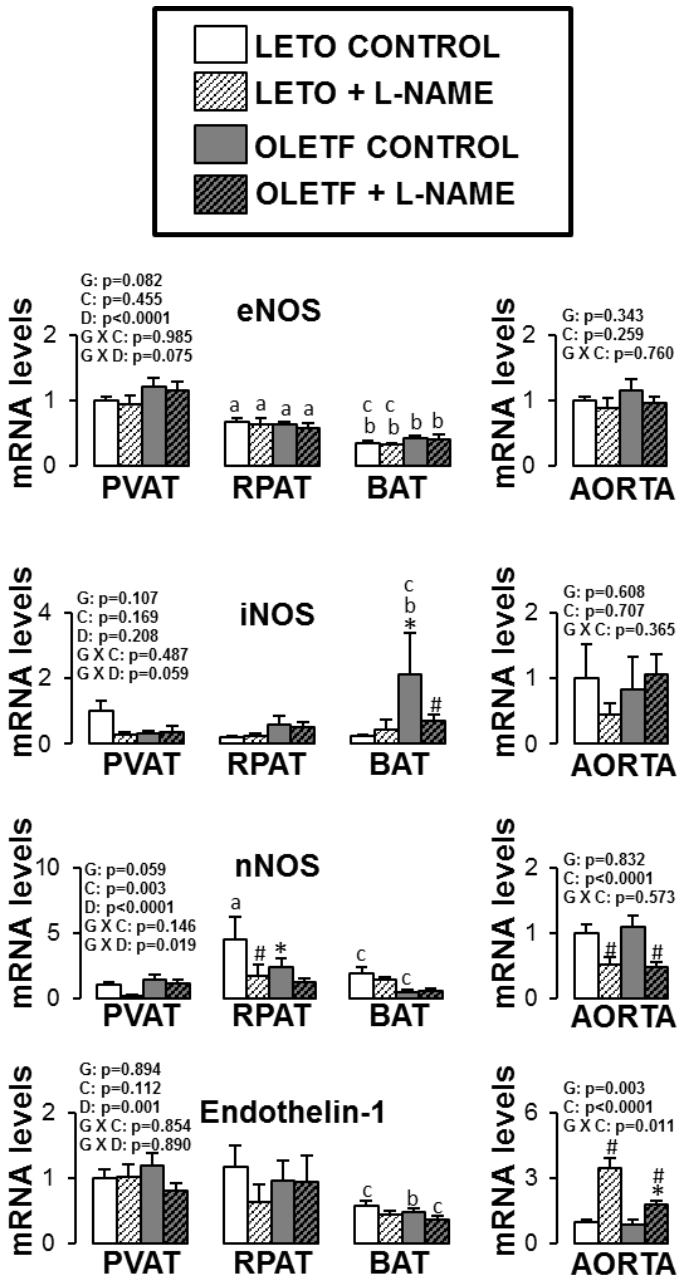

Figure 38. Expression of nitric oxide synthase isoforms and endothelin-1 genes in AT and aorta of LETO and OLETF rats chronically treated without and with L-NAME. Values are fold difference in mRNA and expressed as means ± SE. PVAT in the LETO control group of rats is used as the reference tissue and set at 1 for all AT comparisons. For aorta comparisons, the LETO control is used as the reference group and set at 1. *****Denotes difference ($p<0.05$) from LETO rats; [#]Denotes difference ($p<0.05$) from control rats; [a]Denotes difference ($p<0.05$) between PVAT and RPAT; [b]Denotes difference ($p<0.05$) between PVAT and BAT; [c]Denotes difference ($p<0.05$) between RPAT and BAT. G, group; C, condition; D, fat depot.

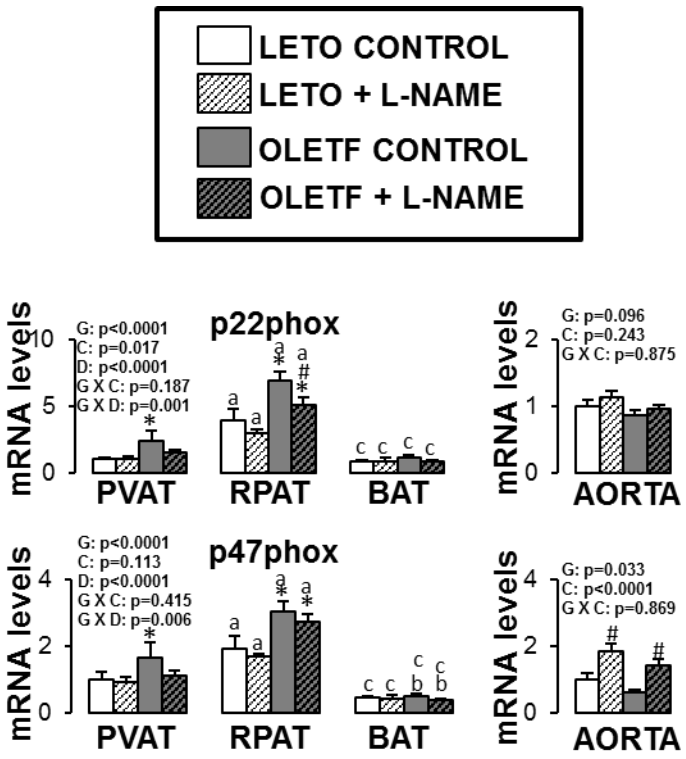

Figure 39. Expression of NADPH oxidase-related genes in AT and aorta of LETO and OLETF rats chronically treated without and with L-NAME. Values are fold difference in mRNA and expressed as means ± SE. PVAT in the LETO control group of rats is used as the reference tissue and set at 1 for all AT comparisons. For aorta comparisons, the LETO control is used as the reference group and set at 1. *****Denotes difference ($p<0.05$) from LETO rats; [#]Denotes difference ($p<0.05$) from control rats; [a]Denotes difference ($p<0.05$) between PVAT and RPAT; [b]Denotes difference ($p<0.05$) between PVAT and BAT; [c]Denotes difference ($p<0.05$) between RPAT and BAT. G, group; C, condition; D, fat depot.

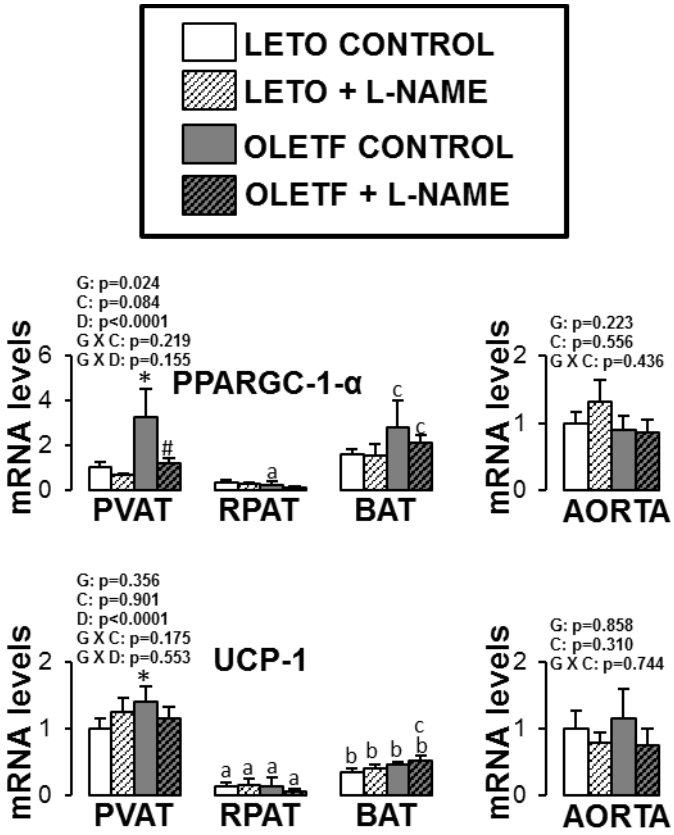

Figure 40. Expression of mitochondria-related genes in AT and aorta of LETO and OLETF rats chronically treated without and with L-NAME. Values are fold difference in mRNA and expressed as means ± SE. PVAT in the LETO control group of rats is used as the reference tissue and set at 1 for all AT comparisons. For aorta comparisons, the LETO control is used as the reference group and set at 1. *****Denotes difference ($p<0.05$) from LETO rats; [#]Denotes difference ($p<0.05$) from control rats; [a]Denotes difference ($p<0.05$) between PVAT and RPAT; [b]Denotes difference ($p<0.05$) between PVAT and BAT; [c]Denotes difference ($p<0.05$) between RPAT and BAT. G, group; C, condition; D, fat depot.

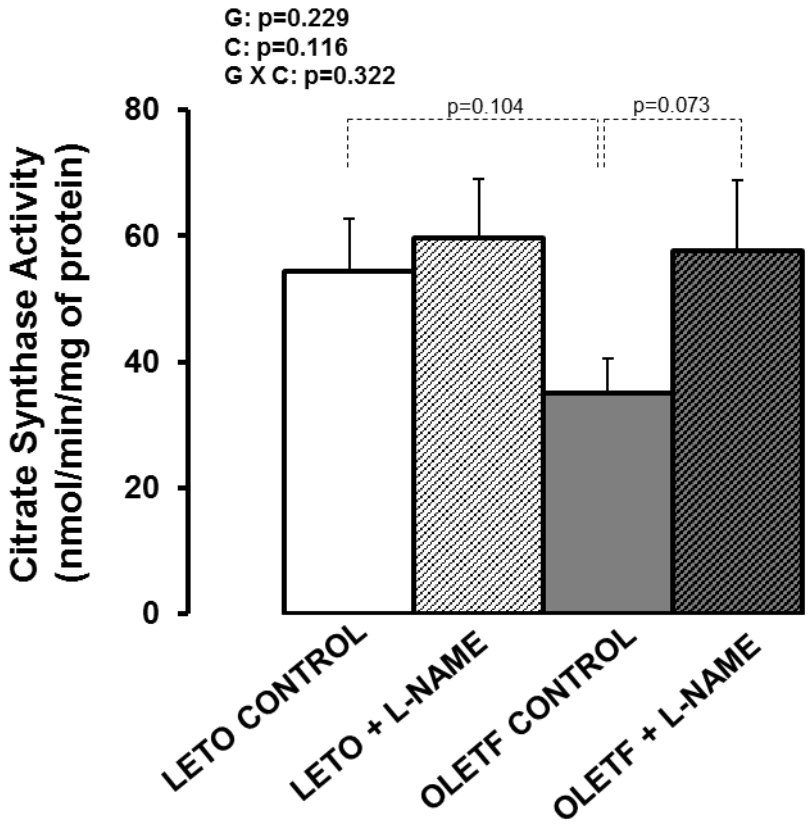

Figure 41. Citrate synthase activity, a marker of mitochondrial content, in retroperitoneal AT of LETO and OLETF rats chronically treated without and with L-NAME. Values are expressed as means ± SE. G, group; C, condition; G X C, group by condition interaction.

f. Discussion

With increasing evidence that AT contributes to the pathogenesis of metabolic and cardiovascular diseases through the local and systemic secretion of pro-inflammatory cytokines (24-31, 37-42), a deeper understanding of the mechanisms responsible for the phenotypic modulation of AT is needed. The main purpose of this study was to test the hypothesis that a decrease in bioavailability of NO would result in increased AT inflammation. This was accomplished by examining the extent to which chronic inhibition of NOS, in the presence or absence of obesity, altered inflammatory gene expression in retroperitoneal white AT, subscapular brown AT, periaortic AT and its contiguous aorta free of perivascular AT. Contrary to our hypothesis, we found that expression of inflammatory genes and markers of immune cell infiltration in all AT depots examined were, by and large, unaltered with chronic administration of L-NAME in both lean and obese rats. This was in contrast with the observation that L-NAME produced a significant upregulation of inflammatory and pro-atherogenic genes in the aorta. Collectively, these findings suggest that the impact of systemic NOS inhibition on inflammatory gene expression is greater in the vascular wall relative to its surrounding perivascular AT, or visceral white and subscapular brown AT depots.

Our finding that NOS inhibition generally did not evoke an increase in inflammatory gene expression in AT was somewhat surprising in light of previous research. Using the eNOS knockout mouse model, Handa et al. (9) demonstrated that reduced eNOS-derived NO signaling is sufficient to induce expression of pro-

inflammatory cytokines and markers of immune cell infiltration in visceral white AT. Likewise, using an eNOS overexpressed mouse model, Sansbury et al. (3) recently showed that increased eNOS activity prevents the obesogenic effects of high-fat diet, in part, by stimulating mitochondrial biogenesis and activity in visceral white AT, thus resulting in a decreased adipocyte size.

A possible explanation for the disparity of findings between these studies and our study may be related to the differences in techniques employed to modulate NO signaling (i.e., eNOS knockout/overexpressed rodent models vs. chronic administration of L-NAME in our study). L-NAME acts as a competitive inhibitor of NOS due to its structural similarity to L-arginine, the substrate of NOS, thus inhibiting all NOS isoforms. Our findings, taken together with data from others using NOS transgenic mouse models (3, 9, 22, 43), suggest that the source of NO (eNOS, iNOS, or nNOS) being modulated may be a determinant of the effects of altered NOS activity on the inflammatory response. Both eNOS and nNOS produce NO in relatively low amounts, whereas iNOS can synthesize remarkably large amounts of NO (44-47). Current evidence indicates that low amounts of NO are beneficial while the large quantities of NO produced by iNOS can be harmful (4, 48). Specifically, it appears that NO derived from eNOS is a key signaling molecule in maintaining a healthy, anti-inflammatory AT phenotype (9), whereas a reduction of NO derived from iNOS may result in reduced both adipocyte size and inflammation. For example, evidence from iNOS knockout mouse studies indicates that ablation of the iNOS gene protects against diet-induced obesity and insulin resistance (43), and in AT, increases expression of mitochondria-related

proteins, and reduces expression of inflammatory cytokines including leptin (22). Hence, given these contrasting roles of eNOS vs. iNOS in modulating AT phenotype, the overall net result when inhibiting all NOS isoforms with L-NAME may be no effect as we indeed largely report in our present study. An alternative explanation could be that the dose of L-NAME at the AT level was insufficient to effectively inhibit NOS isoforms and produce robust genomic effects. Interestingly, there seems to be a downward trend in inflammatory markers in the AT from OLETF L-NAME treated rats vs. OLETF controls (e.g., IL-6, CD4, CD8, CD11C, FoxP3). We speculate this may be evidence of inhibition of the overproduction of NO derived from iNOS in the AT of obese rats. Along these lines, we also observed that L-NAME treatment slightly increased citrate synthase activity, a marker of mitochondrial content, in the retroperitoneal AT of OLETF rats, an effect that would be expected to result from iNOS inhibition (22) and not eNOS inhibition (3). Indeed, current evidence suggests that eNOS-derived NO is an important signal for mitochondrial biogenesis in visceral AT (3).

While NOS inhibition did not produce an effect on AT mRNA levels with the exception of a few genes, we did observe enlargement of adipocyte size and upregulation of inflammatory genes with obesity in the OLETF rat across all AT depots as well as marked differences in gene expression among fat pads. In particular, our data support the idea that perivascular AT surrounding the thoracic aorta has some phenotypic similarities, both morphologically and at the transcriptional level, with brown AT, thus corroborating our recent findings (32). Importantly, in addition to providing evidence of phenotypic divergence among AT

depots, here we show that the effects of hyperphagia-induced obesity on AT gene expression (leptin, MCP-1, VCAM-1, PAI-1, CD4, CD8, CD11c, F4/80, FoxP3, nNOS, CHOP, p22phox, and p47hpox mRNA) appear to be heterogeneous across fat pads.

The overall absence of an L-NAME effect on the phenotype of aortic perivascular AT, and other fat depots examined, is in clear contrast with the NOS inhibition-induced upregulation of inflammatory genes and markers of immune cell infiltration in the contiguous aortic wall. Our data support earlier research demonstrating the atheroprotective role of vascular NO. For example, it has been shown that inhibition of NOS with L-NAME produces atherosclerotic lesions in the aorta of hypercholesterolemic rabbits (49), increases expression of pro-oxidant and inflammatory genes in the aorta of normal rats (5), and increases leukocyte rolling and adhesion in the human microvasculature (6). In addition, there is evidence that mice with targeted disruption of the eNOS gene exhibit abnormal vascular remodeling in response to external carotid artery ligation (8), and mice with eNOS/apoE double knockout exhibit accelerated atherosclerosis, aortic aneurysm formation, and ischemic heart disease (7, 50). One of the unique aspects of our L-NAME study, relative to previous research, is the inclusion of lean and obese rats. We observed an obesity-associated impairment in ACh and SNP-mediated relaxation in aortic rings. In addition, aortas from L-NAME-treated rats, both lean and obese, exhibited complete abrogation of ACh-mediated relaxation. Furthermore, L-NAME treatment reduced SNP-mediated vascular responsiveness and the extent of this effect was similar in both lean and obese rats. The

observation that L-NAME treatment did not abolish between-group differences in SNP-mediated relaxation, suggest that the effect of obesity on vascular responsiveness to NO may not be due to differences in NOS activity.

Of interest, while we observed an effect of obesity on aortic vasomotor function, these effects were not associated with changes in vascular gene expression. Indeed, overall, we did not detect significant differences in aortic mRNA levels between LETO and OLETF rats in the absence of L-NAME. Furthermore, although the vascular effects of NOS inhibition were largely uniform between groups of rats, there were a few exceptions where NOS inhibition unmasked the obesity effect on vascular inflammatory gene expression. Specifically, we noted that induction of E-selectin and IL-6 mRNAs with NOS inhibition was apparent in the obese but not the lean rats. The same was true for other genes including TNF-α and IL-10; however, these effects did not reach statistical significance.

Limitations of the present investigation should be considered. First, our study did not establish whether the reported changes in AT mRNA levels are attributable to alterations in the phenotype of adipocytes and/or resident immune cells within the AT. Similarly, because we studied mRNA levels from whole artery homogenates, it is unknown whether differences in aortic gene expression reported in this study are originating from the endothelium, smooth muscle, or adventitia. Examination of the impact of NOS inhibition and obesity on vascular gene expression with separation of cell populations should be a priority in future studies. Second, all our vasomotor function experiments in the aorta were

performed in the absence of perivascular AT. Future studies are needed to determine if inhibition of NOS in perivascular AT alters vasomotor reactivity. Third, our group and others (5, 15) have previously established that daily consumption of L-NAME in drinking water increases mean arterial pressure in rats. In this regard, because there is extensive evidence that increased blood pressure is a pro-atherogenic stimulus to the vasculature (51), at this time we cannot establish the extent to which the effects of L-NAME on aortic gene expression reported herein are attributable to an increased blood pressure *versus* primarily the direct result of vascular NOS inhibition. This is an important limitation to the present study and further research is necessary to tease out the contribution of increased blood pressure *versus* local removal of NO signaling in modulating vascular gene expression. A potential approach for excluding hypertension-induced changes would be to administer an antihypertensive therapy to L-NAME-treated rats.

In summary, this was the first study to evaluate the effects of systemic NOS inhibition on AT gene expression across different fat pads in lean and obese rats. We provide evidence that expression of inflammatory genes and markers of immune cell infiltration in AT were largely unaltered with chronic administration of L-NAME. This observation is in contrast with the finding that L-NAME caused an overall upregulation of inflammatory genes in the aorta. Taken together, these data suggest that systemic NOS inhibition alters transcriptional regulation of pro-inflammatory genes to a greater extent in the aortic wall compared to its surrounding perivascular AT, as well as relative to visceral white and subscapular brown AT depots.

f. References

1. Ignarro LJ, Buga GM, Wood KS, Byrns RE, Chaudhuri G. Endothelium-derived relaxing factor produced and released from artery and vein is nitric oxide. Proc Natl Acad Sci U S A. 1987;84(24):9265-9. Epub 1987/12/01. PubMed PMID: 2827174; PubMed Central PMCID: PMC299734.

2. Palmer RM, Ferrige AG, Moncada S. Nitric oxide release accounts for the biological activity of endothelium-derived relaxing factor. Nature. 1987;327(6122):524-6. Epub 1987/06/11. doi: 10.1038/327524a0. PubMed PMID: 3495737.

3. Sansbury B, Cummins T, Tang Y, Hellmann J, Holden C, Harbeson M, et al. Overexpression of endothelial nitric oxide synthase prevents diet-induced obesity and regulates adipocyte phenotype. Circulation research. 2012;111:1176-89.

4. Laroux F, Pavlick K, Hines I, Kawachi S, Harada H, Bharwani S, et al. Role of nitric oxide in inflammation. Acta Physiol Scand. 2001;173(1):113-8.

5. Gomez-Guzman M, Jimenez R, Sanchez M, Romero M, O'Valle F, Lopez-Sepulveda R, et al. Chronic (-)-epicatechin improves vascular oxidative and inflammatory status but not hypertension in chronic nitirc oxide-deficient rats. Br J Nutr. 2011;106(9):1337-48.

6. Hossain M, Qadri S, Liu L. Inhibition of nitric oxide synthesis enhances leukocyte rolling and adhesion in human microvasculature. J Inflamm. 2012;9(1):28.

7. Kuhlencordt P, Padmapriya P, Rutzel S, Schodel J, Hu K, Schafer A, et al. Ezetimibe potently reduces vascular inflammation and arteriosclerosis in eNOS-deficient ApoE ko mice. Atherosclerosis. 2009;202(1):48-57.

8. Rudic R, Shesely E, Maeda N, Smithies O, Segal S, Sessa W. Direct evidence for the importance of endothelium-derived nitric oxide in vascular remodeling. J Clin Invest. 1998;101(4):731-6.

9. Handa P, Tateya S, Rizzo N, Cheng A, Morgan-Stevenson V, Han C, et al. Reduced vascular nitric oxide-cGMP signaling contributes to adipose tissue inflammation during high-fat feeding. Arterioscler Thromb Vasc Biol. 2011;31(12):2827-35.

10. Wellen KE, Hotamisligil GS. Obesity-induced inflammatory changes in adipose tissue. J Clin Invest. 2003;112(12):1785-8.

11. Gutierrez D, Puglisi M, Hasty A. Impact of increased adipose tissue mass on inflammation, insulin resistance, and dyslipidemia. Current diabetes reports. 2009;9(1):26-32.
12. Shoelson SE, Lee J, Goldfine AB. Inflammation and insulin resistance. The Journal of Clinical Investigation. 2006;116(7):1793-801. doi: 10.1172/jci29069.

13. Williams I, Wheatcroft S, Shah A, Kearney M. Obesity, atherosclerosis and the vascular endothelium: mechanisms of reduced nitric oxide bioavailability in obese humans. Int J Obes Relat Disord. 2002;26(6):754-64.

14. Siervo M, Jackson S, Bluck L. In-vivo nitric oxide synthesis is reduced in obese patients with metabolic syndrome: application of a novel stable isotopic method. J Hypertens. 2011;29(8):1515-27.

15. Lloyd P, Yang H, Terjung R. Arteriogenesis and angiogenesis in rat ischemic hindlimb: role of nitric oxide. American journal of physiology Heart and circulatory physiology. 2001;281(6):H2528-38.

16. Jenkins NT, Padilla J, Arce-Esquivel AA, Bayless DS, Martin JS, Leidy HJ, et al. Effects of endurance exercise training, metformin, and their combination on adipose tissue leptin and IL-10 secretion in OLETF rats. J Appl Physiol. 2012;113(12):1873-83.

17. Padilla J, Jenkins NT, Roberts MD, Arce-Esquivel AA, Martin JS, Laughlin MH, et al. Differential changes in vascular mRNA levels between rat iliac and renal arteries produced by cessation of voluntary running. Experimental Physiology. 2013;98(1):337-47. doi: 10.1113/expphysiol.2012.066076.

18. Srere PA. Citrate synthase. Methods Enzymol. 1969;13:3-5.

19. Stanford K, Middelbeek R, Townsend K, An D, Nygaard E, Hitchcox K, et al. Brown adipose tissue regulates glucose homeostasis and insulin sensitivity J Clin Invest. 2013;123(1):215-23.

20. Sacks H, Symonds M. Anatomical locations of human brown adipose tissue. Functional relevance and implications in obesity and type 2 diabetes. Diabetes. 2013;62:1783-90.

21. Vasilijevic A, Vojcic L, Dinulovic I, Buzadzic B, Korac A, Petrovic V, et al. Expression pattern of thermogenesis-related factors in interscapular brown adipose tissue of alloxan-treated rats: beneficial effect of L-arginine. Nitric Oxide. 2010;23(1):42-50.

22. Becerril S, Rodriguez A, Catalan V, Sainz N, Ramirez B, Collantes M, et al. Deletion of inducible nitric-oxide synthase in leptin-deficient mice improves brown adipose tissue function. PloS one. 2010;5(6):e10962.

23. Saha S, Ohno T, Ohinata H, Kuroshima A. Effects of nitric oxide synthase inhibition on phospholipid fatty acid composition of brown adipose tissue. Jpn J Physiol. 1997;47(5):477-80.

24. Chatterjee TK, Stoll LL, Denning GM, Harrelson A, Blomkalns AL, Idelman G, et al. Proinflammatory Phenotype of Perivascular Adipocytes. Circulation research. 2009;104(4):541-9. doi: 10.1161/circresaha.108.182998.

25. Payne GA, Kohr MC, Tune JD. Epicardial perivascular adipose tissue as a therapeutic target in obesity-related coronary artery disease. Br J Pharmacol. 2012;165(3):659-69. doi: 10.1111/j.1476-5381.2011.01370.x.

26. Payne GA, Borbouse Ln, Kumar S, Neeb Z, Alloosh M, Sturek M, et al. Epicardial Perivascular Adipose-Derived Leptin Exacerbates Coronary Endothelial Dysfunction in Metabolic Syndrome via a Protein Kinase C-beta Pathway. Arteriosclerosis, Thrombosis, and Vascular Biology. 2012;30(9):1711-7. doi: 10.1161/atvbaha.110.210070.

27. Cheng KH, Chu CS, Lee KT, Lin TH, Hsieh CC, Chiu CC, et al. Adipocytokines and proinflammatory mediators from abdominal and epicardial adipose tissue in patients with coronary artery disease. Int J Obes. 2008;32:268-74.

28. Gorter PM, van Lindert AS, de Vos AM, Meijs MF, GY. vd, Doevendans PA, et al. Quantification of epicardial and peri-coronary fat using cardiac computed tomography: reproducibility and relation with obesity and metabolic syndrome in patients suspected of coronary artery disease. Atherosclerosis. 2008;197:896-903.

29. Greif M, Becker A, SF. v, Lebherz C, Lehrke M, Broedl UC, et al. Pericardial adipose tissue determined by dual source CT is a risk factor for coronary atherosclerosis. Arterioscler Thromb Vasc Biol. 2009;29:781-6.

30. Mazurek T, Zhang L, Zalewski A, Mannion JD, Diehl JT, Arafat H, et al. Human epicardial adipose tissue is a source of inflammatory mediators. Circulation. 2003;108:2460-6.

31. Szasz T, Webb RC. Perivascular adipose tissue: more than just structural support. Clinical Science. 2012;122(1):1-12. doi: 10.1042/cs20110151.

32. Padilla J, Jenkins NT, Vieira-Potter VJ, Laughlin MH. Divergent phenotype of rat thoracic and abdominal perivascular adipose tissues. American journal of physiology Regulatory, integrative and comparative physiology. 2013;304(7):R543-52. Epub 2013/02/08. doi: ajpregu.00567.2012 [pii] 10.1152/ajpregu.00567.2012. PubMed PMID: 23389108; PubMed Central PMCID: PMC3627942.

33. Fitzgibbons TP, Kogan S, Aouadi M, Hendricks GM, Straubhaar J, Czech MP. Similarity of mouse perivascular and brown adipose tissue and their resitance to diet-induced inflammation. American journal of physiology Heart and circulatory physiology. 2011;301:H1425-H37.

34. Jenkins NT, Padilla J, Rector RS, Laughlin MH. Influence of regular physical activity and caloric restriction on beta-adrenergic and natriuretic peptide receptor expression in retroperitoneal adipose tissue of OLETF rats. Exp Physiol. 2013;In press.

35. Bunker A, Arce-Esquivel AA, Rector RS, Booth FW, Ibdah JA, Laughlin MH. Physical activity maintains aortic endothelium dependent relaxation in the obese, type 2 diabetic OLETF rat. American journal of physiology Heart and circulatory physiology. 2010;298(6):H1889-901.

36. McAllister RM, Newcomer SC, Pope ER, Turk JR, Laughlin MH. Effects of chronic nitric oxide synthase inhibition on responses to acute exercise in swine. J Appl Physiol. 2008;104(1):186-97.

37. Ronti T, Lupattelli G, Mannarino E. The endocrine function of adipose tissue: an update. Clinical endocrinology. 2006;64(4):355-65. doi: 10.1111/j.1365-2265.2006.02474.x.

38. Li FYL, Cheng KKY, Lam KSL, Vanhoutte PM, Xu A. Cross-talk between adipose tissue and vasculature: role of adiponectin. Acta Physiologica. 2011;203(1):167-80. doi: 10.1111/j.1748-1716.2010.02216.x.

39. Lau DCW, Dhillon B, Yan H, Szmitko PE, Verma S. Adipokines: molecular links between obesity and atheroslcerosis. American Journal of Physiology - Heart and Circulatory Physiology. 2005;288(5):H2031-H41. doi: 10.1152/ajpheart.01058.2004.

40. Stohr R, Federici M. Insulin resistance and atherosclerosis: convergence between metabolic pathways and inflammatory nodes. Biochem J. 2013;454(1):1-11.

41. Surmi B, Hasty A. The role of chemokines in recruitment of immune cells to the artery wall and adipose tissue. Vascul Pharmacol. 2010;52:27-36.

42. Anderson E, Gutierrez D, Hasty A. Adipose tissue recruitment of leukocytes. Curr Opin Lipidol. 2010;21(3):172-7.

43. Perreault M, Marette A. Targeted disruption of inducible nitric oxide synthase protects against obesity-linked insulin resistance in muscle. Nature Medicine. 2001;7(10):1138-43.

44. Ichinose F, Hataishi R, Wu J, Kawai N, Rodrigues A, Mallari C, et al. A selective inducible NOS dimerization inhibitor prevents systemic, cardiac, and pulmonoary hemodynamic dysfunction in endotoxemic mice. The American journal of physiology. 2003;285:H2524-H30.

45. Enkhbaatar P, Murakami K, Shimoda K, Mizutani A, Traber L, Phillips G, et al. Inducible nitric oxide synthase dimerization inhibitor prevents cardiovascular and renal morbidity in sheep with combined burn and smoke inhalation injury. The American journal of physiology. 2003;285:H2430-H6.

46. Lincoln J, Hoyle C, Burnstock G. Nitric oxide in Health and Disease: Cambridge University Press; 1997.

47. Stuehr D. Structure-function aspects in the nitric oxide synthases. Ann Rev Pharmacol Toxicol. 1997;37:339-59.

48. Thomas D, Ridnour L, Isenberg J, Flores-Santana W, Switzer C, Donzelli S, et al. The chemical biology of nitric oxide: implications in cellular signaling. Free Radic Biol Med. 2008;45(1):18-31.

49. Cayatte A, Palacino J, Horten K, Cohen R. Chronic inhibition of nitric oxide production accelerates neointima formation and impairs endothelial function in hypercholesterolemic rabbits. Arterioscler Thromb 1994;14(753-759).

50. Kuhlencordt P, Gyurko R, Han F, Scherrer-Crosbie M, Aretz T, Hajjar R, et al. Accelerated atherosclerosis, aortic aneurysm formation, and ischemic heart disease in apolipoprotein E/endothelial nitric oxide synthase double-knockout mice. Circulation. 2001;104(448-454).

51. Padilla J, Jenkins NT, Laughlin MH, Fadel PJ. Blood pressure regulation VIII: resistance vessel tone and implications for a pro-atherogenic conduit artery endothelial cell phenotype. European journal of applied physiology. 2013;in press.

6. ADIPOSE TISSUE AND VASCULAR PHENOTYPIC MODULATION BY VOLUNTARY PHYSICAL ACTIVITY AND DIETARY RESTRICTION IN OBESE INSULIN-RESISTANT OLEFT RATS

a. Note to the reader on authorship

This paper was originally authored by Dr. Jacqueline Crissey, who has granted permission for both the text and figures of this paper to be reproduced in this dissertation. Figure and table numbering has been changed when necessary to follow the numbering scheme of the dissertation. The citation for this paper is as follows:

Crissey, J.M., et al., *Adipose tissue and vascular phenotypic modulation by voluntary physical activity and dietary restriction in obese insulin-resistant OLETF rats.* Am J Physiol Regul Integr Comp Physiol, 2014. **306**(8): p. R596-606.

b. Abstract

Adipose tissue (AT)-derived cytokines are proposed to contribute to obesity-associated vascular insulin resistance. We tested the hypothesis that voluntary physical activity and diet restriction-induced maintenance of body weight would both result in decreased AT inflammation and concomitant improvements in

insulin-stimulated vascular relaxation in the hyperphagic, obese OLETF rat. OLETF rats (age 12 wk) were randomly assigned to sedentary (SED, n=10), wheel running (WR, n=10), and diet restriction (DR, n=10; fed 70% of SED) for 8 weeks. WR and DR rats exhibited markedly lower adiposity (7.1±0.4 and 15.7±1.1% body fat, respectively) relative to SED (27±1.2% body fat), as well as improved blood lipid profiles and systemic markers of insulin resistance. Less adiposity in both WR and DR was associated with decreased AT expression of inflammatory genes (e.g., MCP-1, TNF-α, IL-6) and markers of immune cell infiltration (e.g., CD4, CD8, CD11c, F4/80). The extent of these effects were most pronounced in visceral AT (retroperitoneal) compared to subcutaneous and periaortic AT. Markers of inflammation in brown AT were upregulated with WR but not DR. In periaortic AT, WR and DR-induced reductions in mRNA expression and secretion of cytokines were accompanied with a more athero-protective gene expression profile in the adjacent aortic wall. WR, but not DR, resulted in greater insulin-stimulated relaxation in the aorta; an effect that was in part mediated by a decrease in insulin-induced endothelin-1 activation in WR aorta compared to SED. Collectively, we show in OLETF rats that lower adiposity leads to less AT and vascular inflammation as well as an exercise-specific improvement in insulin-stimulated vasorelaxation.

c. Introduction

More than one-third of Americans are obese (1) and the causes underlying the obesity epidemic appear to be largely related to physical inactivity and over-nutrition, a set of behaviors increasingly prevalent in our society (2-6). Cumulative

evidence indicates that obesity is an important contributor to the development of whole body insulin resistance, type 2 diabetes, and cardiovascular disease (7). A critical link between obesity and its associated metabolic and cardiovascular diseases is thought to be chronic low-grade systemic inflammation (7). In this regard, recent studies implicate adipose tissue (AT) as a local and systemic source of inflammatory cytokines that may be involved in the instigation of vascular insulin resistance and atherosclerosis associated with obesity (8-21). Indeed, excessive lipid accumulation and enlargement of adipocytes in obesity is associated with infiltration of immune cells into AT, contributing to AT inflammation and subsequent secretion of pro-inflammatory cytokines (22). A deeper understanding of the influence of lifestyle modifications on AT inflammation and vascular insulin resistance may lead to more effective strategies aimed at prevention and treatment of obesity-related metabolic and cardiovascular diseases.

Accordingly, we tested the hypothesis that treatment with increased voluntary physical activity or diet restriction-induced maintenance of body weight would result in decreased AT inflammation and concomitant improvements in vasomotor reactivity to insulin in obese, insulin-resistant rats. Given the growing appreciation for phenotypic and functional heterogeneity among AT depots including visceral, subcutaneous, brown and perivascular AT (23-26), we also reasoned that the extent of the effects of physical activity and diet restriction on AT inflammation would be AT depot-specific. Furthermore, we tested the hypothesis that reduced AT expression and secretion of cytokines caused by physical activity

or dietary restriction would be accompanied by a less pro-atherogenic vascular phenotype and enhanced insulin-stimulated vascular relaxation.

d. Methods

Animals

All animal protocols were approved by the University of Missouri Institutional Animal Care and Use Committee. Male OLETF rats were obtained at 4 weeks of age (Japan SLC, Inc. 3371-8, Kotoh-Cho, Hamamatsu, Shizuoka, Japan) and housed individually in cages maintained in temperature-controlled (21ºC) animal quarters with light from 06:00 to 18:00 h and dark from 18:00 h to 06:00 h. At 12 weeks, rats were randomized to one of the following three groups: (i) sedentary (SED; n=10); (ii) voluntary wheel running (WR, n=10); or (iii) sedentary + diet restriction (DR, fed 70% of ad libitum-fed SED animals; n=10). Animals in the WR group were housed with running wheels connected to a Sigma Sport BC 800 bicycle computer (Cherry Creek Cyclery, Foster Falls, VA, USA) for determination of daily running distance. All groups were provided with standard rodent chow (Formulab 5008, Purina Mills, St. Louis, MO) with approximately 26% protein, 18% fat, and 56% carbohydrate. SED and WR groups had *ad libitum* access to food. Body weights and food intakes were recorded on a weekly basis. At 20 weeks of age, rats were anesthetized by intraperitoneal injection of pentobarbital sodium (50 mg/kg). Tissues were harvested and the animals were euthanized by exsanguination in full compliance with the American Veterinary Medical Association Guidelines on Euthanasia. The wheels of the WR group were locked

and food was removed from the cages of all groups ~14 hrs before the rats were sacrificed.

Body composition and blood parameters

On the day of the experiments, body mass was measured to the nearest 0.01 g and, following anesthetization, body composition was determined using a dual energy x-ray absorptiometry instrument (Hologic QDR-1000) calibrated for rodents. In addition, retroperitoneal, epididymal, and omental AT weights were measured to the nearest 0.01 g. Plasma samples were prepared by centrifugation and stored at -80ºC until analysis. Glucose, cholesterol, triglycerides, and non-esterified fatty acids (NEFA) assays were performed by a commercial laboratory (Comparative Clinical Pathology Services, Columbia, MO) on an Olympus AU680 automated chemistry analyzer (Beckman-Coulter, Brea, CA) using commercially available assays according to manufacturer's guidelines. Plasma insulin concentrations were determined using a commercially available, rat-specific ELISA (Alpco Diagnostics, Salem, NH). In addition, plasma and periaortic AT-conditioned medium samples were assayed for concentrations of leptin, MCP-1, TNF-α, and IL-6 using a multiplex cytokine assay (Millipore Milliplex, cat no. RCYTOMAG-80K; Billerica, MA, USA) on a MAGPIX instrument (Luminex Technologies; Luminex Corp., Austin, TX, USA) according to the manufacturer's instructions (26, 27).

Tissue sampling

Perivascular AT surrounding the thoracic aorta, retroperitoneal white AT, inguinal subcutaneous white AT, and interscapular brown AT were quickly excised from the anesthetized rat. For each fat depot, a portion was flash frozen and kept at -80ºC for examination of gene expression and a portion was fixed in neutral-buffered 10% formalin for histology analysis. A portion of perivascular AT surrounding the thoracic aorta was used for in vitro assessment of cytokine secretion as described below. A segment of the thoracic aorta cleaned of perivascular AT and excess adventitia was sectioned into 2 mm rings in cold Krebs for subsequent assessment of vasomotor function. In addition, isolated thoracic aortic segments were kept in RNAlater (Ambion, Austin, TX) for 24 h at 4ºC, then removed from the RNAlater solution and stored at -80ºC until processing.

Cytokine secretion from periaortic AT

A portion of perivascular AT surrounding the thoracic aorta was incubated in Medium 199 at pH 7.4 for 24 hrs (100 mg of AT per 300 ul) under standard culture conditions (37ºC, 5% CO_2) to obtain the corresponding secretomes (SED, WR, and DR) (28). After 24 hrs of incubation, the conditioned media from the AT explants were stored at -80ºC until analysis.

RNA extraction and real-time PCR

AT and aortic samples were homogenized in TRIzol solution using a tissue homogenizer (TissueLyser LT, Qiagen, Valencia, CA). Total RNA was isolated using the Qiagen's RNeasy Lipid Tissue Kit and assayed using a Nanodrop spectrophotometer (Thermo Scientific, Wilmington, DE) to assess purity and concentration. First-strand cDNA was synthesized from total RNA using the High

Capacity cDNA Reverse Transcription kit (Applied Biosystems, Carlsbad, CA). Quantitative real-time PCR was performed as previously described (26, 29, 30) using the CFX Connect™ Real-Time PCR Detection System (BioRad, Hercules, CA). Primer sequences (Table 1) were designed using the NCBI Primer Design tool. All primers were purchased from IDT (Coralville, IA). A 20-µl reaction mixture containing 10 µl iTaq UniverSYBR Green SMX (BioRad, Hercules, CA) and the appropriate concentrations of gene-specific primers plus 4 µl of cDNA template were loaded in each well of a 96-well plate. All PCR reactions were performed in duplicate. PCR was performed with thermal conditions as follows: 95ºC for 10 min, followed by 40 cycles of 95ºC for 15 s and 60ºC for 45 s. A dissociation melt curve analysis was performed to verify the specificity of the PCR products. 18S primers were used to amplify the endogenous control product. Our group has established that 18S is a suitable house-keeping gene for real-time PCR when examining AT and vascular gene expression. In the present study, 18S CTs were not different among the three groups of animals for any of the different tissues examined. mRNA expression values are presented as $2^{\Delta CT}$ whereby ΔCT = 18S CT - gene of interest CT (26, 29, 30). mRNA levels were normalized to the SED group of rats, which was always set at 1.

Table 9. Forward and reverse primer sequences for quantitative real-time PCR

	Primer sequence (5'→3')	
Gene	**Forward**	**Reverse**
18S	GCCGCTAGAGGTGAAATTCTTG	CATTCTTGGCAAATGCTTTCG
Leptin	GACACCCTTAGAGGGGGCTA	AACCCAAGCCCCTTTGTTCA
MCP-1	CTGTCTCAGCCAGATGCAGTTAA	AGCCGACTCATTGGGATCAT
TNF-α	AACACACGAGACGCTGAAGT	TCCAGTGAGTTCCGAAAGCC
IL-6	AGAGACTTCCAGCCAGTTGC	AGCCTCCGACTTGTGAAGTG
E-Selectin	GCCATGTGGTTGAATGTAAAGC	GGATTTGAGGAACATTTCCTGACT
VCAM-1	GAAGGAAACTGGAGAAGACAATCC	TGTACAAGTGGTCCACTTATTTCAATT
ICAM-1	CACAAGGGCTGTCACTGTTCA	CCCTAGTCGGAAGATCGAAAGTC
PAI-1	AGCTGGGCATGACTGACATCT	GCTGCTCTTGGTCGGAAAGA
CD4	ACCCTAAGGTCTCTGACCCC	TAGGCTGTGCGTGGAGAAAG
CD8	CACTAGGCTCCAGGTTTCCG	CGCAGCACTTCGCATGTTAG
CD11c	CTGTCATCAGCAGCCACGA	ACTGTCCACACCGTTTCTCC
F4/80	GCCATAGCCACCTTCCTGTT	ATAGCGCAAGCTGTCTGGTT
FoxP3	CTCCAGTACAGCCGGACAC	GGTTGGGCATCAGGTTCTTG
CHOP	AGAGCCAAAATAACAGCCGGA	ACCGGTTTCTGCTTTCAGGT
GRP78	GCAGTTGCTCACGTGTCTTG	TCCAAGGTGAACACACACCC
p22phox	ACCTGACCGCTGTGGTGAA	GTGGAGGACAGCCCGGA
p47phox	ACGCTCACCGAGTACTTCAACA	TCATCGGGCCGCACTTT
UCP-1	CCGGTGGATGTGGTAAAAAC	CTCCAAGTCGCCTATGTGGT
PPARGC-1-α	GGGGCACATCTGTTCTTCCA	GAGCTGTTTTCTGGTGCTGC

Histology assessments

Formalin-fixed AT samples were processed through paraffin embedment, sectioned at five microns, stained with hematoxylin and eosin for morphometric determinations. Sections were examined using an Olympus BX60 photomicroscope (Olympus, Melville, NY) and photographed at 40x magnification using with a Spot Insight digital camera (Diagnostic Instruments, Inc., Sterling Heights, MI) (26, 27).

Functional assessment of isolated aortic rings

A segment of the thoracic aorta, trimmed of fat and connective tissue, was sectioned into 2 mm rings in cold Krebs. Rings were then mounted on wire feet connected to isometric force transducers and submerged in 20mL baths containing physiological Krebs solution maintained at 37ºC for 1 hour to allow for equilibration. Aortic rings were stretched to optimal length which ranged from 130 to 140% of passive diameter. Vasoreactivity was assessed with cumulative concentration-response curves of acetylcholine (ACh, 10^{-10} to 10^{-4} M), insulin (10 to 10,000 µIU/mL), sodium-nitro-prusside (SNP, 10^{-10} to 10^{-4} M), and endothelin-1 (ET-1, 10^{-10} to 10^{-7} M). A submaximal concentration of phenylephrine ($3e^{-7}$ M) was used to preconstrict all vessels prior to acetylcholine, insulin and SNP relaxation curves. The contribution of ET-1 in altering insulin-stimulated relaxation was assessed by incubating the rings with tezosentan (3 µM for 20 min), a nonselective ET-1 receptor blocker. For insulin, ACh, and SNP curves, relaxation at each concentration was measured and expressed as percent maximum relaxation,

where 100% is equivalent to loss of all tension developed in response to phenylephrine (31).

Statistical analysis

The effects of WR and DR on all dependent variables were evaluated using a one-way ANOVA. Dose-response curves from vasomotor function experiments were analyzed using a two-way (group x dose) ANOVAs. When appropriate, the Fishers protected least significant difference post hoc was used. All data are presented as mean ± standard error (SE). For all statistical tests, the alpha level was set at 0.05. All statistical analyses were performed with SPSS V21.0.

e. Results

As shown in Figure 1, rats with access to running wheels increased daily running distance from week 12 to week 15 (~8km/day), after which running distance gradually declined to ~6km/day at 20 weeks. These are similar voluntary running distances as we have previously reported in this animal model. WR and DR rats weighed less and had improved body composition profiles (e.g., lower total percent body fat and less visceral adipose tissue mass) compared to SED rats (all $p<0.05$). As summarized in Table 2, compared to the SED group, WR and DR plasma had lower fasting total cholesterol, LDL cholesterol, HDL cholesterol, triglycerides, NEFAs, glucose, and leptin (all $p<0.05$). In addition, WR had improved HOMA-IR, lower plasma insulin, and lower circulating MCP-1 compared to SED rats (all $p<0.05$).

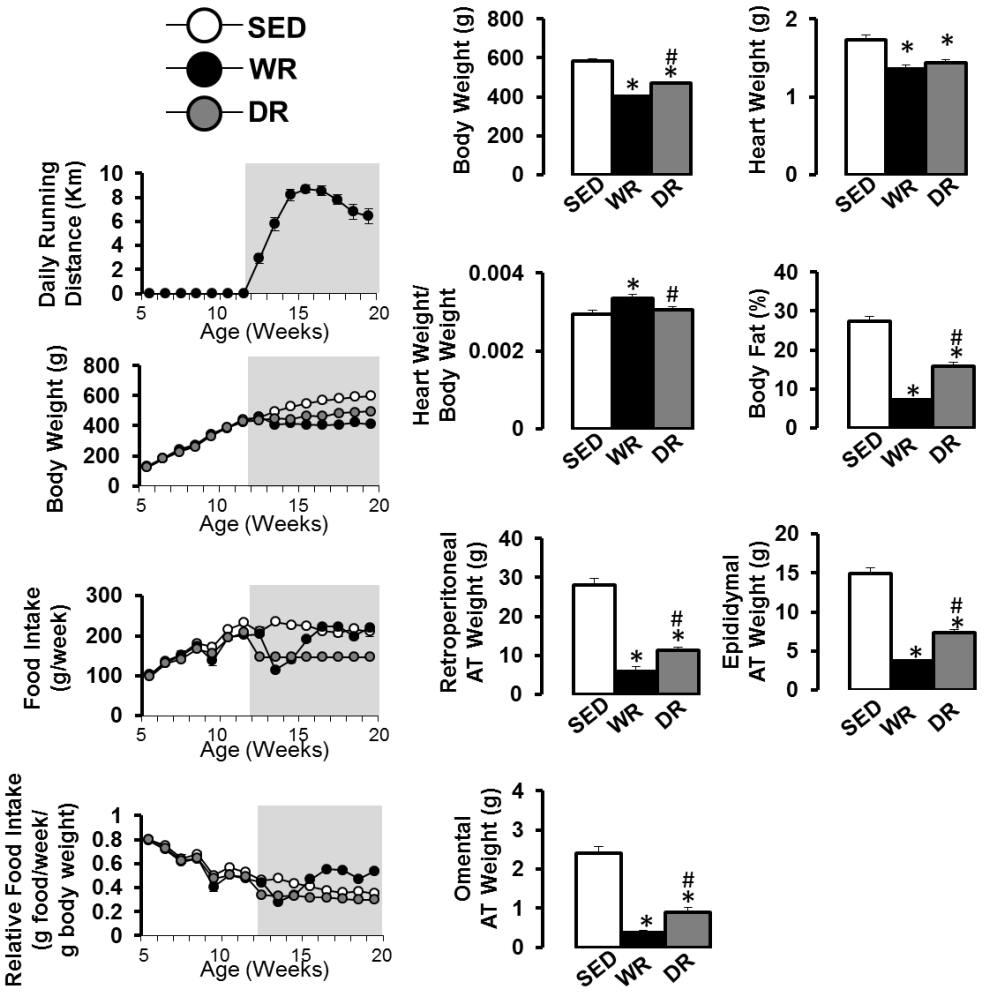

Figure 42. Body composition and food intake in sedentary (SED), wheel running (WR), and diet restriction (DR) OLETF rats. Values are expressed as means ± SE. Body fat, heart weights, and fat pad weights were obtained at 20 weeks (time of sacrifice). *****Denotes difference ($p<0.05$) from SED rats; #Denotes difference ($p<0.05$) from WR rats.

Table 10. Fasting plasma characteristics in sedentary (SED), wheel running (WR), and diet restriction (DR) OLETF rats

Variable	SED	WR	DR
Total cholesterol, mg/dl	110.7±4.4	69.7±2.8*	78.0±1.1*
LDL cholesterol, mg/dl	46.4±3.9	29.6±1.8*	34.5±0.8*
HDL cholesterol, mg/dl	33.2±0.7	29.9±1.3*	29.1±0.5*
Triglycerides, mg/dl	155.0±6.5	51.1±2.7*	71.9±4.0*#
NEFA, mmol/l	0.57±0.05	0.19±0.01*	0.31±0.03*#
Insulin, ng/ml	30.8±10.1	6.9±0.7*	19.5±3.2
Glucose, mg/dl	311.6±9.5	196.1±4.9*	223.1±10.6*#
HOMA-IR index	24.1±8.2	3.4±0.4*	11.1±2.2
Leptin, ng/ml	260.1±39.0	2.2±0.3*	63.9±24.7*
MCP-1, pg/ml	197.1±8.5	144.3±9.4*	194.4±26.4#
TNF-α, pg/ml	6.5±0.3	5.3±0.5	6.6±0.5#
IL-6, pg/ml	204.4±66.0	173.6±56.7	194.5±66.3

Abbreviations: LDL, low density lipoprotein; HDL, high density lipoprotein; NEFA; non-esterified fatty acids; HOMA-IR, homeostasis model assessment of insulin resistance; MCP-1, monocyte chemotactic protein-1; TNF-α, tumor necrosis factor alpha; IL-6, interleukin 6.

*****Denotes difference ($p<0.05$) from SED rats; #Denotes difference ($p<0.05$) from WR rats.

Figure 2 illustrates representative histological photographs of retroperitoneal AT, subcutaneous AT, interscapular brown AT, and periaortic AT. As shown, WR and DR had less lipid deposition in brown and periaortic AT as well as decreased adipocyte size in white AT. Consistent with our previous report (26), a clear structural similarity between thoracic perivascular AT and interscapular brown AT was noted.

Retroperitoneal AT of WR and DR rats exhibited reduced expression of leptin, MCP-1, TNF-α, IL-6 (Figure 3), PAI-1, ICAM-1 (Figure 4), CD4, CD8, CD11c, F4/80, FOXP3 (Figure 5), p22 phox, and p47phox (Figure 6) relative to SED (all $p<0.05$). Furthermore, WR resulted in increased expression of PPARGC-1α, and DR resulted in decreased expression of GRP78 and CHOP (all $p<0.0.5$). Subcutaneous AT of WR and DR rats exhibited reduced expression of leptin and MCP-1 relative to SED (Figure 3; all $p<0.05$). Interscapular brown AT of WR and DR rats exhibited reduced expression of leptin (Figure 3) and PAI-1 (Figure 4) relative to SED (all $p<0.05$). Furthermore, WR resulted in increased expression of MCP-1, TNF-α ($p=0.06$), IL-6 (Figure 3), E-selectin (Figure 4), CD4 ($p=0.06$), F4/80 ($p=0.06$) (Figure 5), and p47phox (Figure 6; all $p<0.05$ unless otherwise indicated); whereas DR resulted in reduced expression of UCP-1 (Figure 7; $p<0.05$). Periaortic AT of WR and DR rats exhibited reduced expression of leptin, MCP-1, TNF-α (Figure 3), CD11c (Figure 5), and UCP-1 (Figure 7) relative to SED (all $p<0.05$). Furthermore, WR resulted in reduced expression of PAI-1 (Figure 4), CD8

(Figure 5) and increased expression of VCAM-1 (Figure 4; all $p<0.05$). On the other hand, DR resulted in reduced expression of IL-6 (Figure 3), E-selectin, ICAM-1 (Figure 4), CD4, F4/80 (Figure 5), p22phox, and p47phox (Figure 6; all $p<0.05$).

Aorta of WR and DR rats exhibited reduced expression of IL-6 (Figure 3), E-selectin, VCAM-1 (Figure 4), CD4, CD8, F4/80 (Figure 5), GRP78 and CHOP (Figure 6) relative to SED (all $p<0.05$). Furthermore, WR resulted in reduced expression of leptin (Figure 3); whereas DR resulted in reduced expression of MCP-1 (Figure 3), CD11c (Figure 5), and increased expression of PAI-1 (Figure 4; all $p<0.05$).

As illustrated in Figure 7, WR and DR rats exhibited reduced periaortic AT-derived secretion of leptin, IL-6 (all $p<0.05$), and MCP-1 ($p=0.09$ and $p=0.11$, respectively) relative to SED. Periaortic-derived secretion of TNF-α was similar among groups ($p>0.05$).

Insulin-stimulated aortic relaxation was significantly greater in WR rats relative to SED and DR rats (Figure 9). Treatment of aortic rings with tezosentan, a non-selective ET-1 receptor blocker, largely removed differences in insulin-stimulated relaxation between WR and SED rats. That is, tezosentan increased insulin-stimulated relaxation in the SED ($p=0.057$) but had no effect in WR or DR ($p>0.05$). A small decrease in ACh-mediated relaxation was observed in DR rats at the highest dose of ACh. In addition, we observed no differences in ET-1-mediated contraction or SNP-mediated relaxation among groups ($p>0.05$).

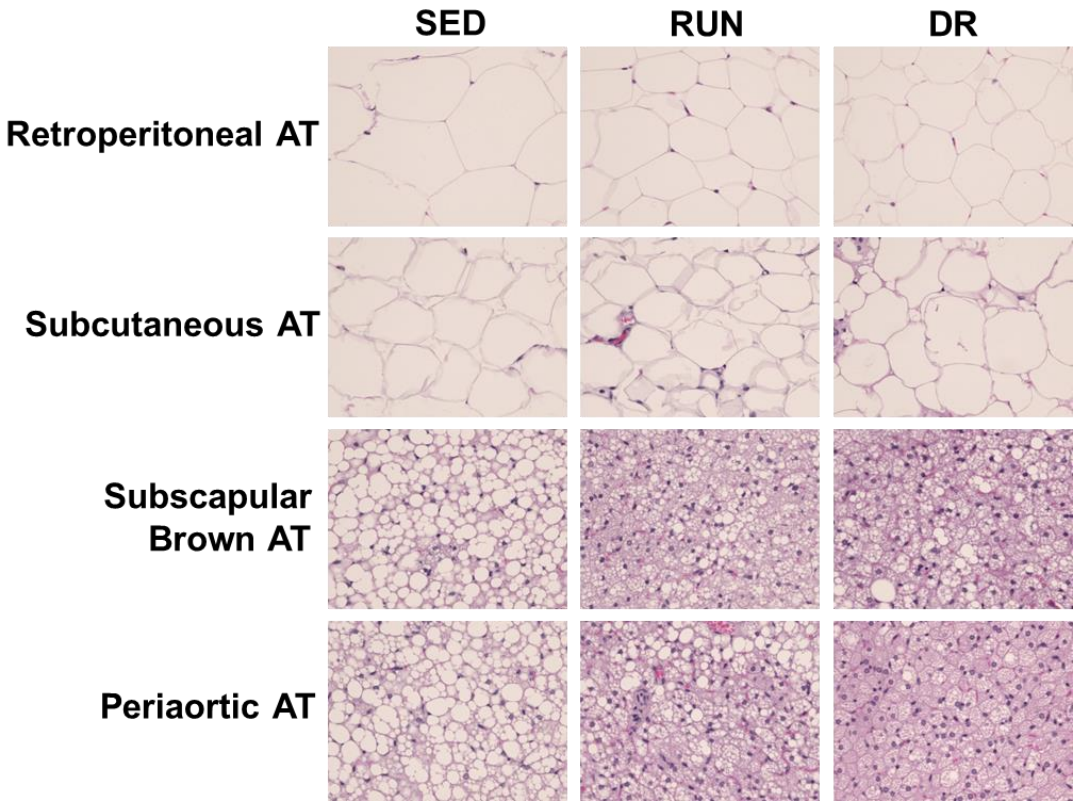

Figure 43. Representative histology photographs (40X magnification) of retroperitoneal AT, subcutaneous AT, interscapular brown AT, and periaortic AT in sedentary (SED), wheel running, (WR), and diet restriction (DR) OLETF rats.

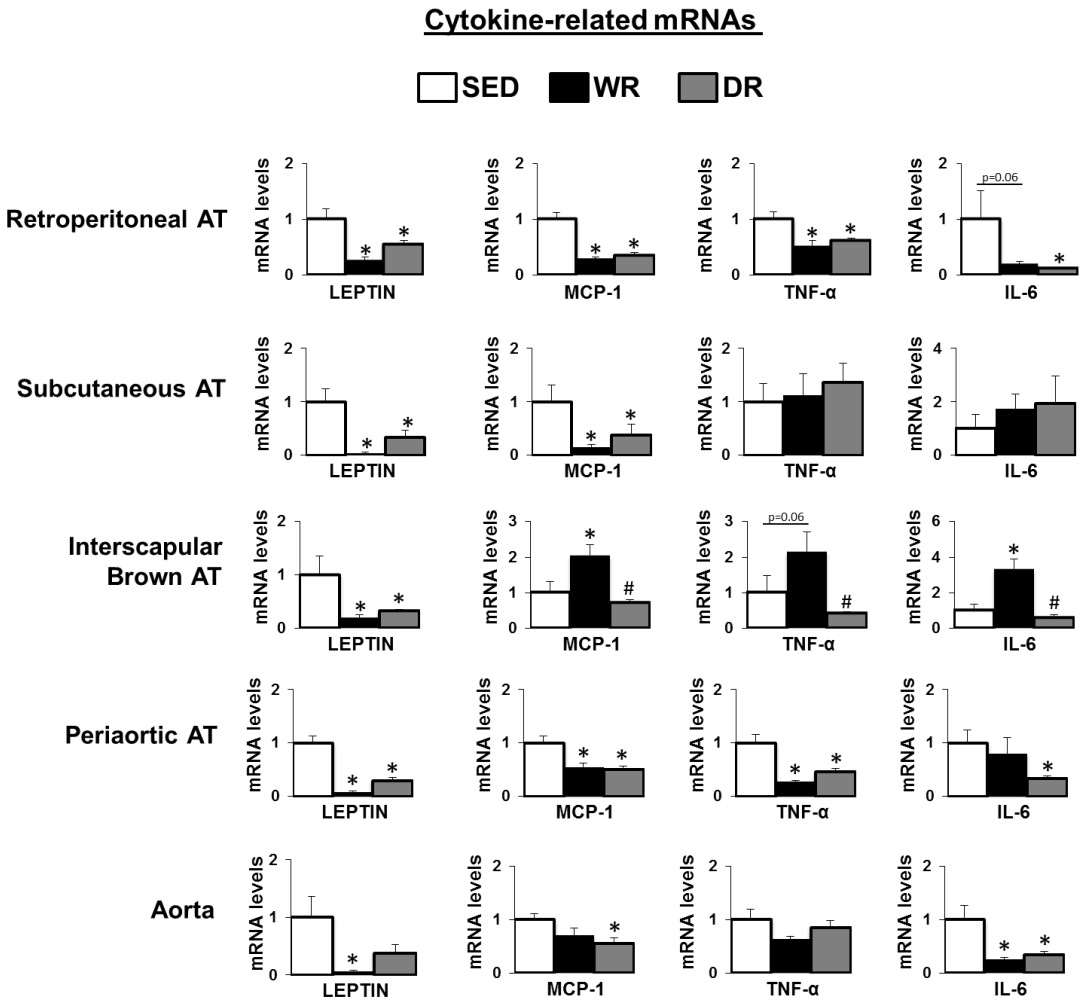

Figure 44. Expression of cytokine-related genes in ATs and aorta of sedentary (SED), wheel running (WR), and diet restriction (DR) OLETF rats. Values are expressed as means ± SE. For each gene, SED is used as the reference group and set at 1. *****Denotes difference ($p<0.05$) from SED rats; $^{\#}$Denotes difference ($p<0.05$) from WR rats.

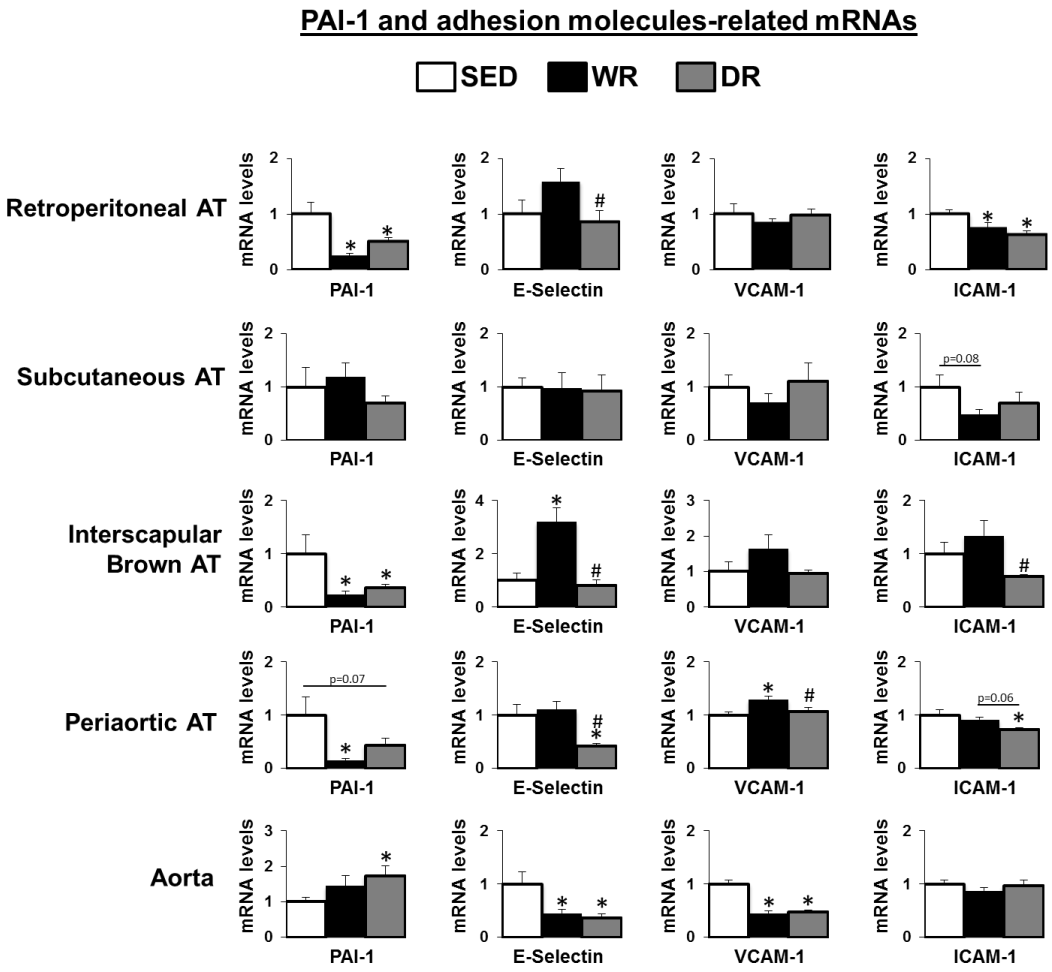

Figure 45. Expression of plasminogen activator inhibitor-1 (PAI-1) and adhesion molecules-related genes in ATs and aorta of sedentary (SED), wheel running (WR), and diet restriction (DR) OLETF rats. Values are expressed as means ± SE. For each gene, SED is used as the reference group and set at 1. *****Denotes difference ($p<0.05$) from SED rats; #Denotes difference ($p<0.05$) from WR rats.

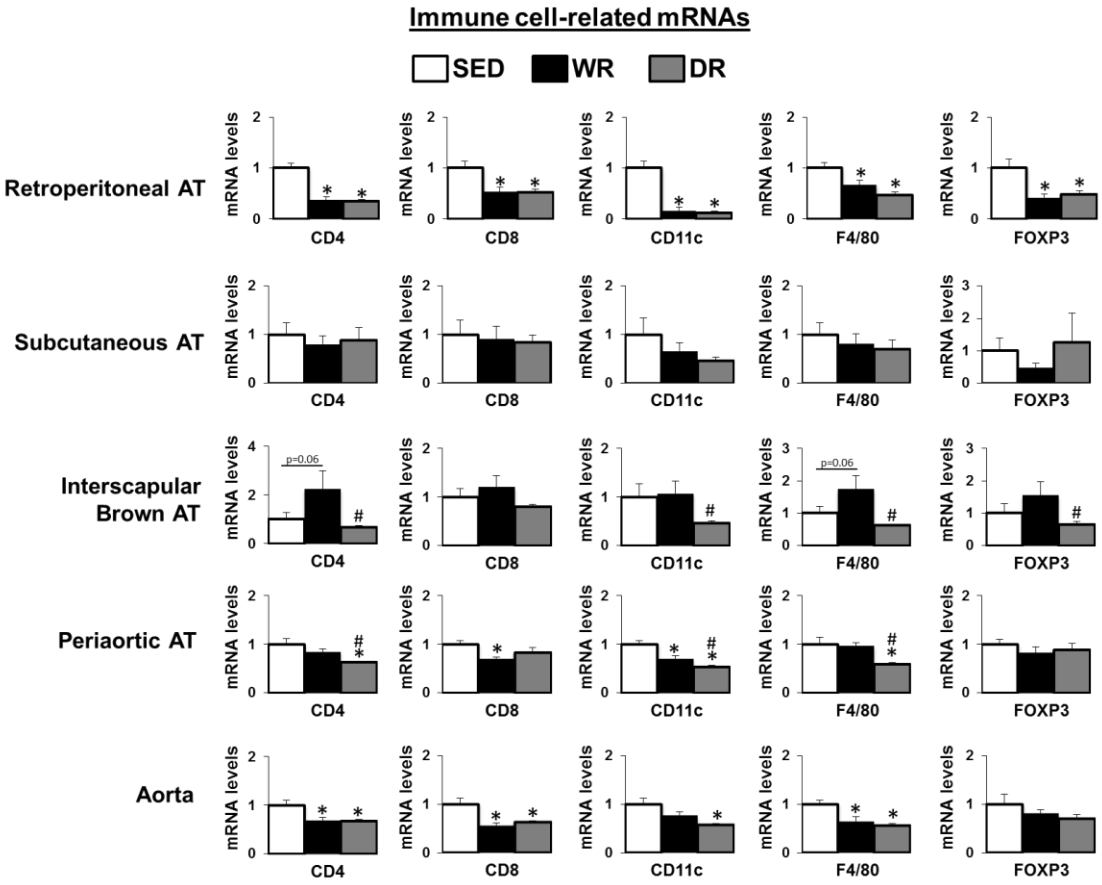

Figure 46. Expression of immune cell-related genes in ATs and aorta of sedentary (SED), wheel running (WR), and diet restriction (DR) OLETF rats. Values are expressed as means ± SE. For each gene, SED is used as the reference group and set at 1. *****Denotes difference ($p<0.05$) from SED rats; #Denotes difference ($p<0.05$) from WR rats.

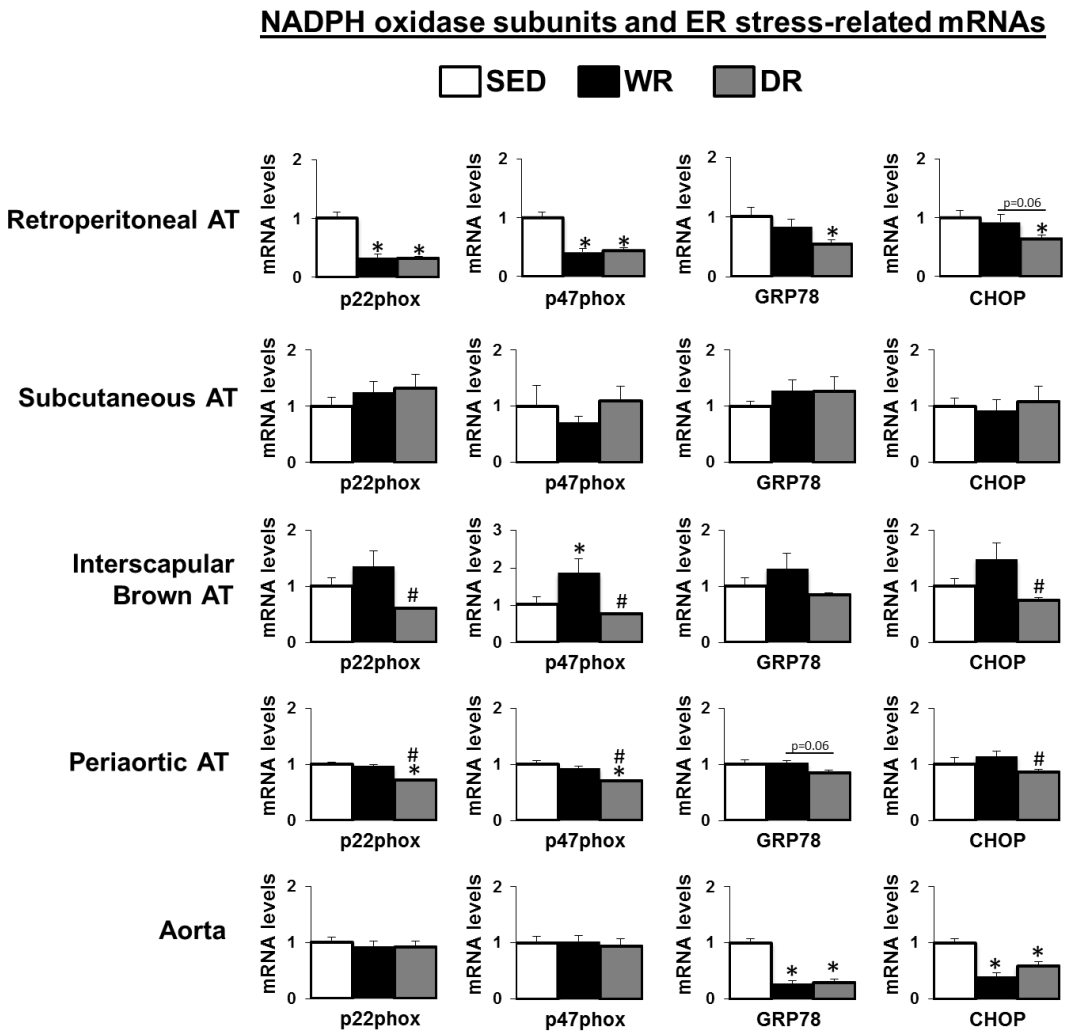

Figure 47. Expression of NADPH oxidase subunits and endoplasmic reticulum (ER) stress-related genes in ATs and aorta of sedentary (SED), wheel running (WR), and diet restriction (DR) OLETF rats. Values are expressed as means ± SE. For each gene, SED is used as the reference group and set at 1. *****Denotes difference ($p<0.05$) from SED rats; #Denotes difference ($p<0.05$) from WR rats.

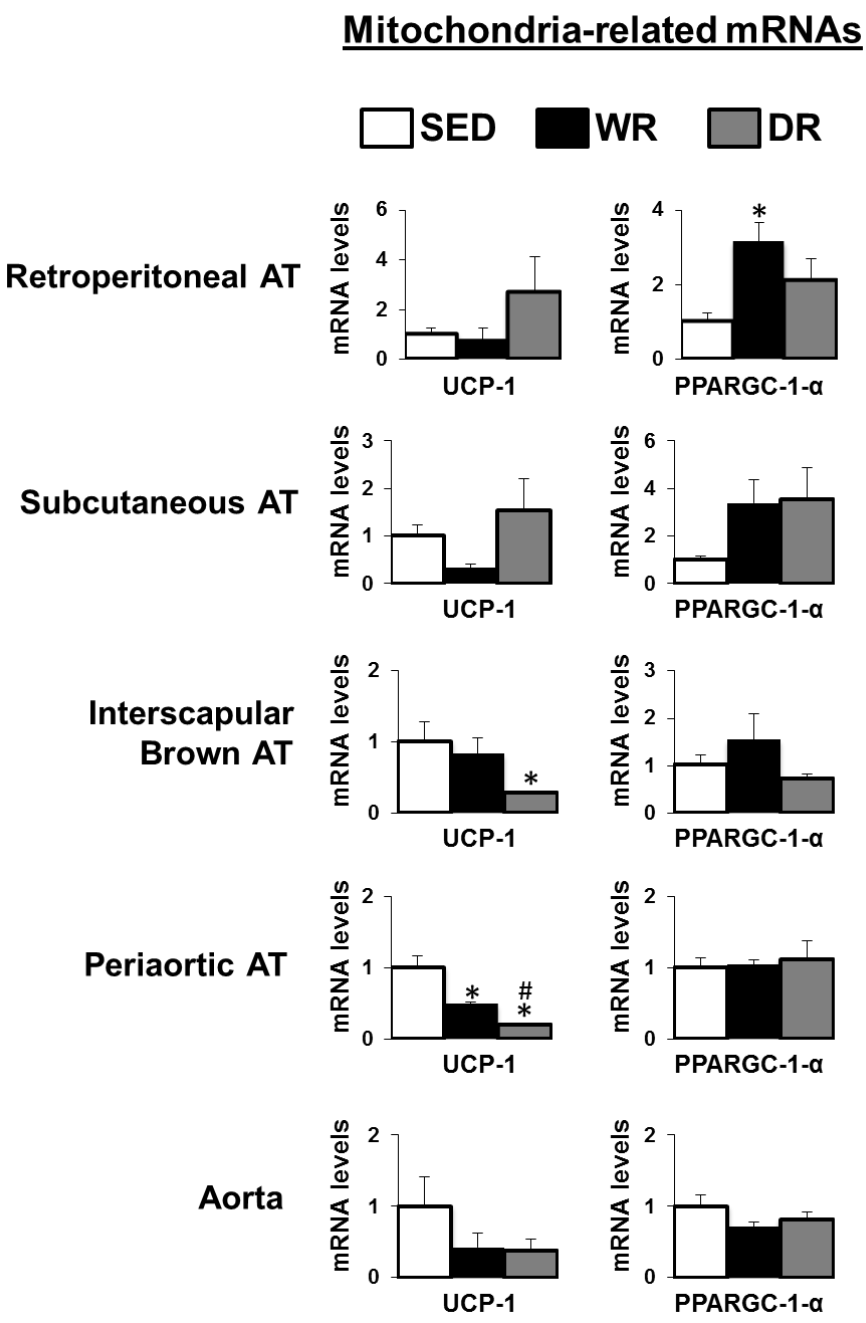

Figure 48. Expression of mitochondria-related genes in ATs and aorta of sedentary (SED), wheel running (WR), and diet restriction (DR) OLETF rats. Values are expressed as means ± SE. For each gene, SED is used as the reference group and set at 1. *****Denotes difference ($p<0.05$) from SED rats; #Denotes difference ($p<0.05$) from WR rats.

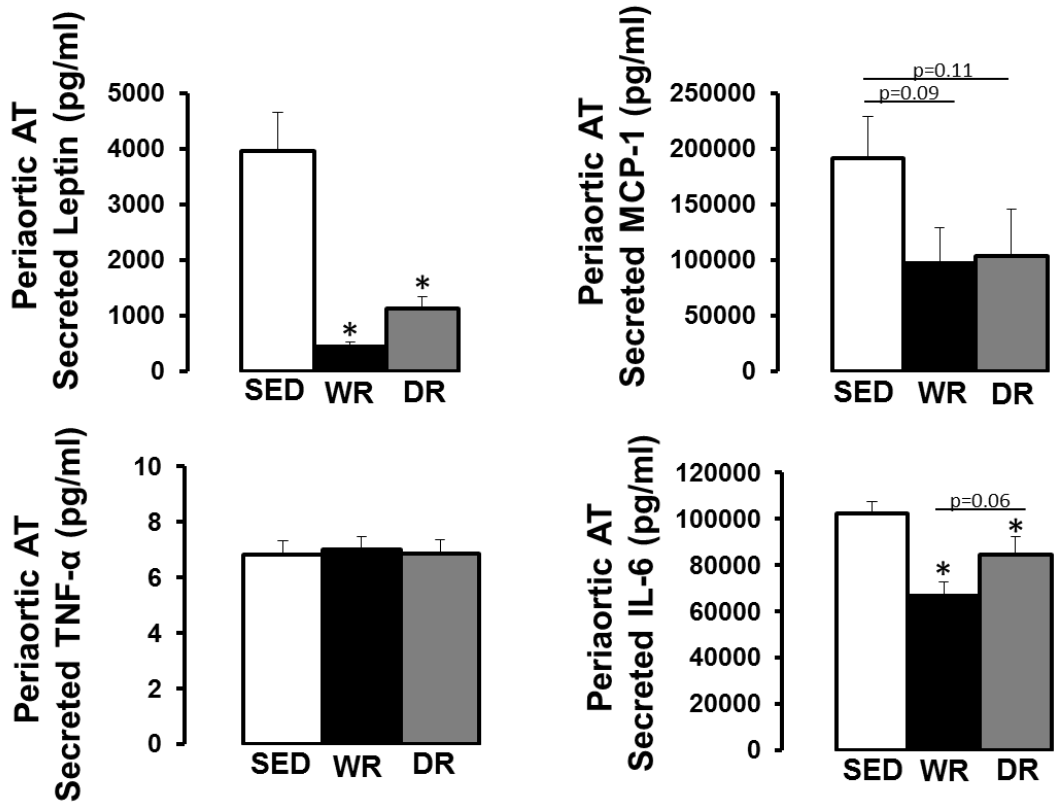

Figure 49. Secretion of cytokines from periaortic AT explants in sedentary (SED), wheel running (WR), and diet restriction (DR) OLETF rats. Values are expressed as means ± SE. *****Denotes difference ($p<0.05$) from SED rats; #Denotes difference ($p<0.05$) from WR rats.

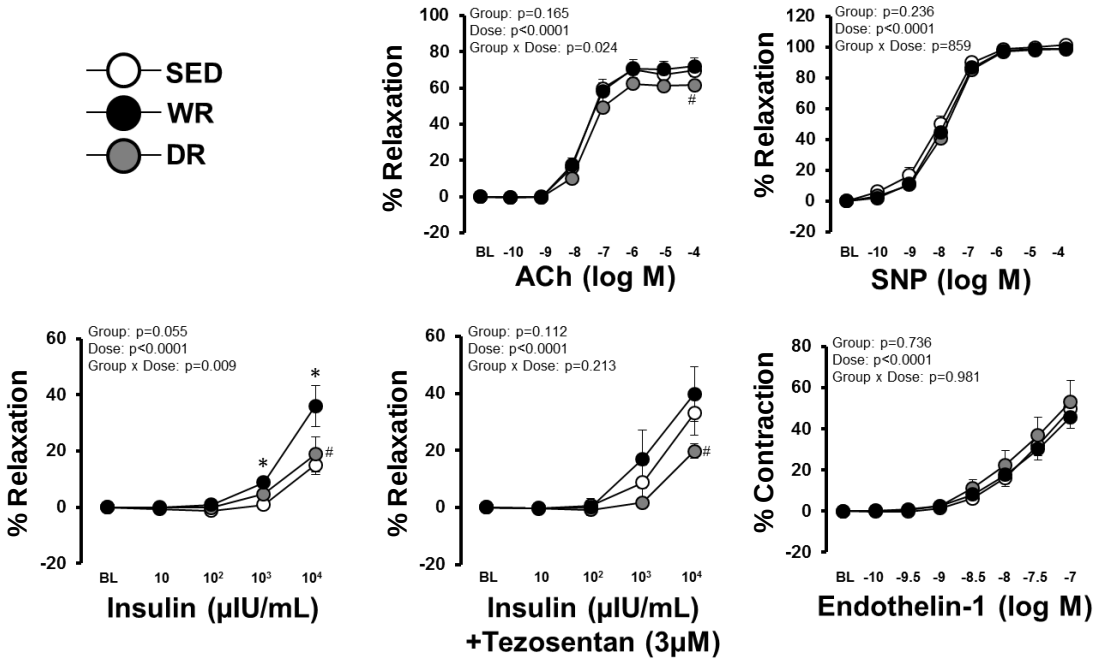

Figure 50. Vasomotor function of thoracic aortic rings in sedentary (SED), wheel running (WR), and diet restriction (DR) OLETF rats. Values are expressed as means ± SE. *****Denotes difference ($p<0.05$) from SED rats; #Denotes difference ($p<0.05$) from WR rats.

f. Discussion

The primary findings of the present study are as follows: (i) treatment with voluntary WR and 30% DR regimen for 8 weeks (starting at 12 weeks of age) resulted in marked reductions in adiposity, improved blood lipid profiles and systemic markers of insulin resistance in the obese OLETF rat model; (ii) reductions in adiposity, through both WR and DR, were associated with decreased AT expression of inflammatory genes and markers of immune cell infiltration, effects that were most pronounced in visceral AT compared to subcutaneous and periaortic AT; (iii) in contrast to other depots, markers of inflammation/immune function in brown AT were upregulated with WR but not DR; (iv) WR and DR-induced reductions in mRNA expression and secretion of cytokines in periaortic AT were accompanied with a more athero-protective gene expression profile in the adjacent aortic wall; and (v) WR, but not DR, resulted in increased insulin-stimulated relaxation in the aorta; an effect that was in part mediated by a decrease in insulin-induced ET-1 mediated activation/contraction in the aorta of WR.

Existing evidence in animals and humans indicates that exercise results in reduced expression of inflammatory genes and markers of immune cell infiltration in white AT (32-37). We found that voluntary WR-induced decreases in adiposity produced, by and large, similar down-regulation of inflammatory genes in white AT (retroperitoneal) to that produced by decreases in adiposity with 30% DR regimen. Thus, our data support the notion that changes in adiposity appear to be the main driving force for the decreased inflammation in white AT. Further research evaluating the effects of physical activity in the absence of changes in adiposity is

needed to elucidate any exercise-specific effects on AT. A unique aspect of the present study was the examination of the effects of WR and DR in several AT depots beyond visceral fat, i.e., subcutaneous, brown, and perivascular AT depots. Overall, our data indicate that the greatest effects of WR and DR on AT gene expression were in visceral AT. While visceral AT is highly susceptible to obesity-mediated inflammation/infiltration of immune cells (32, 34-37), these data suggest that the phenotype of visceral AT is also highly amenable to reductions in adiposity. Given this close link between visceral AT expansion and inflammation in obesity (32, 34-37), it is not surprising that measures of central adiposity in humans relate with metabolic and cardiovascular outcomes (7) and that interventions that result in weight loss are associated with improvements in insulin sensitivity and cardiovascular health (38).

An intriguing finding of the present study is that WR and DR produced differential effects on brown AT gene expression. While both WR and DR produced a down-regulation of leptin and PAI-1 mRNA, WR resulted in the induction of pro-inflammatory genes, markers of immune cell infiltration, and oxidative stress. The finding that WR markedly increased expression of IL-6 in brown AT is of particular interest considering the recent study by Stanford and colleagues (39) demonstrating that brown AT-derived IL-6 is required for the profound effects of brown AT transplantation on glucose homeostasis and insulin sensitivity. Indeed, those authors found that the beneficial metabolic effects of brown AT transplantation were lost when AT used for transplantation was obtained from IL-6 knockout mice (39). Our data combined with the results of Standford et

al. (39) suggest that the beneficial metabolic effects of exercise may be in part mediated by an increased expression of IL-6 in brown AT. To our knowledge, this is the first study to provide evidence that physical activity, but not calorie restriction, is effective in inducing IL-6 expression in brown AT. Our finding that other pro-inflammatory markers (e.g., MCP-1, TNF-α) were also upregulated in brown AT warrants further investigation.

Given the increasing evidence implicating AT surrounding large arteries as a local source of inflammatory cytokines that may be involved in the instigation of vascular dysfunction and atherosclerosis (11-18, 20, 21), a central focus of the present study was to examine the impact of WR and DR on the phenotypic modulation of periaortic AT. Periaortic AT from WR and DR rats clearly exhibited reduced lipid deposition relative to sedentary control rats (Figure 2) and this effect was associated with reduced expression of macrophage (CD11c) and T-cell specific genes (CD4 and CD8), suggesting a decrease in the infiltration of immune cells into periaortic AT. Notably, we also found that WR and DR caused a reduction in periaortic AT-derived secretion of cytokines, such as leptin, IL-6, and MCP-1. To our knowledge this is the first evidence that physical activity and dietary restriction can effectively reduce expression and secretion of cytokines from perivascular AT. The robust reduction in leptin secretion from periaortic AT induced by WR and DR deserves specific attention given direct evidence implicating perivascular AT-derived leptin as a potential contributor to vascular dysfunction. In this regard, Payne et al. (14) elegantly demonstrated that perivascular AT-induced impairment of coronary artery function in metabolic

syndrome pigs was reversed with a recombinant leptin antagonist. Furthermore, there is increasing evidence that leptin, when in excess, induces a pro-inflammatory and pro-oxidant vascular phenotype (40-46). Given our findings that WR and DR reduced systemic inflammation and secretion of cytokines from perioarotic AT, we hypothesized that these effects would be accompanied by an athero-protective phenotype in the adjacent aortic wall. Indeed, we found that both WR and DR resulted in down-regulation of inflammatory genes (e.g., IL-6, E-selectin, VCAM-1), markers of immune cell infiltration (e.g., CD4, CD8, F4/80), and makers of endoplasmic reticulum stress (e.g., GRP78 and CHOP) in the aorta. These findings are consistent with the hypothesis that at the transcriptional level, the effects of physical activity on vascular cell phenotype may be driven by changes in adiposity and the consequent alterations in cytokine secretion from AT.

In contrast to the results where WR and DR had similar effects on gene expression in AT, our results from the aortic vasomotor function experiments indicate that physical activity improved insulin-induced vasorelaxation while DR had no effect. In particular, we found that insulin-stimulated relaxation of the aorta was increased with physical activity but not by a lowering of body weight evoked through dietary restriction. This finding is consistent with previous data from our group showing that insulin-stimulated dilation in skeletal muscle arterioles was enhanced in WR, but not DR, OLETF rats (47). Herein we also report that differences in insulin-stimulated vasorelaxation between WR and SED rats were largely abolished after treatment of aortic rings with a nonselective ET-1 receptor blocker. ET-1 blockade had little to no effect on insulin-induced relaxation in the

aorta from WR animals but produced nearly a 2-fold increase in insulin-induced relaxation in SED. This finding suggests that increases in vasorelaxation to insulin with physical activity were mediated in part by a decrease in ET-1 signaling. Furthermore, to evaluate whether greater insulin-stimulated relaxation in the aorta of WR rats was due to reduced vascular sensitivity to ET-1 and/or decreased vascular production of ET-1, we examined aortic responsiveness to exogenous ET-1 in all three groups of animals. We found similar ET-1 mediated constriction among groups suggesting that it was local insulin-stimulated ET-1 activation, and not the vascular sensitivity to ET-1 *per se* that is likely modulated by physical activity.

Our findings that physical activity, but not DR, increases insulin-stimulated vasorelaxation as a result of decreased insulin-mediated ET-1 activation may be significant in light of evidence indicating that excess ET-1 signaling is an important contributor to the pathogenesis of macro-vascular disease (48). Exercise-induced increases in blood flow and thus shear stress to the artery wall is a likely mechanism by which physical activity exerts an insulin sensitizing effect on the aorta and a decrease in ET-1 (49, 50). This hypothesis is supported by evidence that (i) shear stress reduces expression of ET-1 in cultured endothelial cells (51), (ii) removal of WR for 7 days increases expression of ET-1 in the rat iliac artery (30), (iii) rat soleus muscle feed arteries, known to be chronically exposed to high levels of blood flow display greater insulin-stimulated dilation, as a result of reduced ET-1 activation, than gastrocnemius feed arteries, known to be chronically exposed to lower levels of flow (52), and (iv) inactive lower limbs of spinal cord

injury patients, chronically exposed to low blood flow and shear stress (53), exhibit an enhanced ET-1 mediated basal vascular tone (54).

Another interesting finding of the present study is that the WR-related increase in insulin-stimulated relaxation in the aorta occurred in the absence of changes in ACh-mediated relaxation, a response largely mediated by nitric oxide in rat aorta. Incidentally, compelling evidence from studies using the Zucker obese rat model indicates that impairments in insulin-mediated dilation occurs prior to impairments in ACh-mediated dilation in both skeletal muscle (55) and coronary arterioles (56, 57). It is possible that ACh-mediated dilation was not improved in our WR animals, relative to the sedentary OLETF animals, because no impairment in ACh-mediated dilation may have been present in these 20 week old sedentary rats. Consistent with this hypothesis, data in animals and humans suggest that exercise training does not further improve endothelium-dependent dilation in subjects with a healthy endothelium, likely due to a ceiling effect (58, 59). We did observe, unexpectedly, that DR resulted in a small but significant decrease in ACh-mediated dilation relative to the SED group fed *ad libitum*; this effect was not observed in WR animals.

In summary, we provide evidence that reduced adiposity, owing to either increased physical activity or diet restriction, in the obese, insulin resistant OLETF rat model leads to a marked reduction in the expression of inflammatory genes and markers of immune cell infiltration in visceral and periaortic AT. Our data also demonstrate unique AT depot-specific effects of both increased physical activity and dietary restriction. The anti-inflammatory effects of physical activity and diet

restriction on AT were accompanied with a more athero-protective gene expression profile in the contiguous aorta. Importantly, our results indicate that physical activity enhanced aortic insulin-induced relaxation while diet restriction did not, suggesting that the insulin sensitizing effect on the vasculature is exercise-specific.

g. References

1. Ogden CL, Carroll MD, Curtin LR, Lamb MM, Flegal KM. Prevalence of high body mass index in U.S. children and adolescents, 2007-2008. JAMA. 2010;303(3):242-9.

2. Szostak J, Laurant P. The forgotten face of regular physical exercise: a 'natural' anti-atherogenic activity. Clin Sci. 2011;121:91-106.

3. Booth FW, Laye MJ, Lees SJ, Rector RS, Thyfault JP. Reduced physical activity and risk of chronic disease: the biology behind the consequences. European journal of applied physiology. 2008;102:381-90.

4. Booth FW, Roberts CK, Laye MJ. Lack of exercise is a major cause of chronic disease. Comprehensive Physiology. 2012;2:1143-211.

5. Booth FW, Lees SJ. Fundamental questions about genes, inactivity, and chronic diseases. Physiol Genomics. 2007;28:146-57.

6. Chakravarthy MV, Booth FW. Eating, exercise, and "thrifty" genotypes: connecting the dots toward an evolutionary understanding of modern chronic diseases. Journal of Applied Physiology. 2004;96:3-10.

7. Gutierrez D, Puglisi M, Hasty A. Impact of increased adipose tissue mass on inflammation, insulin resistance, and dyslipidemia. Current diabetes reports. 2009;9(1):26-32.

8. Ronti T, Lupattelli G, Mannarino E. The endocrine function of adipose tissue: an update. Clinical endocrinology. 2006;64(4):355-65. doi: 10.1111/j.1365-2265.2006.02474.x.

9. Li FYL, Cheng KKY, Lam KSL, Vanhoutte PM, Xu A. Cross-talk between adipose tissue and vasculature: role of adiponectin. Acta Physiologica. 2011;203(1):167-80. doi: 10.1111/j.1748-1716.2010.02216.x.

10. Lau DCW, Dhillon B, Yan H, Szmitko PE, Verma S. Adipokines: molecular links between obesity and atheroslcerosis. American Journal of Physiology - Heart and Circulatory Physiology. 2005;288(5):H2031-H41. doi: 10.1152/ajpheart.01058.2004.

11. Szasz T, Webb RC. Perivascular adipose tissue: more than just structural support. Clinical Science. 2012;122(1):1-12. doi: 10.1042/cs20110151.

12. Chatterjee TK, Stoll LL, Denning GM, Harrelson A, Blomkalns AL, Idelman G, et al. Proinflammatory Phenotype of Perivascular Adipocytes. Circulation research. 2009;104(4):541-9. doi: 10.1161/circresaha.108.182998.

13. Payne GA, Kohr MC, Tune JD. Epicardial perivascular adipose tissue as a therapeutic target in obesity-related coronary artery disease. Br J Pharmacol. 2012;165(3):659-69. doi: 10.1111/j.1476-5381.2011.01370.x.

14. Payne GA, Borbouse Ln, Kumar S, Neeb Z, Alloosh M, Sturek M, et al. Epicardial Perivascular Adipose-Derived Leptin Exacerbates Coronary Endothelial Dysfunction in Metabolic Syndrome via a Protein Kinase C-beta Pathway. Arteriosclerosis, Thrombosis, and Vascular Biology. 2012;30(9):1711-7. doi: 10.1161/atvbaha.110.210070.

15. Cheng KH, Chu CS, Lee KT, Lin TH, Hsieh CC, Chiu CC, et al. Adipocytokines and proinflammatory mediators from abdominal and epicardial adipose tissue in patients with coronary artery disease. Int J Obes. 2008;32:268-74.

16. Gorter PM, van Lindert AS, de Vos AM, Meijs MF, GY. vd, Doevendans PA, et al. Quantification of epicardial and peri-coronary fat using cardiac computed tomography: reproducibility and relation with obesity and metabolic syndrome in patients suspected of coronary artery disease. Atherosclerosis. 2008;197:896-903.

17. Greif M, Becker A, SF. v, Lebherz C, Lehrke M, Broedl UC, et al. Pericardial adipose tissue determined by dual source CT is a risk factor for coronary atherosclerosis. Arterioscler Thromb Vasc Biol. 2009;29:781-6.

18. Mazurek T, Zhang L, Zalewski A, Mannion JD, Diehl JT, Arafat H, et al. Human epicardial adipose tissue is a source of inflammatory mediators. Circulation. 2003;108:2460-6.

19. Stohr R, Federici M. Insulin resistance and atherosclerosis: convergence between metabolic pathways and inflammatory nodes. Biochem J. 2013;454(1):1-11.

20. Meijer RI, Bakker W, Alta C-LAF, Sipkema P, Yudkin JS, Viollet B, et al. Perivascular Adipose Tissue Control of Insulin-Induced Vasoreactivity in Muscle Is Impaired in db/db Mice. Diabetes. 2013;62(2):590-8. doi: 10.2337/db11-1603.

21. Lee H-Y, Despres J-P, Koh KK. Perivascular adipose tissue in the pathogenesis of cardiovascular disease. Atherosclerosis. 2013;230(2):177-84.

22. Shoelson SE, Lee J, Goldfine AB. Inflammation and insulin resistance. The Journal of Clinical Investigation. 2006;116(7):1793-801. doi: 10.1172/jci29069.

23. Galvez-Prieto B, Bolbrinker J, Stucchi P, De las Heras AI, Merino B, Arribas S, et al. Comparative expression analysis of the renin-angiotensin system components between white and brown perivascular adipose tissue. Journal of Endocrinology. 2008;197:55-64.

24. Police SB, Thatcher SE, Charnigo R, Daugherty A, Cassis LA. Obesity promotes inflammation in periaortic adipose tissue and angiotensin II-induced abdominal aortic aneurysm formation. Arterioscler Thromb Vasc Biol. 2009;29:1458-64.

25. Fitzgibbons TP, Kogan S, Aouadi M, Hendricks GM, Straubhaar J, Czech MP. Similarity of mouse perivascular and brown adipose tissue and their resitance to diet-induced inflammation. American journal of physiology Heart and circulatory physiology. 2011;301:H1425-H37.

26. Padilla J, Jenkins N, Vieira-Potter VJ, Laughlin MH. Divergent phenotype of rat thoracic and abdominal perivascular adipose tissues. American journal of physiology Regulatory, integrative and comparative physiology. 2013;304(7):R543-52.

27. Jenkins NT, Padilla J, Arce-Esquivel AA, Bayless DS, Martin JS, Leidy HJ, et al. Effects of endurance exercise training, metformin, and their combination on adipose tissue leptin and IL-10 secretion in OLETF rats. J Appl Physiol. 2012;113(12):1873-83.

28. Bailey-Downs LC, Tucsek Z, Toth P, Sosnowska D, Gautam T, Sonntag WE, et al. Aging Exacerbates Obesity-Induced Oxidative Stress and Inflammation in Perivascular Adipose Tissue in Mice: A Paracrine Mechanism Contributing to Vascular Redox Dysregulation and Inflammation. The Journals of Gerontology Series A: Biological Sciences and Medical Sciences. 2013;68(7):780-92. doi: 10.1093/gerona/gls238.

29. Padilla J, Jenkins NT, Lee S, Zhang H, Cui J, Zuidema MY, et al. Vascular transcriptional alterations produced by juvenile obesity in Ossabaw swine. Physiol Genomics. 2013;45(11):434-46. Epub 2013/04/18. doi: physiolgenomics.00038.2013 [pii] 10.1152/physiolgenomics.00038.2013. PubMed PMID: 23592636.

30. Padilla J, Jenkins NT, Roberts MD, Arce-Esquivel AA, Martin JS, Laughlin MH, et al. Differential changes in vascular mRNA levels between rat iliac and renal arteries produced by cessation of voluntary running. Experimental Physiology. 2013;98(1):337-47. doi: 10.1113/expphysiol.2012.066076.

31. Bunker A, Arce-Esquivel AA, Rector RS, Booth FW, Ibdah JA, Laughlin MH. Physical activity maintains aortic endothelium dependent relaxation in the obese, type 2 diabetic OLETF rat. American journal of physiology Heart and circulatory physiology. 2010;298(6):H1889-901.

32. Xu X, Ying Z, Cai M, Xu Z, Li Y, Jiang SY, et al. Exercise ameliorates high-fat diet-induced metabolic and vascular dysfunction, and increases adipocyte progenitor cell population in brown adipose tissue. American Journal of Physiology - Regulatory, Integrative and Comparative Physiology. 2011;300(5):R1115-R25. doi: 10.1152/ajpregu.00806.2010.

33. Bruun JM, Helge JrW, Richelsen Br, Stallknecht B. Diet and exercise reduce low-grade inflammation and macrophage infiltration in adipose tissue but not in skeletal muscle in severely obese subjects. American Journal of Physiology - Endocrinology and Metabolism. 2006;290(5):E961-E7. doi: 10.1152/ajpendo.00506.2005.

34. Vieira V, Valentine R, Wilund K, Antao N, Baynard T, Woods J. Effects of exercise and low-fat diet on adipose tissue inflammation and metabolic complications in obese mice. Am J Physiol Endocrinol Metab. 2009;296:E1164-E71.

35. Gollisch K, Brandauer J, Jessen N, Toyoda T, Nayer A, Hirshman M, et al. Effects of exercise training on subcutaneous and visceral adipose tissue in normal - and high-fat diet-fed rats. Am J Physiol Endocrinol Metab. 2009;297:E495-E504.

36. Kawanishi N, Yano H, Yokogawa Y, Suzuki K. Exercise training inhibits inflammation in adipose tissue via both suppression of macrophage infiltration and acceleration of phenotypic switching from M1 to M2 macrophages in high-fat-diet-induced obese mice. Exerc Immunol Rev. 2010;16:105-18.

37. Kowanishi N, Mizokami T, Yano H, Suzuki K. Exercise attenuates M1 macrophages and CD8+ T cells in the adipose tissue of obese mice. Med Sci Sports Exerc. 2013;45:1684-93.

38. Hamdy O, Ledbury S, Mullooly C, Jarema C, Porter S, Ovalle K, et al. Lifestyle Modification Improves Endothelial Function in Obese Subjects With the Insulin Resistance Syndrome. Diabetes care. 2003;26(7):2119-25. doi: 10.2337/diacare.26.7.2119.

39. Stanford K, Middelbeek R, Townsend K, An D, Nygaard E, Hitchcox K, et al. Brown adipose tissue regulates glucose homeostasis and insulin sensitivity J Clin Invest. 2013;123(1):215-23.

40. Yang R, Barouch LA. Leptin Signaling and Obesity. Circulation research. 2007;101(6):545-59. doi: 10.1161/circresaha.107.156596.

41. Bouloumie A, Marumo T, Lafontan M, Busse R. Leptin induces oxidative stress in human endothelial cells. The FASEB Journal. 1999;13(10):1231-8.

42. Quehenberger P, Exner M, Sunder-Plassmann R, Ruzicka K, Bieglmayer C, Endler G, et al. Leptin Induces Endothelin-1 in Endothelial Cells In Vitro. Circulation research. 2002;90(6):711-8. doi: 10.1161/01.res.0000014226.74709.90.

43. Cirillo P, Angri V, De Rosa S, Cali G, Petrillo G, Maresca F, et al. Pro-atherothrombotic effects of leptin in human coronary endothelial cells. Thrombosis and haemostasis. 2010;103(5):1065-75.

44. Singh P, Peterson TE, Barber KR, Kuniyoshi FS, Jensen A, Hoffmann M, et al. Leptin upregulates the expression of plasminogen activator inhibitor-1 in human vascular endothelial cells. Biochemical and biophysical research communications. 2010;392(1):47-52.

45. Korda M, Kubant R, Patton S, Malinski T. Leptin-induced endothelial dysfunction in obesity. American Journal of Physiology - Heart and Circulatory Physiology. 2008;295(4):H1514-H21. doi: 10.1152/ajpheart.00479.2008.

46. Beltowski J. Leptin and the regulation of endothelial function in physiological and pathological conditions. Clin Exp Pharmacol Physiol. 2012;39(2):168-78.

47. Mikus CR, Rector RS, Arce-Esquivel AA, Libla JL, Booth FW, Ibdah JA, et al. Daily physical activity enhances reactivity to insulin in skeletal muscle arterioles of hyperphagic Otsuka Long-Evans Tokushima Fatty rats. J Appl Physiol. 2010;109(4):1203-10.

48. Pernow J, Shemyakin A, Bohm F. New perspectives on endothelin-1 in atherosclerosis and diabetes mellitus. Life Sci. 2012;91(13-14):507-16. Epub 2012/04/10. doi: S0024-3205(12)00152-X [pii] 10.1016/j.lfs.2012.03.029. PubMed PMID: 22483688.

49. Padilla J, Simmons GH, Bender SB, Arce-Esquivel AA, Whyte JJ, Laughlin MH. Vascular effects of exercise: endothelial adaptations beyond active muscle beds. Physiology. 2011;26(3):132-45.

50. Jenkins NT, Martin JS, Laughlin MH, Padilla J. Exercise-induced signals for vascular endothelial adaptations: implications for cardiovascular disease. Curr Cardiovasc Risk Rep. 2012;6(4):331-46.

51. Toda M, Yamamoto K, Shimizu N, Syotaro O, Kumagaya S, Igarashi T, et al. Differential gene responses in endothelial cells exposed to a combination of shear stress and cyclic stretch. Journal of Biotechnology. 2008;133:239-44.

52. Jenkins NT, Padilla J, Martin JS, Crissey JM, Thyfault JP, Rector R, et al. Differential vasomotor effects of insulin on gastrocnemius and soleus feed arteries in the OLETF rat model: role of endothelin-1. Exp Physiol. 2013;in press.

53. Bell J, Chen D, Bahls M, Newcomer S. Altered resting hemodynamics in lower-extremity arteries of individuals with spinal cord injury. J Spinal Cord Med. 2013;36:104-11.

54. Thijssen DHJ, Ellenkamp R, Kooijman M, Pickkers P, Rongen GA, Hopman MTE, et al. A Causal Role for Endothelin-1 in the Vascular Adaptation to Skeletal Muscle Deconditioning in Spinal Cord injury. Arteriosclerosis, Thrombosis, and Vascular Biology. 2007;27(2):325-31. doi: 10.1161/01.atv.0000253502.83167.31.

55. Eringa EC, Stehouwer CD, Roos MH, Westerhof N, Sipkema P. Selective resistance to vasoactive effects of insulin in muscle resistance arteries of obese Zucker (fa/fa) rats. Am J Endocrinol Metab. 2007;293(5):E1134-9.

56. Oltman C, Richou L, Davidson E, Coppey L, Lund D, Yorek M. Progression of coronary and mesenteric vascular dysfunction in Zucker obese and Zucker diabetic fatty rats. American journal of physiology Heart and circulatory physiology. 2006;291(H1780-H1787).

57. Katakam P, Tulbert C, Snipes J, Erdos B, Miller A, Busija D. Impaired insulin-induced vasodilation in small coronary arteries of Zucker obese rats is mediated by reactive oxygen species. American journal of physiology Heart and circulatory physiology. 2005;288:H854-H60.

58. Jasperse JL, Laughlin MH. Endothelial function and exercise training: evidence from studies using animal models. Med Sci Sports Exerc. 2006;38(3):445-54.

59. Padilla J, Newcomer SC, Simmons GH, Kreutzer KV, Laughlin MH. Long-term exercise training does not alter brachial and femoral artery vasomotor function and endothelial phenotype in healthy pigs. American journal of physiology Heart and circulatory physiology. 2010;299(2):H379-85.

7. DISCONNECT BETWEEN ADIPOSE TISSUE INFLAMMATION AND CARDIOMETABOLIC DYSFUNCTION IN OSSABAW PIGS

a. Note to the reader on authorship

This paper was originally authored by Dr. Victoria Vieira-Potter, who has granted permission for both the text and figures of this paper to be reproduced in this dissertation. Figure and table numbering has been changed when necessary to follow the numbering scheme of the dissertation. The citation for this paper is as follows:

Vieira-Potter, V.J., et al., *Disconnect between adipose tissue inflammation and cardiometabolic dysfunction in Ossabaw pigs.* Obesity (Silver Spring), 2015. **23**(12): p. 2421-9.

b. Abstract

Objective: The Ossabaw pig is emerging as an attractive model of human cardiometabolic disease due to its size and susceptibility to atherosclerosis, among other characteristics. Here we investigated the relationship between adipose tissue inflammation and metabolic dysfunction in this model.

Methods: Young female Ossabaw pigs were fed a western-style high-fat diet (HFD) (n=4) or control low-fat diet (LFD) (n=4) for a period of 9 months and compared for cardiometabolic outcomes and adipose tissue inflammation.

Results: The HFD-fed “OBESE” pigs were 2.5 times heavier ($p<0.001$) than LFD-fed “LEAN” pigs and developed severe obesity. HFD-feeding caused pronounced dyslipidemia, hypertension, insulin resistance (systemic, adipose, and vascular) as well as induction of inflammatory genes, impairments in vasomotor reactivity to insulin and atherosclerosis in the coronary arteries. Remarkably, visceral, subcutaneous and perivascular adipose tissue inflammation (via FACS analysis and RT-PCR) was not increased in OBESE pigs, nor were circulating inflammatory cytokines.

Conclusions: These findings reveal a disconnect between adipose tissue inflammation and cardiometabolic dysfunction induced by western diet feeding in the Ossabaw pig model.

c. Introduction

As obesity continues to increase, so does the prevalence of cardiometabolic diseases including coronary artery disease, stroke, peripheral vascular disease and type 2 diabetes. These disorders are major causes of overall morbidity and mortality in the U.S. and worldwide. Importantly, as obesity leads to cardiometabolic disease in some but not all cases (1), it is imperative that the mechanisms linking obesity to disease be better understood.

It is currently accepted that visceral obesity and insulin resistance (IR) form the ‘common soil’ from which cardiometabolic diseases develop, and that a central feature to this metabolic milieu is adipose tissue (AT) inflammation (2). Visceral AT inflammation, including inflammatory macrophage (Mϕ) polarization, is predictive of metabolic dysfunction in several models with the majority of those conducted in rodents

(3, 4); relationships have also been observed between AT inflammation and metabolic dysfunction in humans (5). Although research strides have been made to better understand such mechanisms, the vast majority of work has been done using rodents, whose size and rapid rate of maturation limits their ability to adequately model human obesity. Additionally, unlike humans, rodents do not develop atherosclerotic lesions, unless genetically modified. The Ossabaw pig model is attractive because, similar to humans, when exposed to caloric excess and physical inactivity, they develop obesity and its metabolic consequences including IR, dyslipidemia, hypertension, and atherosclerosis (6). The pig more closely resembles the human in terms of its size, growth rate, and development of cardiovascular disease and is emerging as a more appropriate obesity model (7). The Ossabaw pig is characterized by the "thrifty phenotype" whereby this breed has adapted to store large amounts of energy during caloric excess (8). Our group (9, 10) and others (11, 12) have been utilizing the Ossabaw as a model of cardiometabolic disease development. We previously demonstrated that significant metabolic changes, as well as AT (9) and vascular (10) transcriptional alterations, occur early in the development of obesity in this model. Interestingly, the obesity that developed over that early period was not associated with increased expression of inflammatory genes conventionally viewed as being associated with obesity in visceral AT (9) and coronary perivascular AT (PVAT) (10).

Although the Ossabaw is emerging as an important model of cardiometabolic dysfunction, the relationship between visceral AT inflammation and metabolic function in this model remains poorly understood. Here, we sought to extend our previous work in juvenile Ossabaw swine (9, 10) and determine the effects of prolonged high fat, high

sucrose diet (HFD) feeding on AT inflammation and cardiometabolic disease. We hypothesized that chronic HFD feeding of female Ossabaw pigs would result in significant cardiometabolic dysfunction in the absence of robust changes in AT inflammation owing to the thrifty phenotype and associated less harmful adipocyte expansion.

d. Methods

Animals, Diets, Blood Pressure, Body Composition, and Tissue Sampling

All procedures were approved by the ACUC at the University of Missouri. Juvenile (5-6 wk-old) female Ossabaw pigs (n=8) obtained from Michael Sturek, Ph.D. at the Ossabaw Swine Resource, Comparative Medicine Program at Purdue University and Indiana University School of Medicine were housed under temperature-controlled (20-23 °C) conditions with a 12 h/12 h light-dark cycle. Pigs were either limit-fed regular miniature pig chow diet (5L80, Lab Diet; 3.03 kcal/g; 10.5% fat, "LEAN" n=4) or a western HFD (5B4L, Lab Diet; 4.14 kcal/g; 40.8% fat and 17.8% high fructose corn syrup, "OBESE" n=4) for nine months. Blood pressure was assessed by tail cuff method (GE Dash 3000) in conscious pigs after 8 ½ months of intervention and was the average of three measurements within 10 minutes. Following the intervention, pigs were weighed, body composition assessed via DXA (Hologic, QDR-1000), euthanized following an 18-20 hour fast, and blood collected for serum analyses via jugular vein. Subcutaneous abdominal (SQAT), visceral omental (OMAT), and PVAT surrounding the left anterior descending (LAD) coronary artery were harvested and processed or

immediately frozen. The distal portion of the LAD coronary artery was dissected and used for vasomotor function experiments.

Serum and AT-Conditioned Media Analysis

Fasting serum glucose, NEFAs, total cholesterol, LDL, HDL, and TGs were analyzed as previously described (10). Insulin was measured using commercial kits (Porcine Insulin ELISA, Mercodia, #10-1200-01). Serum and AT-conditioned media concentrations of interferon gamma (IFN-γ), interleukin (IL) 1 (IL-1β), IL-1 receptor antagonist (IL-1RA), IL-6, IL-10, and tumor necrosis factor (TNF-α) were determined using a porcine-specific multiplex assay (Millipore Multiplex; Billerica, MA, #PCYTMAG-23K). All assays were run in duplicate.

Histology

SQAT, OMAT, and LAD coronary artery rings were fixed and stained with hemotoxylin and eosin, as previously described (9). Digital images were captured with an Olympus BX60 light microscope and Olympus SC 100 camera (Waltham, MA). Adipocyte volume was calculated based on 100 adipocytes/animal from six fields of view using Image J software as described previously (13). Separate slides were stained with porcine-specific anti-scavenger receptor class A (SRA) (Anti MSR-A/CD204, 1:100, Cosmo Bio USA, #KAL-KT022) antibody and examined by an investigator blinded to the treatment groups.

Fluorescence Associated Cell Sorting (FACS)

The stromal vascular cell (SVC) fraction was isolated from whole AT extracted from SQAT, OMAT, and PVAT depots via collagenase digestion as previously

described (13) with slight modifications. The following porcine-specific fluorophore-conjugated antibodies were used: CD3ε-PerCP-Cy5.5 (BD Pharmingen, #561478), CD4a- PECy7 (BD Pharmingen, #561473), CD8a-Alexa Fluor 647 (BD Pharmingen, #561475), and CD68- FITC (Santa Cruz Biotechnology, # sc-7083 FITC). Gating strategies included dead cell discrimination and lymphocyte quantification based on forward/side scatter and included unstained cells, single stain, and FMO controls. Cells were immunophenotyped using a CyAN ADP Analyzer (Beckman Coulter, Inc.) and data analyzed using Summit 5.2 (Beckman Coulter).

RNA Extraction and Quantitative Real-time RT-PCR

Quantitative real-time PCR was performed as previously described (10) and reactions were performed in duplicate. Primer sequences available upon request. 18S was used as house-keeping control gene and cycle thresholds (CT) were not different between groups across for any tissues. mRNA expression values are presented as $2^{\Delta CT}$ whereby ΔCT = 18S CT – gene of interest CT and normalized to LEAN, set at 1.

Cytokine Secretion from AT

A portion of SQAT, OMAT, and PVAT surrounding the LAD coronary artery were incubated in Medium 199 (pH 7.4, 24 hrs) (100 mg AT /500 μl) under standard conditions (37ºC, 5% CO_2) as described (14) to produce AT-conditioned media.

Vasomotor Function Experiments in LAD Coronary Artery Rings

Distal end of the LAD coronary arteries were exposed from the heart and microdissected in the chamber at 4°C. Coronary ring segments were cut into 2-mm rings and mounted in a myograph chamber (Model 610M, Danish Myo Technology, Aarhus,

Denmark) containing physiological salt solution gassed with 95% O_2-5% CO_2 at 37°C, as previously described (10). After a 30-minute equilibration period, an optimal tension (25mN) was applied and then another 30 minutes of equilibration followed. Rings were stimulated with cumulative addition of K+ (30-120 mM) to assess vessel viability. Coronary rings were preconstricted with 10nM U-46619 to induce ~70-80% maximal contraction (i.e. relative to maximal U-46619-induced contraction; data not shown). Concentration-response curves were obtained by cumulative addition of either bradykinin (10^{-12} to 10^{-7}M), insulin (1 to 1000 µIU/mL) or sodium nitroprusside (10^{-9} to 10^{-5}M). Relaxation at each concentration was measured and expressed as percent maximum relaxation, where 100% is equivalent to loss of all tension developed in response to U-46619.

Statistical Analysis

Between group differences were determined using Student's two-tailed t-tests and considered statistically significant if $P<0.05$. Statistical analysis was performed using SPSS 22.0; all data are presented as mean ± SEM.

e. Results

HFD Induces Obesity, IR, and Dyslipidemia

Throughout the study, LEAN pigs were limit-fed to an average of 600 g food/day; whereas the OBESE pigs were limit-fed to an average of 1200 g/day. Compared to LEAN, OBESE were ~2.5X heavier and had 45% more body fat (Table 1). OBESE were considerably larger animals, indicated not only by greater adiposity but also by greater length, lean, bone, and heart mass (Table 1). Adipocytes from OMAT were

more than twice as large in the OBESE than in the LEAN group ($p<0.001$, Figure 1). However, adipocytes from SQAT were not different in size between groups ($p=0.32$, Figure 1). Compared to LEAN, OBESE also had higher fasting total cholesterol, HDL, LDL, NEFAs and TGs (all $P<0.001$, Table 1). OBESE were also considered diabetic based on fasting glucose and were significantly more insulin resistant based on the homeostatic model assessment (HOMA-IR (15)) and adipocyte IR (Adipo-IR (16)) (Table 1). Confirming what others have reported (11), OBESE also had significantly elevated systolic and diastolic blood pressure.

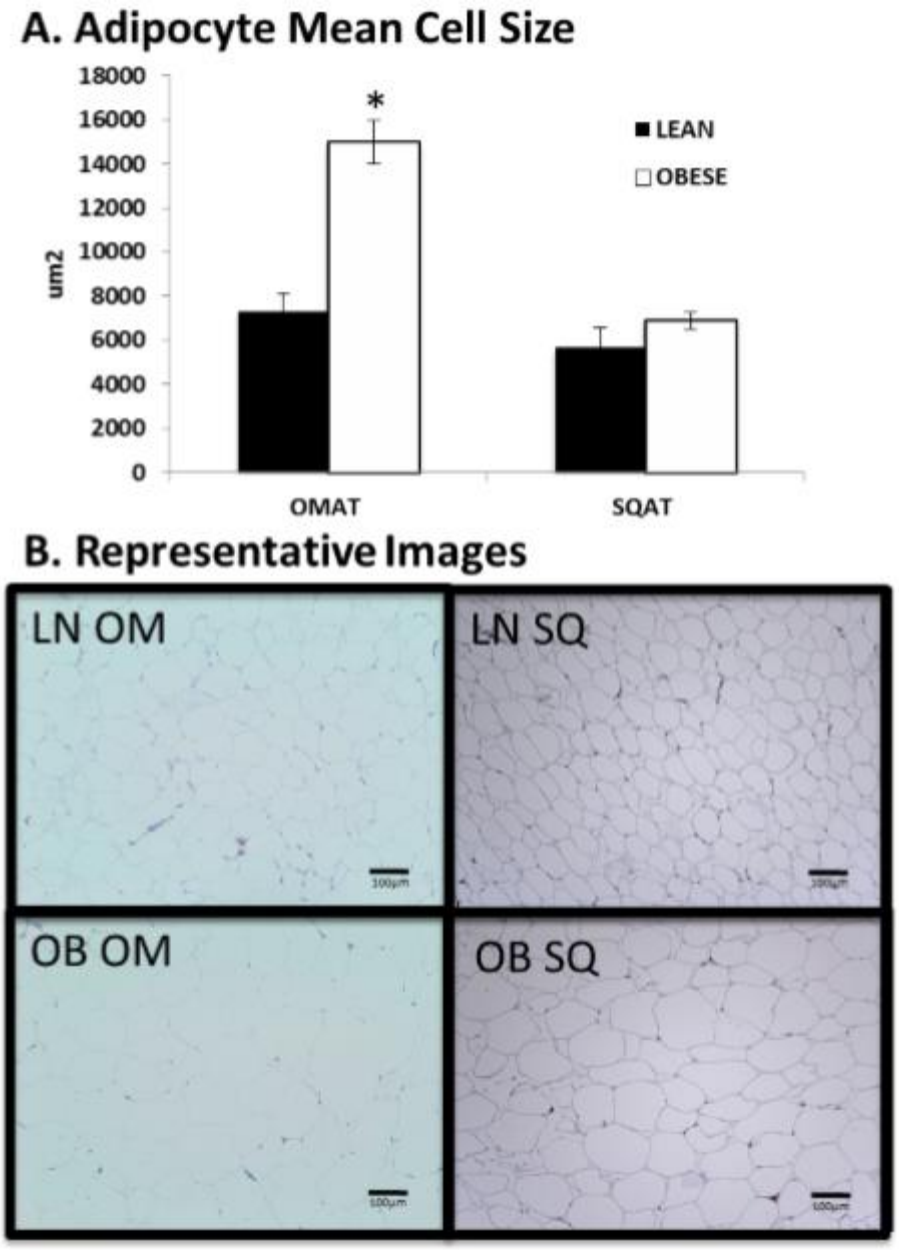

Figure 51: *OBESE pigs have greater mean adipocyte cell size in omental visceral AT (OMAT), but adipocytes from subcutaneous AT (SQAT) were not different between LEAN and OBESE.* A: Mean adipocyte cell size calculated based on counts for 100 adipocytes/animal; n=4 animals/group. B: Representative images for each depot. Data expressed as mean ± SEM; * P<0.05; LN = LEAN; OB=OBESE; OM = OMAT; SQ = SQAT.

Table 11. Body composition and metabolic characteristics of LEAN and OBESE pigs

	LEAN (n=4)	OBESE (n=4)	*P* Value
Body weight, kg	37.3±1.51	100.4±2.00	0.0001
Length, inches	44.0±1.0	56.1±1.1	0.001
Percent body fat, %	29.2±3.13	41.9±1.15	0.009
Percent lean mass, %	72.0±3.6	56.6±0.9	0.006
Blood pressure (Systolic/Diastolic mmHg)	110±3/72±4	130±4/99±8	<0.05
Bone mass, kg	0.80±0.06	1.37±0.065	0.001
Heart mass, kg	0.13±0.013	0.20±0.008	0.001
Total cholesterol, mg/dl	80.0±5.64	189.5±35.2	0.022
LDL-c, mg/dl	31.5±1.5	104.0±21.3	0.014
HDL-c, mg/dl	40.5±3.80	56.25±3.80	0.026
LDL-c:HDL-c	0.79±0.06	1.80±0.3	0.007
Total cholesterol:HDL-c	1.99±0.07	3.29±0.4	0.015
NEFA, mmol/l	0.223±0.085	2.572±0.353	0.001
Triglycerides, mg/dl	27.5±7.5	77.5±14.0	0.02
Glucose, mg/dl	121±10.0	308±47.5	0.008
Insulin, µg/l	0.104±0.017	0.287±0.009	0.017
HOMA-IR	0.91±0.18	6.26±0.96	0.001
Adipo-IR	0.023±0.009	0.736±0.096	<0.001

Values are means ± SEM. LDL, low-density lipoprotein; HDL, high-density lipoprotein, NEFA, nonesterified fatty acids; HOMA-IR, homeostatic model assessment; Adipo-IR, adipocyte IR.

Markers of Inflammation Not Increased in Circulation, AT, or AT-Conditioned Media of OBESE

Of the circulating cytokines measured (IL-10, TNF-α, IFN-γ, IL-1β, IL-1RA, IL-6), only IL-6 was different between OBESE and LEAN with OBESE having ~60% lower circulating values (0.0425±0.006 (LEAN) vs. 0.0165±0.003 (OBESE) pg/mL, *P*=0.012) (Supplementary Figure 1). When media conditioned with AT from LEAN and OBESE was assessed for cytokines (i.e., as indication of AT cytokine production), no between-group differences were observed in any of the cytokines measured . Similarly, no differences in AT immune cell infiltration were observed between OBESE and LEAN pigs. From the SVC fraction, CD68+SVCs (Mϕs) and CD3+, CD3/4+, CD3/8+SVCs (T lymphocytes) were isolated from AT harvested from OMAT, SQAT, and PVAT and quantified via FACS. In concordance with the lack of systemic inflammation in the OBESE, we did not detect increased AT T lymphocytes or Mϕs in the OBESE compared to the LEAN in any of the depots. Finally, in accordance with the lack of evidence of AT inflammatory cell infiltration, it did not appear that OBESE OMAT or SQAT displayed increased Mϕ content as measured via SRA (Mϕ marker) immunostaining (Supp. Fig. 1).

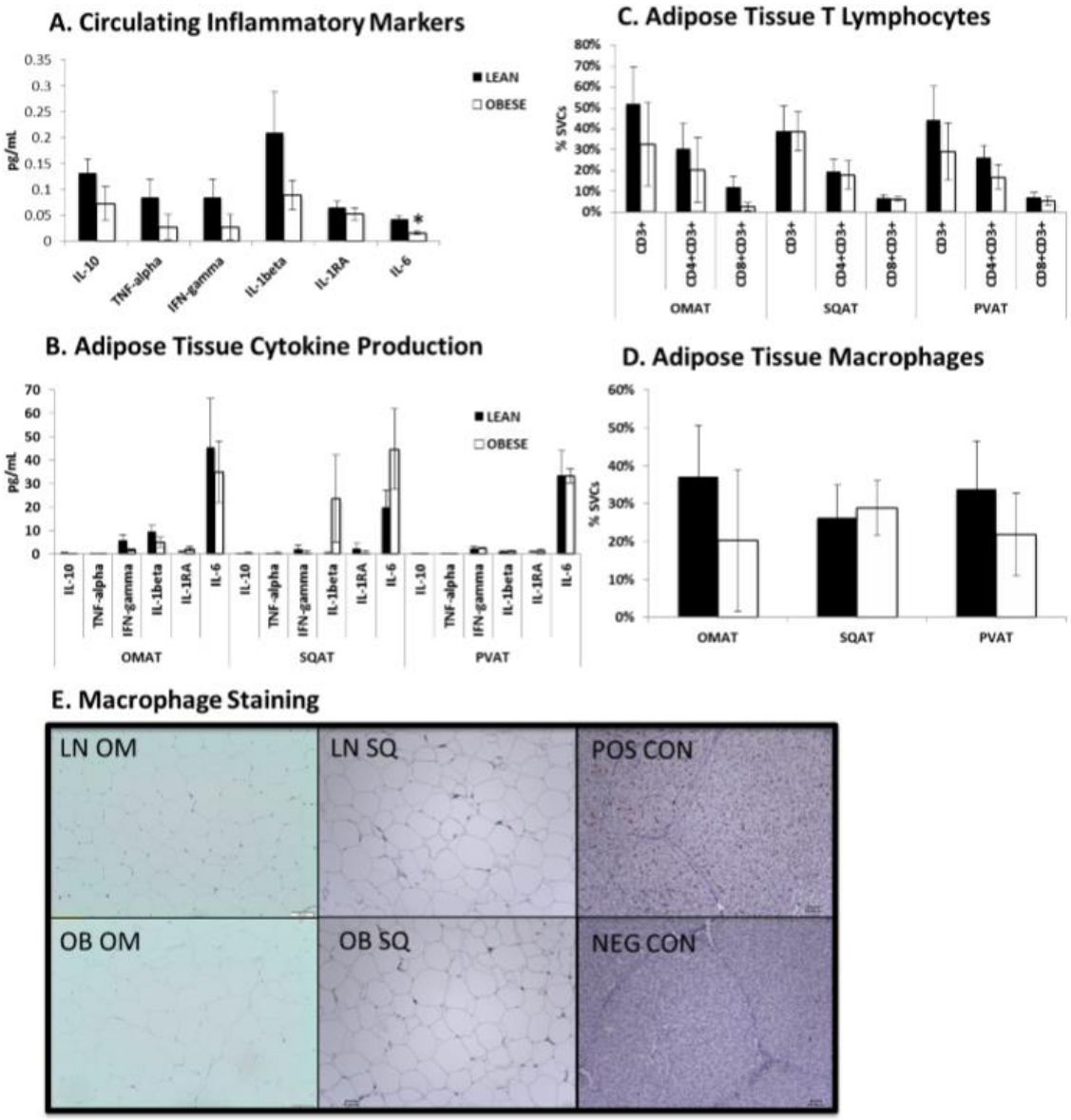

Figure 52. *OBESE pigs do not have greater inflammation compared to LEAN.* A: Serum concentrations of proinflammatory cytokines were not elevated in OBESE; circulating levels of IL-6 were significantly reduced in OBESE compared to LEAN pigs. B: Cytokine production from AT harvested from visceral (e.g., OMAT), subcutaneous (SQAT), and perivascular (PVAT) depots was not increased in OBESE . C: No differences were detected in T lymphocyte infiltration in either of the three depots as measured via FACS (e.g., % positive cells isolated from SVC). D: No differences in CD68+ Mϕ content in either of the three depots as measured via FACS. E: No differences were observed in Mϕ content (indicated by scavenger receptor A-positive staining in images) in OMAT or SQAT between LEAN and OBESE; positive and negative controls were performed in liver tissue. Data expressed as mean ± SEM; * P<0.05.

Little Evidence of AT Inflammation in OBESE Via Gene Expression

To further examine the inflammatory profile of AT from OBESE and LEAN, a comprehensive gene expression panel was analyzed in OMAT and SQAT (Figure 2). In OMAT, only five genes were significantly up-regulated in OBESE pigs. Adiponectin, an AT-secreted protein known to be insulin sensitizing and anti-inflammatory, was elevated ~2-fold and leptin, another AT-secreted protein important in metabolic homeostasis, was ~7-fold higher. IL-6, a cytokine secreted by immune cells as well as adipocytes that is thought to be "immunomodulatory" was ~3-fold higher in OMAT from OBESE animals. No other inflammatory markers were elevated (TNF-α, IFN-γ, toll-like receptor (TLR4), inflammatory T cell markers) except for monocyte chemoattractant protein (MCP-1), important in drawing in Mϕs, which was ~4-fold elevated in OBESE. The T helper cell marker, CD4, trended to be higher among OBESE (*P*=0.076). Interestingly, the naturally occurring anti-oxidant molecule, superoxide dismutase (SOD1) was also marginally elevated in OBESE OMAT as was PPARλ (P=0.08), a nuclear receptor known to enhance adipocyte insulin sensitivity and reduce inflammation (17) (Figure 2A). No markers of Mϕ infiltration were elevated in OBESE compared to LEAN OMAT, while the Mϕ markers CD14 and CD16 were marginally suppressed in OBESE OMAT.

In SQAT, two genes were significantly higher in OBESE: CYBB (GP91-phox), an NADPH oxidase subunit indicative of oxidative stress, and the alternative/anti-inflammatory Mϕ marker known to produce anti-inflammatory cytokines, CD163 (Figure 2B). In stark contrast to other animal models of obesity, gene expression of CD4 (indicative of T helper cells) and CD8 (indicative of cytotoxic T cells) were lower in OBESE compared to LEAN as was the pro-inflammatory cytokine, IFNγ, which is

indicative of inflammatory T cell activation (18) and the Mϕ marker, CD16. Two markers indicative of T regulatory cell (Treg) activation, Foxp3 and CTLA4, were not suppressed in OBESE, however. Tregs have been shown to have anti-inflammatory and insulin-sensitizing properties in AT (19). However, no differences were observed in CD3, CD4, or CD8+ T cells via FACS in SQAT between groups. These findings indicate that the OBESE pigs studied here did not experience increased SQAT T cell and/or Mϕ influx.

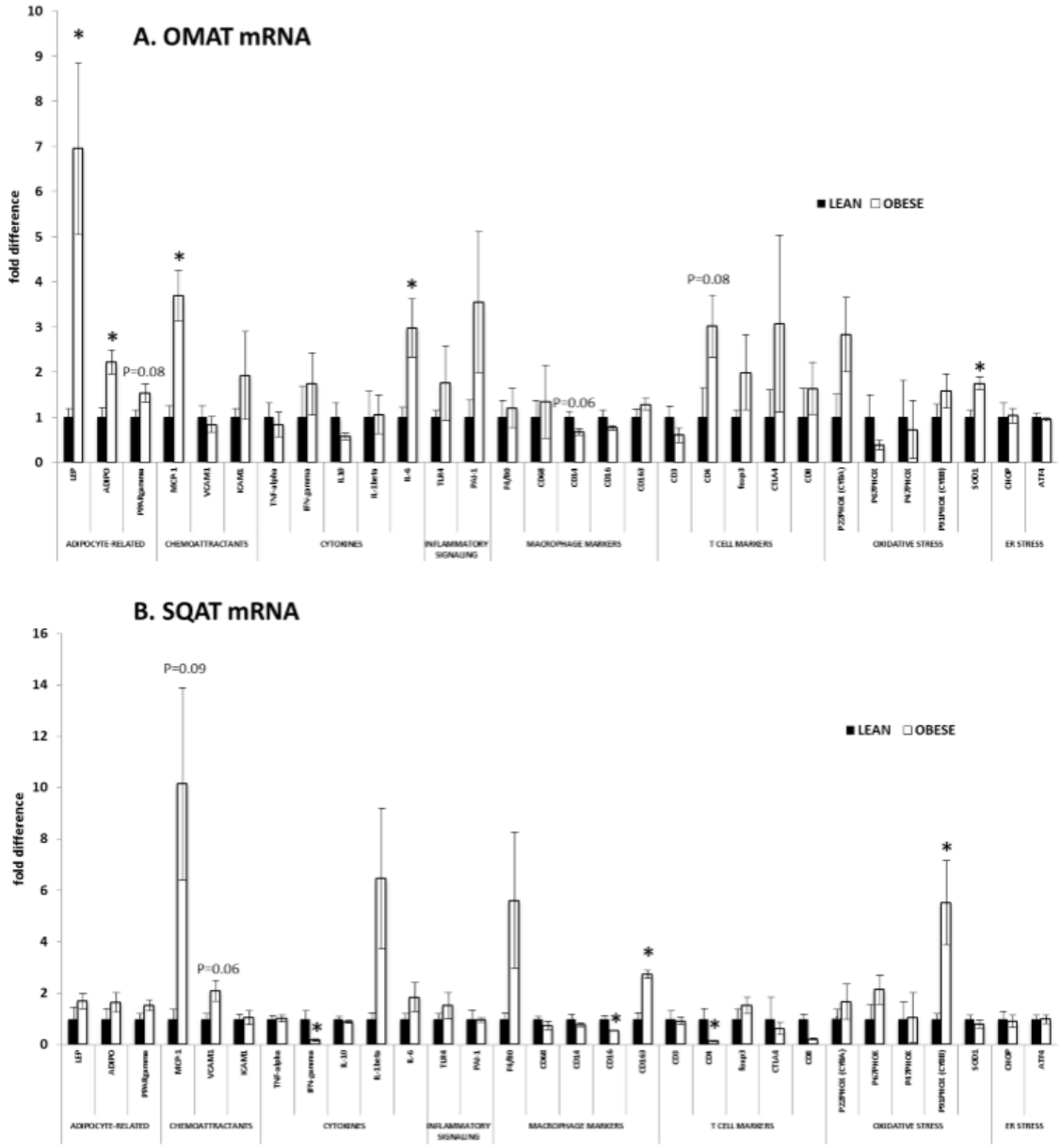

Figure 53: *Little change in AT inflammatory gene expression in OBESE pigs.* A: Omental AT (OMAT) gene expression. B: Subcutaneous AT (SQAT) gene expression. Data expressed as mean ± SEM; * P<0.05

OBESE Have Impaired Insulin-Stimulated Vasorelaxation and Atherosclerotic Lesion Formation in LAD Coronary Arteries Despite no Increase in PVAT Inflammation

The OBESE pigs exhibited evidence of atherosclerotic lesion formation in the LAD coronary arteries upon histological examination. In addition, we noted positive SRA staining on the luminal surface of LAD coronary arteries from OBESE pigs, indicative of greater inflammatory Mϕs. Representative histological images are illustrated in Figure 3A. Similarly, several inflammatory genes were, or trended toward being, up-regulated in the LAD coronary artery of OBESE vs. LEAN including the chemokines, MCP-1 (P=0.057), VCAM1 (P=0.11), and ICAM (P=0.18), the Mϕ marker, F4/80 (P=0.15), and NADPH oxidase subunits, p47Phox (P=0.067) and p91Phox (P<0.05) **(**Figure 3B). We also measured expression of the same genes in PVAT adjacent to the LAD coronary artery. Similar to the lack of inflammation detected in other depots, the PVAT of the OBESE did not express higher inflammatory gene expression (Figure 3C). No genes were significantly different between OBESE and LEAN with the exception of CD3 (P<0.05), CD8 (trending at P=0.09), and IFN-γ (P<0.05), which all were down-regulated in OBESE. As shown in Figure 4, insulin-stimulated relaxation, but not bradykinin or sodium nitroprusside-induced relaxation, in the LAD coronary artery was blunted in OBESE compared to LEAN.

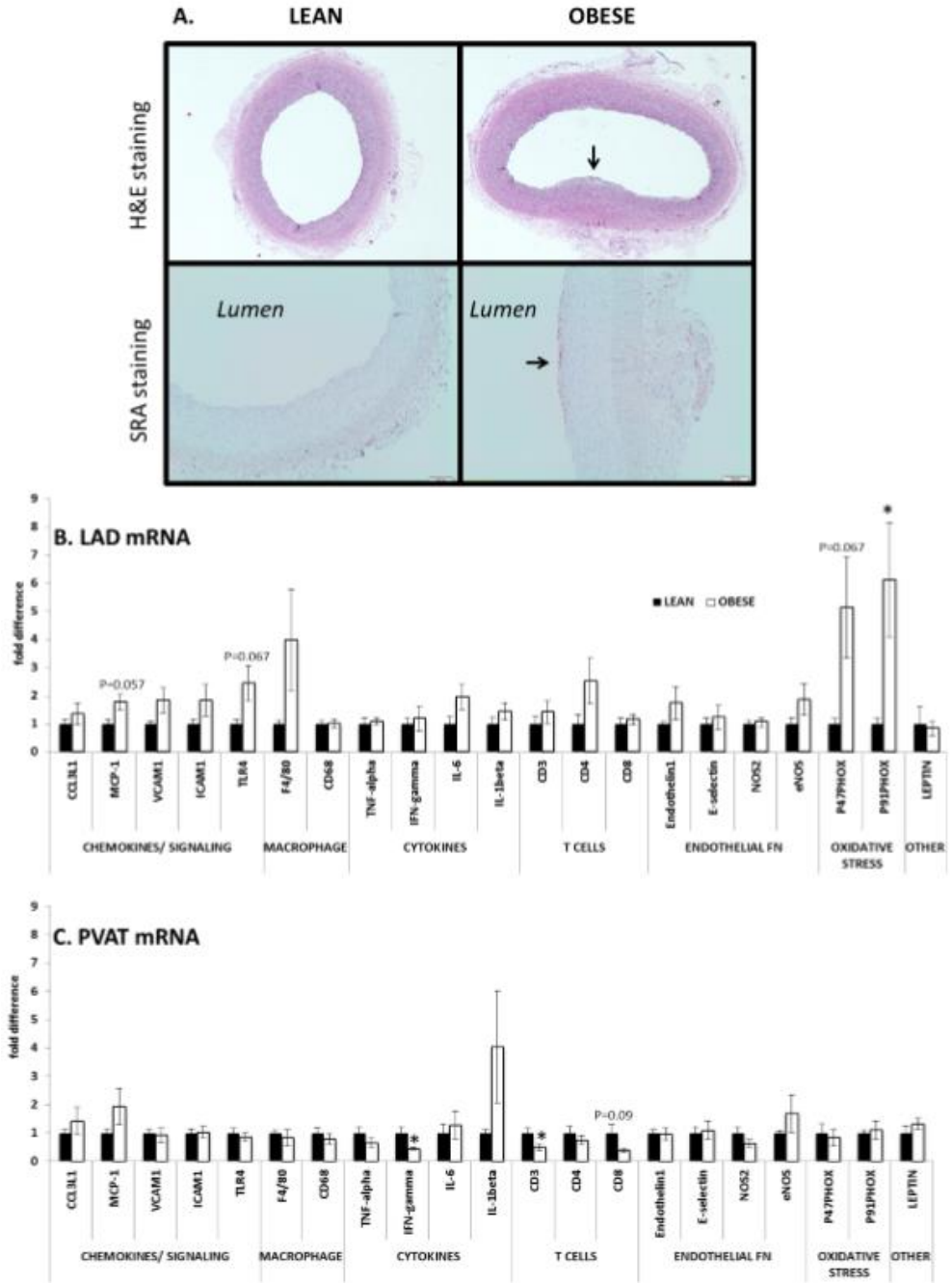

Figure 54: *OBESE pigs develop signs of coronary artery inflammation and atherosclerosis.* A: Representative images of left anterior descending (LAD) coronary artery cross sections indicating lesion formation (indicated by arrow, top panels) and Mϕ staining (SRA staining, bottom panels; positive staining indicated by arrow) in OBESE compared to LEAN. B: Gene expression analysis of LAD. C: Gene expression analysis of AT surrounding the LAD (i.e., perivascular AT, PVAT). Data expressed as mean ± SEM; * P<0.05.

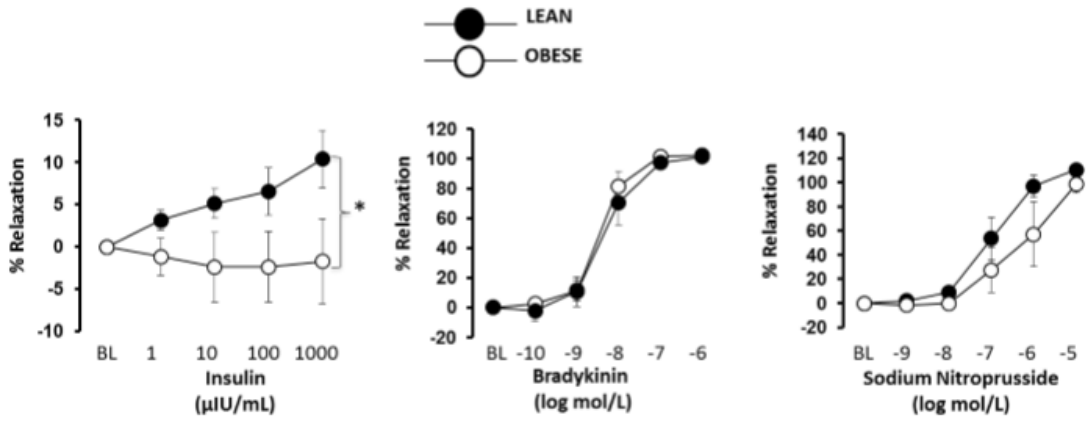

Figure 55: *OBESE pigs exhibit impaired insulin-stimulated relaxation in left anterior descending (LAD) coronary artery.* Data expressed as mean ± SEM; * P<0.05.

f. Discussion

We previously demonstrated that juvenile HFD-fed Ossabaw swine develop obesity and IR, with minimal evidence of AT inflammation (9). Here, we extend our previous work, demonstrating that, despite the fact that continued overconsumption of HFD causes extreme obesity, dyslipidemia, systemic IR, vascular IR, hypertension, as well as coronary artery inflammation and atherosclerotic lesions, female Ossabaw swine remained largely "protected" from the development of AT and systemic inflammation traditionally viewed as "characteristic" of obesity-associated metabolic impairments.

The HFD-fed OBESE pigs did not exhibit increased visceral AT (i.e., OMAT) Mϕ or T cell infiltration assessed by FACS and verified at the level of mRNA in several inflammatory markers including T cell markers (CD3, CD8) and Mϕ markers (CD68, CD14, CD16). The OBESE OMAT expressed higher levels of adiponectin and leptin, which often associate with greater adipocyte size, but the vast majority of inflammatory Mϕ, T cell, and cytokine markers were not increased. However, the chemoattractant, MCP-1, thought to precede immune cell infiltration into AT, was significantly increased in OBESE AT. This is consistent with other findings in this model in the absence of significant inflammatory Mϕ infiltration (11), and may suggest that MCP-1 is recruiting anti-inflammatory rather than inflammatory Mϕs since we observed an increase in the alternative Mϕ marker, CD163, in OBESE SQAT. Gene expression of the nuclear receptor, PPARλ trended higher in OBESE OMAT and SQAT. PPARλ associates with greater insulin sensitivity, less dysregulation of adipocyte lipolysis and an anti-

inflammatory Mϕ profile (17). Also interesting, SOD1 (an antioxidant) was elevated in OBESE OMAT.

Cytokine release from AT explants harvested from the three depots investigated (i.e., SQAT, OMAT, and PVAT) did not differ between groups, nor were there increases in circulating inflammatory cytokines (TNF-α, IFN-γ, IL-1β). Intriguingly, despite increased IL-6 gene expression in OMAT in OBESE pigs, OMAT secretion was unaltered and circulating levels were significantly reduced. This may suggest a disconnect between transcription and translation. IL-6 has been shown to be increased in AT (20) and circulation of obese humans (21) and correlate both inversely (22) and positively (21) with IR. IL-6 has both AT and skeletal muscle origins (23), and considered by some to be both pro- and anti-inflammatory (24). It is possible that reduced skeletal muscle IL-6 may have contributed to reduced circulating levels in the OBESE pigs. This should be addressed in future studies.

Taken together, Ossabaw swine appear to be protected from HFD-induced increases in AT inflammation. These findings correspond with our previous work in juvenile Ossabaw swine fed a HFD shorter-term (9) and another previous report where HFD-feeding failed to increase CD203+ Mϕ infiltration (i.e., less CD203+SVCs isolated from AT of HFD-fed vs control pigs) (11). In that study, CD203 was used as a marker of mature Mϕs similar to the marker we used to identify cells of the Mϕ/monocyte lineage, CD68; both are non-specific Mϕ markers. Interestingly, although HFD reduced total AT Mϕ infiltration in the Faris study, it caused the Mϕ phenotype to change such that a

greater percentage expressed CD16, a marker thought to be associated with inflammatory Mϕ activity (11).

The SQAT is generally considered a healthier AT depot and is characterized by smaller, more insulin sensitive and less inflammatory adipocytes (25). Still, adipocytes in this depot have been shown to expand with obesity in other models, albeit not to the extent to which adipocytes from the visceral region do (5). Reduced expandability of adipocytes from SQAT during the progression of obesity may potentiate ectopic lipid deposition and increase visceral adiposity, all of which contribute to IR (26). The "adipose tissue expandability" hypothesis is that when adipocytes are limited in their ability to expand, this results in adipocyte stress, inflammation and IR (27). The lack of expandability of SQAT adipocytes in the OBESE may have contributed to their larger OMAT adipocytes as well as the increase in systemic IR and dyslipidemia. Our data suggest that this model, compared to others, is protected to some degree in terms of AT inflammation and that less harmful adipocyte 'expandability' may be contributing to this protection. Importantly, AT inflammation is not always present in obese adults (28, 29) and it recently has been reported that overweight children showed little evidence for Mϕs in AT (30). Thus, the lower susceptibility to AT inflammation in the pig may lend support for the use of pig (as opposed to rodent) models to more accurately parallel the metablic manifestations of obesity in humans.

Given the lack of overt AT inflammation, which is the major source of obesity-associated systemic inflammation (31), it was not surprising that OBESE did not have greater systemic inflammation. However, the OBESE pigs developed other features of cardiometabolic dysfunction including hypertension, hyperglycemia, hyperinsulinemia,

hypertriglyceridemia, and impaired insulin-stimulated vasodilation in coronary arteries. The OBESE also developed atherosclerotic lesions and increased coronary artery inflammation and oxidative stress. Indeed, the Ossabaw has been described as one of the best porcine models of metabolic syndrome-induced atherosclerosis (32). The role played by PVAT in the pathophysiology of cardiovascular disease is becoming increasingly appreciated with evidence suggesting that inflammatory factors secreted by PVAT promote inflammation and impair vascular function (33, 34). Remarkably, although significant up-regulation of genes associated with inflammation were detected in the LAD, such genes were not elevated, and many reduced, in PVAT. These findings are consistent with recent data showing that most of the PVAT secreted proteins that were altered with obesity in Ossabaw were not related to classic markers of inflammation or oxidative stress (34). Similarly, our previous microarray analysis in coronary PVAT from juvenile lean and obese Ossabaw revealed only 7 genes were significantly altered with obesity (10), none of which were linked to inflammation or oxidative stress pathways. Together, these findings point to a disconnect between AT inflammation and cardiometabolic dysfunction in the Ossabaw model. An important question is whether this disconnect is specific to the Ossabaw or is consistent across swine breeds. Compared to other models, the Ossabaw is arguably the best model of metabolic syndrome-associated cardiometabolic dysfunction for a variety of reasons including practicality of their smaller size and development of human cardiometabolic manifestations. However, the limited data available in other breeds suggests that pigs in general may not be as susceptible to metabolic inflammation. Female HFD-fed White pigs develop some evidence of systemic inflammation, but no increase in IL-6 or AT

Mϕs (35); Gottingen pigs also appear protected (36). While insufficient data are available to make conclusions regarding the breed-specificity of the lack of AT inflammation documented in our study, the available evidence suggest that the pig model is less susceptible to obesity-induced AT inflammation compared to other models. Another important consideration is that there are known sex differences in obesity-induced AT inflammation such that ovary-intact females are less susceptible to AT inflammation compared to age-matched males; whether this protection would be seen in male Ossabaw pigs is unknown. Unfortunately, the other cited studies (11, 36) investigating metabolic inflammation in pigs were also exclusively in females. We investigated one male Ossabaw pig, age-matched to our experimental sample and fed chow diet, and did not find that he had higher IR or blood lipids compared to the mean values of the females fed chow, but we did find that he had ~7% and 5% more CD68+ Mϕs in SQAT and OMAT, respectively; clearly, with a sample of 1, no conclusions can be made regarding the sex-specificity of our present findings.

Insulin-stimulated relaxation in the LAD coronary artery was blunted in OBESE versus LEAN pigs in the absence of changes in bradykinin-induced relaxation, a response largely endothelium-dependent. In line with this observation, compelling evidence from studies using obese rodents demonstrate that impairments in insulin-stimulated dilation occur prior to impairments in other endothelium-dependent dilators in both skeletal muscle and coronary arteries (37-39). Reciprocally, our group found that an improvement in insulin-induced dilation with physical activity-induced weight loss occurs in the absence of changes in acetylcholine-mediated dilation in rats (14). Thus, it

appears that obesity-related changes in vascular insulin sensitivity do not always correlate with changes in classic measures of endothelium-dependent dilation.

Remarkably, after nine months of HFD feeding, the Ossabaw pigs studied here were largely “protected” from AT and systemic inflammation despite developing severe obesity with visceral adipoctye size expansion, IR, atherosclerosis, and dyslipidemia. These findings suggest that visceral AT inflammation is not a “hallmark feature” of the development of cardiometabolic disease in the female Ossabaw pig model. Given that AT inflammation has been shown to predict adverse metabolic outcomes in humans and rodents (5), determining what factor(s) is “protecting” the Ossabaw from developing inflammation could lead to therapeutic or preventative strategies applicable to human cardiometabolic disease. We speculate that the Ossabaw pig, and perhaps other swine breeds, have evolved to survive despite gross AT expansion owing to their “thrifty” genotype and postulate that this genetically-selected less harmful AT expansion may buffer the Ossabaw pig from a further exacerbation in cardiometabolic pathologies.

g. References

1. Shaharyar S, Roberson LL, Jamal O, Younus A, Blaha MJ, Ali SS, et al. Obesity and metabolic phenotypes (metabolically healthy and unhealthy variants) are significantly associated with prevalence of elevated C-reactive protein and hepatic steatosis in a large healthy brazilian population. Journal of obesity. 2015;2015:178526. Epub 2015/04/04. doi: 10.1155/2015/178526. PubMed PMID: 25838943; PubMed Central PMCID: PMC4369939.

2. Murdolo G, Smith U. The dysregulated adipose tissue: a connecting link between insulin resistance, type 2 diabetes mellitus and atherosclerosis. Nutrition, metabolism, and cardiovascular diseases : NMCD. 2006;16 Suppl 1:S35-8. Epub 2006/03/15. doi: 10.1016/j.numecd.2005.10.016. PubMed PMID: 16530128.

3. Mraz M, Haluzik M. The role of adipose tissue immune cells in obesity and low-grade inflammation. The Journal of endocrinology. 2014;222(3):R113-R27. Epub 2014/07/10. doi: 10.1530/JOE-14-0283. PubMed PMID: 25006217.

4. Vieira-Potter VJ. Inflammation and macrophage modulation in adipose tissues. Cellular microbiology. 2014. Epub 2014/07/31. doi: 10.1111/cmi.12336. PubMed PMID: 25073615.

5. Kloting N, Fasshauer M, Dietrich A, Kovacs P, Schon MR, Kern M, et al. Insulin-sensitive obesity. Am J Physiol Endocrinol Metab. 2010;299(3):E506-15. Epub 2010/06/24. doi: 10.1152/ajpendo.00586.2009. PubMed PMID: 20570822.

6. Dyson MC, Alloosh M, Vuchetich JP, Mokelke EA, Sturek M. Components of metabolic syndrome and coronary artery disease in female Ossabaw swine fed excess atherogenic diet. Comparative medicine. 2006;56(1):35-45. Epub 2006/03/09. PubMed PMID: 16521858.

7. Koopmans SJ, Schuurman T. Considerations on pig models for appetite, metabolic syndrome and obese type 2 diabetes: From food intake to metabolic disease. European journal of pharmacology. 2015. Epub 2015/03/31. doi: 10.1016/j.ejphar.2015.03.044. PubMed PMID: 25814261.

8. Neel JV. Diabetes mellitus: a "thrifty" genotype rendered detrimental by "progress"? American journal of human genetics. 1962;14:353-62. Epub 1962/12/01. PubMed PMID: 13937884; PubMed Central PMCID: PMC1932342.

9. Toedebusch RG, Roberts MD, Wells KD, Company JM, Kanosky KM, Padilla J, et al. Unique transcriptomic signature of omental adipose tissue in Ossabaw swine: a model of childhood obesity. Physiol Genomics. 2014;46(10):362-75. Epub 2014/03/20. doi: 10.1152/physiolgenomics.00172.2013. PubMed PMID: 24642759; PubMed Central PMCID: PMC4042183.

10. Padilla J, Jenkins NT, Lee S, Zhang H, Cui J, Zuidema MY, et al. Vascular transcriptional alterations produced by juvenile obesity in Ossabaw swine. Physiol Genomics. 2013;45(11):434-46. Epub 2013/04/18. doi: physiolgenomics.00038.2013 [pii] 10.1152/physiolgenomics.00038.2013. PubMed PMID: 23592636.

11. Faris RJ, Boddicker RL, Walker-Daniels J, Li J, Jones DE, Spurlock ME. Inflammation in response to n3 fatty acids in a porcine obesity model. Comparative medicine. 2012;62(6):495-503. Epub 2012/01/01. PubMed PMID: 23561883; PubMed Central PMCID: PMC3527754.

12. Zhang X, Li ZL, Woollard JR, Eirin A, Ebrahimi B, Crane JA, et al. Obesity-metabolic derangement preserves hemodynamics but promotes intrarenal adiposity and macrophage infiltration in swine renovascular disease. American journal of physiology Renal physiology. 2013;305(3):F265-76. Epub 2013/05/10. doi: 10.1152/ajprenal.00043.2013. PubMed PMID: 23657852; PubMed Central PMCID: PMC3742861.

13. Vieira Potter VJ, Strissel KJ, Xie C, Chang E, Bennett G, Defuria J, et al. Adipose tissue inflammation and reduced insulin sensitivity in ovariectomized mice occurs in the absence of increased adiposity. Endocrinology. 2012;153(9):4266-77. Epub 2012/07/11. doi: 10.1210/en.2011-2006. PubMed PMID: 22778213; PubMed Central PMCID: PMC3423617.

14. Crissey JM, Jenkins NT, Lansford KA, Thorne PK, Bayless DS, Vieira-Potter VJ, et al. Adipose tissue and vascular phenotypic modulation by voluntary physical activity and dietary restriction in obese insulin-resistant OLETF rats. American journal of physiology Regulatory, integrative and comparative physiology. 2014;306(8):R596-606. Epub 2014/02/14. doi: 10.1152/ajpregu.00493.2013. PubMed PMID: 24523340; PubMed Central PMCID: PMCPMC4043131.

15. Matthews DR, Hosker JP, Rudenski AS, Naylor BA, Treacher DF, Turner RC. Homeostasis model assessment: insulin resistance and beta-cell function from fasting plasma glucose and insulin concentrations in man. Diabetologia. 1985;28(7):412-9. Epub 1985/07/01. PubMed PMID: 3899825.

16. Malin SK, Kashyap SR, Hammel J, Miyazaki Y, DeFronzo RA, Kirwan JP. Adjusting glucose-stimulated insulin secretion for adipose insulin resistance: an index of beta-cell function in obese adults. Diabetes care. 2014;37(11):2940-6. Epub 2014/08/21. doi: 10.2337/dc13-3011. PubMed PMID: 25139885; PubMed Central PMCID: PMC4207203.

17. Odegaard JI, Ricardo-Gonzalez RR, Goforth MH, Morel CR, Subramanian V, Mukundan L, et al. Macrophage-specific PPARgamma controls alternative activation and improves insulin resistance. Nature. 2007;447(7148):1116-20. Epub 2007/05/23. doi: 10.1038/nature05894. PubMed PMID: 17515919; PubMed Central PMCID: PMC2587297.

18. Blazquez R, Sanchez-Margallo FM, de la Rosa O, Dalemans W, Alvarez V, Tarazona R, et al. Immunomodulatory Potential of Human Adipose Mesenchymal Stem Cells Derived Exosomes on in vitro Stimulated T Cells. Frontiers in immunology. 2014;5:556. Epub 2014/11/22. doi: 10.3389/fimmu.2014.00556. PubMed PMID: 25414703; PubMed Central PMCID: PMC4220146.

19. Feuerer M, Herrero L, Cipolletta D, Naaz A, Wong J, Nayer A, et al. Lean, but not obese, fat is enriched for a unique population of regulatory T cells that affect metabolic parameters. Nat Med. 2009;15(8):930-9. Epub 2009/07/28. doi: 10.1038/nm.2002. PubMed PMID: 19633656; PubMed Central PMCID: PMC3115752.

20. Bastard JP, Jardel C, Bruckert E, Blondy P, Capeau J, Laville M, et al. Elevated levels of interleukin 6 are reduced in serum and subcutaneous adipose tissue of obese women after weight loss. The Journal of clinical endocrinology and metabolism. 2000;85(9):3338-42. Epub 2000/09/22. doi: 10.1210/jcem.85.9.6839. PubMed PMID: 10999830.

21. van Beek L, Lips MA, Visser A, Pijl H, Ioan-Facsinay A, Toes R, et al. Increased systemic and adipose tissue inflammation differentiates obese women with T2DM from obese women with normal glucose tolerance. Metabolism: clinical and experimental. 2014;63(4):492-501. Epub 2014/01/29. doi: 10.1016/j.metabol.2013.12.002. PubMed PMID: 24467914.

22. Mauer J, Chaurasia B, Goldau J, Vogt MC, Ruud J, Nguyen KD, et al. Signaling by IL-6 promotes alternative activation of macrophages to limit endotoxemia and obesity-associated resistance to insulin. Nature immunology. 2014;15(5):423-30. Epub 2014/04/01. doi: 10.1038/ni.2865. PubMed PMID: 24681566; PubMed Central PMCID: PMC4161471.

23. Munoz-Canoves P, Scheele C, Pedersen BK, Serrano AL. Interleukin-6 myokine signaling in skeletal muscle: a double-edged sword? The FEBS journal. 2013;280(17):4131-48. Epub 2013/05/15. doi: 10.1111/febs.12338. PubMed PMID: 23663276; PubMed Central PMCID: PMC4163639.

24. Starkie R, Ostrowski SR, Jauffred S, Febbraio M, Pedersen BK. Exercise and IL-6 infusion inhibit endotoxin-induced TNF-alpha production in humans. FASEB journal : official publication of the Federation of American Societies for Experimental Biology. 2003;17(8):884-6. Epub 2003/03/11. doi: 10.1096/fj.02-0670fje. PubMed PMID: 12626436.

25. Bolinder J, Kager L, Ostman J, Arner P. Differences at the receptor and postreceptor levels between human omental and subcutaneous adipose tissue in the action of insulin on lipolysis. Diabetes. 1983;32(2):117-23. Epub 1983/02/01. PubMed PMID: 6337893.

26. Alligier M, Gabert L, Meugnier E, Lambert-Porcheron S, Chanseaume E, Pilleul F, et al. Visceral fat accumulation during lipid overfeeding is related to subcutaneous adipose tissue characteristics in healthy men. The Journal of clinical endocrinology and metabolism. 2013;98(2):802-10. Epub 2013/01/04. doi: 10.1210/jc.2012-3289. PubMed PMID: 23284008.

27. Virtue S, Vidal-Puig A. Adipose tissue expandability, lipotoxicity and the Metabolic Syndrome--an allostatic perspective. Biochimica et biophysica acta. 2010;1801(3):338-49. Epub 2010/01/09. doi: 10.1016/j.bbalip.2009.12.006. PubMed PMID: 20056169.

28. Apovian CM, Bigornia S, Mott M, Meyers MR, Ulloor J, Gagua M, et al. Adipose macrophage infiltration is associated with insulin resistance and vascular endothelial dysfunction in obese subjects. Arterioscler Thromb Vasc Biol. 2008;28(9):1654-9. Epub 2008/06/21. doi: 10.1161/ATVBAHA.108.170316. PubMed PMID: 18566296; PubMed Central PMCID: PMC2728436.

29. Le KA, Mahurkar S, Alderete TL, Hasson RE, Adam TC, Kim JS, et al. Subcutaneous adipose tissue macrophage infiltration is associated with hepatic and visceral fat deposition, hyperinsulinemia, and stimulation of NF-kappaB stress pathway. Diabetes. 2011;60(11):2802-9. Epub 2011/10/26. doi: 10.2337/db10-1263. PubMed PMID: 22025778; PubMed Central PMCID: PMC3198061.

30. Tam CS, Tordjman J, Divoux A, Baur LA, Clement K. Adipose tissue remodeling in children: the link between collagen deposition and age-related adipocyte growth. The Journal of clinical endocrinology and metabolism. 2012;97(4):1320-7. Epub 2012/01/20. doi: 10.1210/jc.2011-2806. PubMed PMID: 22259057.

31. Festa A, D'Agostino R, Jr., Williams K, Karter AJ, Mayer-Davis EJ, Tracy RP, et al. The relation of body fat mass and distribution to markers of chronic inflammation. International journal of obesity and related metabolic disorders : journal of the International Association for the Study of Obesity. 2001;25(10):1407-15. Epub 2001/10/24. doi: 10.1038/sj.ijo.0801792. PubMed PMID: 11673759.

32. Hamamdzic D, Wilensky RL. Porcine models of accelerated coronary atherosclerosis: role of diabetes mellitus and hypercholesterolemia. Journal of diabetes research. 2013;2013:761415. Epub 2013/07/12. doi: 10.1155/2013/761415. PubMed PMID: 23844374; PubMed Central PMCID: PMC3697774.

33. Villacorta L, Chang L. The role of perivascular adipose tissue in vasoconstriction, arterial stiffness, and aneurysm. Hormone molecular biology and clinical investigation. 2015. Epub 2015/02/27. doi: 10.1515/hmbci-2014-0048. PubMed PMID: 25719334.

34. Owen MK, Witzmann FA, McKenney ML, Lai X, Berwick ZC, Moberly SP, et al. Perivascular adipose tissue potentiates contraction of coronary vascular smooth muscle: influence of obesity. Circulation. 2013;128(1):9-18. Epub 2013/05/21. doi: 10.1161/CIRCULATIONAHA.112.001238. PubMed PMID: 23685742; PubMed Central PMCID: PMC3755741.

35. Busnelli M, Manzini S, Froio A, Vargiolu A, Cerrito MG, Smolenski RT, et al. Diet induced mild hypercholesterolemia in pigs: local and systemic inflammation, effects on vascular injury - rescue by high-dose statin treatment. PloS one. 2013;8(11):e80588. Epub 2013/11/22. doi:10.1371/journal.pone.0080588. PubMed PMID: 24260430; PubMed Central PMCID: PMC3829827.

36. Rodgaard T, Skovgaard K, Moesgaard SG, Cirera S, Christoffersen BO, Heegaard PM. Extensive changes in innate immune gene expression in obese Gottingen minipigs do not lead to changes in concentrations of circulating cytokines and acute phase proteins. Animal genetics. 2014;45(1):67-73. Epub 2013/10/11. doi: 10.1111/age.12090. PubMed PMID: 24106888.

37. Eringa EC, Stehouwer CD, Roos MH, Westerhof N, Sipkema P. Selective resistance to vasoactive effects of insulin in muscle resistance arteries of obese Zucker (fa/fa) rats. American jou rnal of physiology Endocrinology and metabolism. 2007;293(5):E1134-9. Epub 2007/07/12. doi: 10.1152/ajpendo.00516.2006. PubMed PMID: 17623751.

38. Katakam PV, Tulbert CD, Snipes JA, Erdos B, Miller AW, Busija DW. Impaired insulin-induced vasodilation in small coronary arteries of Zucker obese rats is mediated by reactive oxygen species. American journal of physiology Heart and circulatory physiology. 2005;288(2):H854-60. Epub 2005/01/15. doi: 10.1152/ajpheart.00715.2004. PubMed PMID: 15650157.

39. Oltman CL, Richou LL, Davidson EP, Coppey LJ, Lund DD, Yorek MA. Progression of coronary and mesenteric vascular dysfunction in Zucker obese and Zucker diabetic fatty rats. American journal of physiology Heart and circulatory physiology. 2006;291(4):H1780-7. Epub 2006/05/23. doi: 10.1152/ajpheart.01297.2005. PubMed PMID: 16714356.

8. CONCLUSIONS

a. Discussion and Future Directions

From work with other researchers culminating in publications by them, it became rapidly apparent that within-tissue signaling can influence vascular structure and function. Previous work from this lab which is included in this paper illustrates that different tissue beds can feature different secretomes, which in turn can alter overall prognosis as well as vessel responsiveness and structure(1, 2). Additionally, obesity can modify secretomes in deleterious fashion with respect to vessel function, and exercise training can reverse these secretome changes, as can pharmaceutical administration(3-5). With this previous data indicating that obesity has profound effects on vessel function, in conjunction with data from other researchers demonstrating capillarity decrease in obese humans and animals, we developed our hypothesis that IGF2R, IGF2, uPAR, and TGFβ were altered in obesity as to promote capillarity decrease.

In our data, we observed decreased capillarity in our non-lean animals in conjunction with no significant change in any of the factors we were measuring, contrary to our hypothesis that IGF2R, IGF2, uPAR, and TGFβ would differ significantly with induction of obesity as compared to our lean control rats. In Figure 56 we summarize a new hypothesis schema, with our proposal that pro-angiogenic activity is maintained in obese individuals, but hampered by uncharacterized anti-angiogenic mechanisms, increased rarefaction of capillaries, or both. Beginning at the top of the schema, obesity results from calorie intake in excess of daily need, often in conjunction with diminished

physical activity as a result of lifestyle factors or injury. We have data showing that capillarity decreases as a result of obesity induction, but which also shows that factors we hypothesized would be elevated with the end result of promoting capillarity decrease- IGF2R and TGFβ – did not change significantly relative to control, and that factors we hypothesized would decrease with the end result of not promoting capillarity increase – IGF2 and uPAR – either slightly increased or did not change significantly relative to control. As a consequence, we hypothesize that capillarity decrease in obesity is driven by either other anti-angiogenic mechanisms, increased capillary rarefaction, or a combination of both.

At present we do not know why IGF2R, IGF2, uPAR, and TGFβ are present at levels similar to our lean controls, but we hypothesize that this may be a compensatory response to a decrease in capillary density driven by other mechanisms. This capillary density decrease then promotes increase in IGF2 expression to sustain nutrient delivery. Meanwhile IGF2R, uPAR, and TGFβ expression returns to levels as seen in lean individuals, resulting in the same contribution to new vessel growth in obese individuals as seen in lean individuals, with the discrepancy in capillarity arising from other mechanisms. An alternative hypothesis would be capillarity changes without a corresponding change in any of the factors excepting a later increase in IGF2. Both possibilities are summarized in Figure 56. As prior work has suggested that all four factors are altered in obesity in fetuses and young animals, leading us to our hypotheses about alteration in adult animals, it may further imply these factors change over time if they are altered in young individuals but not significantly so in older individuals.

We have one issue in the LETO HFD data set. These data were excluded from Figure 15 TGFβ because there were insufficient data points to allow valid conclusions. Additional data points may be needed, but if the LETO HFD animals display the same differences in respect to obesity induction versus LETO control diet rats, as between LETO control and OLETF control rats, we would anticipate that we would also see a drop in TGFβ. While this would be a suitable observation to follow on in future experiments, we do not believe it greatly impacts our earlier overall conclusions.

In developing any future experiments to clarify the data I obtained in my own thesis work, I would begin by hypothesizing that I would observe differences in the expression of these four factors between groups, as animals respond to diet and intervention by weight changes and development of diabetes if I conducted a future set of experiments in which I was able to test animal samples over time – for example, testing our LETO and OLETF groups earlier than age 32 weeks, at age 20 weeks and age 26 weeks. Specifically, we would hypothesize that one of two sequences would occur as outlined in Figure 57. Both obesity and diabetes is induced followed by progressive decrease in capillarity in conjunction with a capillarity-decreasing change in these four factors, followed by an capillary-increasing change in these four factors as a compensatory response, or these four factors are maintained at or slightly above normal physiological levels during the time course from obesity and diabetes induction to when we sacrificed them. Before I address multiple samples over time, however, I must account for the fact that while we examined our data on the basis of obesity, diabetes may cause capillary rarefaction as well.

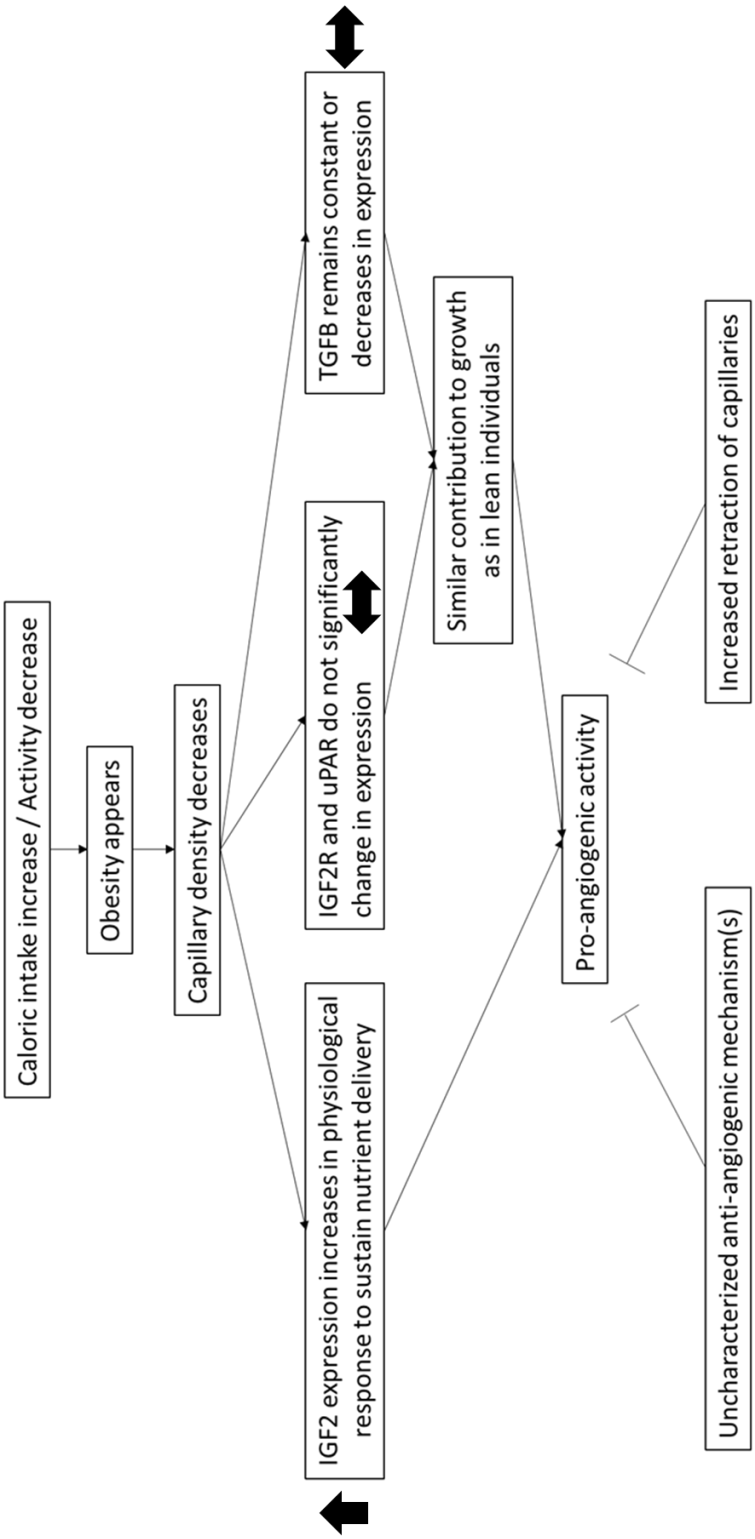

Figure 56: New proposed schema for IGF2R and coordinated factors in obesity

Figure 57: Two separate proposed progressions to account for observed changes in IGF2R, IGF2, uPAR, and TGFβ

The arc of diabetes

One consideration to be made in interpreting our data is whether the rats' diabetic status may have contributed to capillarity changes, independent of their obesity status. In OLETF rats, there is an extensive record of diabetes onset in concurrence with obesity (6). As early as 25 weeks of age, significant impaired B-cell insulin signaling and content occurs compared to control, and even extended out to 65 weeks of age, control rats still maintain B-cells in the pancreas as compared to their counterparts who display complete loss and fibrosis at that age (7, 8). On a structural basis, these pancreas islets display a hyperplastic phenotype and fibrosis beginning as early as ten weeks of age, progressing to atrophy at 40 weeks of age (9). Prior research has also suggested there is some divergence in phenotypes among OLETF rats with respect to islet function, with heavier diabetic rats having more typical capillarity within islets while leaner diabetic rats have sparser capillarity, resulting in a more severe phenotype in the latter group (10).

Referring to other animal and human studies, there has been extensive records of decreased capillarity in db/db, C57BL/6, and steptozotocin-knockout models of rats and mice (11-15) Diabetic pigs have also been shown to display decreases in capillarity, and human diabetic explants have shown capillarity decreases and pericyte loss (16).

A study released on the same animals reflected in our data by Linden et. al. showed that OLETF sedentary animals showed clear evidence of diabetes, with hyperglycemia and glucose levels differing significantly from OLETF EX animals, though not OLETF FR animals. Insulin levels were similar, although this can be explained by

way of loss of beta-cell function in the sedentary animals, while insulin levels were controlled in the other two groups by way of intervention(17).

The question then becomes how further work may determine what proportion of capillarity changes is derived from obesity and what is derived from diabetes. The primary difficulty lies in how obesity promotes insulin resistance which then leads to the development of type II diabetes. One could sidestep this with administration of streptozotocin alone which is toxic to pancreas beta cells, however this is said to more closely replicate type I diabetes than type II diabetes.

A better solution might be to mitigate obesity as a driving factor by first inducing obesity, then allowing diabetes to either develop as a consequence of obesity or inducing it quickly by way of low-dose streptozotocin administration. The animal can then be placed on an exercise or calorie restriction regimen to reduce body fat percentage, bringing them down from an obese state as quickly as possible. When maintained at a lean body mass following induction of obesity and beta-cell destruction to induce diabetes, the model should recapitulate the negative effects of prior obesity and diabetes, while removing the immediate effects of obesity, meaning diabetes will have a greater proportional contribution to physiological changes.

Prior studies using the streptozotocin protocol have set their fat content for regular chow around 12%, and high fat chow around 40%, and used one injection of between 30-45 mg/kg, although some studies have used two or more injections(18-20). A preliminary treatment protocol then, might attempt to recapitulate our LETO/OLETF study, but with LETO alone or a different strain of rat, in order to eliminate any variables arising from the OLETF rat's hyperphagia. We would receive the rats at age four weeks

and raise them on regular chow until age 8 weeks, at which point we would subdivide them into low fat diet and high fat diet cohorts. They would continue until age 20 weeks, at which point the low-fat diet and high fat diet cohorts would be internally subdivided into animals receiving streptozotocin treatment and those without. A weight loss protocol, likely beginning immediately after streptozotocin treatment, would then bring the animals back down to a lower body fat percentage. An outline of the protocol is shown in Figure 57.

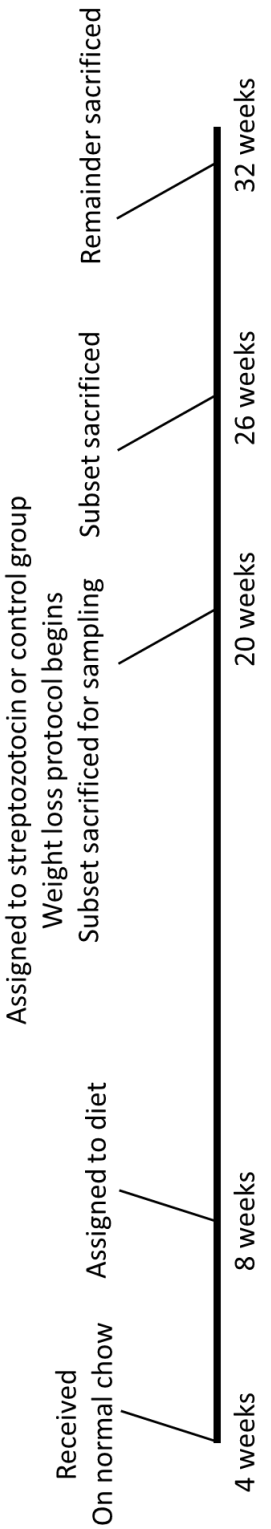

Figure 58: Proposed protocol for elucidating impact of diabetes on IGF2R, IGF2, uPAR, and TGFβ

Sex

Another consideration at hand is the effect of sex on capillarity during obesity. Prior research has shown sex differences in cardiovascular function, both at baseline and during obesity(21). These sex differences can be attributed in part due to gonadal hormones, but are also due to non-hormone derieved influences, which could include either sex chromosome composition or sex-dependent gene regulation(22). Gonadal hormone withdrawal in the case of ovariectomy is shown to give rise to microvessel destabilization and capillary rarefaction in the dura mater of pigs (23, 24). In humans, hypertension is shown to reduce tissue capillary density by 33% in men relative to women, which is relevant as hypertension is a potential consequence of both diabetes and obesity(21). Additionally, chronic heart failure is shown to result in a vastus lateralis capillary density decrease in men relative to women(25).

It is abundantly clear that any animal data that is extended to humans must include female animal data to build support for any hypotheses that there is a difference between human men and women in respect to mechanism function in capillary density changes. However, OLETF rats are unsuitable for this purpose as the company which controls the strain does not make female OLETF rats available for purchase, likely to control the strain for commercial purposes. As such, any experiments involving female rats would require using a different strain in which both male and female rats are readily available.

We suggest that any experiments could proceed as previously outlined for male rats. It may be necessary to monitor estrous cycle owing to the previously established effects of ovarian hormones on capillarity. Serum monitoring for estradiol levels is

feasible, although it may be prudent to use non-invasive monitoring to reduce stress on animals(26).

b. The effects of obesity, and the known effect of exercise intervention on vasomotor function

In obesity and during insulin resistance, pathological vessel remodeling and change in vasomotor function is known to occur, owing to a wide variety of factors such as hypertension, abnormal sympathetic activation, and changes in the renin-angiotensin-aldosterone system among others(27, 28). Physological changes are seen ranging from the endothelial cell layer with vasoactive factor handling, to the vascular smooth muscle layer with decrease in function and loss of myogenic tone, to the extracellular matrix where an increase in ECM density and remodeling occurs(28-30).

In the endothelial cell layer, one of the primary dysfunctions is shown in the synthesis and handling of NO, where increase in NADPH oxidase can provide ROS for NO conversion to perioxynitrite(31, 32). Vessel responsiveness to other factors such as Ach is shown to be blunted during insulin resistance as well(33). This general insensitivity to vasoactive substances likely accounts for attenuation of skeletal muscle blood flow during exercise in diabetes relative to non-diabetic counterparts, with Ach insensitivity, lack of capillary recruitment, and general ischemia observed. (34, 35).

From our images of muscle cross-sections, we performed measurements of the physical dimensions of arterioles, as shown in Figure 58. In short, we measured the diameter across the widest part of the vessel twice, once from the outermost edge to

the opposite outermost edge, and once from the innermost edge to the opposite innermost edge. We also measured the vessel wall at the thickest location.

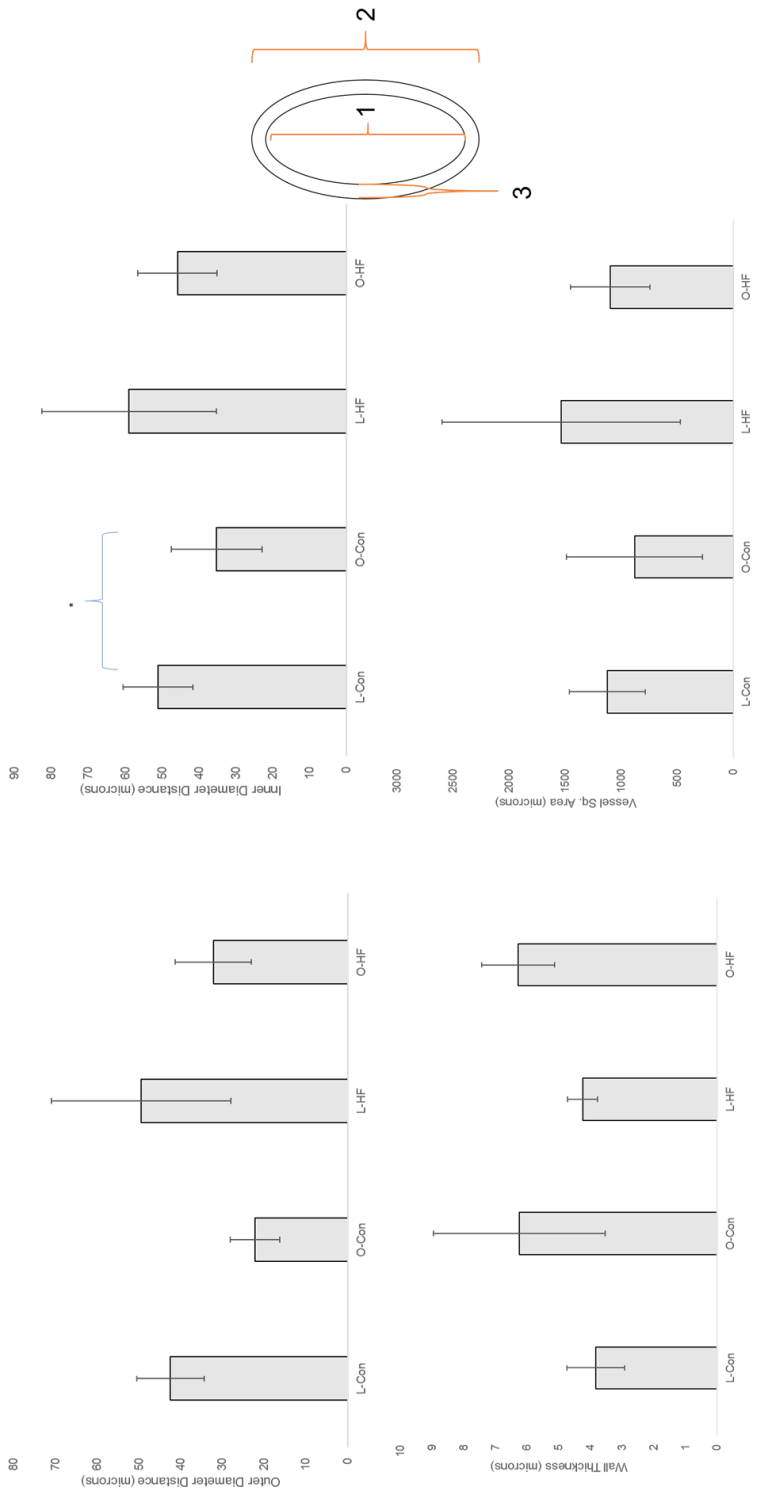

Figure 59: Measurements of physical dimensions of large vessels.

The data did not support the hypothesis that dietary or strain-induced obesity alters macrovessel outer diameter, inner diameter, wall thickness, or vessel cross-sectional area. The sole exception is a significant decrease ($p<0.05$) between the inner diameters of L-CON and O-CON vessels. This is contrary to our initial hypothesis that induction of diet or strain obesity would cause thickening of vessel walls, and we suggest our low n-values ($n = 4-5$) may account for the large variance in standard error seen. We hypothesize that with additional data points, we would observe similar outcomes to what is reported in the literature with regard to vessel wall thickening in obesity.

Even though we did not measure the changes in vessel parameters in response to exercise and calorie restriction for our specific cohort outlined in previous data, prior work indicates that exercise training can improve vasomotor responsiveness even during insulin resistance. Studies have shown that endurance exercise training and interval sprint training can improve responsiveness of vessels to insulin or Ach administration, dependent on fiber type of associated skeletal muscle(33, 36-38). This increase arises from several factors, including increase in eNOS, decrease in stiffness, and an increase in capillary recruitment(37).

c. Other effects on capillarity

Inflammation, shear stress, and the venous system

Despite our focus on the four factors, IGF2R, IGF2, uPAR, and TGFβ, other items such as the immune system and the venous system can contribute to capillarity changes. Pathological activation of the immune system can promote vascular

remodeling at several different steps. Hypertensive stimuli can activate dendritic cells which then work to promote hypertension, while NADPH oxidase can mediate angiotensin-II induced infiltration of macrophages into the vessel wall(39, 40). Damage-associated molecular patterns (DAMPs) can also act via Toll-like receptors to cause abnormal immune activation in the circulation leading to hypertension and pathological remodeling (41, 42). Additionally, macrophage colony-stimulating factor, when knocked out, demonstrates less endothelial dysfunction and remodeling during the development of hypertension (43).

Shear stress also plays a role in vascular remodeling, as mechanical force can provoke responses in the endothelium as a result of both endothelial cell sensitivity and varying degrees of shear stress(44-46). This can lead to reduction of the vessel diameter by physical changes in the vessel wall and changes in smooth muscle tone(47-49).

In evaluating the effects of the venous system on capillarity, the key point is that the microcirculation can be physically set up such that arterioles and venules run parallel to each other, with capillaries forming a web between them. This permits the possibility of venous signaling to “earlier” areas of the tissue as well as to arterioles, in a paracrine fashion.

Previous work has demonstrated that norepinephrine injected into vessels residing post-arteriole but pre-venule, and endogenous factors such as NO released from hemoglobin in the low oxygen environment of the venule, will diffuse from the venule to nearby arterioles and effect action on the arteriole. (50-54). Also observed is

that mechanical impact on venules in the form of shear stress can result in signaling to arterioles, as well as other mechanical factors such as muscle contraction(55-58).

With prior studies demonstrating that immediate paracrine action can be effected by diffusion of substances across the venule wall and through the extracellular space to neighboring arterioles, it is possible that bloodflow changes due to capillary rarefaction, as well as tissue stress signaling arising from capillary rarefaction, could then promote venule-arteriole communication to promote new vessel growth as part of a physiological response to improve nutrient and oxygen delivery to tissue. This would then account for maintenance of IGF2R, IGF2, uPAR, and TGFβ at, or above, normal physiological levels for promotion of growth.

d. Concluding remarks

In summary, while we have shown that none of the four factors we examined seem to change significantly with respect to obesity and one sampling at age 32 weeks, there remains several avenues of investigation to further examine these factors. These include multiple samplings over time to determine if these factors change as animals undergo pathological changes, as well as determining if diabetes may account for some of these capillarity changes rather than obesity being the sole determinant. The impact of sex, and to what extent inflammation and venous communication play a role in these animals and in conjunction with these factors is also an exciting line of investigation.

e. References

1. Roberts MD, Bayless DS, Company JM, Jenkins NT, Padilla J, Childs TE, et al. Elevated skeletal muscle irisin precursor FNDC5 mRNA in obese OLETF rats. Metabolism: clinical and experimental. 2013;62(8):1052-6. Epub 2013/03/19. doi: 10.1016/j.metabol.2013.02.002. PubMed PMID: 23498898; PubMed Central PMCID: PMCPMC3688677.

2. Vieira-Potter VJ, Lee S, Bayless DS, Scroggins RJ, Welly RJ, Fleming NJ, et al. Disconnect between adipose tissue inflammation and cardiometabolic dysfunction in Ossabaw pigs. Obesity (Silver Spring, Md). 2015;23(12):2421-9. Epub 2015/11/03. doi: 10.1002/oby.21252. PubMed PMID: 26524201; PubMed Central PMCID: PMCPMC4701582.

3. Crissey JM, Jenkins NT, Lansford KA, Thorne PK, Bayless DS, Vieira-Potter VJ, et al. Adipose tissue and vascular phenotypic modulation by voluntary physical activity and dietary restriction in obese insulin-resistant OLETF rats. American journal of physiology Regulatory, integrative and comparative physiology. 2014;306(8):R596-606. Epub 2014/02/14. doi: 10.1152/ajpregu.00493.2013. PubMed PMID: 24523340; PubMed Central PMCID: PMCPMC4043131.

4. Padilla J, Jenkins NT, Thorne PK, Lansford KA, Fleming NJ, Bayless DS, et al. Differential regulation of adipose tissue and vascular inflammatory gene expression by chronic systemic inhibition of NOS in lean and obese rats. Physiological reports. 2014;2(2):e00225. Epub 2014/04/20. doi: 10.1002/phy2.225. PubMed PMID: 24744894; PubMed Central PMCID: PMCPMC3966247.

5. Jenkins NT, Padilla J, Arce-Esquivel AA, Bayless DS, Martin JS, Leidy HJ, et al. Effects of endurance exercise training, metformin, and their combination on adipose tissue leptin and IL-10 secretion in OLETF rats. Journal of applied physiology (Bethesda, Md : 1985). 2012;113(12):1873-83. Epub 2012/09/29. doi: 10.1152/japplphysiol.00936.2012. PubMed PMID: 23019312; PubMed Central PMCID: PMCPMC3544496.

6. Okauchi N, Mizuno A, Zhu M, Ishida K, Sano T, Noma Y, et al. Effects of obesity and inheritance on the development of non-insulin-dependent diabetes mellitus in Otsuka-Long-Evans-Tokushima fatty rats. Diabetes research and clinical practice. 1995;29(1):1-10. Epub 1995/07/01. PubMed PMID: 8593753.

7. Zhao J, Zhang N, He M, Yang Z, Tong W, Wang Q, et al. Increased beta-cell apoptosis and impaired insulin signaling pathway contributes to the onset of diabetes in OLETF rats. Cellular physiology and biochemistry : international journal of experimental cellular physiology, biochemistry, and pharmacology. 2008;21(5-6):445-54. Epub 2008/05/06. doi: 10.1159/000129637. PubMed PMID: 18453752.

8. Fukaya N, Mochizuki K, Tanaka Y, Kumazawa T, Jiuxin Z, Fuchigami M, et al. The alpha-glucosidase inhibitor miglitol delays the development of diabetes and dysfunctional insulin secretion in pancreatic beta-cells in OLETF rats. European journal of pharmacology. 2009;624(1-3):51-7. Epub 2009/10/13. doi: 10.1016/j.ejphar.2009.09.048. PubMed PMID: 19818342.

9. Kawano K, Hirashima T, Mori S, Natori T. OLETF (Otsuka Long-Evans Tokushima Fatty) rat: a new NIDDM rat strain. Diabetes research and clinical practice. 1994;24 Suppl:S317-20. Epub 1994/10/01. PubMed PMID: 7859627.

10. Mizuno A, Noma Y, Kuwajima M, Murakami T, Zhu M, Shima K. Changes in islet capillary angioarchitecture coincide with impaired B-cell function but not with insulin resistance in male Otsuka-Long-Evans-Tokushima fatty rats: dimorphism of the diabetic phenotype at an advanced age. Metabolism: clinical and experimental. 1999;48(4):477-83. Epub 1999/04/17. PubMed PMID: 10206441.

11. Gonzalez-Quesada C, Cavalera M, Biernacka A, Kong P, Lee DW, Saxena A, et al. Thrombospondin-1 induction in the diabetic myocardium stabilizes the cardiac matrix in addition to promoting vascular rarefaction through angiopoietin-2 upregulation. Circulation research. 2013;113(12):1331-44. Epub 2013/10/02. doi: 10.1161/circresaha.113.302593. PubMed PMID: 24081879; PubMed Central PMCID: PMCPMC4408537.

12. Gilbert RE. Endothelial loss and repair in the vascular complications of diabetes: pathogenetic mechanisms and therapeutic implications. Circulation journal : official journal of the Japanese Circulation Society. 2013;77(4):849-56. Epub 2013/03/19. PubMed PMID: 23503045.

13. Bonner JS, Lantier L, Hasenour CM, James FD, Bracy DP, Wasserman DH. Muscle-specific vascular endothelial growth factor deletion induces muscle capillary rarefaction creating muscle insulin resistance. Diabetes. 2013;62(2):572-80. Epub 2012/09/25. doi: 10.2337/db12-0354. PubMed PMID: 23002035; PubMed Central PMCID: PMCPMC3554359.

14. Ashoff A, Qadri F, Eggers R, Johren O, Raasch W, Dendorfer A. Pioglitazone prevents capillary rarefaction in streptozotocin-diabetic rats independently of glucose control and vascular endothelial growth factor expression. Journal of vascular research. 2012;49(3):260-6. Epub 2012/03/30. doi: 10.1159/000335214. PubMed PMID: 22456468.

15. Ko SH, Cao W, Liu Z. Hypertension management and microvascular insulin resistance in diabetes. Curr Hypertens Rep. 2010;12(4):243-51. Epub 2010/06/29. doi: 10.1007/s11906-010-0114-6. PubMed PMID: 20582734; PubMed Central PMCID: PMCPMC3020573.

16. Hinkel R, Hoewe A, Renner S, Ng J, Lee S, Klett K, et al. Diabetes Mellitus-Induced Microvascular Destabilization in the Myocardium. J Am Coll Cardiol. 2017;69(2):131-43. Epub 2017/01/14. doi: 10.1016/j.jacc.2016.10.058. PubMed PMID: 28081822.

17. Linden MA, Sheldon RD, Meers GM, Ortinau LC, Morris EM, Booth FW, et al. Aerobic exercise training in the treatment of non-alcoholic fatty liver disease related fibrosis. The Journal of physiology. 2016;594(18):5271-84. Epub 2016/04/23. doi: 10.1113/jp272235. PubMed PMID: 27104887; PubMed Central PMCID: PMCPMC5023692.

18. Zhang M, Lv XY, Li J, Xu ZG, Chen L. The characterization of high-fat diet and multiple low-dose streptozotocin induced type 2 diabetes rat model. Experimental diabetes research. 2008;2008:704045. Epub 2009/01/10. doi: 10.1155/2008/704045. PubMed PMID: 19132099; PubMed Central PMCID: PMCPMC2613511.

19. Srinivasan K, Viswanad B, Asrat L, Kaul CL, Ramarao P. Combination of high-fat diet-fed and low-dose streptozotocin-treated rat: a model for type 2 diabetes and pharmacological screening. Pharmacological research. 2005;52(4):313-20. Epub 2005/06/28. doi: 10.1016/j.phrs.2005.05.004. PubMed PMID: 15979893.

20. Reed MJ, Meszaros K, Entes LJ, Claypool MD, Pinkett JG, Gadbois TM, et al. A new rat model of type 2 diabetes: the fat-fed, streptozotocin-treated rat. Metabolism: clinical and experimental. 2000;49(11):1390-4. Epub 2000/11/25. doi: 10.1053/meta.2000.17721. PubMed PMID: 11092499.

21. Huxley VH. Sex and the cardiovascular system: the intriguing tale of how women and men regulate cardiovascular function differently. Advances in physiology education. 2007;31(1):17-22. Epub 2007/03/01. doi: 10.1152/advan.00099.2006. PubMed PMID: 17327577.

22. Wang J, Bingaman S, Huxley VH. Intrinsic sex-specific differences in microvascular endothelial cell phosphodiesterases. American journal of physiology Heart and circulatory physiology. 2010;298(4):H1146-54. Epub 2010/02/09. doi: 10.1152/ajpheart.00252.2009. PubMed PMID: 20139324; PubMed Central PMCID: PMCPMC2853420.

23. Glinskii OV, Abraha TW, Turk JR, Rubin LJ, Huxley VH, Glinsky VV. Microvascular network remodeling in dura mater of ovariectomized pigs: role for angiopoietin-1 in estrogen-dependent control of vascular stability. American journal of physiology Heart and circulatory physiology. 2007;293(2):H1131-7. Epub 2007/05/15. doi: 10.1152/ajpheart.01156.2006. PubMed PMID: 17496211; PubMed Central PMCID: PMCPMC3332330.

24. Glinskii OV, Huxley VH, Glinskii VV, Rubin LJ, Glinsky VV. Pulsed estrogen therapy prevents post-OVX porcine dura mater microvascular network weakening via a PDGF-BB-dependent mechanism. PloS one. 2013;8(12):e82900. Epub 2013/12/19. doi: 10.1371/journal.pone.0082900. PubMed PMID: 24349391; PubMed Central PMCID: PMCPMC3857298.

25. Huxley VH, Wang J. Cardiovascular sex differences influencing microvascular exchange. Cardiovascular research. 2010;87(2):230-42. doi: 10.1093/cvr/cvq142. PubMed PMID: 20495187; PubMed Central PMCID: PMCPMC2895545.

26. Caligioni C. Assessing Reproductive Status/Stages in Mice. Current protocols in neuroscience / editorial board, Jacqueline N Crawley [et al]. 2009;Appendix:Appendix-4I. doi: 10.1002/0471142301.nsa04is48. PubMed PMID: 19575469; PubMed Central PMCID: PMCPMC2755182.

27. Briones AM, Aras-Lopez R, Alonso MJ, Salaices M. Small artery remodeling in obesity and insulin resistance. Current vascular pharmacology. 2014;12(3):427-37. Epub 2014/05/23. PubMed PMID: 24846232.

28. Jia G, Aroor AR, DeMarco VG, Martinez-Lemus LA, Meininger GA, Sowers JR. Vascular stiffness in insulin resistance and obesity. Frontiers in physiology. 2015;6:231. Epub 2015/09/01. doi: 10.3389/fphys.2015.00231. PubMed PMID: 26321962; PubMed Central PMCID: PMCPMC4536384.

29. Caballero AE, Arora S, Saouaf R, Lim SC, Smakowski P, Park JY, et al. Microvascular and macrovascular reactivity is reduced in subjects at risk for type 2 diabetes. Diabetes. 1999;48(9):1856-62. Epub 1999/09/10. PubMed PMID: 10480619.

30. Schofield I, Malik R, Izzard A, Austin C, Heagerty A. Vascular structural and functional changes in type 2 diabetes mellitus: evidence for the roles of abnormal myogenic responsiveness and dyslipidemia. Circulation. 2002;106(24):3037-43. Epub 2002/12/11. PubMed PMID: 12473548.

31. Rask-Madsen C, King GL. Mechanisms of Disease: endothelial dysfunction in insulin resistance and diabetes. Nature clinical practice Endocrinology & metabolism. 2007;3(1):46-56. Epub 2006/12/21. doi: 10.1038/ncpendmet0366. PubMed PMID: 17179929.

32. Pacher P, Beckman JS, Liaudet L. Nitric oxide and peroxynitrite in health and disease. Physiological reviews. 2007;87(1):315-424. Epub 2007/01/24. doi: 10.1152/physrev.00029.2006. PubMed PMID: 17237348; PubMed Central PMCID: PMCPMC2248324.

33. Martin JS, Padilla J, Jenkins NT, Crissey JM, Bender SB, Rector RS, et al. Functional adaptations in the skeletal muscle microvasculature to endurance and interval sprint training in the type 2 diabetic OLETF rat. Journal of applied physiology (Bethesda, Md : 1985). 2012;113(8):1223-32. Epub 2012/08/28. doi: 10.1152/japplphysiol.00823.2012. PubMed PMID: 22923508; PubMed Central PMCID: PMCPMC3472489.

34. Kingwell BA, Formosa M, Muhlmann M, Bradley SJ, McConell GK. Type 2 diabetic individuals have impaired leg blood flow responses to exercise: role of endothelium-dependent vasodilation. Diabetes care. 2003;26(3):899-904. Epub 2003/03/01. PubMed PMID: 12610056.

35. Womack L, Peters D, Barrett EJ, Kaul S, Price W, Lindner JR. Abnormal skeletal muscle capillary recruitment during exercise in patients with type 2 diabetes mellitus and microvascular complications. J Am Coll Cardiol. 2009;53(23):2175-83. Epub 2009/06/06. doi: 10.1016/j.jacc.2009.02.042. PubMed PMID: 19497445; PubMed Central PMCID: PMCPMC2722783.

36. Laughlin MH, Roseguini B. Mechanisms for exercise training-induced increases in skeletal musde blood flow capacity: differences with interval sprint training versus aerobic endurance training. Journal of physiology and pharmacology : an official journal of the Polish Physiological Society. 2008;59 Suppl 7:71-88. Epub 2009/03/11. PubMed PMID: 19258658; PubMed Central PMCID: PMCPMC2654584.

37. Cocks M, Shaw CS, Shepherd SO, Fisher JP, Ranasinghe A, Barker TA, et al. Sprint interval and moderate-intensity continuous training have equal benefits on aerobic capacity, insulin sensitivity, muscle capillarisation and endothelial eNOS/NAD(P)Hoxidase protein ratio in obese men. The Journal of physiology. 2016;594(8):2307-21. Epub 2015/02/04. doi: 10.1113/jphysiol.2014.285254. PubMed PMID: 25645978; PubMed Central PMCID: PMCPMC4933110.

38. Dela F, Larsen JJ, Mikines KJ, Ploug T, Petersen LN, Galbo H. Insulin-stimulated muscle glucose clearance in patients with NIDDM. Effects of one-legged physical training. Diabetes. 1995;44(9):1010-20. Epub 1995/09/01. PubMed PMID: 7657022.

39. Kirabo A, Fontana V, de Faria AP, Loperena R, Galindo CL, Wu J, et al. DC isoketal-modified proteins activate T cells and promote hypertension. J Clin Invest. 2014;124(10):4642-56. Epub 2014/09/23. doi: 10.1172/jci74084. PubMed PMID: 25244096; PubMed Central PMCID: PMCPMC4220659.

40. Liu J, Yang F, Yang XP, Jankowski M, Pagano PJ. NAD(P)H oxidase mediates angiotensin II-induced vascular macrophage infiltration and medial hypertrophy. Arterioscler Thromb Vasc Biol. 2003;23(5):776-82. Epub 2003/03/15. doi: 10.1161/01.atv.0000066684.37829.16. PubMed PMID: 12637340.

41. McCarthy CG, Goulopoulou S, Wenceslau CF, Spitler K, Matsumoto T, Webb RC. Toll-like receptors and damage-associated molecular patterns: novel links between inflammation and hypertension. American journal of physiology Heart and circulatory physiology. 2014;306(2):H184-96. Epub 2013/10/29. doi: 10.1152/ajpheart.00328.2013. PubMed PMID: 24163075; PubMed Central PMCID: PMCPMC3920129.

42. Singh MV, Abboud FM. Toll-like receptors and hypertension. American journal of physiology Regulatory, integrative and comparative physiology. 2014;307(5):R501-4. Epub 2014/06/13. doi: 10.1152/ajpregu.00194.2014. PubMed PMID: 24920728; PubMed Central PMCID: PMCPMC4214832.

43. De Ciuceis C, Amiri F, Brassard P, Endemann DH, Touyz RM, Schiffrin EL. Reduced vascular remodeling, endothelial dysfunction, and oxidative stress in resistance arteries of angiotensin II-infused macrophage colony-stimulating factor-deficient mice: evidence for a role in inflammation in angiotensin-induced vascular injury. Arterioscler Thromb Vasc Biol. 2005;25(10):2106-13. Epub 2005/08/16. doi: 10.1161/01.atv.0000181743.28028.57. PubMed PMID: 16100037.

44. Lu D, Kassab GS. Role of shear stress and stretch in vascular mechanobiology. Journal of the Royal Society Interface. 2011;8(63):1379-85. doi: 10.1098/rsif.2011.0177. PubMed PMID: 21733876; PubMed Central PMCID: PMCPMC3163429.

45. Davies PF, Tripathi SC. Mechanical stress mechanisms and the cell. An endothelial paradigm. Circulation research. 1993;72(2):239-45. Epub 1993/02/01. PubMed PMID: 8418981.

46. DePaola N, Gimbrone MA, Jr., Davies PF, Dewey CF, Jr. Vascular endothelium responds to fluid shear stress gradients. Arterioscler Thromb. 1992;12(11):1254-7. Epub 1992/11/11. PubMed PMID: 1420084.

47. Langille BL, O'Donnell F. Reductions in arterial diameter produced by chronic decreases in blood flow are endothelium-dependent. Science (New York, NY). 1986;231(4736):405-7. Epub 1986/01/24. PubMed PMID: 3941904.

48. Bevan JA, Laher I. Pressure and flow-dependent vascular tone. FASEB journal : official publication of the Federation of American Societies for Experimental Biology. 1991;5(9):2267-73. Epub 1991/06/01. PubMed PMID: 1860618.

49. Wechezak AR, Viggers RF, Sauvage LR. Fibronectin and F-actin redistribution in cultured endothelial cells exposed to shear stress. Laboratory investigation; a journal of technical methods and pathology. 1985;53(6):639-47. Epub 1985/12/01. PubMed PMID: 4068668.

50. Tigno XT, Ley K, Pries AR, Gaehtgens P. Venulo-arteriolar communication and propagated response. A possible mechanism for local control of blood flow. Pflugers Archiv : European journal of physiology. 1989;414(4):450-6. Epub 1989/08/01. PubMed PMID: 2798041.

51. Hester RL. Venular-arteriolar diffusion of adenosine in hamster cremaster microcirculation. The American journal of physiology. 1990;258(6 Pt 2):H1918-24. Epub 1990/06/01. PubMed PMID: 2360679.

52. Hester RL, Hammer LW. Venular-arteriolar communication in the regulation of blood flow. American journal of physiology Regulatory, integrative and comparative physiology. 2002;282(5):R1280-5. Epub 2002/04/18. doi: 10.1152/ajpregu.00744.2001. PubMed PMID: 11959667.

53. Stamler JS, Jia L, Eu JP, McMahon TJ, Demchenko IT, Bonaventura J, et al. Blood flow regulation by S-nitrosohemoglobin in the physiological oxygen gradient. Science (New York, NY). 1997;276(5321):2034-7. Epub 1997/06/27. PubMed PMID: 9197264.

54. Ellsworth ML. Red blood cell-derived ATP as a regulator of skeletal muscle perfusion. Med Sci Sports Exerc. 2004;36(1):35-41. Epub 2004/01/07. doi: 10.1249/01.mss.0000106284.80300.b2. PubMed PMID: 14707765.

55. Boegehold MA. Shear-dependent release of venular nitric oxide: effect on arteriolar tone in rat striated muscle. The American journal of physiology. 1996;271(2 Pt 2):H387-95. Epub 1996/08/01. PubMed PMID: 8770074.

56. Falcone JC, Meininger GA. Arteriolar dilation produced by venule endothelium-derived nitric oxide. Microcirculation (New York, NY : 1994). 1997;4(2):303-10. Epub 1997/06/01. PubMed PMID: 9219222.

57. Kuo L, Arko F, Chilian WM, Davis MJ. Coronary venular responses to flow and pressure. Circulation research. 1993;72(3):607-15. Epub 1993/03/01. PubMed PMID: 8431988.

58. Saito Y, Eraslan A, Lockard V, Hester RL. Role of venular endothelium in control of arteriolar diameter during functional hyperemia. The American journal of physiology. 1994;267(3 Pt 2):H1227-31. Epub 1994/09/01. PubMed PMID: 8092290.

VITA

David Bayless was born and raised in the Kansas City metro area, to Linton Bayless of the Kansas City metro area and Sara Deubner of California. He attended Truman State University for his undergraduate education, receiving a B.A. in Biology, and worked at A.T. Still Unversity with George Carlson before coming to the University of Missouri.

In his free time, he enjoys exercise training, both running in a continuance of his cross country days and weight training, as well as his hobby work in assembling and painting miniatures.